

Extended Arm Polyphenylene Dendrimers: Synthesis and Characterization

Dissertation zur Erlangung des Grades
„Doktor der Naturwissenschaften“
am Fachbereich Chemie und Pharmazie
der Johannes Gutenberg-Universität in Mainz

vorgelegt von

Ekaterina Vladimirovna Andreitchenko

geb. in Sankt-Petersburg, Russland

Mainz, 2006

Die vorliegende Arbeit wurde in der Zeit von Mai 2002 bis November 2005 am Max-Planck-Institut für Polymerforschung in Mainz unter der Leitung von Prof. Dr. K. Müllen durchgeführt.

Herrn Professor Dr. K. Müllen danke ich für die sehr interessante Themenstellung and für seine wissenschaftliche Förderung.

Contents

1 Introduction

- 1.1 The dendrimer concept 1
- 1.2 Chemical synthesis of dendrimers 2
- 1.3 Flexible dendrimers 5
- 1.4 Molecular structure 5
- 1.5 Properties of dendritic macromolecules compared to linear polymers 7
- 1.6 Rigid dendrimers 8
- 1.7 Synthesis of polyphenylene dendrimers through Diels-Alder cycloaddition 10
 - 1.7.1 Divergent synthesis 12
 - 1.7.2 Convergent synthesis 12
- 1.8 The influence of the cores and the branching units on the shape of the polyphenylene dendrimers 15
- 1.9 Functionalization of polyphenylene dendrimers 16
 - a) Prior group introduction, the cyclopentadienone route 17
 - b) Posteriori Group Introduction 19
 - c) Electrophilic Aromatic Substitution 19
- 1.10 Practical applications of dendrimers 20
- 1.11 Motivation 21
- 1.12 Literature for Chapter 1 24

2 Extended Arm Polyphenylene Dendrimers

- 2.1 Introduction 28
- 2.2 Synthesis of the new branching unit **2.1** bearing tris-(*para*-phenylene ethynylene)arms 28
- 2.3 Synthesis of the new extended arm branching unit **3.1** 30
- 2.4 The synthesis of "exploded" dendrimers up to the sixth generation 35
- 2.5 MALDI-TOF MS applied to the extended dendrimers 38
- 2.6 ¹H NMR analysis of exploded dendrimers 49
- 2.7 Size exclusion chromatography (SEC) 52

- 2.8 Multi-angle laser light scattering size exclusion chromatography (MALLS-SEC) 62
- 2.9 Vibrational spectroscopy (IR/Raman) 63
- 2.10 Visualisation of the exploded dendrimers by structural simulation 64
- 2.11 Dynamic light scattering (DLS) 65
- 2.12 Transmission electron microscopy (TEM) 68
- 2.13 Atomic Force Microscopy (AFM) 74
- 2.14 Guest molecules and their monitoring by the quartz microbalance (QMB) technique 81
- 2.15 Shortening the arms slightly: “semi-extended” dendrimers bearing a biphenyl - instead of a terphenyl spacer 87
- 2.16 Characterization of the dendrimers with biphenyl spacer 90
- 2.17 Outlook: dendrimers with biphenyl spacers for future application 92
- 2.18 Literature for Chapter 2 95

3 Synthesis and Hydrogenation of Dendrimers possessing internal -C≡C- Triple bonds

- 3.1 Introduction 101
- 3.2 Synthesis of new cyclopentadienone branching unit bearing the *para*-phenylene ethynylene arms (**5.1**) 101
- 3.3 Synthesis of the first-generation dendrimer with branching unit **5.1** 104
- 3.4 Synthesis of the second- and third-generation dendrimers bearing eight internal triple bonds 108
- 3.5 Heterogeneous catalysis of hydrogenation: some principal considerations 110
- 3.6 Hydrogenation of the second-generation dendrimer **5.6** 113
- 3.7 Hydrogenation of the third-generation dendrimer **5.7** 116
- 3.8 Further effects caused by hydrogenation of internal -C≡C- triple bond
 - 3.8.1 UV-Vis absorption of the second- and third-generation dendrimers 118
 - 3.8.2 Raman spectroscopy of the third-generation dendrimers **5.7** and **5.9** 119
 - 3.8.3 Diffusion-ordered 2D NMR (DOSY) of the third-generation dendrimers **5.7** and **5.9** 120
- 3.8.4 Incorporation of guest molecules 122
- 3.9 Literature for Chapter 3 123

4 Dendronization of a Chromophore Core by means of the New Extended Arm 3.1

- 4.1 Introduction 125
- 4.2 Synthesis of dendronized perylene dyes using the branching unit **3.1** 127
- 4.3 Characterization of dendronized chromophore dendrimers **6.5-6.10** 130
- 4.4 Optical properties
 - 4.4.1 Absorption and emission 132
 - 4.4.2 Fluorescence quenching experiment 135
 - 4.4.3 Fluorescence correlation spectroscopy (FCS) 137
- 4.5 Literature for Chapter 4 145

5 Summary 147

6 Experimental Part

- 6.1 Reagents and solvents 158
- 6.2 Instruments and analysis 159
- 6.3 General procedures 161
- 6.4 Synthesis of the extended arm polyphenylene dendrimers (for Chapter 2) 162
- 6.5 Synthesis of the semi-extended arm polyphenylene dendrimers (for Chapter 2) 178
- 6.6 Synthesis of the dendrimers possessing eight inner -C≡C- triple bonds and their hydrogenation (for Chapter 3) 185
- 6.7 Synthesis of the extended arm polyphenylene dendrimers with perylenedimide core (for Chapter 4) 195
- 6.8 Literature for Chapter 6 200

Abbreviations

AFM	atomic force microscopy
Calcd.	calculated
Da	Dalton
DLS	dynamic light scattering
DOSY	diffusion-ordered (NMR spectrum)
EDA	ethylenediamine
FD MS	field desorption mass spectrometry
G1-G6	first-sixth generation number
HPLC	high performance liquid chromatography
IR	infrared
MALDI-TOF	matrix assisted laser desorption ionization time of flight (MS)
MALLS	multiple angle laser light scattering
MS	mass spectrometry
M_n	number average molecular weight
M_w	weight average molecular weight
M	molecular weight (calculated molecular mass)
NMR	nuclear magnetic resonance
PAMAM	poly-(amino amine)
PDI	1) poly-dispersity index, 2) perylene-3,4,9,10-tetracarboxdimides
PDs	polyphenylene dendrimers
PS	poly-(styrene)
RI	refractive index
R_F	retention factor
r.t.	room temperature
SEC	size exclusion chromatography
TBAF	tetrabutylammoniumfluoride trihydrate
Td	tetraphenylmethane core
TEM	transmission electron microscopy
THF	tetrahydrofuran
TiPS	triisopropylsilyl group
UV-Vis	ultraviolet-visible (light)
QMB	quartz microbalance

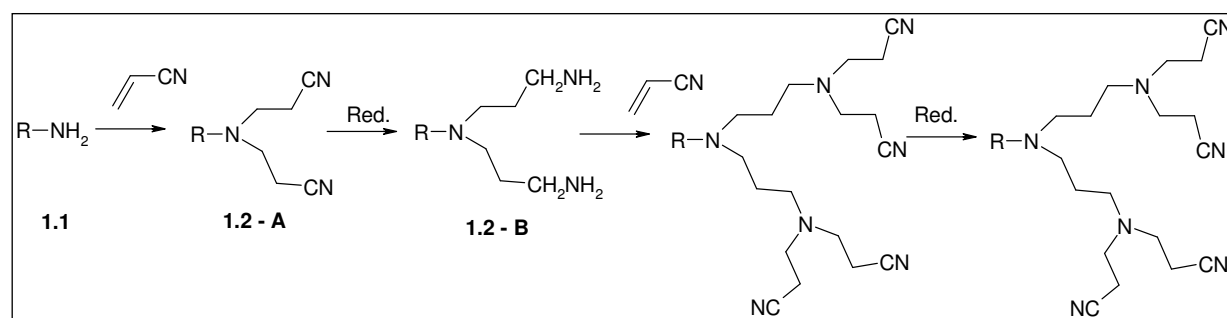
1 Introduction

1.1 The dendrimer concept

Traditional polymers, according to Staudinger,^[1-3] may be divided into three major macromolecular architectures: (I) linear (plexiglass, nylon), (II) cross-linked (rubber, epoxies), and (III) branched (low density polyethylene). As the fourth major of macromolecular architecture dendritic polymers have evolved; they consist of four sub-categories: random hyperbranched,^[3-4] dendigraftes,^[3] dendrons,^[3] and dendrimers.^[3,5] The present dissertation is concerned with the last category, namely that of dendrimers, exclusively.

A dendrimer is generally described as a macromolecule, which is characterized by its extensively branched 3D structure that provides a high degree of surface functionality and versatility. Its structure is always built around a central multi-functional core molecule, with branches and end-groups. Dendrimers are synthesised in a stepwise manner, i.e. each successive shell, known as a generation, is formed in an individual step.

In 1978 Vögtle and co-workers reported the first preparation, separation and mass spectrometric characterization of a basic dendrimer structure.^[5-6] These authors produced a cascade in an iterative sequence of reaction steps, in which each additional reaction gave a higher generation material (Scheme 1.1). The reaction of a monoamine **1.1**, as a starting material, with acrylonitrile via Michael addition led to the synthesis of desired dinitrile **1.2-A** which was reduced to the terminal diamine **1.2-B**, serving as a branching unit. Then the molecule **1.2-B** was subjected to the same reaction sequence to generate a heptaamine. This was the first synthesis of a cascade molecule and during the 1980's only a handful of additional research papers on cascade molecules were published.^[5]



Scheme 1.1: First synthesis of a cascade molecular architecture.

Subsequently, Denkewalter et. al. obtained patents on the first divergent preparation of dendritic polypeptides based on amino acids as the monomeric building block.^[7]

The term ‘‘dendrimer’’ was first offered by Tomalia in 1984. The word ‘‘dendrimer’’ derives from the Greek word ‘‘dendron’’ meaning ‘‘tree’’ and ‘‘meros’’ meaning ‘‘part’’. Other names for dendrimers are ‘‘arborols’’ from Latin also referring to a tree, and ‘‘cascade polymers’’. Although the earlier name ‘‘cascade molecule’’ is connected more directly to nomenclature, the expression ‘‘dendrimer’’ has now been generally accepted.^[8] Since the 1990’s after significant advances in analytical methods the field blossoms.

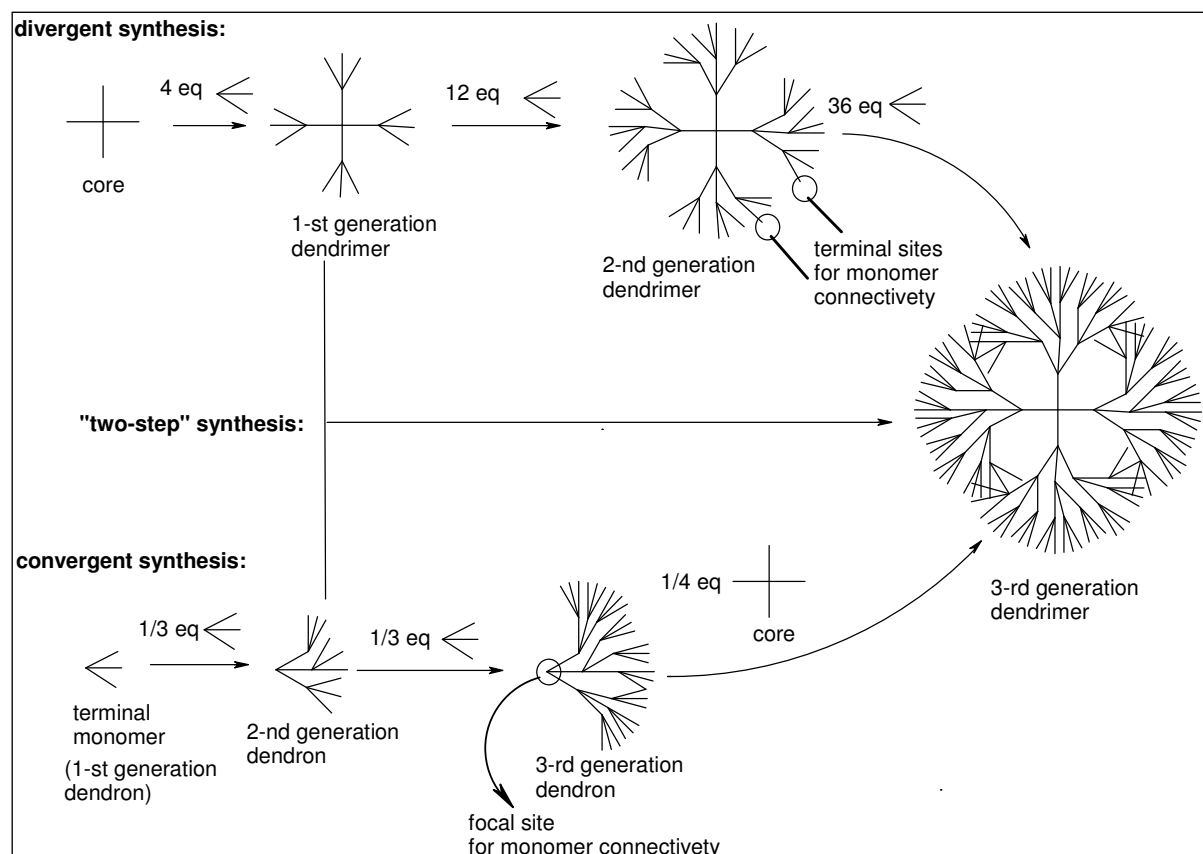
1.2 Chemical synthesis of dendrimers

Dendrimer synthesis can be achieved through different methods.^[6-18] However, divergent (a) and convergent (b) syntheses are the most common and extended methods (Scheme 1.2).

In the divergent approach the dendrimer is prepared from the core as the starting point and built up generation by generation. However the high number of reactions which have to be performed on a single molecule demands very effective transformations (99 + % yield) to avoid defects. In the divergent way problems occur from an incomplete reaction of the end groups, since these structure defects accumulate with the build up of further generation.^[8] As the side products possess similar physical properties, chromatographic separation is not always possible. Therefore the higher generations of divergently constructed dendrimers always contain certain structural defects. To prevent side reactions and to force reactions to completion a large excess of reagents is required, however this causes some difficulties in the purification of the final product.

The convergent approach starts from the surface and ends up at the core, where the dendrimer segments (dendrons) are coupled together. In this way only a small number of reactive sites are functionalized in each step, giving a small number of possible side-reactions per step. Therefore each synthesized generation of dendrimers can be purified, although purification of the high-generation dendrons becomes more cumbersome because of increasing similarity between reactants and formed product.^[9-10] But with proper purification after each step dendrimers without defects can be obtained by the convergent approach. On the other side, the convergent approach does not allow the formation of high generations because steric problems occur in the reactions of the dendrons and the core molecule.

Fundamental contributions to divergent dendrimer synthesis have been reported by Vögtle,^[6] Denkewalter,^[7] Meijer,^[11] Mülhaupt,^[12] Tomalia,^[13] and Newkome^[14]; early classical examples of the convergent approach to dendrimer synthesis can be found in the work of Frechet,^[15] Miller,^[16] and Moore.^[17]



Scheme 1.2: Dendrimer synthesis (schematically depicted).

Other synthetic approaches:^[18] combined synthesis (divergent-convergent, Scheme 1.2),^[18a, 18b] double-stage convergent growth,^[18c, 18d] and double exponential growth^[18e-18h] are known. The double-stage convergent growth approach allows for the preparation of larger dendrimers in less time and with greater ease than the single-stage approach. In the double-stage growth process a dendritic molecule carries at least one reactive functional group at each of its numerous chain extremities. This dendritic molecule is prepared by convergent growth (Figure 1.1) and is then used as a core to attach other preformed dendritic fragments through their single focal point reactive group (Figure 1.1): the first stage of this approach is the preparation of the hypercore moiety, which in the second stage reacts with a dendritic fragment to form a final dendrimer.

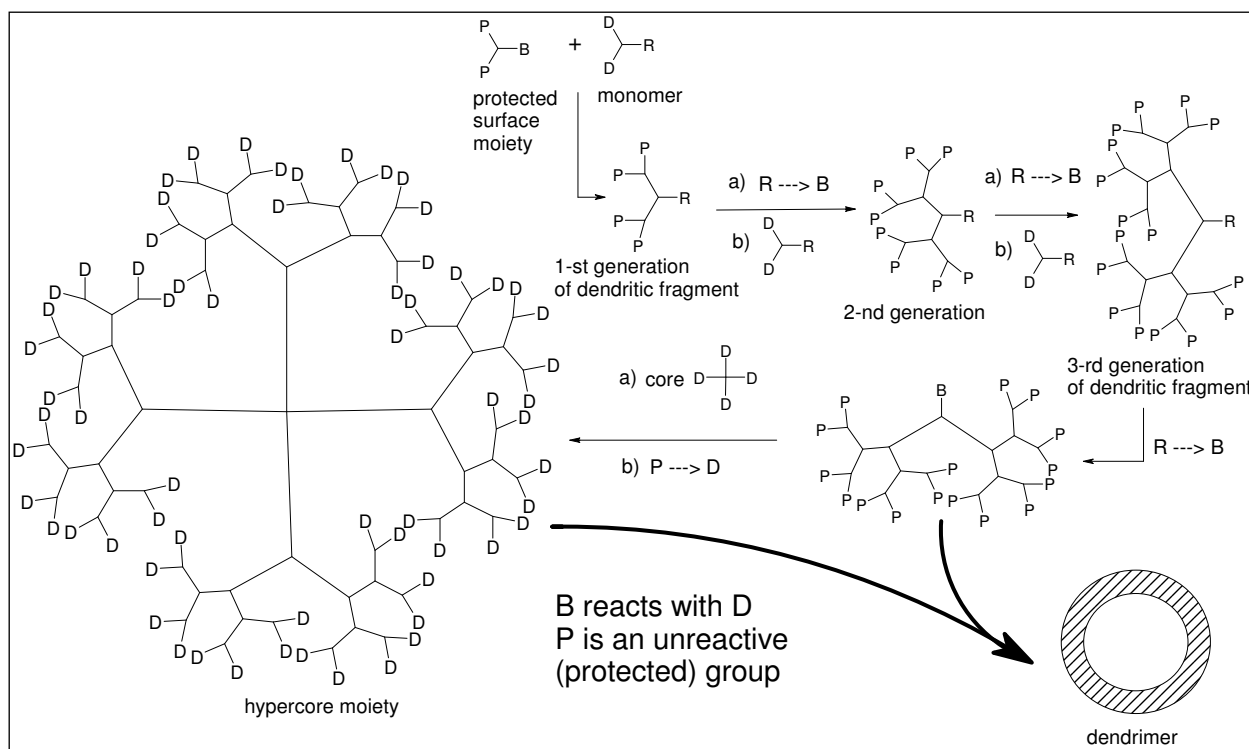


Figure 1.1: Double-Stage Convergent Growth Approach.

The double exponential dendrimer growth is an accelerated convergent scheme for the preparation of monodendrons via a bi-directional synthesis^[18h] (Figure 1.2). The final third generation macromolecule (Figure 1.2) can be prepared in only nine synthetic steps from the starting material, while the conventional convergent growth scheme would require seven generations to reach this same size (14 synthetic steps).

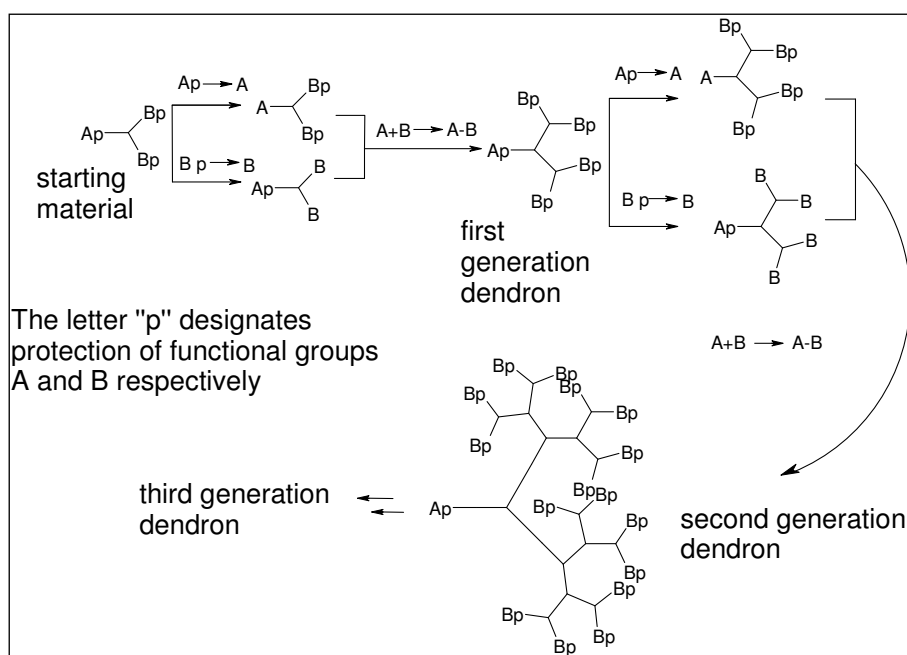
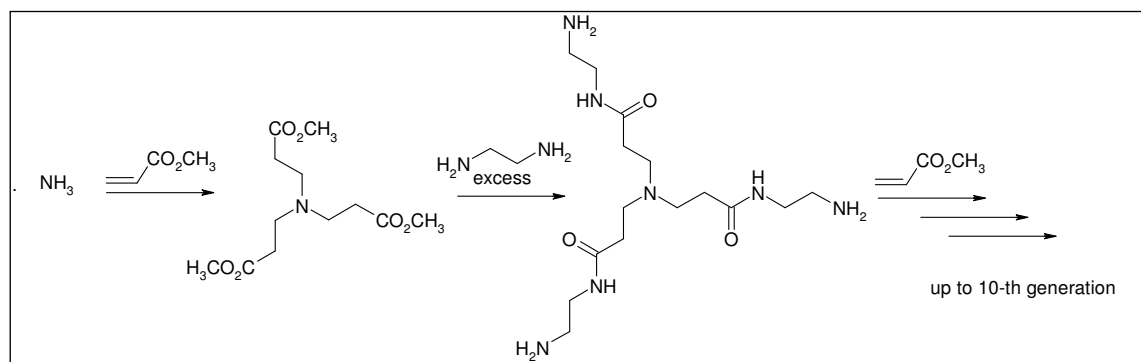


Figure 1.2: Double Exponential Dendrimer Growth.

1.3 Flexible dendrimers

Tomalia revived the concept of highly branched, monodisperse molecules^[13] when he developed the family of so called polyamidoamine (PAMAM) dendrimers (Scheme 1.3). PAMAM dendrimers are synthesized by the divergent approach. Ethylenediamine, ammonia or cystamine were used as cores and allowed to undergo iterative, two-steps reaction sequences consisting of a) an alkylation of primary amines by Michael addition to methyl acrylate and b) amidation of ester groups with a large excess of ethylenediamine to produce terminal amine groups. Repeating these iterative sequences created the high generations. At the same time, Newkome's group independently reported the synthesis of similar macromolecules named arborols.^[14]

PAMAM dendrimers constitute the first dendrimer family to be widely used, produced in kilogram scale and distributed commercially; they represent the most extensively characterized and best-understood series at this time.^[2] An other most commonly studied dendrimer is the Frechet-type polyether composition.^[2, 15] A novel P-dendrimer series up to the twelfth generation with the highest theoretical molecular mass (3 030 289 Da) is a part of Majoral's work.^[5, 19]



Scheme 1.3: Synthesis of PAMAM-dendrimers.

1.4 Molecular structure

Dendrimers of lower generations have highly asymmetric shape and possess more open structures as compared to higher generation dendrimers. As the chains growing from the core the molecules become longer and more branched, dendrimers adopt a globular shape.^[20] Dendrimers with higher generation number become densely packed as they extend out to the periphery, which forms a closed membrane-like structure. When a critically branched state is

reached, dendrimers cannot grow any further because of a lack of space.^[21-22] This is called the "starburst effect". In PAMAM dendrimer synthesis, this is observed after the tenth generation. The increasing branching density with each additional generation is also believed to have striking effects on the structure of dendrimers. They are characterized by the presence of internal cavities and by a large number of reactive end groups (Figure 1.3).

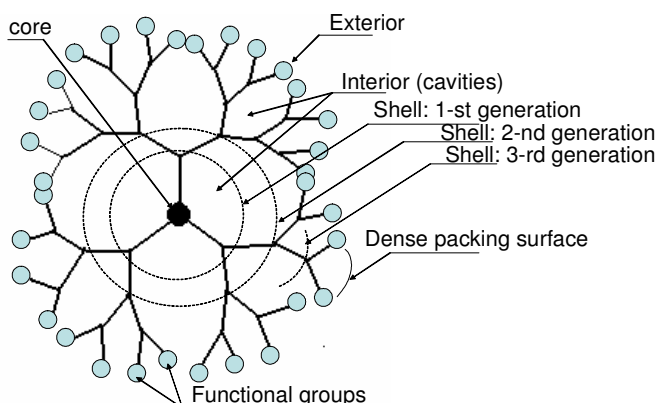
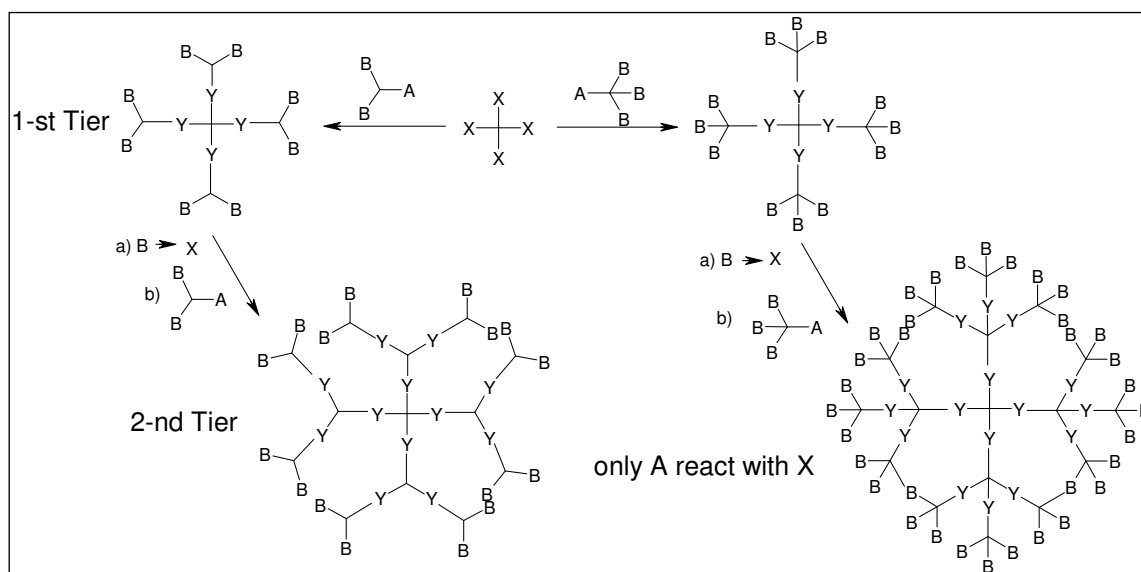


Figure 1.3: Concepts of core, generation and cavities.

There are different types of the building unit (monomer) bearing variable numbers of the reactive groups. The monomer AB_2 designates one reactive moiety and two masked groups which will be activated after the sequential growth of the dendrimer. In this case, the number of reactive surface sites is doubled with every generation (Scheme 1.4). In the case of branching monomer AB_3 , the reactive sites increase three-fold.



Scheme 1.4: Examples of divergent synthesis for dendrimer construction, using branching monomers with differing number of reactive units.

In practice, the monomers AB_2 and AB_3 are widely used, only a few monomers AB_4 and AB_5 have been employed for the rapid synthesis of dendrimers.^[5]

The nomenclature of dendrimers according to the IUPAC nomenclature is challenging because of the molecular size, high number of branching repeating units and functional groups. To simplify the name, an abbreviation sometimes will be used in the present work. The name is formed in the following way: 1- the generation number; 2-abbreviated name of core, 3- number of the functional groups on the surface. Two examples are presented in Figure 1.4.

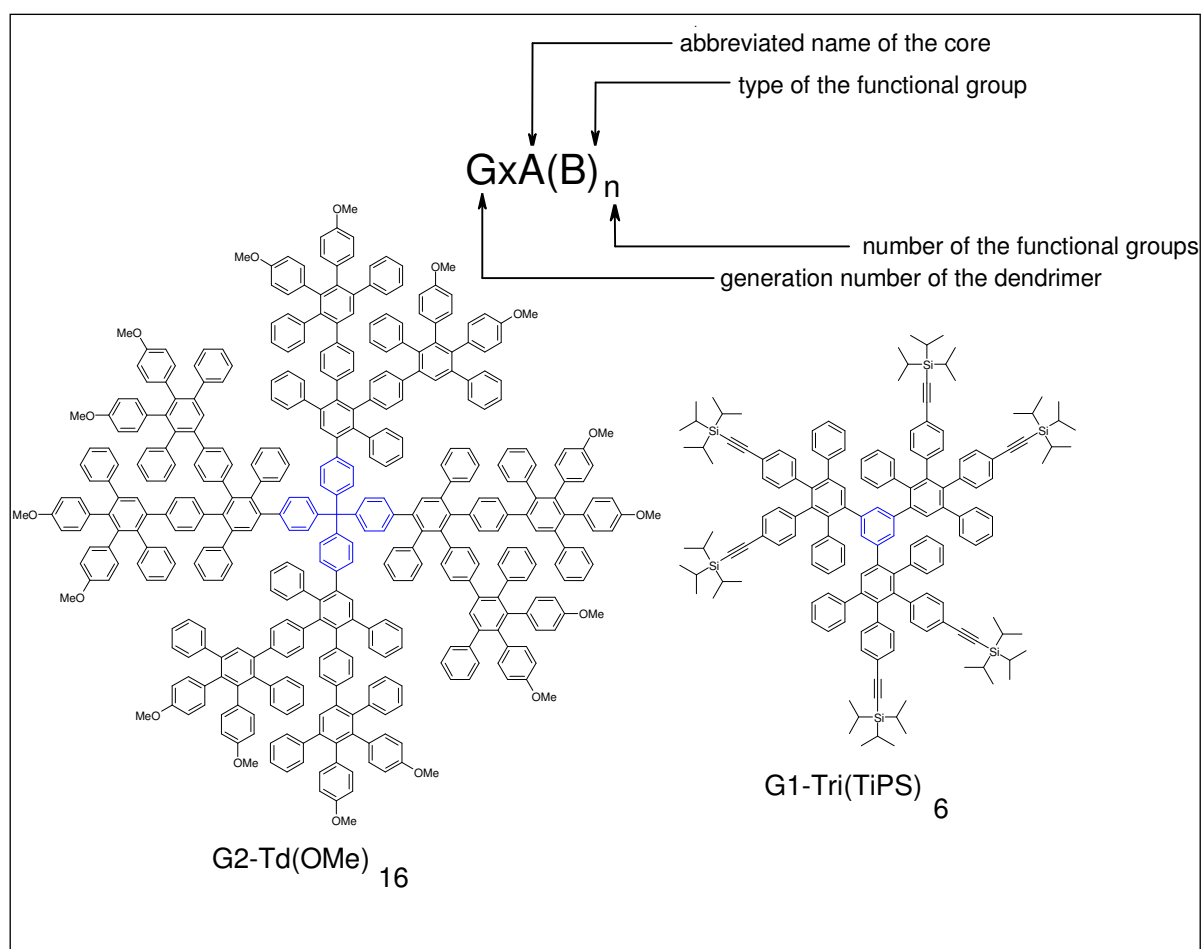


Figure 1.4: Nomenclature of typical dendrimers originating from the Müllen group.

1.5 Properties of dendritic macromolecules compared to linear polymers

Unlike linear polymers, dendrimers are monodisperse macromolecules. The classical polymerization process, which results in linear or slightly branched polymers, is usually random in nature and produces molecules of different size, whereas size and molecular mass

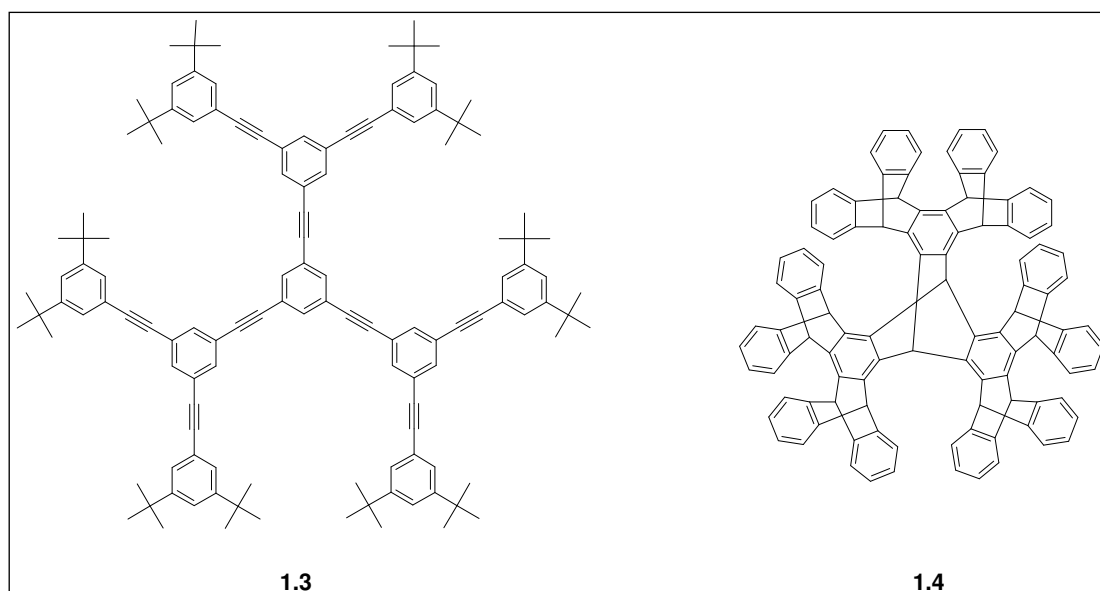
of dendrimers can be specifically controlled during synthesis. Because of their molecular architecture, dendrimers show strongly altered physical and chemical properties when compared to traditional linear polymers.^[3,21]

Whereas in solution, linear chains exist as flexible coils, the dendrimer structure resembles a tightly packed ball. This has a great impact on their rheological properties^[3] such that dendrimer solutions have significantly lower viscosity than those of linear polymers.^[21] For classical polymers the intrinsic viscosity increases continuously with molecular mass. Conversely, in the case of dendrimers, the intrinsic viscosity often goes through a maximum at the fourth generation and then begins to decline.^[3, 22-23] The presence of many chain-ends is responsible for high solubility and miscibility.^[4] Thus, the solubility of dendritic polyesters was found to be considerably higher than that of analogous linear polyester. An important difference between linear polymers and dendrimers is that in a dendrimer the many branches give rise to a very high number of terminal functional groups in each molecule, while a linear polymer molecule possesses two terminal functional groups only.^[24-25] Because of their globular shape and the presence of internal cavities dendrimers have some unique properties. The most important feature is the possibility to encapsulate guest molecules in the macromolecule interior of a dendrimer.

1.6 Rigid dendrimers

The majority of work reported up to now is devoted to dendrimers with arms made up of flexible units. The first suggestion about the fact that the ends of the branches at a given generation are not on the surface but may be buried within the molecule was proposed by Lescañes and Muthukumar.^[26] Both a Monte Carlo simulation by Mansfield and Klushin^[27] and a molecular dynamic simulation by Murat and Grest^[28] showed a density maximum at the core with a monotonic decrease to the edge, except for a slight local minimum at small radial distances for large dendrimers. This state was experimentally confirmed by Rubinstein and Boris^[29] who noted, that if the branches of the starburst were very rigid, so that the persistence length of a test branch were greater than its contour length, then each successive generation would be at a further radial distance and a relatively hollow interior would result. A few publications only deal with dendrimers with rather rigid arms built up from phenylene units (Schemes 1.5-1.6), as introduced by Moore and Xu (**1.3**),^[17] Hart (**1.4**),^[30] Miller and Neenan (**1.5**),^[31, 32] Müllen (**1.6**).^[33-35]

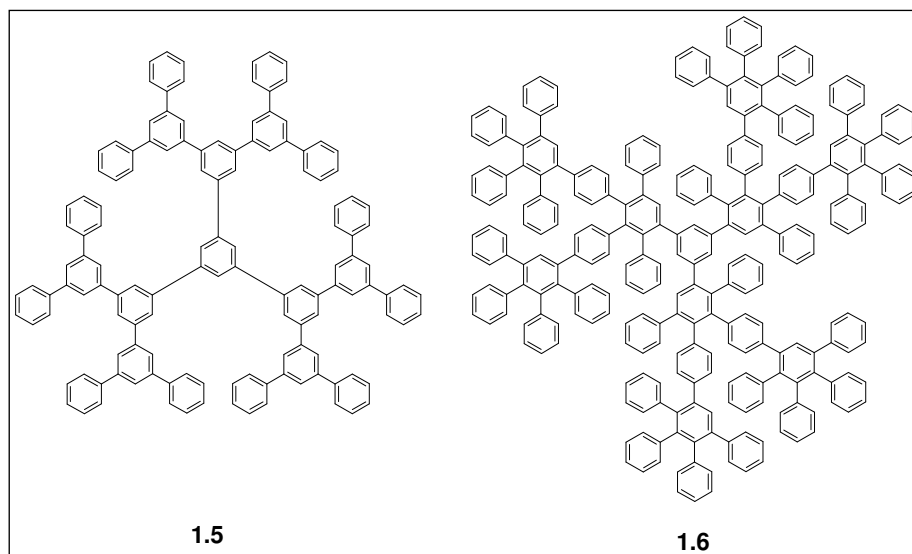
Dendrimers prepared from rigid units have a more precisely defined three-dimensional structure compared to their flexible counterparts. The rigid repeating units impose geometrical restrictions and thus little conformational freedom arises. Such freedom comes mainly from the rotational movement which depends on steric effect and/ or hydrogen bonding.^[24] The rigidity of the dendritic branches generates stable intramolecular free volumes (voids) with definite structures. Moore and Xu (**1.3**) reported the convergent preparation of rigid dendritic wedges based on 1,3,5-trisubstituted phenylacetylenic linkages and they enlarged the size of stiff dendrimers using differently sized branching units at each generation,^[17] while Hart presented an iptycene dendrimer containing three large cavities (**1.4**), each lined with six benzene rings.^[30]



Scheme 1.5: Examples of rigid dendrimers.

Miller and Neenan synthesized other stiff dendrimers, known as polyphenylene macromolecules, using a 1,3,5-trisubstituted benzene (**1.5**) as core, via convergent synthesis based on the Suzuki-type conditions up to second and third generations.^[16, 31] These dendrimers exhibit conformational isomerism due to rotational mobility around C-C σ -conformation chains.

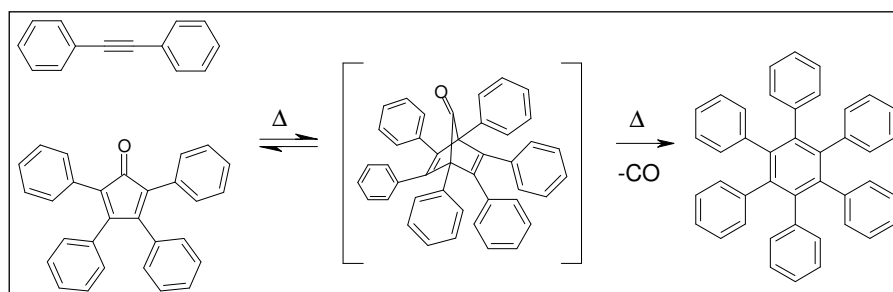
Other polyphenylene dendrimers were prepared in Müllen's group under Diels-Alder conditions, (for example based on the core 1,3,5-triethynylbenzene **1.6**), they will be discussed in detail in the next paragraph. This new type of dendrimer leads to dendritic structures with well defined shapes and diameters.



Scheme 1.6: Second generation of polyphenylene dendrimers, obtained by palladium catalyzed coupling via a convergent approach (**1.5**) and by Diels-Alder cycloaddition via a divergent approach (**1.6**).

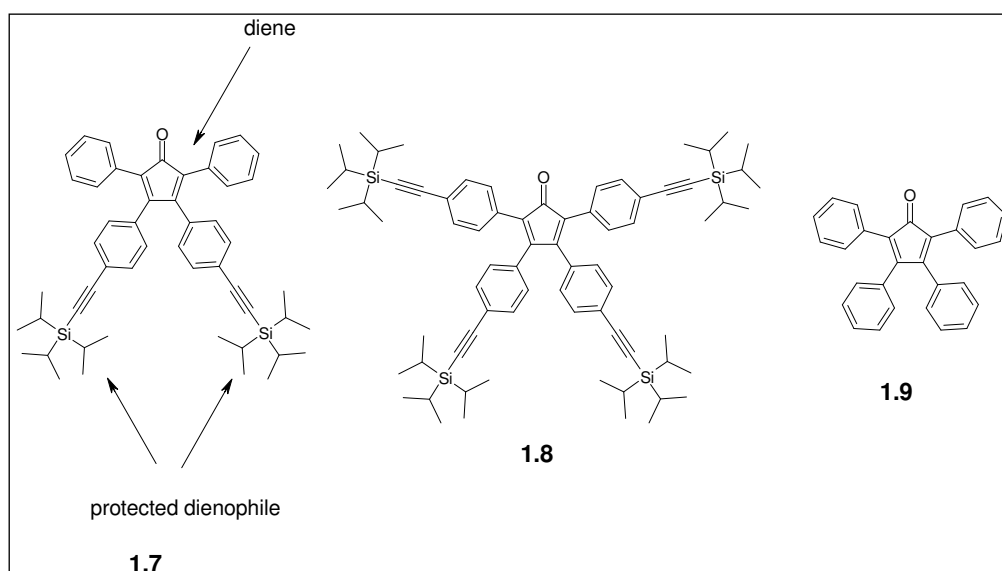
1.7 Synthesis of polyphenylene dendrimers through Diels-Alder cycloaddition

In 1997 Müllen's group reported on both types of approaches to produce polyphenylene dendrimers (PDs) where a Diels-Alder reaction was the centre of the reactions.^[33-35] The [2+4] Diels-Alder cycloaddition of tetraphenylcyclopentadienones to ethynes, known since 1933, is quantitative (yield is above 99 %)^[36] and profits from the elimination of carbon monoxide to afford phenyl substituted benzene (Scheme 1.7).

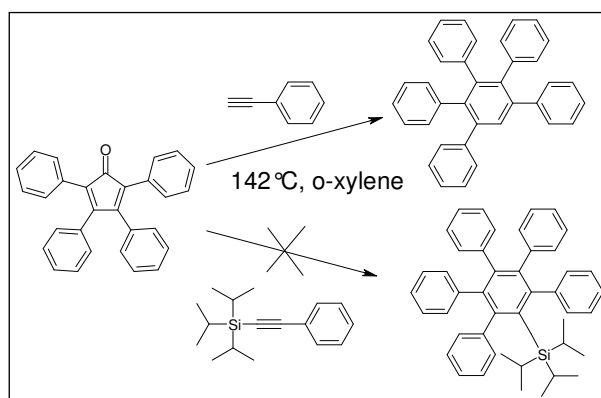


Scheme 1.7: Diltley-reaction to form hexaphenylbenzene.

In order to use the Dilthey reaction^[36] for dendrimer synthesis, the A₂B type branching unit 3,4-bis[4-(tri-*iso*-propylsilylethynyl)-phenyl]-2,5-diphenyl-cyclopentadienone (**1.7**) was introduced (Scheme 1.8). This molecule contains tetraphenylcyclopentadienone as a diene subunit for the Diels-Alder cycloaddition, and two ethynes as protected dienophile functions. The latter are protected against self-cycloaddition by the bulky triisopropylsilyl (TiPS) substituents (Scheme 1.9).



Scheme 1.8: Branching units: A₂B type **1.7**, A₄B type **1.8**, and A₀B type **1.9** for dendrimer termination.



Scheme 1.9: TiPS-group as a steric inhibitor for the Diels-Alder cycloaddition.

The branching unit A₄B (**1.8**) has two additional protected ethyne functionalities,^[35] which gives the respective generation number dendrimer with twice as many functional groups. However, a lower maximum number of generation is accessible with the latter because of the steric hindrance. After the isolation of a certain ethynyl-TiPS decorated dendrimer, the

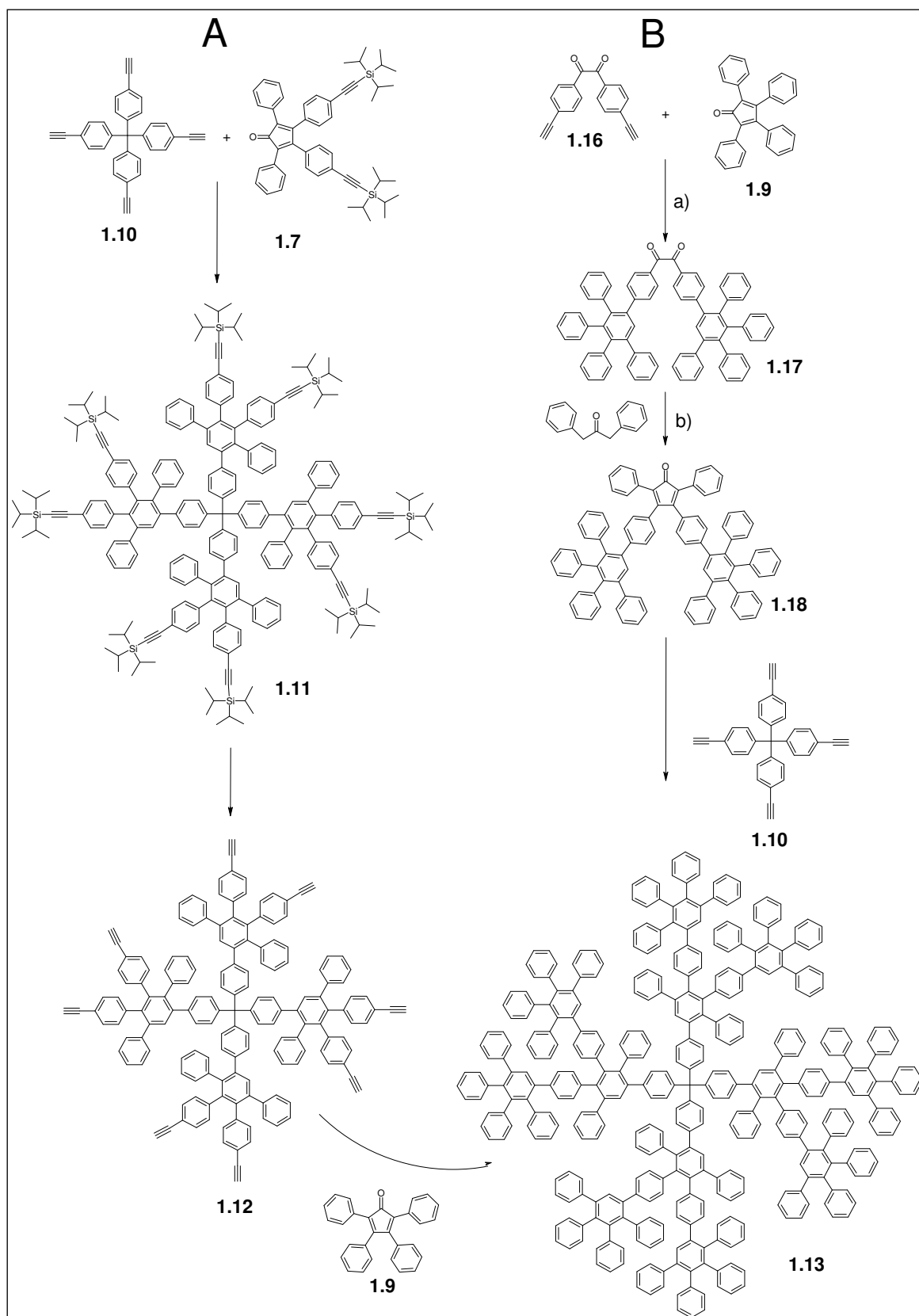
protecting groups can be removed easily by tetrabutylammoniumfluoride trihydrate restoring reactivity for a subsequently Dilthey-reaction. The other branching unit **1.9**, less sterically demanding and commercial available, is used for the termination step.

1.7.1 Divergent synthesis (A)

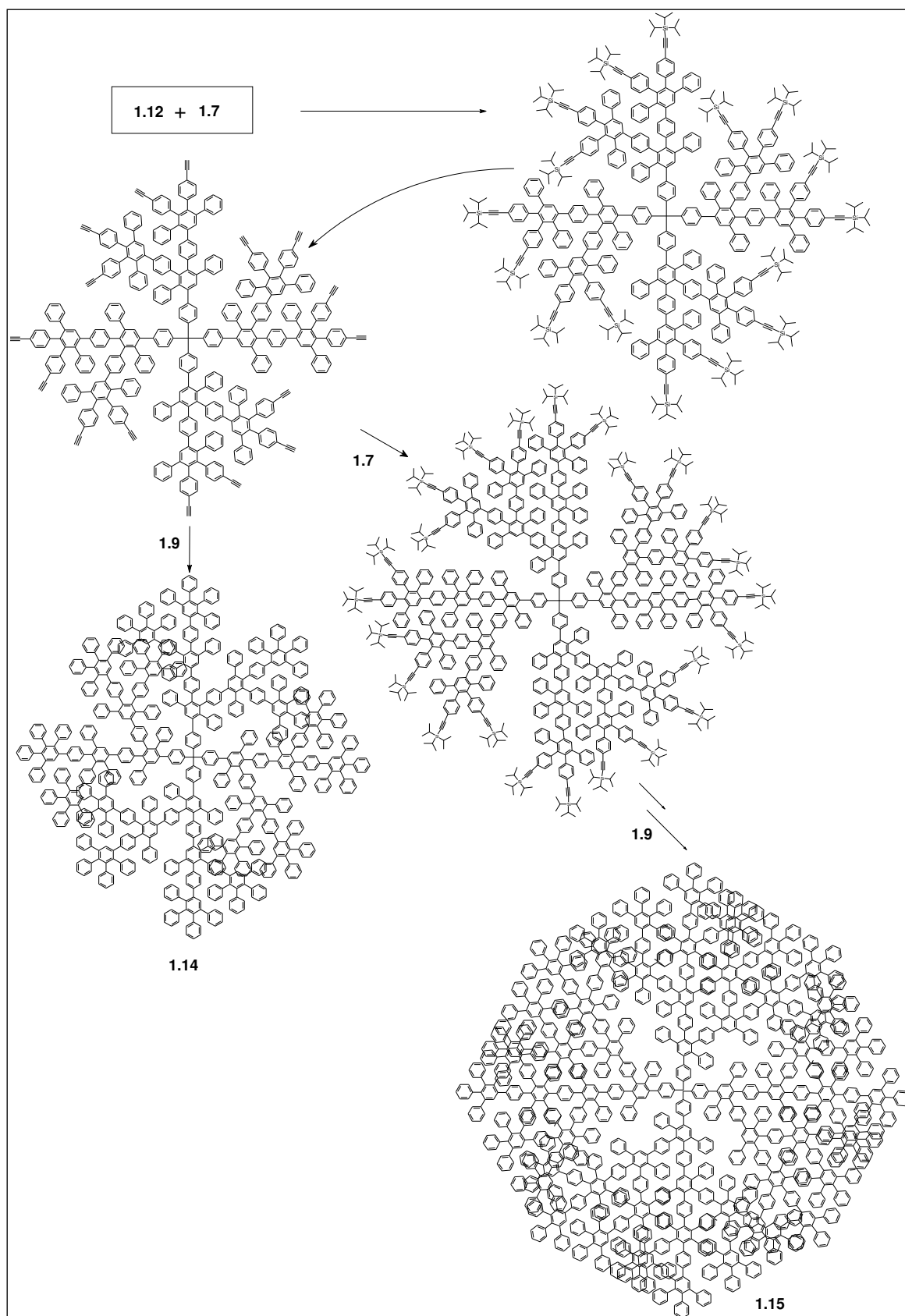
The synthesis of polyphenylene dendrimers is based on two alternating reactions: a) "growth step" - the Diels-Alder cycloaddition of the branching unit (**1.7**), bearing two protective TiPS groups, to phenylene substituted ethynyls and b) "deprotection step" – the desilylation of the triisopropylsubstituted alkynes.^[35] The starting material for the Diels-Alder reaction is the core tetrakis-(4-ethynylphenyl)-methane (**1.10**) (Scheme 1.10) and the branching unit **1.7** to yield the first generation dendrimer with eight TiPS-protected groups (**1.11**). After the removal of the TiPS groups, the dendrimer with eight terminal ethynyl units (**1.12**) reacts with tetraphenylcyclopentadienone (**1.9**) to afford a terminal second-generation dendrimer **1.13**. If the first generated deprotected dendrimer **1.12** reacts with the branching unit **1.7** the cycle is repeated till the final third- and fourth-generation dendrimers (**1.14** and **1.15** respectively, Scheme 1.11).

1.7.2 Convergent synthesis (B)

A convergent method was developed for the growth of the polyphenylene dendrimers only up to the second generation^[34] (Scheme 1.10). This synthesis is based on two alternating orthogonal reactions: a) the Diels-Alder cycloaddition of tetraphenylcyclopentadienones to phenylene substituted ethynyls and b) the Knoevenage-condensation of benzils with 1,3-diphenylacetones to cyclopentadienones. The starting compound is 4,4'-diethynyl-benzyl (**1.16**) featuring two ethynylic dienophilic units and one ethanedione function. The two-fold Diels-Alder reaction of an excess of **1.9**, which is regarded as a first-generation dendron, with **1.16** leads to the second-generation benzilic dendron **1.17**. The Knoevenagel condensation of **1.17** with 1,3-diphenylacetone gives the second-generation cyclopentadienone dendron **1.18** which is used for the final step. Its four-fold cycloaddition to the core **1.10** produces the second generation polyphenylene dendrimer (**1.13**). The attempt to synthesis of the next (third) generation cyclopentadienone dendron failed, because the Knoevenagel condensation of the third-generation benzilic dendron, obtained from the Diels-Alder cycloaddition of **1.18** with **1.16**, with 1,3-diphenylacetone was incomplete.



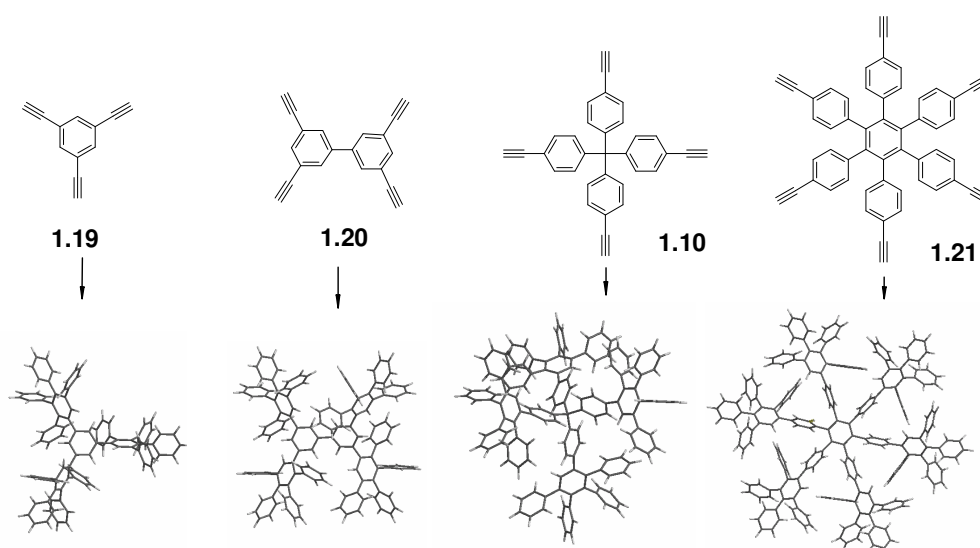
Scheme 1.10: Two alternative approaches to the second-generation polyphenylene dendrimer: divergent (A) and convergent synthesis (B) via Diels-Alder cycloaddition.



Scheme 1.11: Divergent synthesis of the third- and fourth-generation polyphenylene dendrimers.

1.8 The influence of the cores and the branching units on the shape of the polyphenylene dendrimers

The variation of the cores causes the branches to grow in certain given directions^[35] as shown in Scheme 1.12 where the cores are based on 1,3,5-triethynylbenzene (**1.19**), 3,3',5,5'-tetraethynylbiphenyl (**1.20**), tetrakis(4-ethynylphenyl)methane (**1.10**) and hexakis(4-ethynylphenyl)benzene (**1.21**). According to the simulations of Bredas et al,^[37] the dendrimer with core **1.19** adopts a false-propeller structure without rotational symmetry, and the one with core **1.21** a true-propeller shape. They differ in the orientation of the branches around the center of the molecule. The biphenyl core **1.20** leads to the dumb-bell shaped molecule, while dendrimers based on tetrahedral core **1.10** with a diabolo-like molecular shape resemble the shape of the core very well.^[35, 38] Due to the large number of benzene rings around the central methane unit, the branches are hindered in their rotations and this lowers the internal mobility of the molecule compared to the one based on the biphenyl core **1.20**. The stiffness of dendrimers is influenced not only by the various cores but also by the type of branching units (Scheme 1.8). Using different degrees of branching, the density of the dendrimers is differentiated. The A₄B-type branching unit **1.8** containing four dienophiles allows the growth of four branches from each functional group thus increasing the density of the dendrimers, however leading to the lower generation number due to the steric hindrance.



Scheme 1.12: Molecular modelling of the first-generation dendrimers with different cores employing the branching unit **1.9**.

Rosenfeldt compared the fourth-generation urea-functionalized poly(propyleneamine) dendrimer (Figure 1.5, molecule A) with the fourth-generation polyphenylene dendrimer based on the biphenyl core (Figure 1.5, molecule B).^[39]

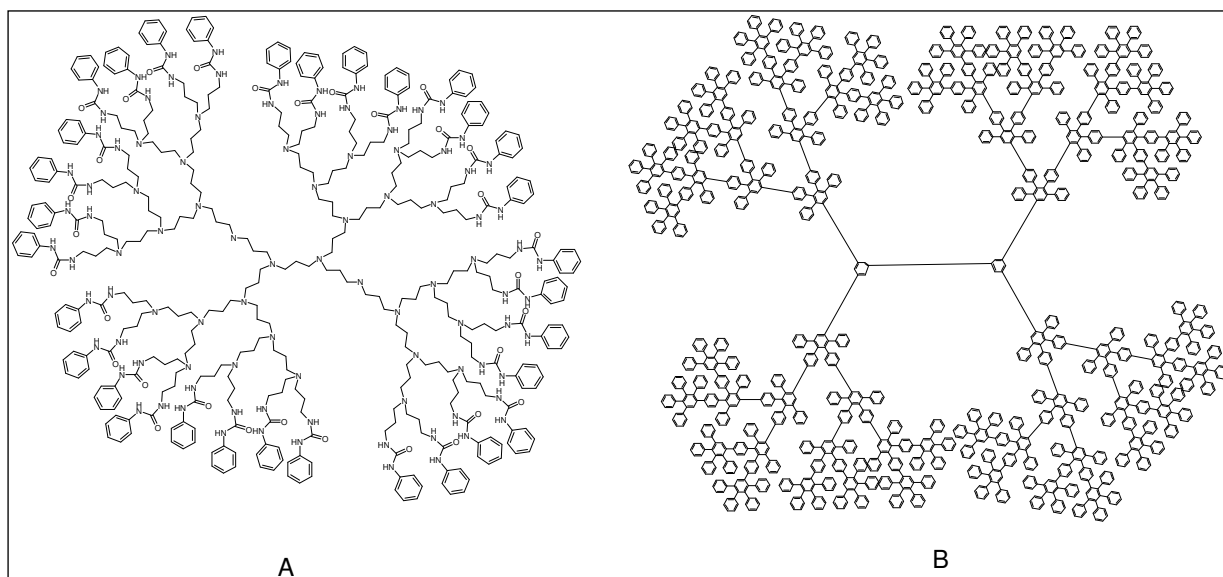


Figure 1.5: The flexible dendrimer A^[41] and the rigid dendrimer B^[40]

The structure A (Figure 1.5) exhibits its maximum density at the core of the molecule ("dense-core model") because the end groups are folding back precisely into the voids created by stretching.^[42] As all most flexible dendrimers, structure A has a vast number of conformations that are generated by rotation about the bonds between these units. A totally different situation arises in structure B (Figure 1.5). In this case the benzene rings are connected either linearly (para) or at an angle of 60° (ortho) or 120° (meta) to each other. Hence, the rotation about the bonds between the rings cannot change the structure of the molecule profoundly and no back-folding of the terminal groups is possible.^[39] Structure B represents the "dense-shell model" in which a hollow core is surrounded by a densely packed shell of the end groups. This polyphenylene dendrimer conform with de Gennes's theory,^[43] which states that all subsequent branches extend to the periphery of the molecule.

1.9 Functionalization of polyphenylene dendrimers

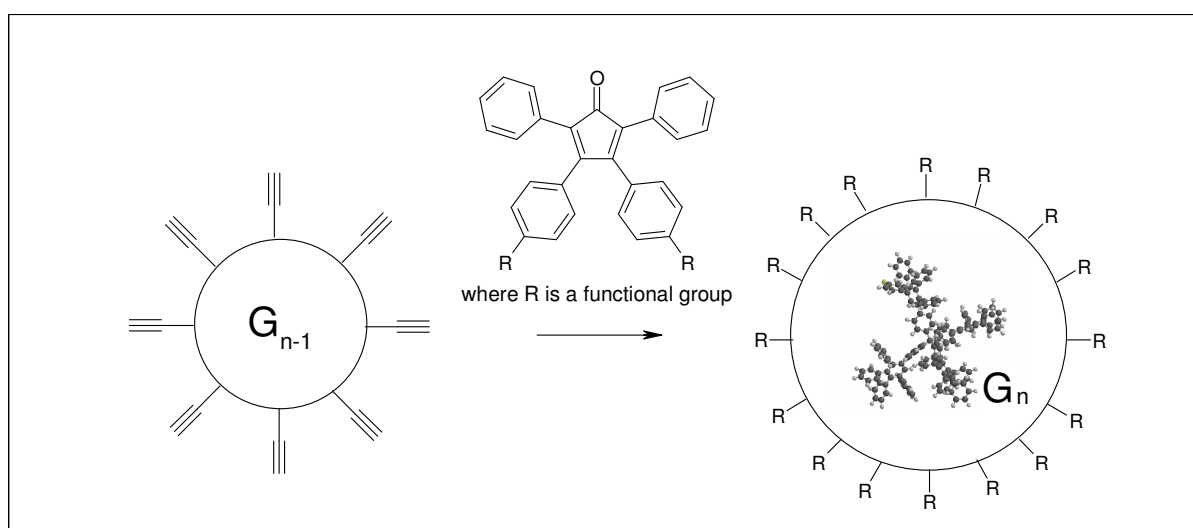
As mentioned above, the various types of the cores and some branching units (for example, A₄B) strongly influence the structure of polyphenylene dendrimers. However, the introduction of functional groups at the periphery does not change the shape of the polyphenylene dendrimers,

because these are rigid and back-folding of the branches is prevented, contrary to the condition of flexible dendrimers.^[41] Müllen's group was able to functionalize the polyphenylene dendrimers via three different methods:^[38]

- the use of functionalized cyclopentadienones,
- polymer-analogous reactions (group conversions),
- electrophilic aromatic substitution.

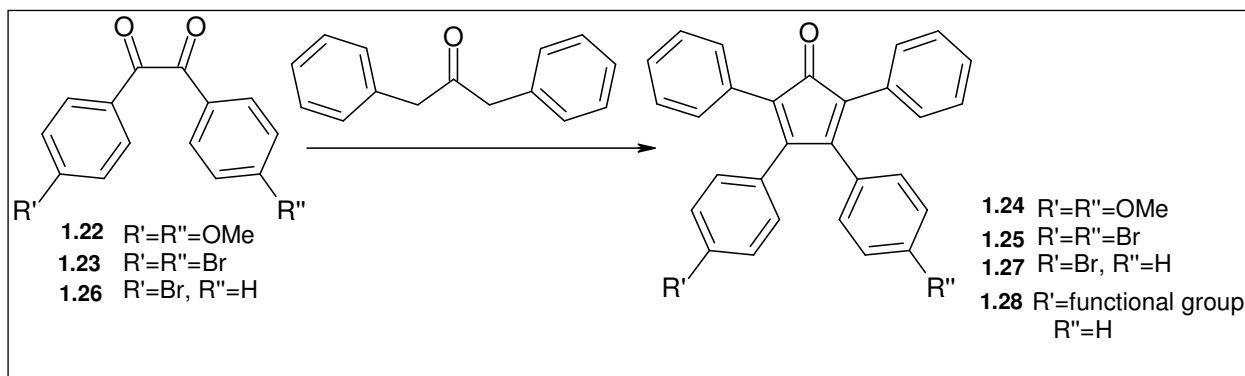
a) Prior group introduction, the cyclopentadienone route

By means of this synthetic approach, cyclopentadienone building units carrying the functional groups are used for the outer shell of the dendrimer (Scheme 1.13) leading to a defined number of peripheral groups R.

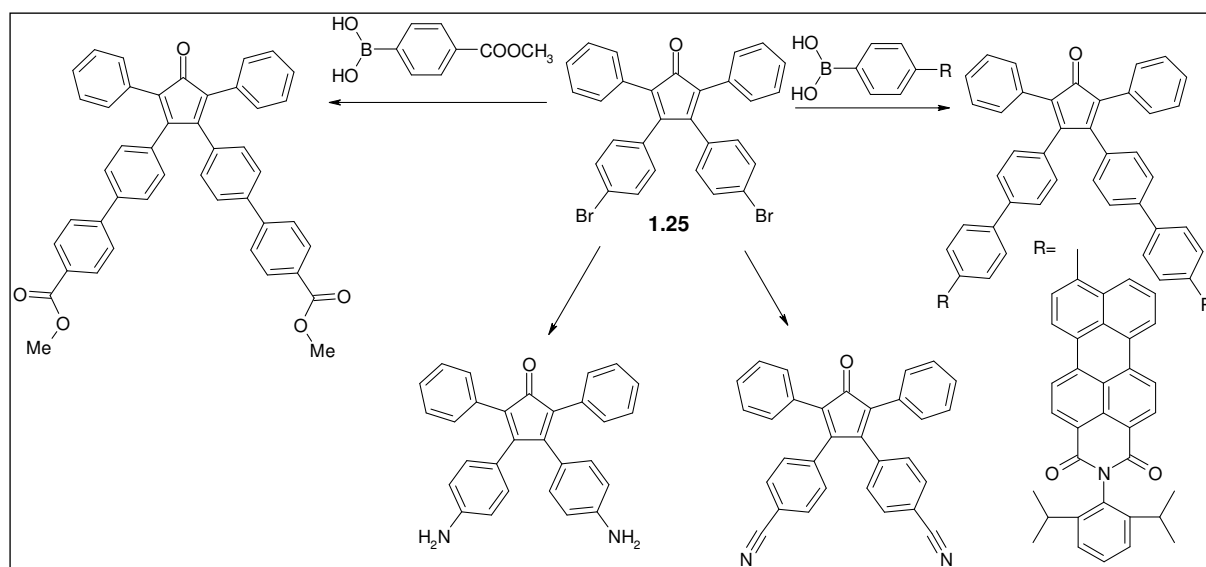


Scheme 1.13: Functionalization of polyphenylene dendrimers via the cyclopentadienone-route.

This method gives defined, monodisperse, defect-free functionalized dendrimers, which are easily purified because of the high mass differences between the cyclopentadienone and the final dendrimer. On the other side, for each new functionality, an appropriate cyclopentadienone building unit has to be synthesized. This approach is achieved via a Knoevenagel reaction of an already functionalized bibenzyl and 1,3-diphenylacetone (Scheme 1.14). For instance, a commercially available 4,4'-dimethoxybibenzyl **1.22** or 4,4'-dibromobenzyl **1.23** with 1,3-diphenylacetone give the cyclopentadienone carrying two methoxy- or bromo- substituents (**1.24** and **1.25** respectively). The bromo- substituent of the dibromocyclopentadienone **1.25** can then be converted quantitatively into a cyano- or amino- functions^[38] (Scheme 1.15).



Scheme 1.14: Synthesis of functionalized cyclopentadienones via the Knoevenagel reaction.

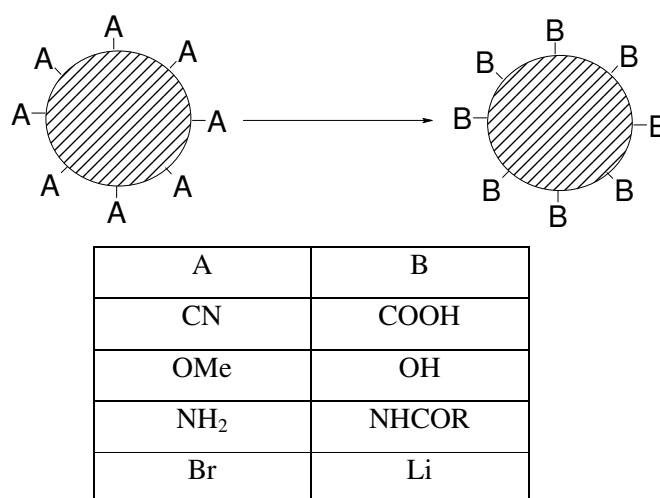
Scheme 1.15: Synthesis of various functionalized cyclopentadienones.^[41, 44]

Since the Diels-Alder reaction takes place at high temperature, it is important to use functional groups which are thermally stable. Other functionalized cyclopentadienones can be synthesized via Suzuki reaction of **1.25** with the boronic ester of benzene^[44] bearing the required functional groups, many of which now are commercially available (Scheme 1.15). There are also other variants of decorated cyclopentadienones containing thiomethyl, thiophenyl, halogen groups.^[38] A mono-substituted functionalized cyclopentadienone **1.27** (Scheme 1.14) plays an important role in the synthesis of the desymmetrised three-dimensional polyphenylene dendrimers. Müllen et. al. have synthesized a large range of mono-substituted cyclopentadienones (**1.28**) bearing fluorescent dyes, charge-transporting units, biotin units for attaching the dendrimers to

biologically active molecules, sulphur containing groups for binding to gold electrodes, and ethylene oxide chains for water solubility.^[45]

b) Posteriori Group Introduction

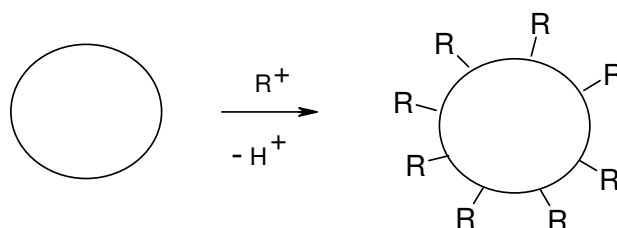
The conversion of an already existing group A on the dendrimer into a substituent B by subsequent addition of an electrophile has been accomplished (Scheme 1.16). In the ideal case, this reaction should be quantitative, but the possibility of incomplete conversions or byproducts must always be considered.^[46]



Scheme 1.16: Polymer-analogous reactions on polyphenylene dendrimers.^[38]

c) Electrophilic Aromatic Substitution

Electrophilic aromatic substitutions on the final dendrimer, such as the introduction of chloromethyl, aminomethyl and sulfonic acid groups, has been achieved (Scheme 1.17).^[47]



Scheme 1.17: Functionalization via electrophilic aromatic substitution of unsubstituted polyphenylene dendrimer.

It is a quickest method for derivatisation of the dendrimers, because no further functionalized cyclopentadienones have to be synthesized, but this approach leads to a statistical distribution of the functionalities over the surface of the dendrimer. It is nevertheless possible to adjust the approximate number of groups via the electrophile/dendrimer ratio.

1.10 Practical applications of dendrimers

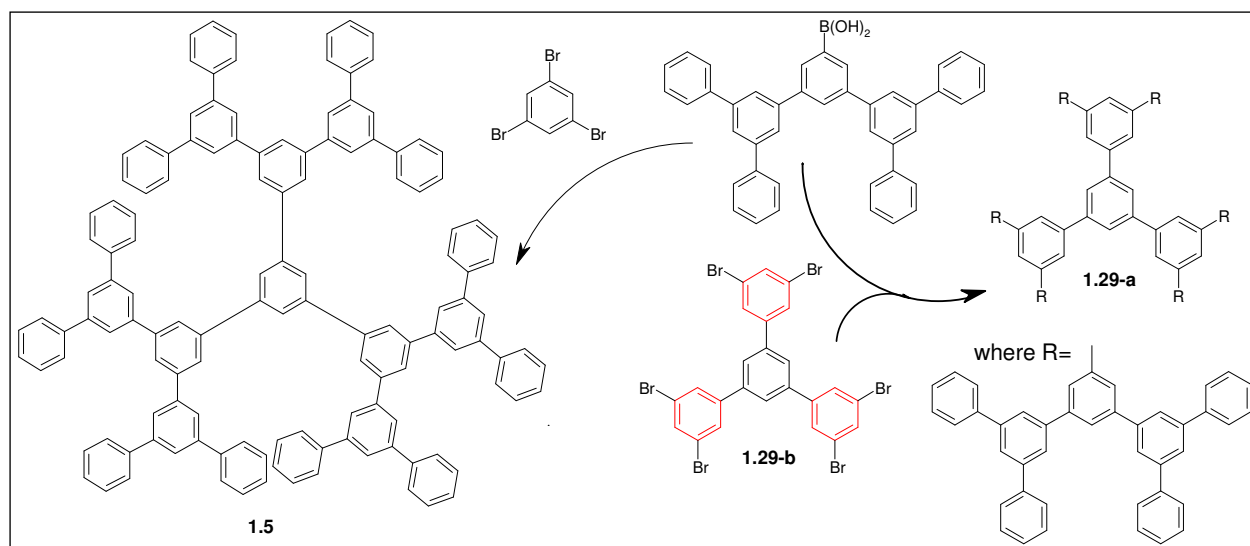
Nowadays, there are many variable dendrimers, each with specific properties. The surface, the interior and the core can be tailored for different sorts of applications. Many potential applications of dendrimers are based on their unparalleled molecular uniformity, multifunctional surface and presence of internal cavities. These specific properties render dendrimers attractive in modern high technology as exemplified by biomedical and industrial applications.^[10, 21] Dendrimers have found biomedical use^[9]; in this context *in vitro* diagnostics,^[10] contrast agents for magnetic resonance tomography,^[48] carriers for drug delivery,^[10] boron neutron capture therapy,^[49] nanoscale reactors^[50] and micelle mimicry^[51] should be mentioned. Dendrimers also serve to improve industrial processes. For example, dendrimers, which are multifunctionalized at their periphery with metal-containing catalytically active sites, promote the polymerization of monomers; they are easily separated and recovered from the reaction mixture by filtration method.^[52] Majoral-type dendrimers have functionalized groups with numerous transition metals and are attractive as catalysts.^[53] Metalated dendrimers for the electrochemical reduction of CO₂ to CO are known.^[54] Dendrimers can encapsulate insoluble materials or metal ions and transport them into a solvent within their interior. Some functionalized dendrimers can be used to extract strongly hydrophilic compounds from water into liquid CO₂.^[55]

The PDs, known since 1997 only, display unique features such as high stiffness, shape persistence, nanometer dimension which render them suitable for the use as chemical and thermally inert nanosupports for chromophores, and catalysts.^[38] Certain PDs have been employed as organic templates and supramolecular assemblies, in surface functionalization, gene transfection,^[38] and in diagnosis.^[56] The development of PDs is continued.

1.11 Motivation

As was mentioned earlier, the polyphenylene dendrimers (PDs) possess unique features like the dimensionally stable inner cavities and control over the locations of the chain ends. The PDs are particularly interesting with respect to selective incorporation of guest molecules: the size of the inner cavities increases with the variable shapes of the core and with increasing generation number. However, the synthesis of PDs around various cores with branching unit **1.7** has been so far limited to the fourth generation^[35, 38] due to the de Gennes dense packing problem.^[43]

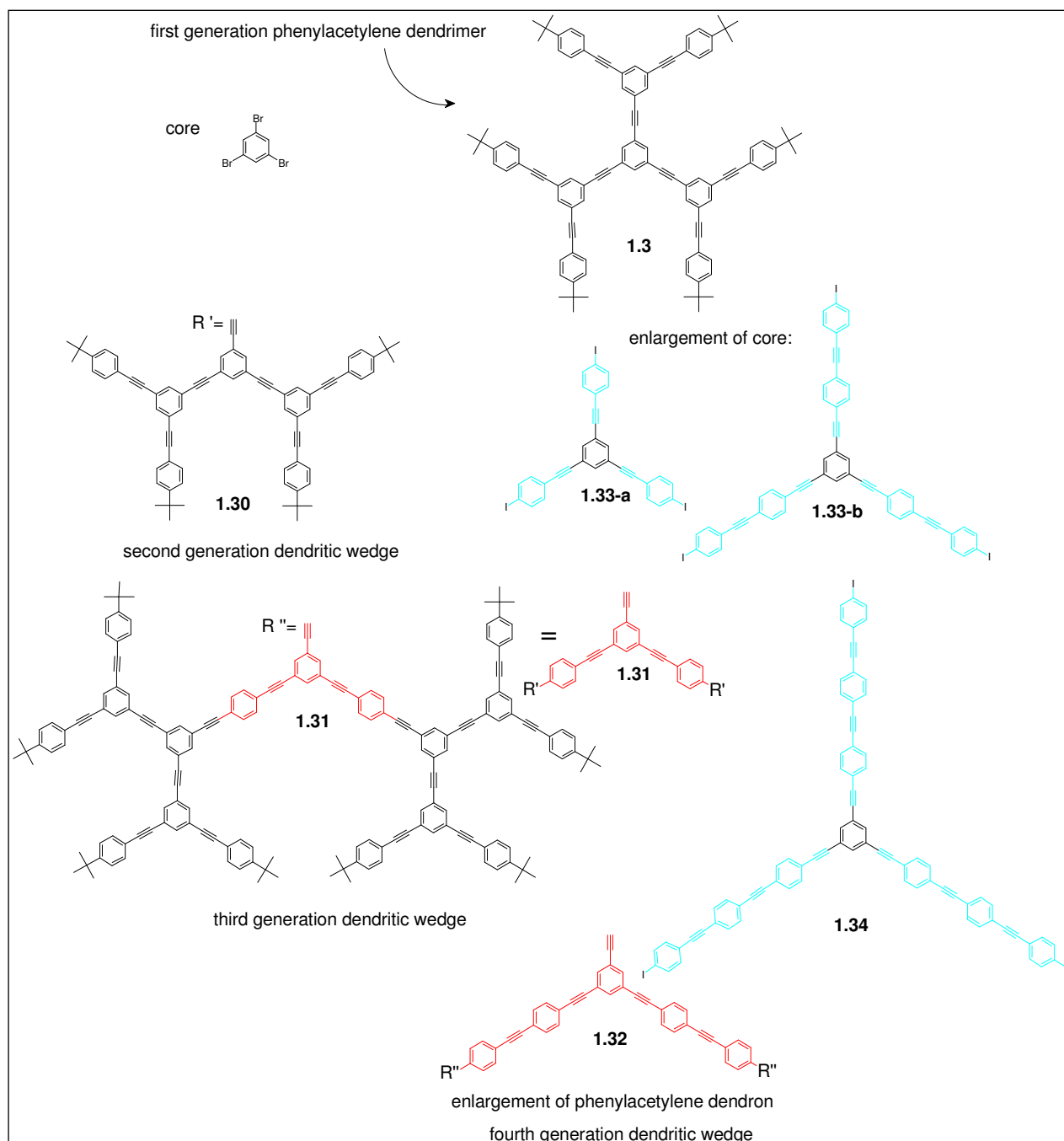
The same problem arose with other known rigid dendrimers, which were also synthesized up to the fourth generation only.^[17, 57, 58] Miller and Neenan prepared second-generation polyphenylene dendrimer **1.5** based on the 1,3,5-tri-substituted benzene core. This species contains 22 phenyl rings. To achieve a 46-phenylene dendrimer **1.29-a**, they extended the core **1.29-b** (Scheme 1.18).^[57]



Scheme 1.18: Enlargement of Miller-type dendrimers.

Other examples are the convergently prepared dendrimers by Moore and Xu. Their second-generation polyphenylacetylene dendritic wedge **1.30** (Scheme 1.19) was coupled to the core 1,3,5-tribromobenzene to form the second-generation phenylacetylene dendrimer. The third generation was realized by the use of an elongated monomer (red part of **1.31** in Scheme 1.19) indicating that increased spacer length should allow facile construction of large, rigid dendrimers.^[17, 58] Moore et. al. also employed the concept of dendritic spacer elongations in the construction of a series of polyphenylene cascades (enlargement of the dendritic wedge **1.32** and

the extended cores **1.33-a**, **1.33-b**, and **1.34**, Figure 1.6). Thus, the fourth-generation dendritic wedge (**1.32**) was coupled to the enlarged core (**1.34**) to generate 4th generation dendrimer with 12.5 nanometers in molecular diameter.^[5, 58]



Scheme 1.19: Enlargement of Moore-type dendrimers.

The method of avoidance of steric inhibition to dendritic construction through the use of increasingly longer spacer moieties gave rise to the acronym SYNDROME (SYNthesis of Dendrimers by Repetition Of Monomer Enlargement). These dendrimers are shape- and

dimension-persistent, which plays an important role in the development of molecular frameworks that require strict control of functional groups juxtaposition.^[5]

In the case of the polyphenylene dendrimers, steric hindrance may be prevented by the same strategy: either by extension of cores (Figure 1.6) or by introducing linear rigid arms into the branching unit **1.7** in the 3,4-position of 2,5-diphenylcyclopentadienone to generate a new extended branching unit **1.35** (Figure 1.6).

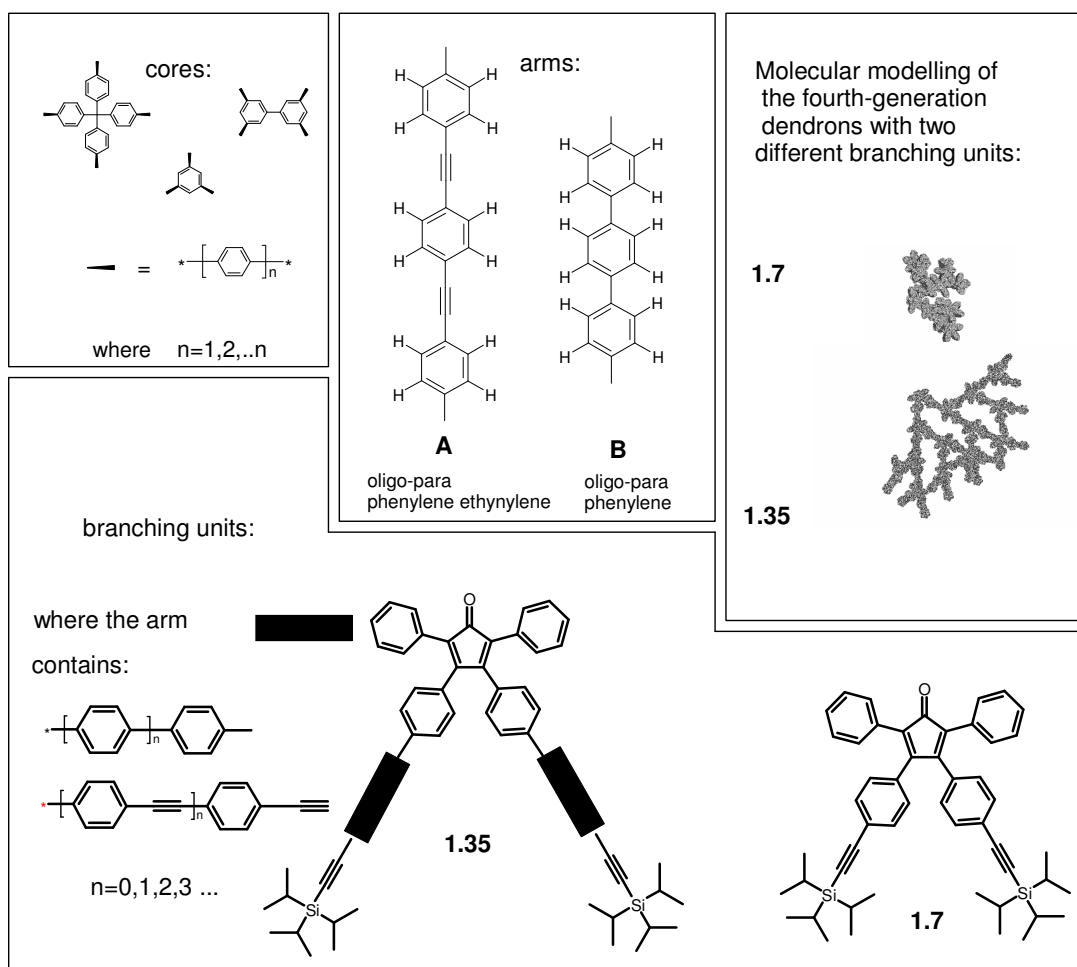


Figure 1.6: Sketch for the enlargement of Müllen-type dendrimers.

According to the molecular simulation, the enlargement of the core would not significantly increase the attainable generation number since steric hindrance arises mainly from the dendrons.^[35] (Space filling molecular modelling of the fourth-generation dendrons in Figure 1.6). On the contrary, the extension of the arm in the cyclopentadienone **1.35** should considerably decrease crowding in the 4th generation, relieving steric strain because the distance between arms in the dendrons on the surface is quite large. This should allow further additions of the extended branching unit **1.35** to form 5th, 6th or even higher generation dendrimers. The goal of the present

work is to create extremely large monodisperse polyphenylene dendrimers boasting diameters that exceed 20 nm or more. The tetraphenylmethane core is considered optimal, in order to generate PDs which display tetrahedral shape at the lower generations and approach spherical shape for higher generations. For this aim, it was decided to introduce the extended branching unit **1.35**. There are alternative approaches to synthesize the linear arm of **1.35** (**A** and **B** in Figure 1.6): either oligo-*para*-phenylene ethynylene (**A**) or oligo-*para*-phenylene (**B**) could be used as the enlargement. In the present dissertation, the preparation of hydrocarbon dendrimers will be extended to fifth- and sixth-generation specimen, which requires careful attention to the nature of the dendrons. In order to abate steric crowding at the periphery which would limit the accessible generation number, long extended arms based on oligo-*para*-phenylene units will be introduced leading to a class appropriately named “exploded dendrimers”. As an aside, these dendrimer should exhibit fairly large cavities which could serve one desired role of dendrimers, namely that of functioning as a host for guest molecules (Chapter 2).

An ideal component of a long extended arm would be the ethynylene unit. Therefore the latter will also be included into the dendrons. Among others, it offers the possibility of converting a rigid arm (alkyne-based) into a flexible arm (alkane-based) by means of dendrimer hydrogenation (Chapter 3). Whether this will be feasible is not immediately clear since the alkyne sites inside a dendrimer may not be accessible to a catalyst surface (heterogeneous hydrogenation).

1.12 Literature for Chapter 1

1. H. Staudinger. From Organic Chemistry to Macromolecules. **1970**, Wiley-Interscience: New York.
2. D.A. Tomalia. *Aldrichimica*. **2004**, 37, 2, 39-55.
3. J.M.J. Frechet; D.A. Tomalia. Dendrimers and other dendritic polymers. **2001**, John Wiley & Sons, Ltd.
4. a) P.J. Flory. Principles of Polymer Chemistry; Cornell University Press: Ithaca NY, **1953**;
b) P.J. Flory. *Am. Chem. Soc.* **1941**, 63, 3083. c) P.J. Flory. *Am. Chem. Soc.* **1952**, 74, 2718.
5. G.R. Newkome; C.N. Moorefields; F. Vögtle. Dendrimers and dendrons. **2001**, Wiley-VCH.
6. E. Buhleier; W. Wehner; F. Vogtle. *Synthesis-Stuttgart*. **1978**, 155-158.
7. R.G. Denkewalter; J.F. Kolc; W.J. Lukasavage. Macromolecular Highly Branched Homogenous Compound. U.S. Pat. 4.-410.688, **1983**.

8. M. Fischer; F. Vögtle. *Angew. Chem., Int. Ed. Engl.* **1999**, 38, 884-905.
9. U. Boas; P.M.H. Heegaard. *Chem. Soc. Rev.* **2004**, 33, 43-63.
10. P. Hodge. *Nature.* **1993**, 362, 18-19.
11. E.M.M. Brabander-van den Berg; E.W. Meijer. *Angew. Chem., Int. Ed. Engl.* **1993**, 32, 1308-1311.
12. C. Wörner; R. Mülhaupt. *Angew. Chem., Int. Ed. Engl.* **1993**, 32, 1306-1308.
13. a) D.A. Tomalia; H. Baker; J.R. Dewald; M. Hall; G. Kallos; S. Martin; J. Roeck; J. Ryder; P. Smith. *Polym. J.* **1985**, 17, 117-132. b) D.A. Tomalia. *Aldrichimica Acta.* **1993**, 26, 91-101.
14. G.R. Newkome; Z.Q. Yao; G.R. Baker; V.K. Gupta. *J. Org. Chem.* **1985**, 50, 2003-2004.
15. a) C.J. Hawker; J.M.J. Frechet. *J. Am. Chem. Soc.* **1990**, 112, 7638-7647. b) C.J. Hawker; J.M.J. Frechet. *Chem. Soc., Chem. Commun.* **1990**, 1010-1013.
16. T.M. Miller; T.X. Neenan. *Chem. Mater.* **1990**, 2, 346-349.
17. a) Z.F. Xu; J.S. Moore. *Angew. Chem., Int. Ed. Engl.* **1993**, 32, 1354-1357. b) J.S. Moore; Z. Xu. *Macromolecules.* **1991**, 24, 5893-5894.
18. a) G.J. Capitosti; C.D. Guerrero; D.E. Binkley, Jr.; C.S. Rajesh; D.A. Modarelli. *J. Org. Chem.* **2003**, 68, 247-261; b) A. Herrmann; T. Weil; V. Sinigersky; U.-M. Wiesler; T. Vosch; J. Hofkens; F.C. De Schryver; K. Müllen. *Chem. Eur. J.* **2001**, 22, 4844; c) K.L. Wooley; C.J. Hawker; J.M.J. Frechet. *J. Am. Chem. Soc.* **1991**, 113, 4252-4261; d) Z. Xu; M. Kahr; K.L. Walker; C.L. Wilkins; J.S. Moore. *J. Am. Chem. Soc.* **1994**, 116, 4537-4550; e) T. Kawaguchi; K.L. Walker; C.L. Wilkins; J.S. Moore. *J. Am. Chem. Soc.* **1995**, 117, 2159-2165; f) Y. Hirayama; Y. Sakamoto; K. Yamaguchi; S. Sakamoto; M. Iwamura. *Tetradendron Letters.* **2005**, 46, 1027-1030; g) G.M. Dykes; L.J. Brierley; D.K. Smith; P.T. McGrail; G.J. Seeley. *Chem. Eur. J.* **2001**, 7, 4730; h) T. Kawaguchi; K.L. Walker; C.L. Wilkins; J.S. Moore. *J. Am. Chem. Soc.* **1995**, 117, 2159-2165.
19. a) V. Maraval; R. Laurent; B. Donnadieu; M. Mauzac; A.-M. Caminade; J.-P. Majoral. *J. Am. Chem. Soc.* **2000**, 122, 2499-2511; b) M.-L. Lartigue, B. Donnadieu, C. Galliot, A.-M. Caminade, J.-P. Majoral. *Macromolecules.* **1997**, 30, 7335-7337.
20. G. Caminati; D.A. Tomalia. *J. Am. Chem. Soc.* **1990**, 112, 8515-8522.
21. B. Klajnert; M. Bryszewska. *Acta Biochimica Polonica.* **2001**, 48, 1, 199-208.
22. a) J.M.J. Frechet. *Science.* **1994**, 263, 170-1715; b) J.M.J. Frechet, C.J. Hawker, I. Gitsov, J.W. Leon. *J.M.S. – Pure Appl.Chem.* **1999**, A33 (10), 1399.
23. T.H. Mourey; S.R. Turner; M. Rubenstein; J.M.J. Frechet; C.J. Hawker; K.L. Wooley. *Macromolecules.* **1992**, 25, 2401-2406.

24. A. de Padua; J.A. de Miranda-Neto; I.M. Xavier, Jr.; F. Moraes. *J. Mathematical Chemistry*. **1997**, 22, 97-106
25. D.A. Tomalia; A.M. Naylor; W.A. Goddard III. *Angew. Chem. Int., Ed. Engl.* **1990**, 29, 138-175.
26. R.L. Lescanes; M. Muthukumar. *Macromolecule*. **1990**, 23, 2280-2288.
27. M.L. Mansfield; L.I. Klushin. *Macromolecules*. **1993**, 26, 4262-4268.
28. M. Murat; G.S. Grest. *Macromolecules*. **1996**, 29, 1278.
29. D. Boris; M. Rubinstein. *Macromolecules*. **1996**, 29, 7251-7260.
30. H. Hart. *Pure Appl. Chem.* **1993**, 65, 27-34.
31. T.M. Miller; T.X. Neenan. *J. Amer. Chem. Soc.* **1992**, 114, 1018-1025.
32. T.M. Miller; T.X. Neenan; H.E. Bair. *Polym. Prepr.* **1991**, 32, 627-628.
33. a) F. Morgenroth; E. Reuther; K. Müllen. *Angew. Chem., Int. Ed. Engl.* **1997**, 36, 631. b) F. Morgenroth; C. Kubel; K. Müllen. *J. Mater. Chem.* **1997**, 7, 1207-1211.
34. U.-M. Wiesler, K. Müllen. *J. Chem. Soc. Chem. Commun.* **1999**, 2293-2294.
35. U.-M. Wiesler; A.J. Berresheim; F. Morgenroth; G. Lieser; K. Müllen. *Macromolecules*. **2001**, 34, 187-199.
36. a) W. Dilthey; W. Schommer; H. Dierichs; O. Trösken. *Chem. Berichte*. **1933**, 66, 1627; b) W. Dilthey; G. Hurtig. *Chem. Berichte*. **1934**, 67, 2004.
37. P. Brocorens; E. Zojer; J. Cornil; Z. Shuai; G. Leising; K. Müllen; J.L. Bredas. *Synth. Met.* **1999**, 100, 141.
38. U.-M. Wiesler; T. Weil; K. Müllen. *Topics in Current Chemistry*, Vol. 212; Springer Verlag, Berlin-Heidelberg **2001** (F. Vögtle. *Dendrimers III. Design, Dimension, Function*).
39. S. Rosenfeldt; N. Dingenouts; D. Pötschke; M. Ballauff; A.J. Berresheim; K. Müllen; P. Lindner. *Angew. Chem., Int. Ed. Engl.* **2004**, 43, 109-112.
40. K. Müllen; F. Morgenroth. *Tetrahedron*. **1997**, 53, 15349-15366.
41. S. Roselfeldt; N. Dingenouts; Ballauff; N. Werner; F. Vögtle; P. Lindner. *Macromolecules*. **2002**, 35, 8098-8105.
42. a) I.O. Götze; C.N. Likos. *Macromolecules*. **2003**, 36, 8189-8197; b) H.M. Harreis; C.N. Likos; M. Ballauf. *J. of Chem. Phys.* **2003**, 118, 1979-1988.
43. P.G. de Gennes; H. Hervet. *J. Phys. (Paris)*. **1983**, 44, L351-L360.
44. a) R.E. Bauer. Ph-D dissertation, University of Mainz, **2005**; b) T. Weil. Ph-D dissertation, University of Mainz, **2001**; c) T. Weil; U.-M. Wiesler; A. Hermann; R. Bauer; J. Hofkens; F.C. De Schryver; K. Müllen. *J. Am. Chem. Soc.* **2001**, 123, 8101-8108.

45. A.C. Grimsdale; R. Bauer, T. Weil; N. Tchegotareva; J. Wu; M. Watson; K. Müllen. *Synthesis-Stuttgart*. **2002**, 9, 1229-1238.
46. M.P. Stevens. *Polymer chemistry*. **1999**, Oxford University Press.
47. U.-W. Wiesler. Ph-D dissertation, University of Mainz, **2000**.
48. a) L.H. Bryant; M.W. Brechbiel; C. Wu; J.W.M. Bulte; V. Herynek; J.A. Frank. *J. Magn. Reson. Imaging*. **1999**, 9, 348-352. b) M.W. Bourne; L. Margerun; N. Hylton; B. Campion; J.J. Lai; N. Derugin; C.B. Higgins. *J. Magn. Reson. Imaging*. **1996**, 6, 305-310.
49. a) M.F. Hawthorne. *Angew. Chem., Int. Ed. Engl.* **1993**, 32, 950-984, b) R.F. Barth; D.M. Adams; A.H. Soloway; F. Alam; M.V. Darby. *Bioconjug. Chem.* **1994**, 5, 58-66. c) L. Liu; R.F. Barth; D.M. Adams; A.H. Soloway. *Hematotherapy*. **1995**, 4, 477-483. d) J. Capala; R.F. Barth; M. Bendayam; M. Lauson; D.M. Adams; A.H. Solowaya; R.A. Fenstermaker; J. Carlsson. *Bioconjug. Chem.* **1996**, 7, 7-15.
50. D.A. Tomalia; P.R. Dvornic. *Nature*. **1994**, 617-618; and references herein.
51. a) J.F.G.A. Janssen; E.M.M. de Brabander-van den Berg; E.W. Meijer. *Science*. **1994**, 266, 1226-1229. b) G.R. Newkome; C.N. Moorefield; G.R. Baker; M.J. Saunders; S.H. Grossman. *Angew. Chem., Int. Ed. Engl.* **1991**, 30, 1178-1180.
52. J.W.J. Knapen; A.W. van der Made; J.C. de Wilde; P.W.N.M. van Leeuwen; P. Wijkens; D.M. Grove; G. van Koten. *Nature*. **1994**, 372, 659-660.
53. M. Bardaji; M. Kustos; A.-M. Caminade; J.-P. Majoral; B. Chaudret. *Organometallics*. **1997**, 16(3), 403-410.
54. a) A.M. Herring; B.D. Steffey; A. Miedaner; S.A. Wander; D.L. DuBois. *Inorg. Chem.* **1995**, 34, 1100-1109, b) A. Miedaner; C.J. Curtis; R.M. Barkley; D.L. DuBois. *Inorg. Chem.* **1994**, 33, 5482-5490.
55. A.I. Cooper; J.D. Londono; G. Wignall; J.B. McClain; E.T. Samulki; J.S. Lin; A. Dobrynin; M. Rubinstein; A.L.C. Burke; J.M.J. Frechet; J.M. Desimone. *Nature*. **1997**, 389, 368-371.
56. G. Mihov; I. Scheppelmann; K. Müllen. *J. Org. Chem.* **2004**, 69, 8029-8037 and their references.
57. T.M. Miller; T.N. Neenan; R. Zayas; H.E. Bair. *J. Amer. Chem. Soc.* **1992**, 114, 1018-1025.
58. Z. Xu, K.L. Walker; C.L. Wilkins; J.S. Moore. *J. Am. Chem. Soc.* **1994**, 116, 4537-4550.

2 Extended Arm Polyphenylene Dendrimers

2.1 Introduction

In this chapter the synthesis of novel dendrimers possessing very long arms as part of the dendrons will be explored. The arm **A** (Figure 1.6, Chapter 1) in which the benzene rings are separated by alkyne units possesses two advantages over the terphenyl arm **B**: (1) For the same number of phenyl rings, the length of arm **A** considerably exceeds that of arm **B**. This should effect less pronounced crowding at the dendrimer surface, (2) The separation of neighbouring benzene rings by the intervening triple bond eliminates *ortho-ortho* hydrogen compression strain. Therefore momentary conformations in which neighbouring benzene rings are coplanar will be tolerated. This will effect the π -conjugation in the arm **A** compared to **B**.

Since the synthesis of an extended arm **1.35** (Chapter 1) bearing more than 3 *para*-phenylene units is a demanding task, a terphenyl segment was selected in which triple bonds were inserted between every phenylene pair. Therefore, a new branching unit with the tris-(*para*-phenylene ethynylene)-arm **2.1** (Scheme 2.1, Chapter 2.2) was initially chosen as an extended arm.

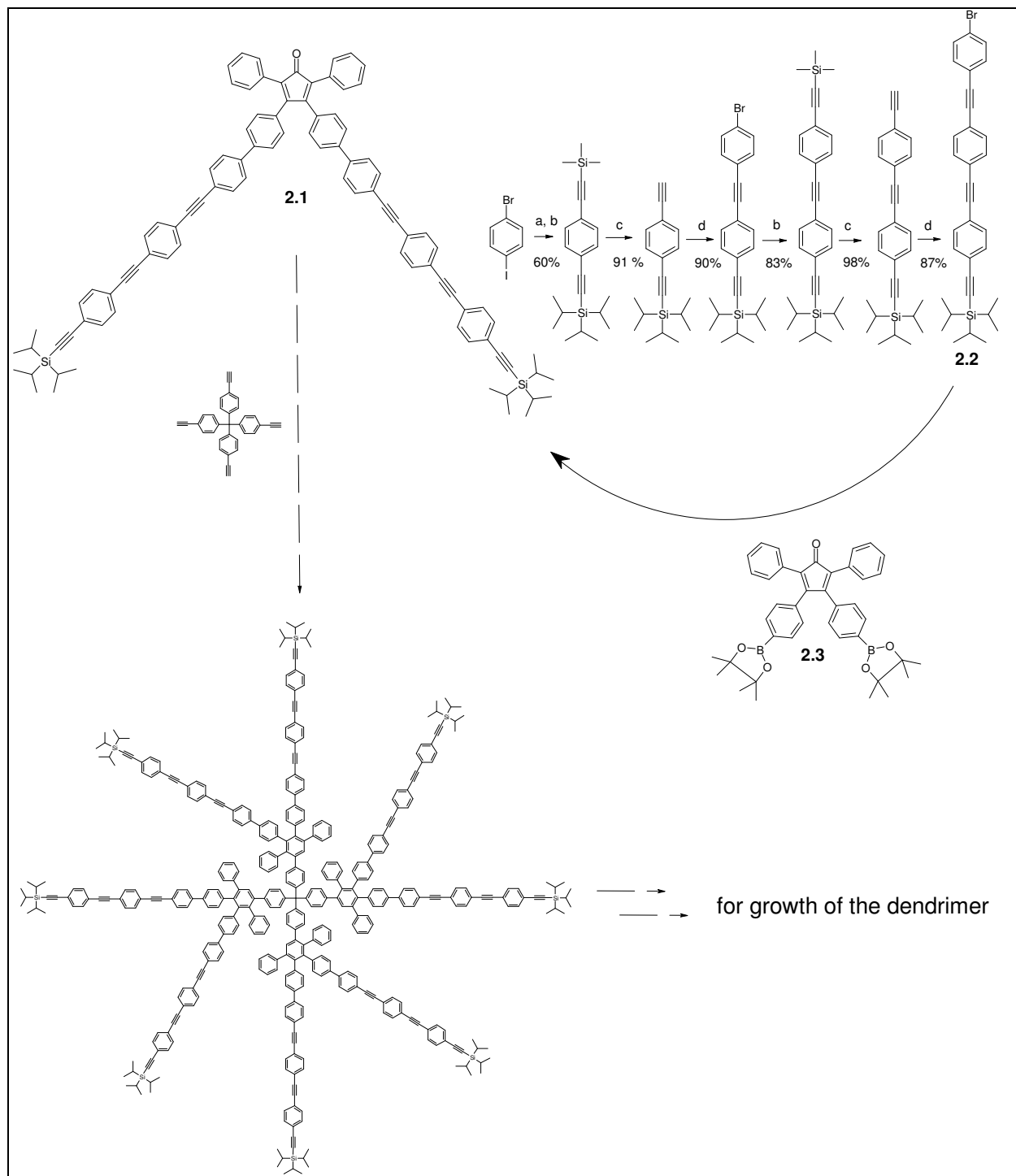
2.2 Synthesis of the new branching unit **2.1** bearing tris-(*para*-phenylene ethynylene)-arms

As shown in Scheme 2.1, the synthesis of the extended branching unit **2.1** consists of the seven-step preparation of the arm **2.2** via a sequence of Sonogashira-Hagihara coupling and subsequent alkynyl-deprotection steps, and the final Suzuki-coupling of **2.2** to 3,4-bis[4-(4,4,5,5-tetramethyl-1,3,2-dioxaborolan-2-yl)phenyl]-2,5diphenylcyclopentadienone (**2.3**).^[1]

This latter synthesis was accompanied by the formation of the side product from mono-substitution of cyclopentadienone, which arose from de-boronation, typically during the Suzuki coupling.^[2]

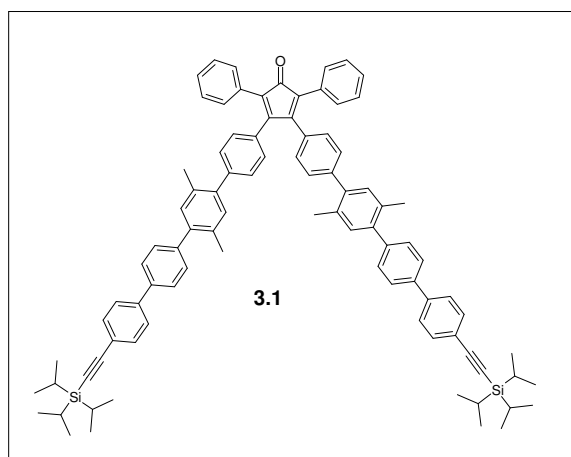
The crude material **2.1** was subjected to purification both by flash column chromatography and size exclusion chromatography (SEC). In all cases the product **2.1** contained 5-7% impurity, purification was impeded by the strong interaction of **2.1** with silica gel during

column chromatography. Therefore, all efforts for a complete purification failed. This prevented the use of **2.1** for the synthesis of dendrimers.



Scheme 2.1: Synthesis of the new branching unit **2.1** bearing tris-(*para*-phenylene ethynylene)arms; a) ^[3a] HC≡CSi(*i*Pr)₃, CuI, PPh₃, Pd(PPh₃)₂Cl₂, piperidine, 24 h, rt; b) ^[3a] HC≡CSi(CH₃)₃, CuI, PPh₃, Pd(PPh₃)₂Cl₂, piperidine, 15 h, 60 °C; c) ^[3a, 3b] K₂CO₃, MeOH, THF, 4 h, rt; d) ^[3c, 3d] 1-bromo-4-iodobenzene, CuI, PPh₃, Pd(PPh₃)₂Cl₂, THF, NEt₃, 24 h, rt.

Because of the aforementioned purification problem, the branching unit **2.1** was replaced by a new one **3.1** (Scheme 2.2). In the building block **3.1** two triple bonds are absent, i.e. there is a conversion of tris-(*para*-phenylene ethynylene) arm into a *para*-quaterphenylene arm which bears a terminal alkynyl unit only. The absence of triple bonds was expected to decrease the strong interaction of **3.1** with silica gel in the column chromatography, thus rendering purification possible.



Scheme 2.2: The proposed new extended branching unit possessing quaterphenylene ethynyl arms.

2.3 Synthesis of the new extended arm branching unit **3.1**

Before engaging in experimental details, it is worth while to contemplate about the effect, extremely long rigid arms will have on the structure of the resulting dendrimers. This can be profitably done by the comparison of dendrimers with two different branching units, **1.7** and **3.1**. Their images were generated by programs Spartan and POV-Ray. The maximum radius was taken as the length of the longest, linear oligophenylene arm for each generation measured from the centre of core to the outermost phenyl-H atom, using Spartan Pro with the molecular force field MMFF (see Chapter 2.10). These radii are listed in Table 2.1. From Figure 2.1 and Table 2.1, it is seen that the expected radii of extended arm dendrimers using the new branching unit **3.1** are more than twice as large as those with the branching unit **1.7** in the respective generations. Blue colour on the surface of dendrimer indicates the functional groups, red colour points towards the branching units inside the dendrimer. The fourth generation with building block **1.7** has higher density on the surface (blue colour is

predominantly seen, while fourth-generation dendrimer (G4-Td) with the new building block **3.1** has comparatively low density up to G7 (red colour is predominantly seen).

Table 2.1 Calculated radii (in nm) of two different dendrimer types:

Type of dendrimers	Number of generations					
	G1	G2	G3	G4	G5	G6
"exploded" dendrimers (with new branching unit, 3.1)	2.7	4.8	6.9	9.1	11.2	13.4
general polyphenylene dendrimers (with branching unit 1.7)	1.3	2.2	3.0	3.8	-	-

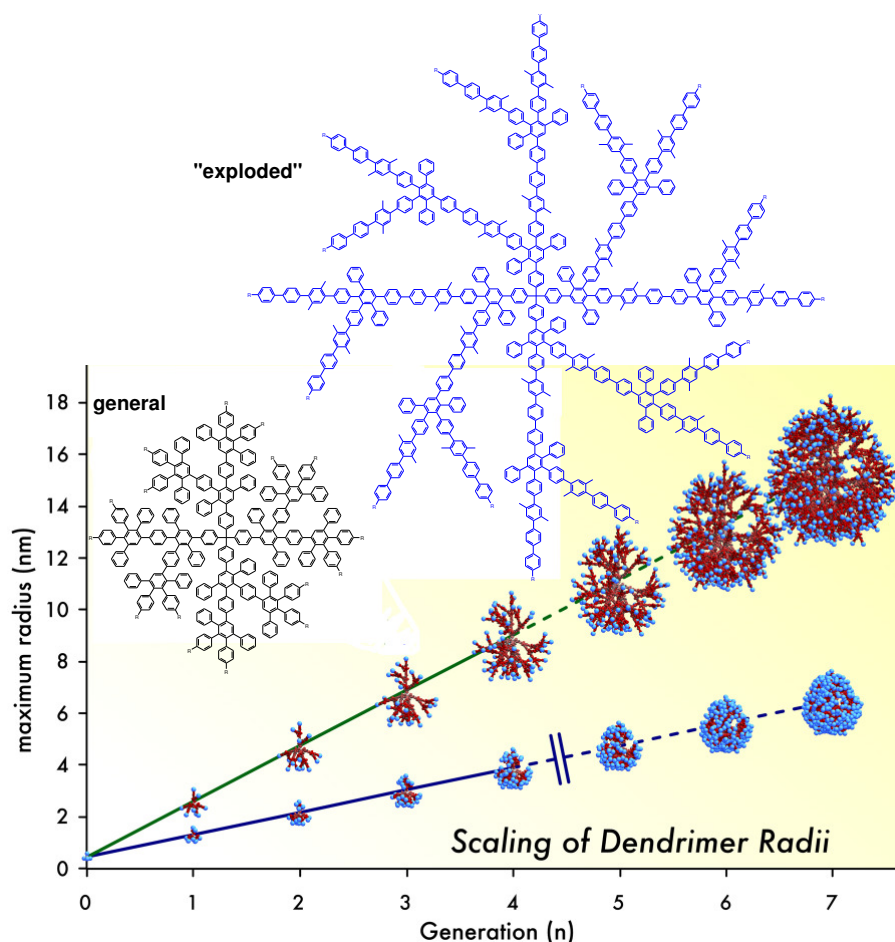
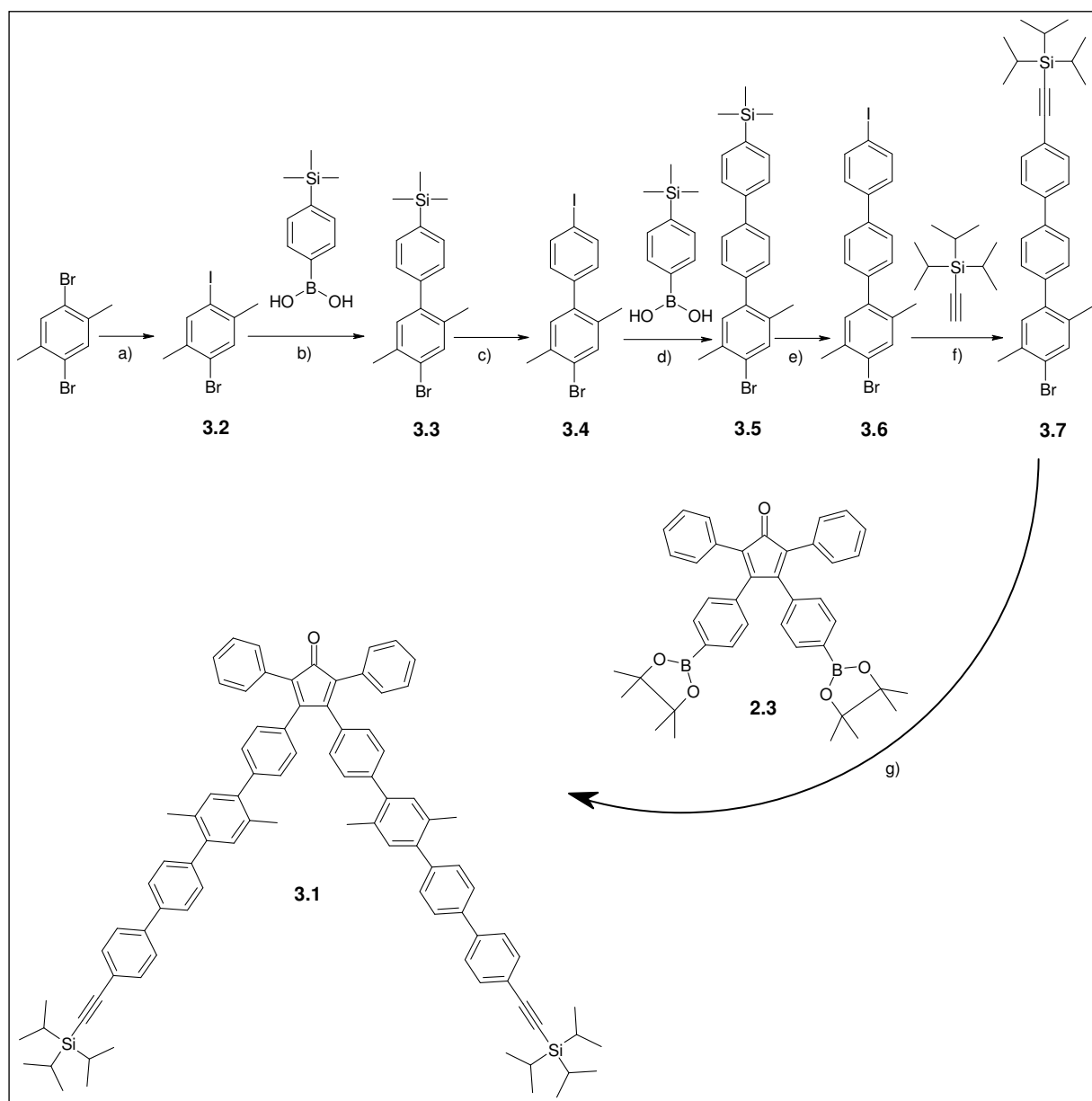


Figure 2.1: Comparison of size and shape for general and extended polyphenylene dendrimers. (Courtesy C. Clark, Jr., the illustrations were generated by the programs Spartan and POV-Ray).

According to molecular modelling, it should therefore be possible to extend the approach to the G6 and G7 dendrimers because of low steric hindrance at the periphery. Dendrimers with the new branching unit **3.1** will be called extended or "exploded", those with the branching unit **1.7** are named general or ordinary.



Scheme 2.3: Synthesis of the extended arm branching unit **3.1**: a) *n*-BuLi, THF, -80 °C, ICH₂CH₂I, 65%; b) K₂CO₃, Pd(PPh₃)₄, toluene, water, reflux, 62%; c) ICl, CCl₄, CH₂Cl₂, 0 °C, 96%; d) K₂CO₃, Pd(PPh₃)₄, toluene, water, ethanol, reflux, 83%; e) ICl, CH₂Cl₂, 0 °C, 87%; f) PdCl₂(PPh₃)₂, CuI, PPh₃, NEt₃, CH₂Cl₂, 80%; g) K₂CO₃, Pd(PPh₃)₄, toluene, water, ethanol, reflux, 48%.

Scheme 2.3 depicts the synthesis of the new building block **3.1**, which contains three additional *para*-phenylene units at the 3,4 positions of 2,5 diphenylcyclopentadienone. This new branching unit is called “extended”.

The synthesis starts from commercially available 1,4-dibromo-2,5-dimethyl-benzene. The methyl groups were included to increase the solubility of the *para*-terphenylene unit **3.6**. In the first step an exchange of one bromine atom by iodine to form 1-bromo-4-iodo-2,5-methylbenzene (**3.2**) permits formation of an unsymmetrically substituted biphenyl derivative **3.3** by means of Suzuki coupling, since the cross-coupling proceeds with very high selectivity at C-I over C-Br^[4] to generate the product **3.3** in high purity. The unsymmetrical *para*-phenylene derivative **3.4** forms after an exchange of the protecting trimethylsilyl group **3.3** by iodine.^[5] Suzuki coupling of **3.4** with 4-trimethylsilylphenylboronic acid gives the next unsymmetrically substituted terphenyl derivative **3.5**. For another C-TMS/C-I conversion dichloromethane was used as a better solvent instead of tetrachloromethane to yield **3.6**. Using common solvents such as THF, toluene or piperidine for the Sonogashira-Hagihara reaction the formation of **3.7** was impossible: compound **3.6** failed to react even after 3 days. However, dichloromethane as a solvent yielded **3.7** in 12 hours in 80% yield. Like the Suzuki reaction, the Sonogashira-Hagihara reaction also selectively proceeded at the C-I position.^[3-a] All reactions exhibited good to excellent yield. The molecule **3.1** was synthesized via Suzuki coupling of the new arm **3.7** and 3,4-bis[4-(4,4,5,5-tetramethyl-1,3,2-dioxaborolan-2-yl)phenyl]-2,5diphenylcyclopentadienone^[1] (**2.3**) in a yield of 48% only. The only fair yield may be traced (1) to the fact that two consecutive reactions are involved, each contributing with its inherent yield, (2) to the large, functionalized nature of the building blocks and (3) to the possibility of partial deboronation, competing with C-C coupling. Non-optimal yields in the preparation of branching units, based on Suzuki coupling, have been encountered previously in our group.^[9b, 9c]

The new cyclopentadienone **3.1** showed a single peak in its mass spectrum with a mass 1258 g/mol which agreed with the calculated molecular mass. Furthermore, ¹H and ¹³C NMR spectra, HPLC, FDMS and elementary analysis proved the purity of compound **3.1**. The presence of methyl groups in the branching unit **3.1** accords with the ¹H NMR (Figure 2.2) and H-H COSY NMR spectra (Figure 2.3). The ¹H NMR spectrum showed two peaks ($\delta=2.32$ and 2.26 ppm) which can be assigned to the two methyl groups. The H-H COSY NMR spectrum agreed with the presence of a quaterphenyl arm, one phenylene group being

substituted in the 2,5-positions by two methyl groups. A full assignment of all protons was not feasible, however.

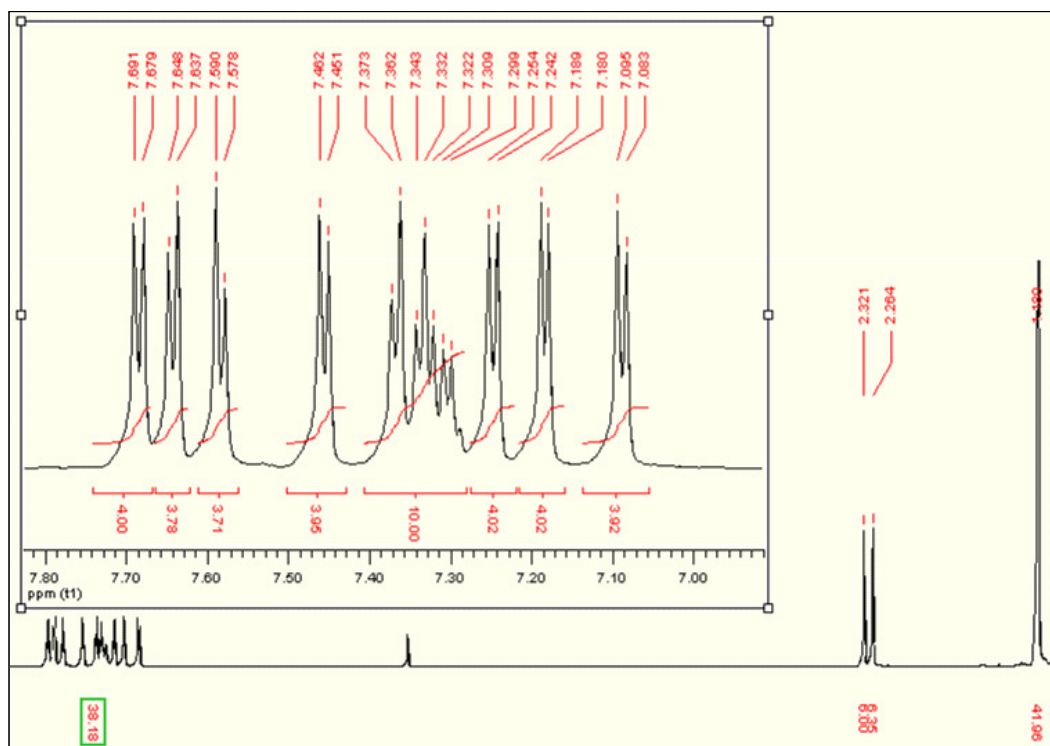


Figure 2.2: ^1H NMR spectrum of **3.1** (60 mg) in 1 ml CD_2Cl_2 , 700 MHz, r.t.

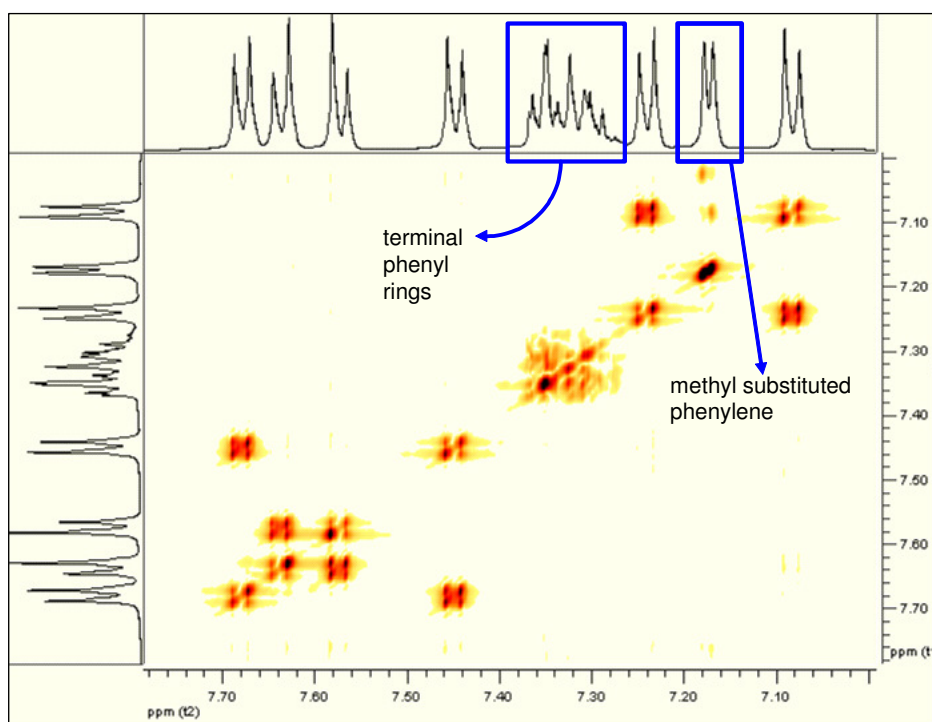


Figure 2.3: H-H COSY NMR spectrum of the extended branching unit **3.1**, CD_2Cl_2 , 500 MHz, r.t.

2.4 Synthesis of "exploded" dendrimers up to the sixth generation

The synthesis of new polyphenylene dendrimers is outlined in Schemes 2.4-2.5 and is based on the divergent method. The first step involved the Diels-Alder coupling of the tetra-(4-ethynylphenyl)methane core (**1.10**) with an excess of the extended arm cyclopentadienone **3.1** (1.3 equivalent of **3.1** per one ethynyl group) to yield a first-generation dendrimer bearing eight TiPS protecting groups (**3.8**). The removal of excess **3.1** was accomplished by means of column chromatography. Compound **3.8** was identified by the MALDI TOF technique. Its spectrum is presented in Figure 2.4, which showed a single peak (calcd. 5444, found 5443) and confirmed its monodispersity: a potential defect, resulting from incomplete [2+4] cycloaddition during dendrimer growth, would have been detected because each un-reacted ethynyl group of the core results in a mass difference of 1230. ^1H NMR spectra, an additional tool, confirmed the absence of the signal from the ethynyl groups ($-\text{C}\equiv\text{CH}$).

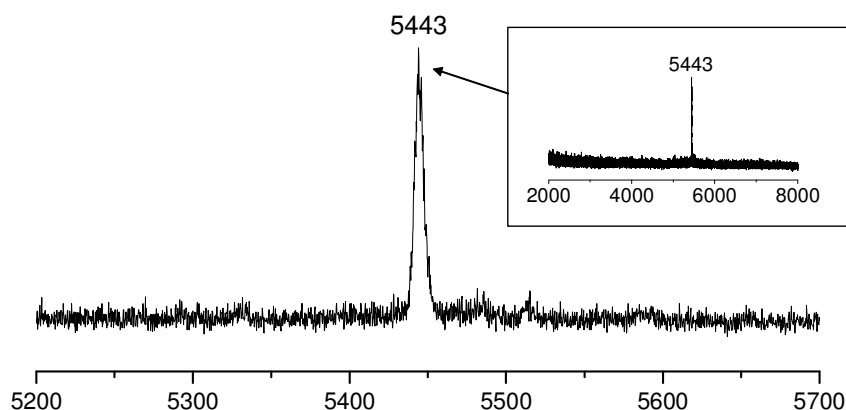
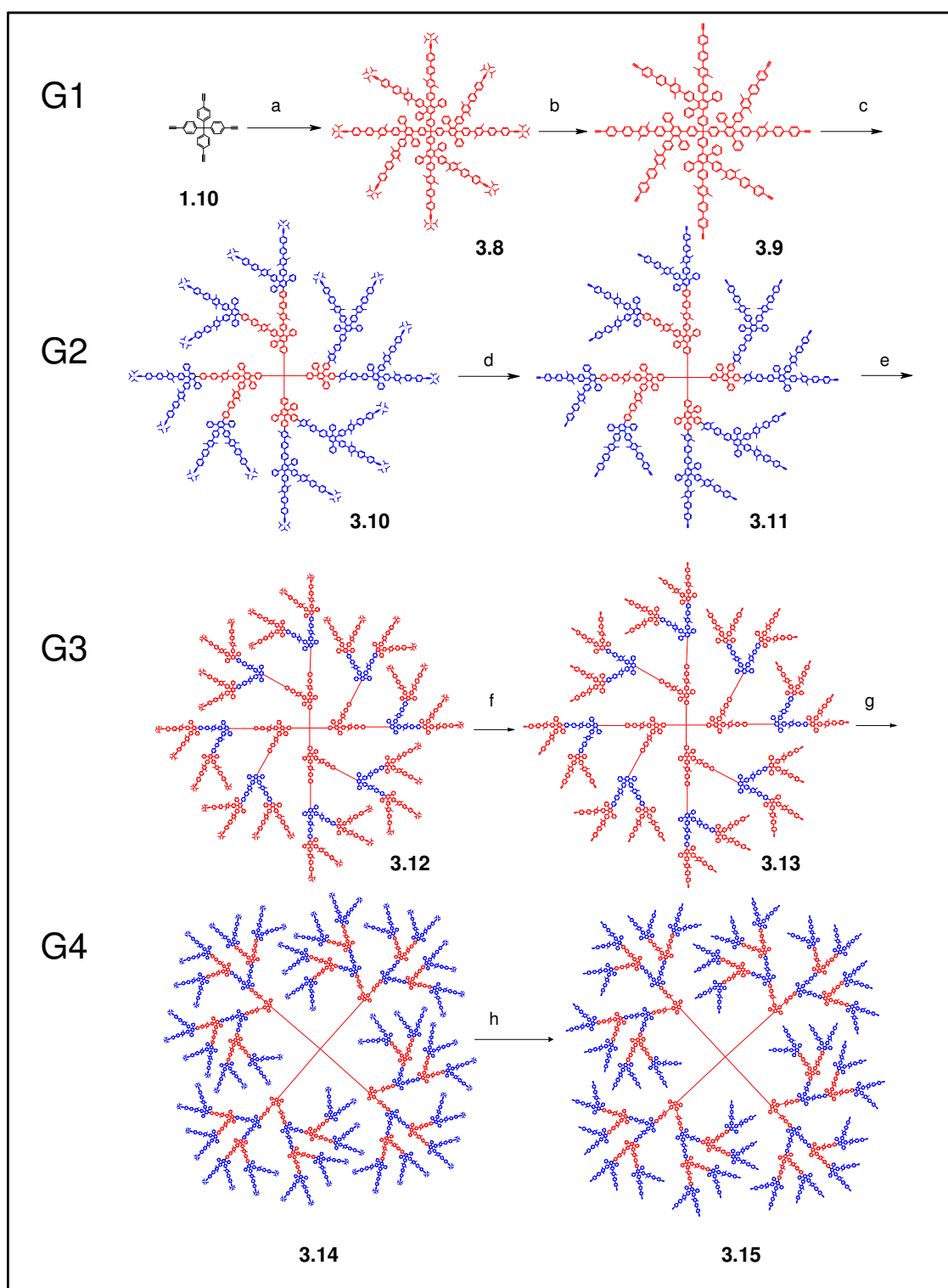


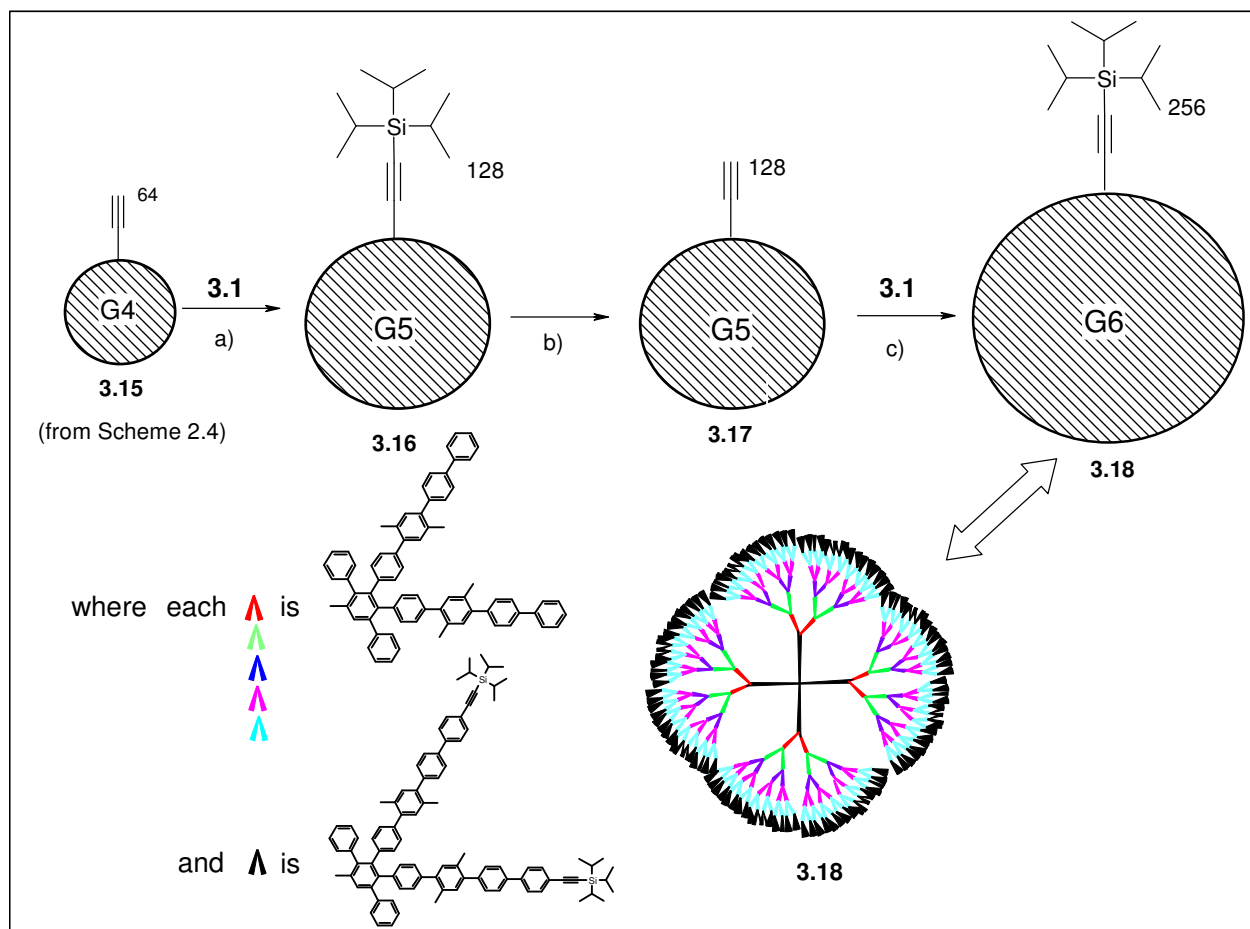
Figure 2.4: MALDI-TOF MS of the first-generation dendrimer **3.8** (reflector mode, Ag^+).

The removal of the TiPS groups by tetrabutylammoniumfluoride trihydrate (TBAF) gave the first-generation dendrimer with eight terminal ethynyl units, **3.9**. Compound **3.9**, after quenching with water and precipitation into methanol, was ready for subsequent dendrimer growth. The cycle was repeated through the fifth-generation dendrimer **3.16**, and a final coupling yielded the sixth-generation dendrimer **3.18** (Scheme 2.5).

The synthesis of extended G2-G6 dendrimers with TiPS groups (**3.10**, **3.12**, **3.14**, **3.16** and **3.18**) via Diels-Alder cycloaddition was carried out in refluxing *o*-xylene. The excess of the branching unit **3.1** was increased with growing generation number (1.5 eq. of **3.1** per 1 ethynyl group of **3.9** to form **3.10**; and 4 eq. of **3.1** per 1 ethynyl group of **3.17** to obtain **3.18**).



Scheme 2.4: Synthesis of first- through fourth-generation extended dendrimers with a tetraphenylmethane core: a), c), e), g) **3.1**, *o*-xylene, reflux; b), d), f), h) tetrabutylammonium fluoride trihydrate, THF, r.t.; a) 85%, b) 76%, c) 96%, d) 75%, e) 87%, f) 75%, g) 75%, h) 86%.



Scheme 2.5: Synthesis of fifth- and sixth-generation dendrimers, a), c) *o*-xylene, reflux; b) tetrabutylammonium fluoride trihydrate, THF, r.t.; a) 65%, b) 58%, c) 75%.

The separation of G2-G6 with *TiPS* groups (**3.10**, **3.12**, **3.14**, **3.16** and **3.18**) from the excess of building unit **3.1** was carried out in the following way: after cooling to room temperature, the reaction mixture was concentrated *in vacuo* (the maximum amount of *o*-xylene was evaporated) and the residue was dropped into acetone. The precipitate was collected by filtration and was loaded onto a layer of silica (1x1 cm), washed with acetone until the filtrate remained colourless. The stationary phase was dried and extracted with THF. The THF solution was filtered and concentrated to a viscous solution (1-2 mL) and dropped into acetone. After filtration, the solid was washed with acetone, methanol and dried *in vacuo* to yield the dendrimers.

The complete removal of the *TiPS* protecting groups for all dendrimers in the series which gave **3.9**, **3.11**, **3.13**, **3.15** and **3.17** required no more than 1 hour. Synthetic details for all compounds are given in the Experimental Section. All new dendrimers **3.8-3.18** are soluble in

common solvents, such as THF, dichloromethane, tetrachloroethane, and insoluble in acetone, methanol, nonpolar solvents as hexane, pentane.

To characterize these dendrimers, analytical methods, such as MALDI-TOF MS and NMR spectroscopy were applied. To get an idea of their sizes and shapes, molecular modelling, dynamic light scattering and direct visualization method such as transition electron microscopy (TEM) and atomic force microscopy (AFM) were used. All of these methods and their results are presented in the following paragraphs.

2.5 MALDI-TOF MS applied to the extended dendrimers

All dendrimers up to the fourth generation (**3.8-3.15**) were characterized by the MALDI-TOF mass spectrometry. The MALDI-TOF mass spectra were recorded by two techniques: reflector and linear mode. In the case of lower generation dendrimers, the instrument with the reflector mode was used. For higher generation dendrimers the linear mode was employed, as typical for other dendrimers.^[6] The single peak of the new species G1-Td-(TiPS)₈ (**3.8**) from the reflector MS is shown in Figure 2.4 with high resolution, the width of the peak is 11 Da. It confirms the purity of the dendrimer, since side products were not observed.

The MALDI-TOF MS of the extended G2-Td-(TiPS)₁₆ (**3.10**) recorded in both modes are depicted in the Figure 2.5 (A, B). In the reflector mode a single peak was observed, its width is rather narrow, about 30 Da, thus confirming the monodispersity of **3.10**. It was noticed that in the linear mode there are peaks pointing to the presence of dimer, trimer, tetramer, pentamer etc. This indicates clustering, a phenomenon interesting in itself (see below), which occurs during the MALDI-TOF measurement.^[7, 8] Monodispersity is also supported by the SEC data obtained for **3.10** which show a monomodal elution peak (Figure 2.18). It was observed, that in the linear mode, the width of peak of **3.10** with molecular mass (M) 13935 Da is about 400 Da. With increasing M the width of peaks increases as well. However, thanks to the reflector measurement, it is clear that the extended dendrimer G2-Td-(TiPS)₁₆ (**3.10**) is monodisperse. The double measurements (reflector and linear modes) were observed only for the compound **3.10**. The peaks of the higher generation dendrimers (**3.11-3.15**) could be detected only in the linear mode. MALDI-TOF MS of the deprotected second generation dendrimer **3.11** (Figure is not shown here) exhibited gas-phase clusters up to octamers (as

well as in the case of **3.10** in Figure 2.5-B) where the molecular ion is the base peak with the non-specific aggregates (dimer, trimer, tetrameric etc.) decreasing in intensity exponentially. The same phenomenon was observed with other types of dendrimers^[8, 9a] where the highly branched very open architecture of the dendrimers suggests that the cluster formation may occur through an interlocking of the branches of the dendrimers in a type of host-guest linking^[8] in the gas-phase.

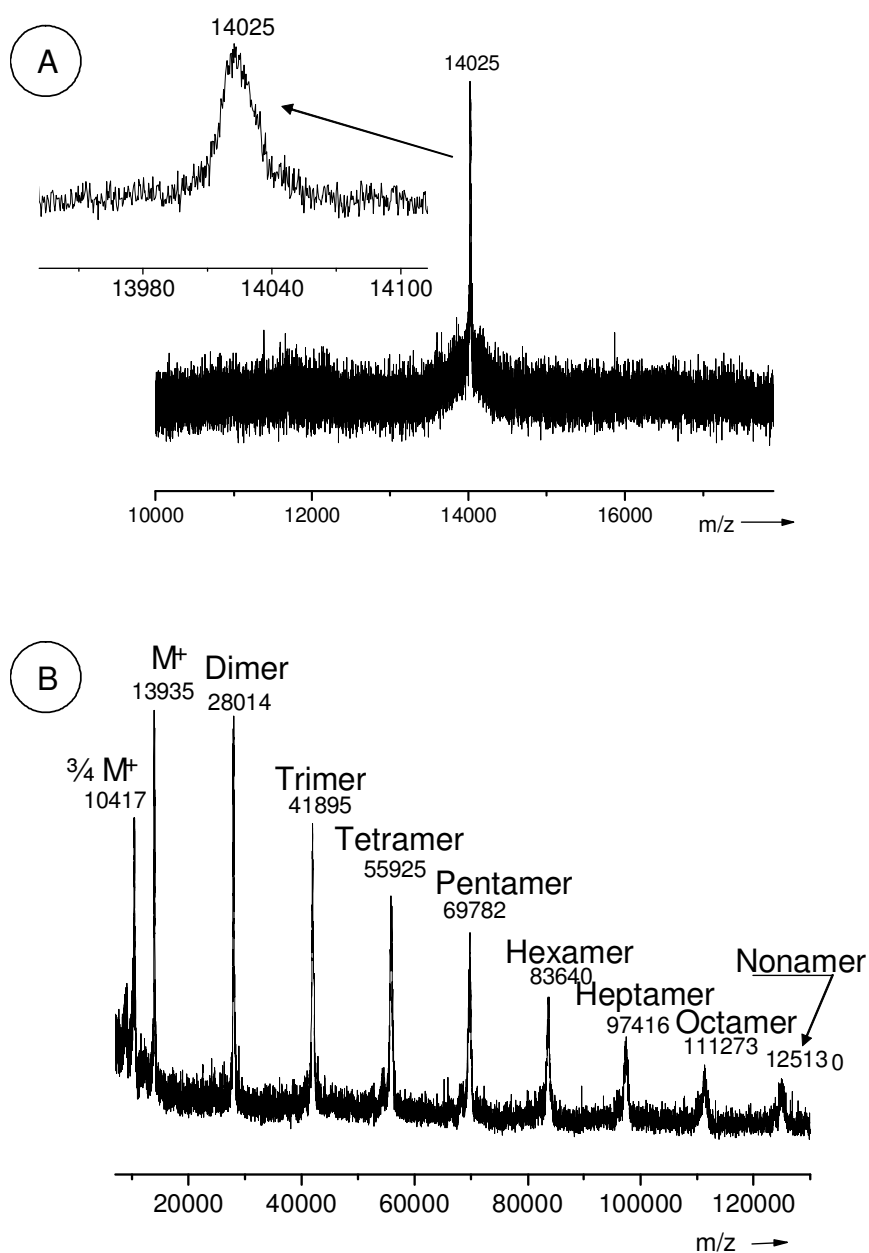


Figure 2.5: MALDI-TOF MS (in Da) of second-generation dendrimer **3.10** with TiPS protecting groups in different modes; **A** - reflector mode, Ag^+ ; **B** - linear mode, K^+ .

MALDI-TOF MS of the third-generation dendrimers **3.12** (Figure 2.6, calcd: 31102, found 31168) and **3.13** (not shown here) gave single peaks, where their molecular masses are in good agreement with the theoretical ones. Fortunately, the width of the peaks ranges within 470-570 Da, which is much less than the mass difference of potential defects (1230 Da).

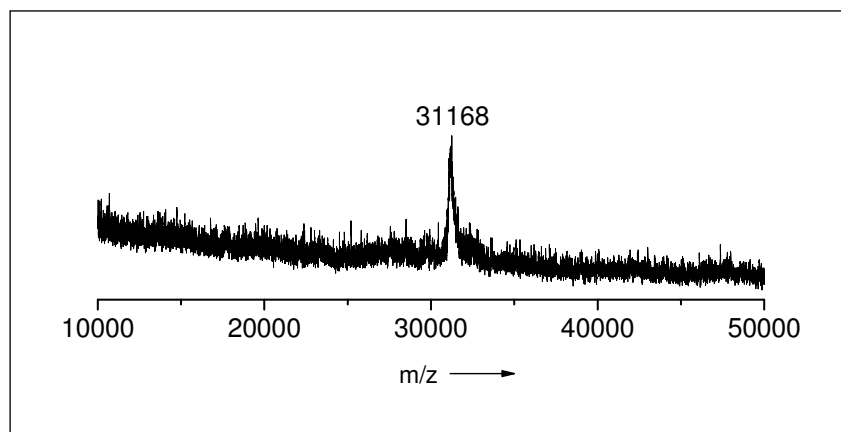


Figure 2.6: MALDI-TOF MS of third-generation dendrimer with 32 TiPS groups, **3.12** (linear mode, dithranol, without salt).

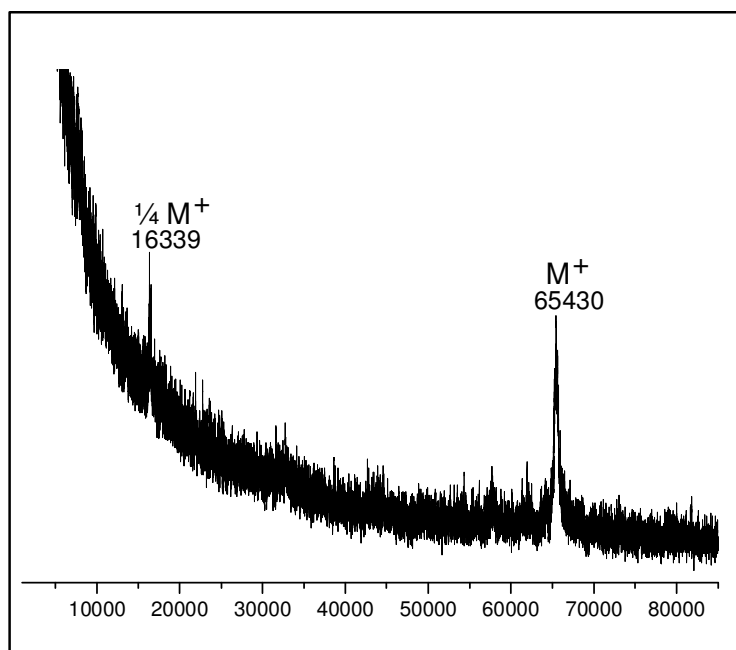


Figure 2.7: MALDI-TOF mass spectrum (dithranol, K^+) of G4 (**3.14**).

Figure 2.7 depicts the MALDI-TOF MS of the exploded dendrimer G4-Td-(TiPS)₆₄ (**3.14**), where in addition to the molecular ion (calcd 65495, found 65430), a fragmentation at the core was also observed (calcd 16370, found 16339). This fragmentation mechanism, where one dendron is removed from the core, has typically been observed for polyphenylene dendrimers bearing a tetraphenylmethane core.^[9a]

The G4-deprotected dendrimer **3.15** (Figure 2.8, calcd 55450, found 55539) was the last molecule in the synthesis of the exploded dendrimers, whose peak could be detected in the MALDI-TOF spectrum as a single ion.

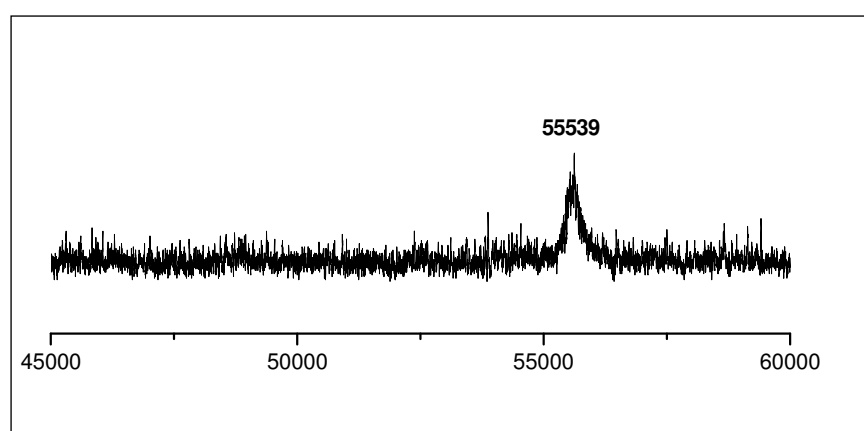


Figure 2.8: MALDI-TOF MS of fourth-generation dendrimer with 62 ethynyl groups, **3.15** (linear mode, without salt).

For the extended dendrimer G5-Td-(TiPS)₁₂₈ (**3.16**), using dithranol as matrix, no ions could be observed in the MALDI-TOF spectrum. However, using (2-[(2*E*)-3-(4-*tert*-butylphenyl)-2-methylprop-2-enylidene]malononitrile (DCTB)^[10] as a matrix and sufficient laser power, many peaks were detected. Among these peaks a weak signal for the molecular ion (calcd. 134162, found 135290) was found (Figure 2.9).

In general there are two suggestions for the formation of the multitude of fragments: 1) the fifth generation was not synthesized quantitatively and 2) fragmentation of dendrimer by laser energy takes place.

The first suggestion seems improbable, because it is evident that **3.16** was formed exclusively since 128 TiPS groups are seen in the ¹H NMR spectrum (Figure 2.15) in the correct relative intensity with regard to the expected alkyl/aryl ratio (more details in paragraph 2.6).

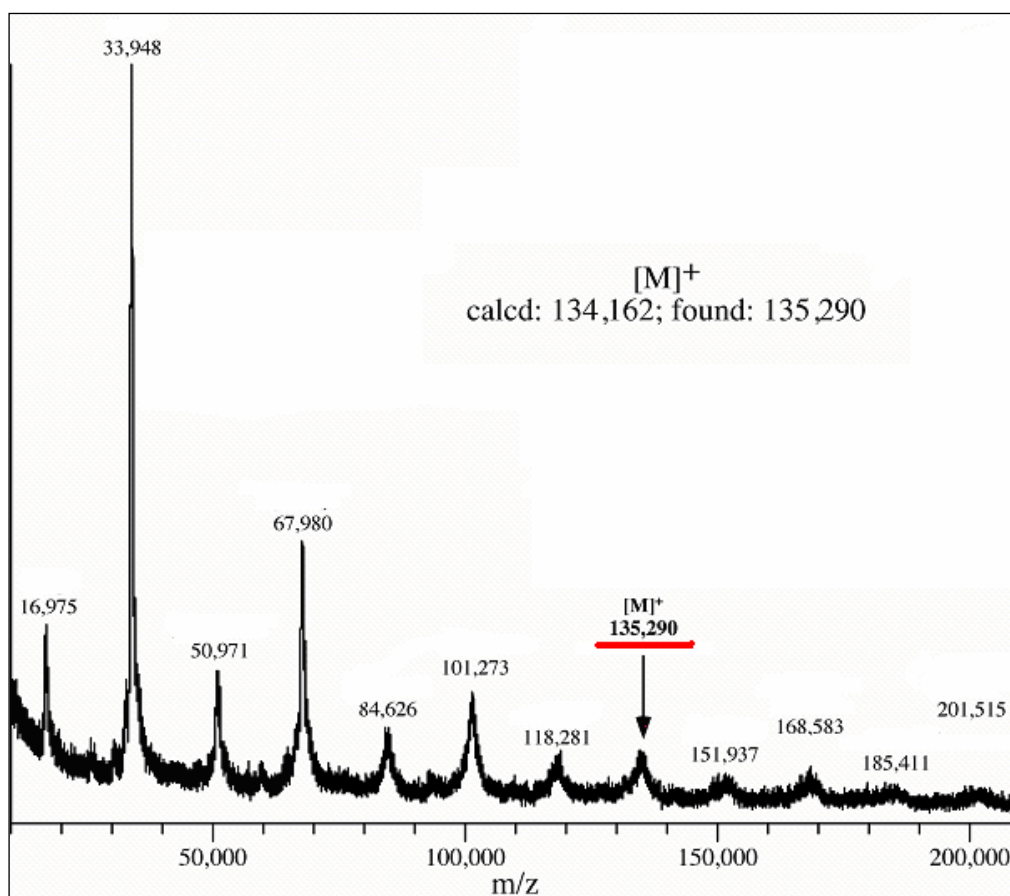


Figure 2.9: MALDI-TOF mass spectrum (DCTB) of G5-Td-(TiPS)₁₂₈ (**3.16**): where 16975 is $\frac{1}{8} M^+$; 33948 = $\frac{1}{4} M^+$; 50971 = $\frac{1}{4} M^+ + \frac{1}{8} M^+$; 67980 = $\frac{1}{2} M^+$; 84626 = $\frac{1}{2} M^+ + \frac{1}{8} M^+$; 101273 = $\frac{3}{4} M^+$; 118281 = $\frac{3}{4} M^+ + \frac{1}{8} M^+$; 135290 = M^+ ; 151937 = $M^+ + \frac{1}{8} M^+$; 168583 = $\frac{3}{4} M^+ + 2 (\frac{1}{8} M^+)$; 185411 = $M^+ + 3 (\frac{1}{8} M^+)$; and 201515 = $M^+ + 4 (\frac{1}{8} M^+)$.

Moreover, peaks at 16 975, 33 948 and 50 971 Da should have originated from the fragmentation of **3.16** during the ionization process because no elution peaks were detected at the lower molecular weight region in SEC analysis (Figure 2.18). Therefore, one can safely assume that degradation occurs during MALDI measurements, in the course of sample preparation or during and/or after UV laser irradiation. Degradation consecutive to laser irradiation is more likely.

UV spectra of **3.16** dendrimer showed broad absorption band between 258-345 nm with a peak maximum at 300 nm (Figure 2.10).

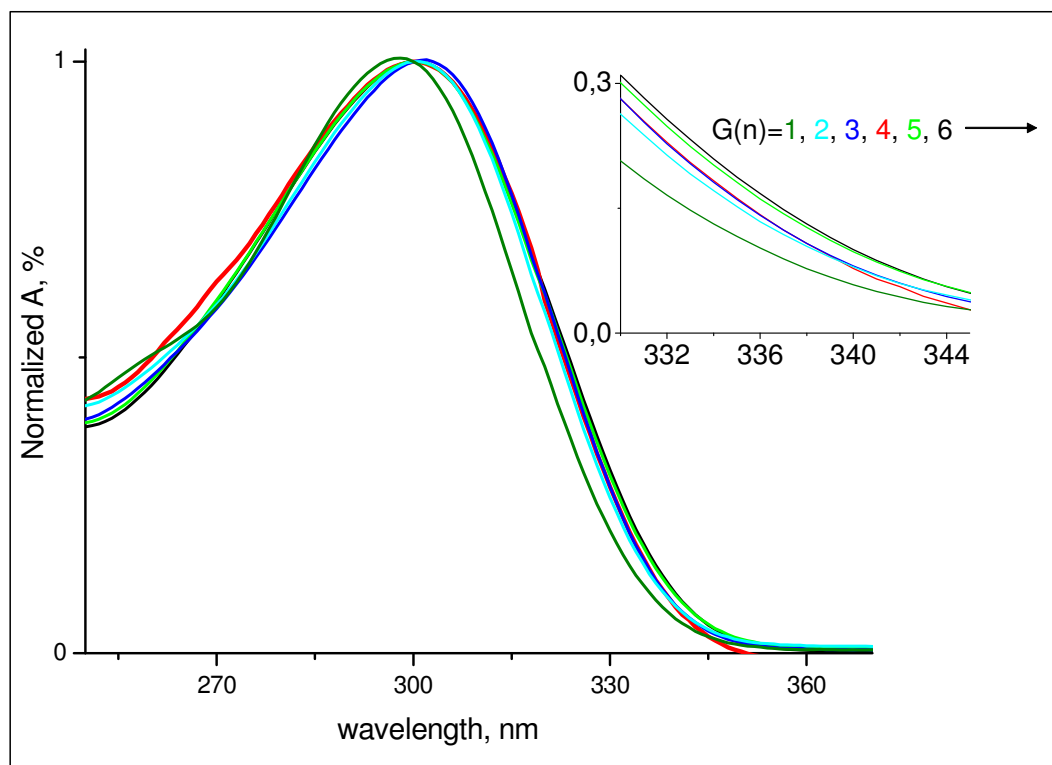


Figure 2.10: UV-vis spectra of extended G1-G6 dendrimers (**3.8**, **3.10**, **3.12**, **3.14**, **3.16**, and **3.18**) in dichloromethane

UV-vis spectra of G1-G6 (**3.8-3.18**) in dichloromethane shift gradually towards higher wavelength with increasing generation (Figure 2.10). The UV-Vis spectra of the dendrimer **3.16** showed a broad absorption band between 258-345 nm with a maximum peak at 300 nm. Therefore, when the pulsed laser beam from MALDI-TOF instrument (337 nm) hits the analyte, molecule **3.16** absorbs energy. Accordingly in the MALDI-TOF technique, laser ionization may cause the dissociation of the dendrimer **3.16**. Some bonds in **3.16** may be broken because of a) stabilization of fragments by resonance and b) metastability of ion. As there is no strong parent peak at 135 kDa, the sample apparently fragmented into species $\frac{3}{4} M^+$, $\frac{1}{2} M^+$, $\frac{1}{4} M^+$, $\frac{1}{8} M^+$. These fragments then can recombine forming new peaks (for example, $M^+ + \frac{1}{8} M^+$, $\frac{1}{2} M^+ + \frac{1}{8} M^+$). They all attest to the formation of **3.16** in the original synthesis.

Increasing the relative amount of the matrix, the use of soft laser power, or the introduction of cationization agents did not improve the signal intensity of the molecular ion.

Similar fragmentations of triazine dendrimers by Takagi et. al.^[11] and higher generations of phosphorus-containing dendrimers by Majoral et. al.^[12] were observed, where fragmentations also occurred due to the relatively strong absorption of the dendrimers in the range of the wavelength of the laser. The molecular peaks of extended G5-Td-(ethynyl)₁₂₈ **3.17** and G6-Td-(TiPS)₂₅₆ **3.18** were not observed in MALDI-TOF MS.

Although dendrimer chemistry is now highly developed, the molecular masses of the largest dendrimers escaped detection by the MALDI-TOF technique. For example, in the case of giant organo-silicon dendrimers up to ninth generation (with M=177 147 Da), MALDI-TOF measurement was recorded only up to fourth generation with mass 108 664 Da.^[13] Another report presented spherical cyclophosphazene dendrimers up to the fifth generation with M=1832 420 Da; however, mass spectroscopy was useful up to second generation only.^[14]

In the case of PAMAM dendrimers, the molecular masses of the highest generation numbers, generating highly multiply charged ions, were measured by Electrospray Ionization Mass Spectrometry (EI MS).^[15] We did not use this method for our exploded type dendrimers, as these species consist of non-charged polyphenylenes. The characterization of Majoral's giant phosphorus-containing dendrimers (highest generation number G-12 with theoretical molecular mass 3 030 289 Da) had to rely on other methods, such NMR, IR spectroscopy, elemental analysis, TEM, and AFM.^[16-17]

As mentioned earlier, the peak of **3.18** with molecular mass higher than 260 kDa was not seen in the MALDI-TOF technique in our institute, because microchannel plates (MCP) in this MALDI-TOF spectrometry are used as a detector. This most standard ion detector is known to suffer from a considerable decrease in sensitivity for large ion masses.^[18] MCPs depend on secondary electron emission, which becomes increasingly inefficient as molecular mass increases and impact velocity decreases. They can now be replaced by cryogenic detectors, that spot large, slow-moving ions or neutrals with 100 % efficiency.^[18]

A very recent paper reported initial results from the first commercially available MALDI-TOF mass spectrometer with a superconducting tunnel junction detector (STJ).^[19] This detector technology measures the kinetic energy of the particles impacting the detector, which can be correlated to the charge of the particles. The new equipment was able to analyze high-mass proteins within the mega Dalton range. This work points to the potential of detecting molecular ions of extremely high mass; however, the authors stated that there are still many

unanswered questions. For example, the ionization of high-mass molecules without fragmentation or dissociation has proven challenging, high-mass calibrants and matrixes are also not well developed.

In collaboration with the Zenobi group (ETH Zurich), the exploded dendrimers G4-Td-(TiPS)₆₄ (**3.14**), G5-Td-(TiPS)₁₂₈ (**3.16**) and G6-Td-(TiPS)₂₅₆ (**3.18**) were studied by means of MALDI-TOF MS equipment with a STJ detector.

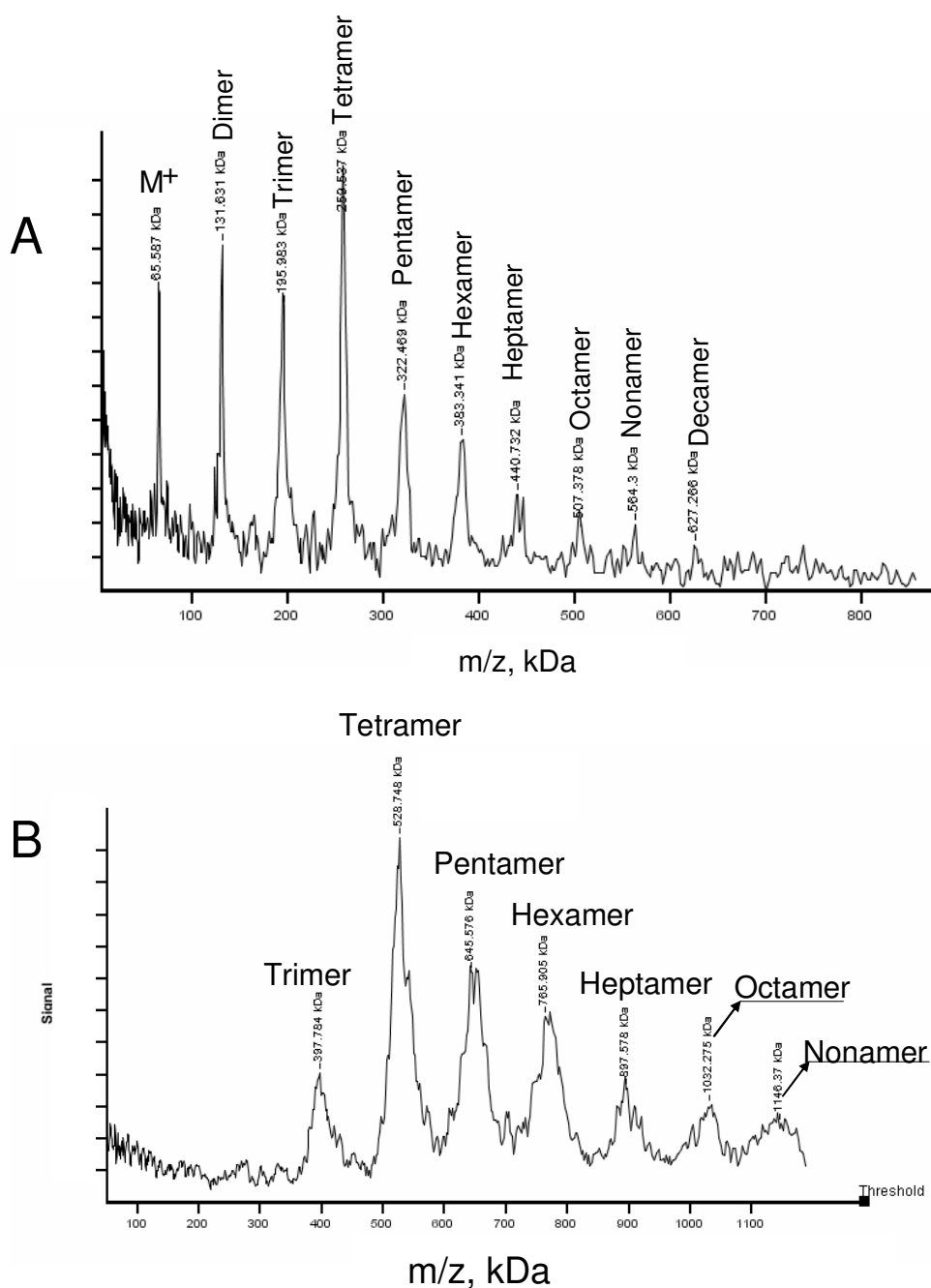


Figure 2.11: **A** - MALDI-TOF MS with STJ detector for G4-Td-(TiPS)₆₄ (**3.14**), and **B** - MALDI-TOF MS with STJ detector for G5-Td-(TiPS)₁₂₈ (**3.16**).

The following sample preparation proved to be optimal, the best condition for the preparation was optimized: the analyte (approximately 0.1 mg) was dissolved in a mixture of 0.25 mol/L dithranol and 0.025 mol/L potassium acetate in THF, then this mixture was diluted ten-fold by addition of THF. The results are depicted in Figures 2.11- 2.12. For G4-Td-(TiPS)₆₄ (**3.14**), signals appear which pertain to the monomer at 65.6 kDa and to oligomers at higher masses (Figure 2.11-A).

No monomer peaks were found for both G5-Td-(TiPS)₁₂₈ (**3.16**) (Figure 2.11-B) and G6-Td-(TiPS)₂₅₆ (**3.18**) (Figure 2.12), however there were peaks corresponding to trimers up to nonamers for **3.16** and tetramer up to heptamers for **3.18**. The strongest peaks of **3.14**, **3.16**, and **3.18** were observed for the tetramers (250 kDa, 529 kDa, and 1024 kDa respectively).

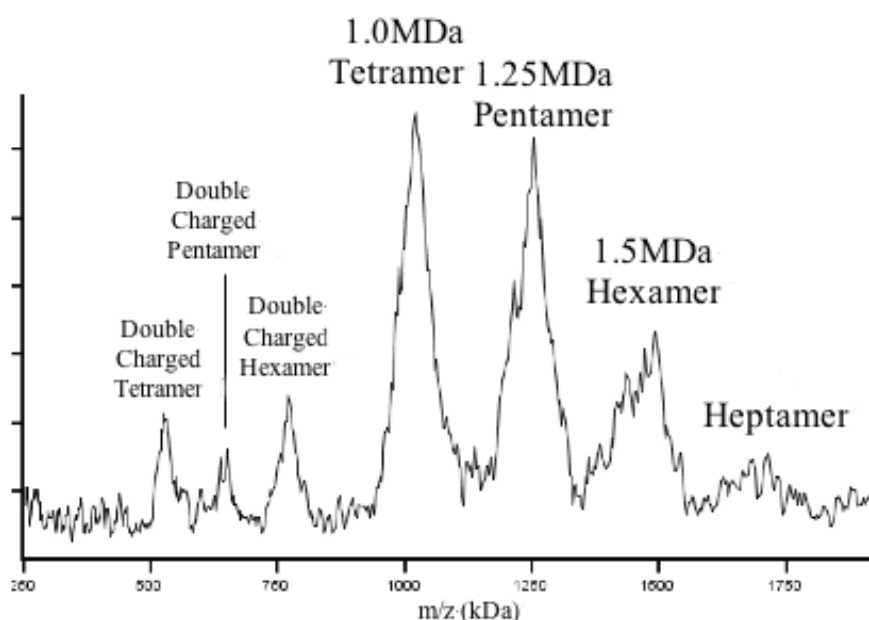


Figure 2.12: MALDI-TOF MS with STJ detector for G6-Td-(TiPS)₂₅₆ (**3.18**).

From Figure 2.13 we see that with the increasing of the molecular masses (increasing of the number of the oligomers), their observed molecular masses increasingly deviate from the calculated molecular masses (see comparison between red and black lines). For example, a found molecular mass (65.6 kDa) of the monomer G4 matched the calculated one (65.5 kDa), however, the found molecular mass of its decamer (507 kDa) is lower than the calculated (524 kDa). It is worth to stress, that the calculated molecular masses of hexamer for G4 (393 kDa) and trimer for G5 (402 kDa) are similar (A₄ and A₅, Figure 2.13), but their found molecular

masses are lower and the difference between the calculated/found masses are randomly different: 9.4 kDa for A₄ and 4.7 kDa for A₅. Analogously, with the calculated masses of B₄, B₅, and B₆ (524 kDa, 537 kDa, and 543 kDa respectively), their found masses are lower than the expected ones by the amounts of 16 kDa, 8 kDa, and 15 kDa respectively. The comparison of the others oligomers with different dendrimers are listed in the Table 2.2.

It confirms that the accuracy in the case of high masses is lower than in the case of the lower molecular masses. Thus, based on this observation, we could not expect to obtain the exact peak of tetramer for sixth generation (E₆). As its monomer was not detected, its experimental molecular mass was computed by dividing the mass of tetramer (1086 kDa) to get 256 kDa. This result falls short of the calculated mass (271.6 kDa) by 15.5 kDa. As was mentioned earlier, the calibration for such high masses is still not well developed, leaving open many questions. However, from the Table 2.2 it is clear, that the value of the differences between the calculated and found masses is not strictly dependent on the molecular masses. There should be other instrumental factors such as calibration, width of the peaks, and therefore limited resolution.

Table 2.2: Differences between calculated M and found M from MALDI-TOF MS with STJ detector:

	(Calc. M in kDa), $\Delta = M_{\text{calcd.}} - M_{\text{found}}$ (unit of kDa); number of point from Figure 2.13				
G4, 3.14	(393) $\Delta=9$; A ₄	(524) $\Delta=16$; B ₄			
G5, 3.16	(402) $\Delta=4.7$; A ₅	(537) $\Delta=8$; B ₅	(671) $\Delta=25$; C ₅	(805) $\Delta=39$; D ₅	(1073) $\Delta=41$; E ₅
G6, 3.18		(543) $\Delta=15$; B ₆	(679) $\Delta=26.7$; C ₆	(815) $\Delta=41$; D ₆	(1086) $\Delta=62$; E ₆

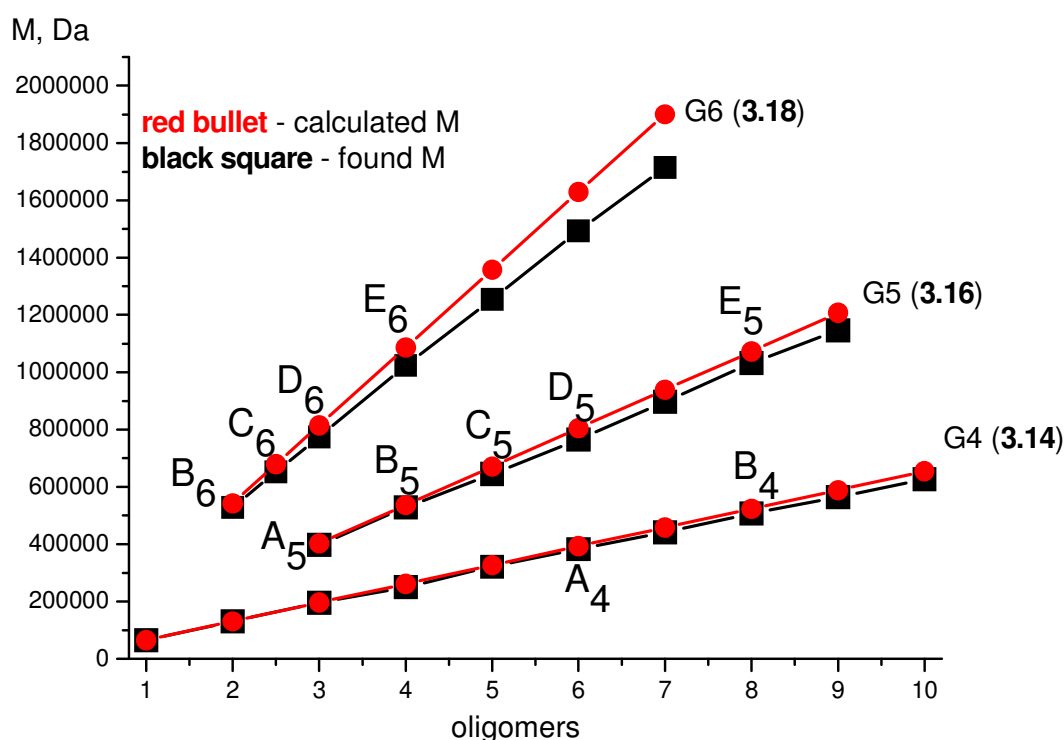


Figure 2.13: Comparison of the differences between the calculated molecular mass (M) and found M from MALDI-TOF MS with STJ detector for G4-G6 dendrimers (**3.14**, **3.16**, and **3.18**).

At this point, as the molecular masses of the new exploded dendrimers **3.8-3.18** seem to be well established, judging from the MALDI-TOF data, it is instructive to put the results into perspective. Particularly, it is illuminating to compare the molecular masses of the exploded type with those of more conventional type for each generation number. This is done diagrammatically in Figure 2.14.

It is seen that the extended arm dendrimers experience an enormous mass increase per generation added, i.e. the mass/generation number curve has a very steep slope. Clearly, decreased steric hindrance of the extended arm favours the extension to higher generations. Note, that polyphenylene dendrimers based on the branching unit **1.7** only reached G4 whereas branching unit **3.1** made G6 accessible and even higher generations appear feasible. Furthermore, while PAMAM dendrimers based on ethylenediamine (EDA) was built up to G8,^[20] the mass increase per generation falls short of that encountered for the exploded type.

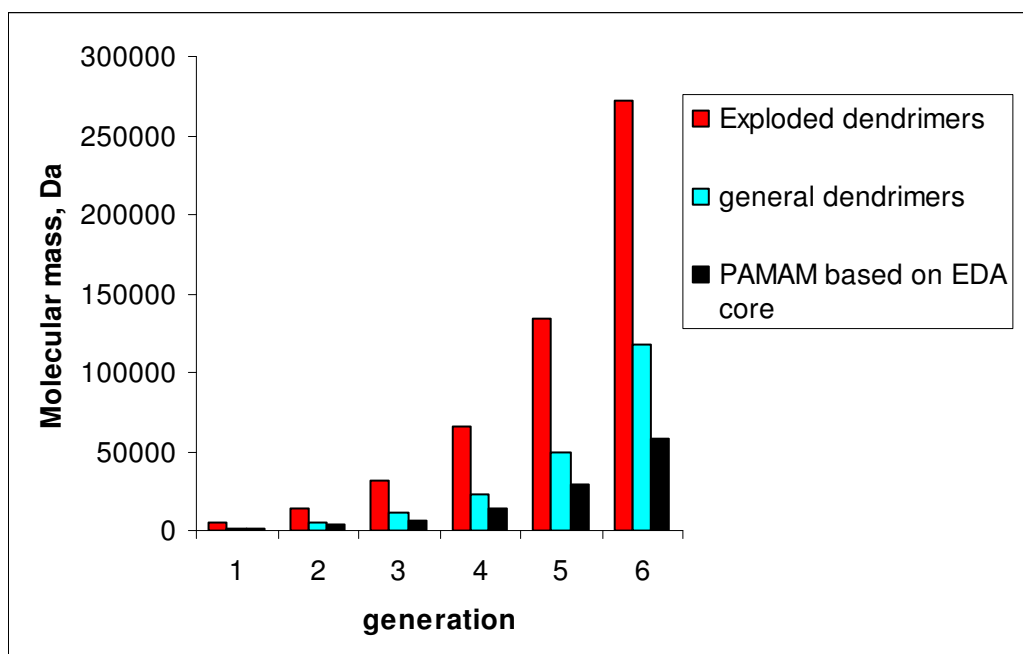


Figure 2.14: Theoretical molecular masses of exploded and regular polyphenylene dendrimers and their comparison with PAMAM dendrimers based on EDA core. The number of terminal groups of all dendrimers is the same for each generation number. They are doubled with every generation and the mass increases with the geometric progression.^[21]

2.6 ¹H NMR analysis of exploded dendrimers

Dendrimers frequently are characterized by classical methods such as ¹H NMR and ¹³C NMR spectroscopy. However, in many cases NMR spectroscopy has been found to be of little use in determining structural defects at higher generations because of the "self-similarity" inherent in the dendritic architecture.^[22] On the other side, a combination of the NMR and MALDI-TOF techniques is quite suitable for dendrimer characterization. Deviations from quantitative transformation are often observed in MALDI-TOF MS.

¹H NMR spectra for **3.8**, **3.10**, **3.12**, **3.14**, and **3.16** (G1-G5 with TIPS groups) are depicted in Figure 2.15. The experimentally found intensity ratio of the aromatic to the methyl proton signals and that of the aromatic to the alkyl group signals from the TIPS groups correspond to the expected composition. As anticipated from the presence of identical structural units in the dendrons, the ¹H NMR spectra for the various generation dendrimers differ only marginally. For better resolution the higher boiling solvent C₂D₂Cl₄ was used for **3.12** (G3), **3.14** (G4),

3.16 (G5) in order to increase conformational mobility of the phenyl rings and reduce line widths.

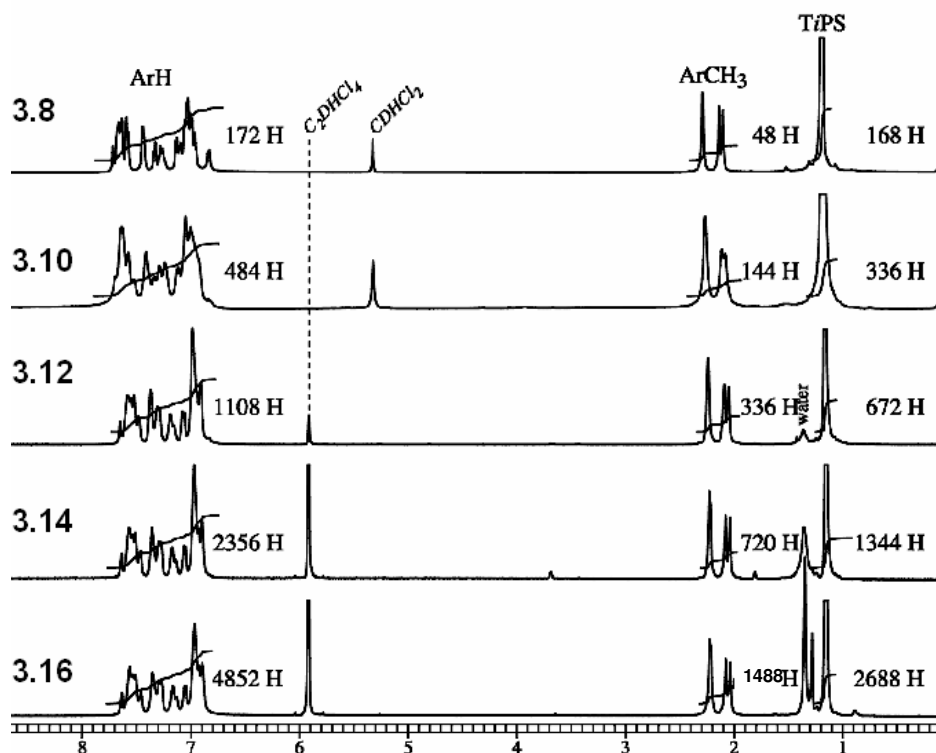


Figure 2.15: ^1H NMR of G1-G5 with TiPS groups (**3.8** in 500 MHz, r.t, CD_2Cl_2 ; **3.10** in 700 MHz, r.t, CD_2Cl_2 ; **3.12**, **3.14**, and **3.16** in 700 MHz, 393 K, $\text{C}_2\text{D}_2\text{Cl}_4$).

The synthesis of G5-Td-(TiPS)₁₂₈ (**3.16**) was also carried out in a NMR tube. The used solvent was tetrachloroethane (10 eq of branching unit **3.1** per 1 acetylene group). At the start of the reaction the signal from the acetylene group was seen at 3.09 ppm (Figure 2.16). During 4 hours signal intensity from the acetylene group decreased significantly and after 8 hours was not detected any more. The inherent weakness of the acetylene proton NMR signal does not make this a test for quantitative conversion. Notwithstanding, the ^1H NMR experiment implies that the Diels-Alder cycloaddition takes place rather quickly.

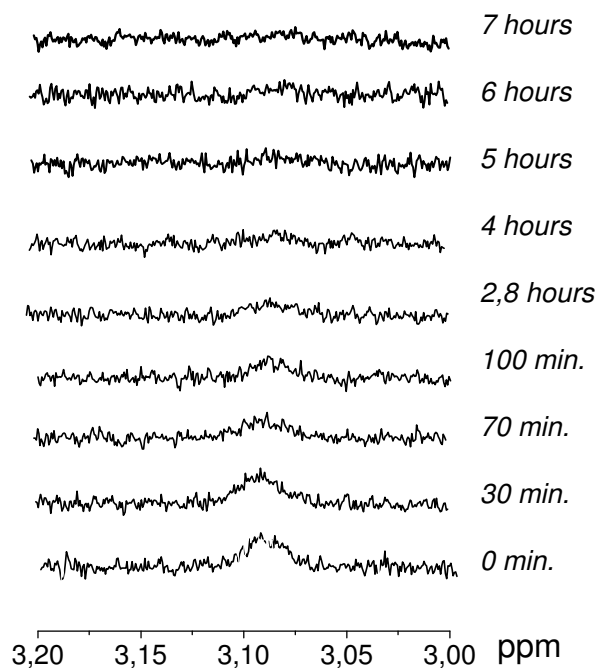


Figure 2.16: The formation of **3.16** during Diels-Alder reaction in $C_2D_2Cl_4$, 411 K, 500 MHz.

Figure 2.17 shows an 1H NMR comparison of G5-Td-(TiPS) $_{128}$ (**3.16**), G5-Td-(ethynyl) $_{128}$ (**3.17**), and G6-Td-(TiPS) $_{256}$ (**3.18**). They exhibit peaks for aromatic, methyl and TiPS groups.

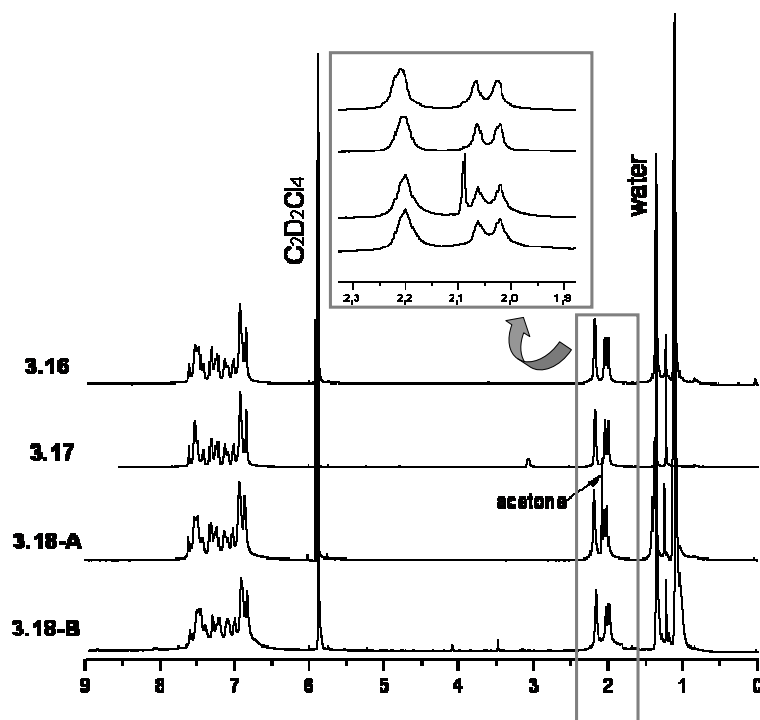


Figure 2.17: 1H NMR spectra of **3.16**, **3.17**, and **3.18** (700 MHz, 373 K, $C_2D_2Cl_4$).

In the case of G6-Td-(TiPS)₂₅₆ an additional peak at 2.09 ppm appeared pointing to acetone (Figure 2.17, **3.18-A**). To remove the solvent acetone completely (Figure 2.17, **3.18-B**), the sample **3.18** was heated at 100 °C under *vacuum* for 3 days. The expected intensity ratio of the aromatic to the methyl proton signals in **3.18** (Figure 2.17, **3.18-B**) corresponded to the experimentally found composition. As expected, formation of the G6 species **3.18** is accompanied by a disappearance of the alkyne proton signal at $\delta=3.08$ ppm, present in the G5 species **3.17**.

The ¹H NMR spectra, in addition to MALDI-TOF MS, confirmed the formation of the exploded dendrimers **3.8**, **3.10**, **3.12**, **3.14**, **3.16**, and **3.18**.

2.7 Size exclusion chromatography (SEC)

Being based on linear polymer standards size exclusion chromatography (SEC, also named gel permeation chromatography GPC) is commonly applied for the characterization of various dendrimers.^[16] Results obtained from SEC provide qualitative information on dimension and monodispersity of dendrimers. A polydispersity close to 1.0 does not guarantee the monodispersity of dendrimers of high generations.^[23] The ratio M_w/M_n obtained by SEC between 1.03-1.05 is characteristic for monodisperse dendrimers. The molecular masses derived from the SEC results only give order of magnitudes rather than precise values. They allow an unequivocal determination of the respective generation, however.

The SEC traces (Figure 2.18) show a progressive decrease in the elution volume for each subsequent generation **3.8**, **3.10**, **3.12**, **3.14**, **3.16**, and **3.18**. The incremental decrease Δ (mL) in the elution volume was smaller going to the fifth- and sixth-generation dendrimers (**3.16**, **3.18**), as was also observed with other dendrimers.^[24] The peak shape confirmed that the dendrimer is smaller than the exclusion limit of the column. The ratio M_w/M_n of G1-G4 is in the range 1.03-1.05 (Table 2.3). In the case of G5 (**3.16**) and G6 (**3.18**), larger width of the peaks suggests broader polydispersities (PDI=1.10 and 1.46 for **3.16** and **3.18** respectively) when compared with smaller generation dendrimers.

Table 2.3: Molecular weight distribution, elution volumes and polydispersity of exploded dendrimers.

dendrimers	V, mL	Δ , mL	SEC PDI	SEC M_n (PS), g/mol	theoretical molecular mass (M), Da
G1 TIPS, 3.8	24.94	-	1.04	8300	5336
G2 TIPS, 3.10	23.01	1.93	1.05	22000	13924
G3 TIPS, 3.12	21.92	1.09	1.03	41300	31101
G4 TIPS, 3.14	20.45	1.47	1.05	88500	65454
G5 TIPS, 3.16	19.89	0.56	1.10	117200	134162
G6 TIPS, 3.18	19.40	0.49	1.46	136711	271577

Furthermore, the shoulders seen for G5 and G6 presumably result from aggregation, as has been observed previously for large generation dendrimers.^[17, 25-26]

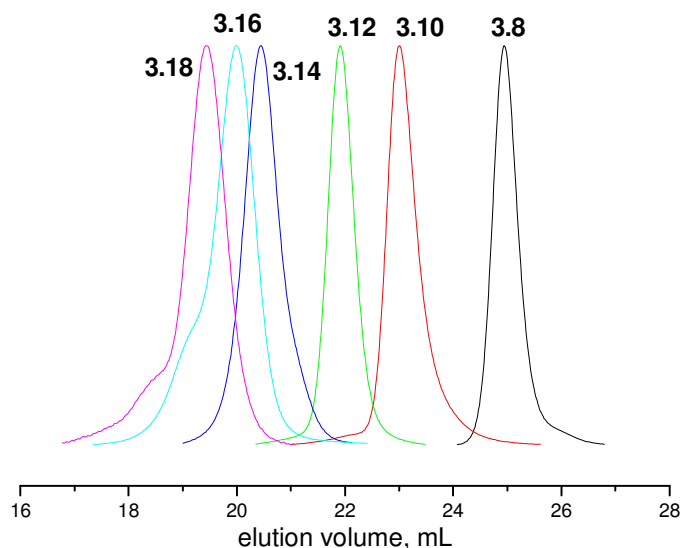


Figure 2.18: SEC elution profiles for TiPS ethynyl functionalized, polyphenylene dendrimers (**3.8**, **3.10**, **3.12**, **3.14**, **3.16** and **3.18**) in THF, using SEC columns with 500 Å, 104 Å, and 106 Å porosities.

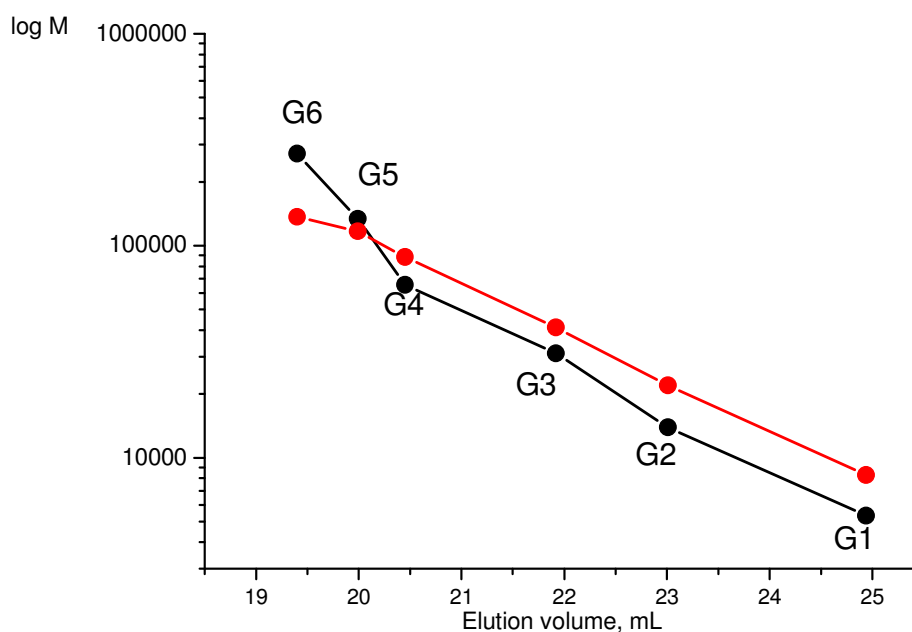


Figure 2.19: Semilogarithmic plot of SEC weight average molecular weight vs retention volumes for polystyrene standards (red line) and extended dendrimers (black line) (3.8, 3.10, 3.12, 3.14, 3.16, and 3.18).

Based on the data from Table 2.3, Figure 2.19 shows a plot of the logarithm of molecular weight versus elution volume for both the dendrimers G1-G6 (black line) and the polystyrene standards (red line). The data for the polystyrene standards follow a relatively straight line up to the mass corresponding to G6, whereas those for the dendrimers lie on a straight line only up to G4. This is in agreement with what was noticed originally by Aharoni^[27] and observed in the case of other dendrimers.^[12, 28] However, the continuation from G4 to G6 has a larger slope than the preceding part. Apparently, the bigger dendrimers (G5-G6) are delayed in the SEC more than expected from an extrapolation. From the Table 2.3 it is also seen that the increments of the elution volumes (Δ) of higher dendrimers (G5-G6) are smaller than those of the lower generations (G1-G4). It is noticed (Table 2.3) that the dendrimers G5 (3.16) and G6 (3.18) with nominal masses 134162 and 271577, exhibit SEC polystyrene equivalents M_w of 117200 and 136711 respectively. This observation may be interpreted by the fact that G5 and G6 dendrimers are denser and more compact, than G1-G4 dendrimers. The use of polystyrene standards in SEC of higher dendrimers must therefore be considered problematic. This is not unexpected, given the obvious difference in molecular shape of polystyrene compared to dendrimers.^[29]

In order to determine the optimal reaction time for the conversion **3.15** \rightarrow **3.16** and to ascertain, that SEC peaks presented in Figure 2.18 actually reflect completion of the reaction, the synthesis of **3.16** from deprotected **3.15** was repeated and monitored by subjecting samples to SEC measurement as the reaction progresses.

The SEC traces are depicted in the Figure 2.20. The reaction was carried out in *o*-xylene on a small scale: 2 mg of the starting material **3.15** were treated with the extended cyclopentadienone **3.1**, taken in excess (10 eq of **3.1** per acetylene group, which is 8 times more than in the large scale preparation). The samples (ca 0.01 mL) from the reaction mixture were collected at the certain times (5 min, 30 min, 1 hour, 2 hs, 3 hs, 4 hs, 8 hs, 1 day, 2 days, 3 days and 6 days from the starting of the Diels-Alder cycloaddition) and diluted in THF. All samples were applied to one SEC at the same day. Figure 2.20 shows that the Diels-Alder reaction proceeds fairly rapidly.

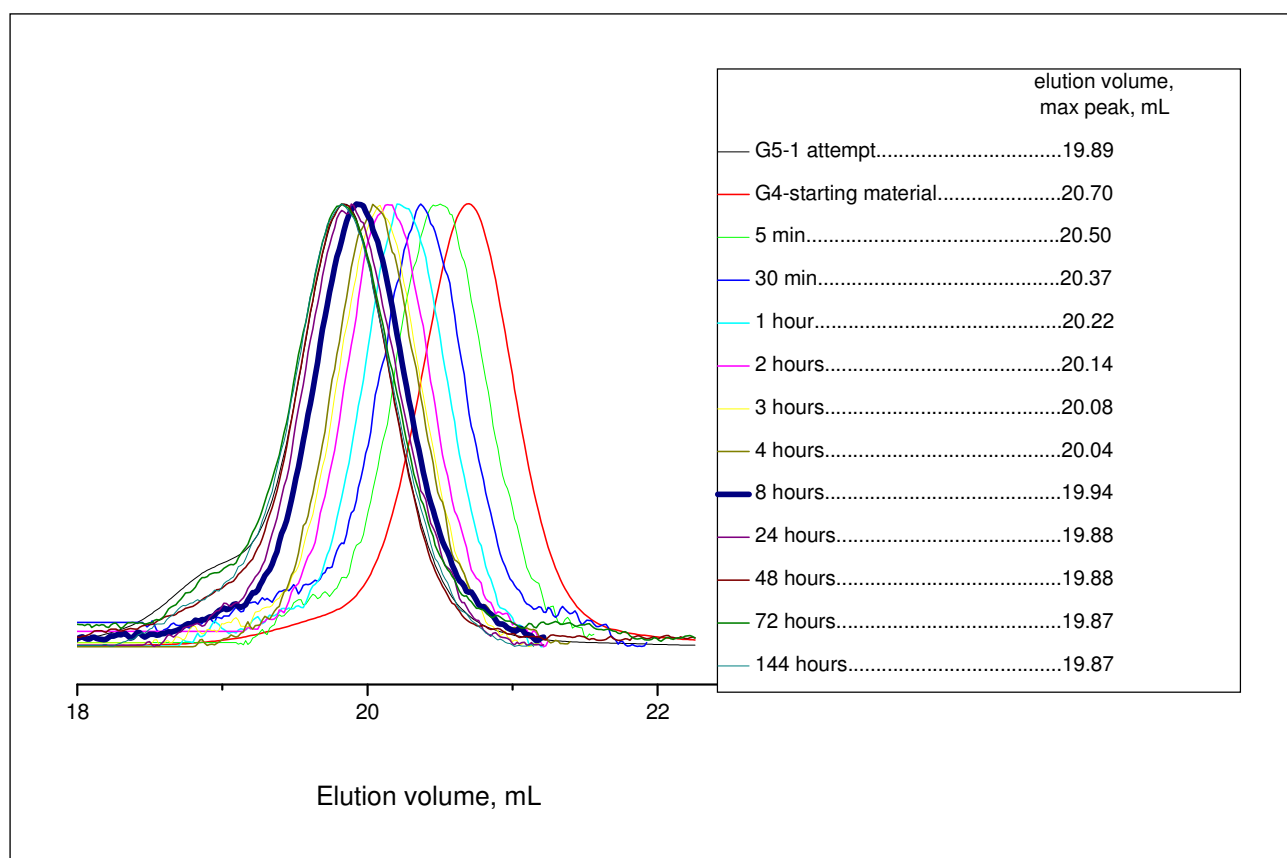


Figure 2.20: SEC control during the reaction time for the synthesis of G5-Td-(TiPS)₁₂₈ (**3.16**) from **3.15**, *o*-xylene, reflux.

However, with increasing reaction time, the time increments required to effect shifts to smaller elution volume become increasingly larger: whereas a change from 20.70 (starting material) to 19.94 mL takes place during 8 hours, at the final stage of the experiment the change from 19.94 mL to 19.89 mL requires 40 hours. The shoulder at smaller elution volume (pointing to aggregation) develops only during the final stage of Diels-Alder cycloaddition, after 24 hours that is.

As was mentioned before, the size of the shoulder changed with the concentration of **3.16** in THF in the sample used for SEC. The higher the concentration, the bigger the shoulder observed. Plausibly, in concentrated solution the dendrimer **3.16** is more prone to engage in aggregation.

A number of studies have addressed the effect of macromolecular architecture on physical and chemical properties.^[30-32] Comparative studies involving different macromolecular architectures have seldom been performed due to the synthetic difficulties intrinsic to the preparation of molecular structures sufficiently similar to enable comparisons between dendrimers and their architectural isomers.^[33-35]

For example, Harth et al.^[35] reported the synthesis and characterization of monodisperse architectural isomers of poly(benzyl ether) dendrons and dendrimers with a porphyrin core, ranging from exact linear analogues to four- and eight- arm star polymers also containing a central porphyrin (Figure 2.21). Characterization of the different structural isomers by SEC gave evidence for the influence of macromolecular configuration on hydrodynamic volume. These studies implied that the dendrimer A (Figure 2.21) has a significantly smaller hydrodynamic volume than does the isomeric eight-arm star B, which in turn is substantially smaller than the four-arm star C. In this case, the isomers A, B, and C have almost the same molecular mass, but the calibration of SEC using linear polystyrene standards led to accurate molecular weight for the linear four-arm star (C) only, which shows the highest structural similarity to the polystyrene standards. Clearly, the linear portion of the macromolecule dominates the hydrodynamic properties of the four-arm star leading to a less spherical disposition in solution. In the case of the eight-arm star (B) and dendrimers (A), the increased branching caused a progressively larger deviation when compared to linear polystyrene standards.^[35]

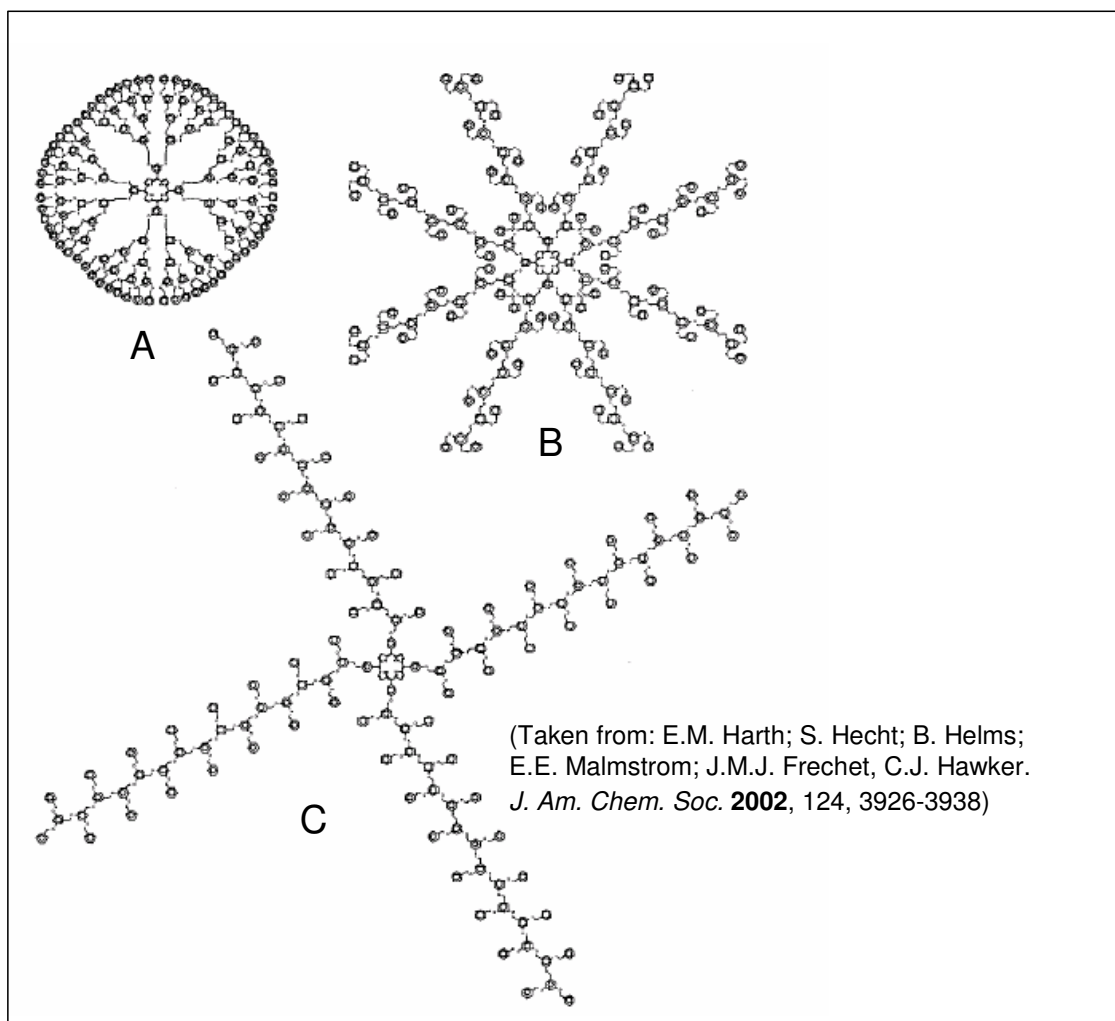
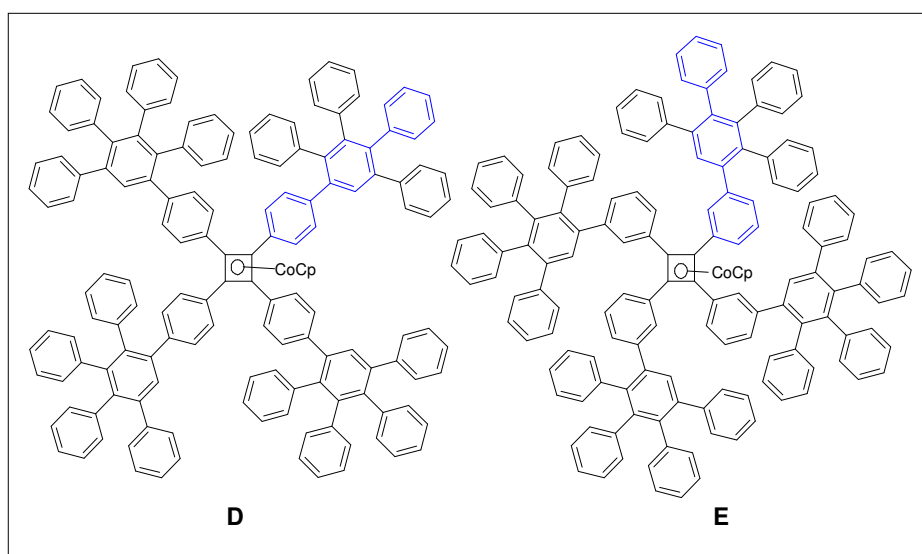


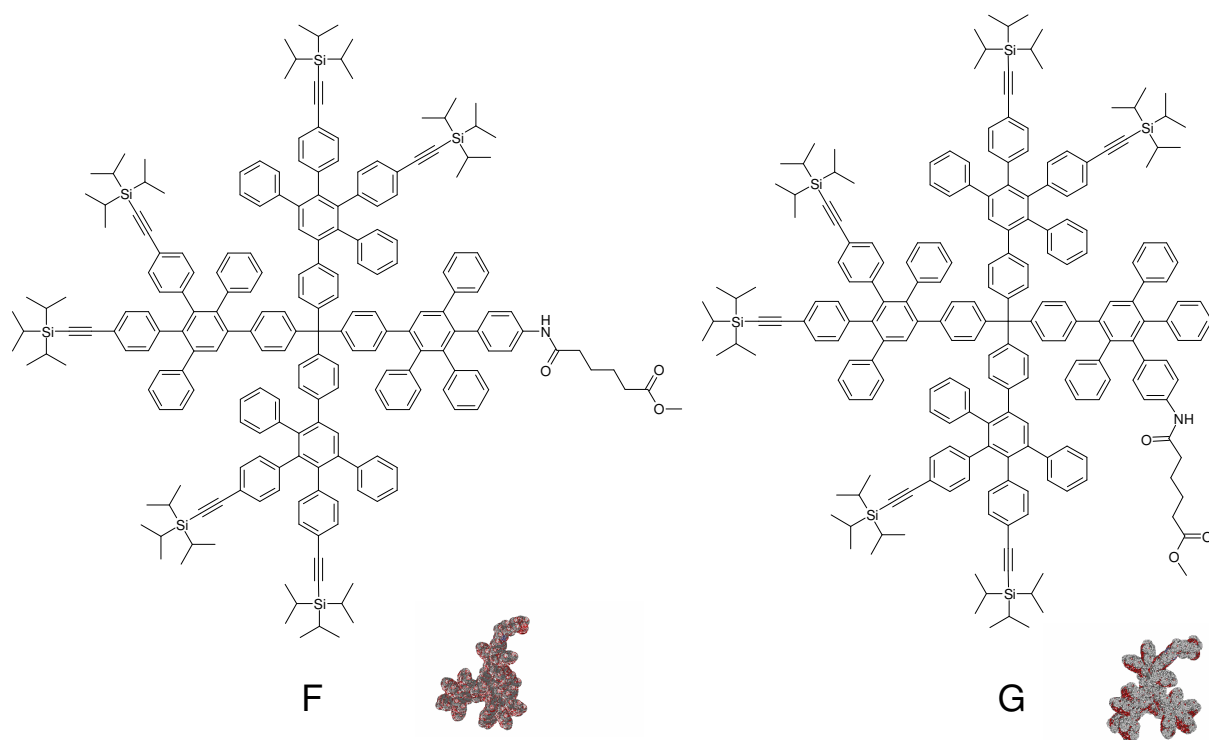
Figure 2.21: Three different macromolecular architectures of Frechet-type dendrimers of similar mass but large difference in radial extension.



Scheme 2.6: Bunz-type organometallic polyphenylene dendrimers.

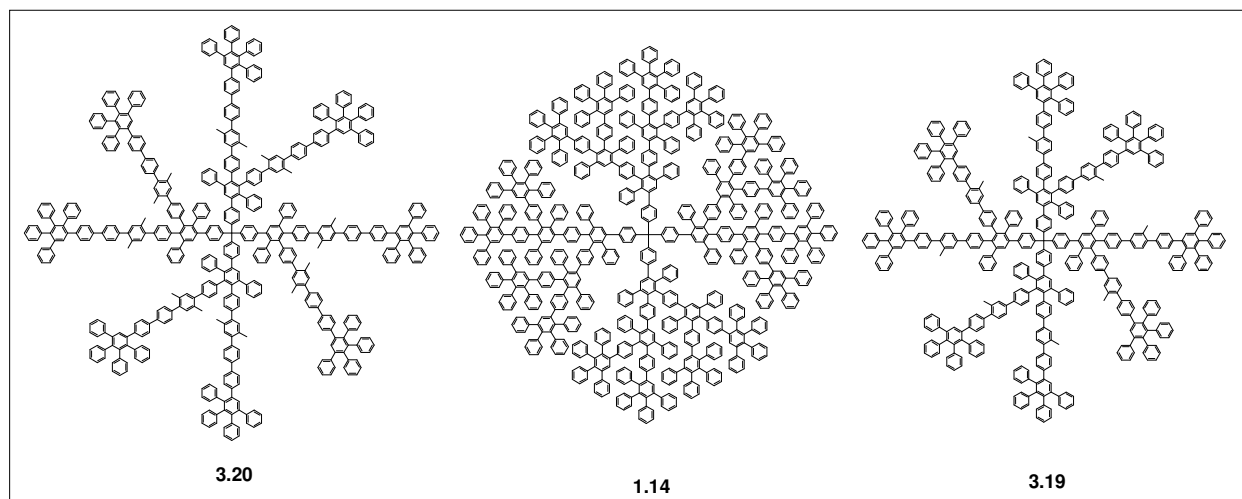
Bunz et. al.^[33] compared two isomers of rigid organometallic polyphenylene dendrimers containing 24 phenyl rings (Scheme 2.6). The more extended structure D (Scheme 2.6) has a shorter retention time than E (Scheme 2.6), and thus features a higher hydrodynamic volume.

Two regioisomeric desymmetrized polyphenylene dendrimers (Scheme 2.7), bearing polar ester group, were successfully separated by flash chromatography. The isomer G (Scheme 2.7) had lower retention volume ($R_f=0.66$) than isomer F ($R_f=0.73$). This separation was only possible because the defined spatial structure of the dendrimer led to substantial differences of their physical properties, further evidence of the shape-persistence of the dendritic polyphenylene structure.^[36]



Scheme 2.7: Müller-type desymmetrized polyphenylene dendrimers.

Here we compare three polyphenylene dendrimers (Scheme 2.8): the third-generation general dendrimer (**1.14**) and two second-generation dendrimers (**3.19** and **3.20**) using the branching units **3.1** and **4.1** respectively (the synthesis of **4.1** is reported in Chapter 2.15). These three dendrimers have similar radii according to molecular modelling and dynamic light scattering (Table 2.4). Their nominal molecular masses are compared with the molecular masses obtained from SEC (Figure 2.22) and listed in the Table 2.4.



Scheme 2.8: Three different polyphenylene dendrimers with similar estimated diameter.

From Figure 2.22 it is seen that although the masses obey the sequence $3.19 < 3.20 < 1.14$, the order of elution volumes is $3.20 < 1.14 < 3.19$.

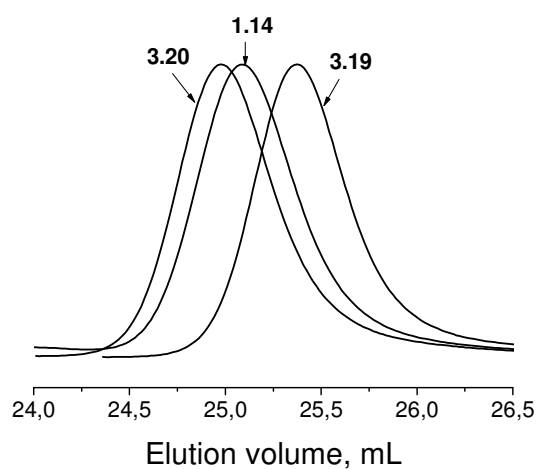


Figure 2.22: SEC of three different polyphenylene dendrimers.

Table 2.4: Calculated M and M based on PS of three different PDs with similar diameters:

	calculated M, Da	SEC, found M _p (PS), Da	calculated radius, nm	DLS, found radius, nm
3.19	6216	7227	3.0	2.1
3.20	6936	8816	3.4	2.42
1.14	10974	8342	3.0	2.2 ^[9a]

Based on this sequence, it is clear, that hydrodynamic properties of polyphenylene dendrimers have a pronounced influence on the elution volume. Obviously, molecular mass and shape both govern the elution volumes (V) determined in size exclusion chromatography and a steady decrease of V with increasing molecular mass is not to be expected. The observed comparatively small decrease in elution volume on going from **3.14** to **3.18** is a case in point.

It is important to mention that in a sample tube of a solution of **3.17** in tetrachloroethane, prepared for ^1H NMR spectroscopy, after a few days at ambient temperature a precipitate formed. This was not observed for the lower generation dendrimers. This again indicates that aggregation seems to be favoured for G5 and higher polyphenylene dendrimers. The SEC of G5-Td-(ethynyl)₂₅₆ (**3.17**) is presented in (Figures 2.23-2.24) with its polydispersity of 4.11 with regards to the tendency to aggregation.

The next step to prepare G6 (**3.18**) was attempted. The conversion from **3.17** to **3.18** was checked by SEC as well (the samples ca 0.01 mL from the reaction mixture were collected at the certain times and diluted in THF, all samples were applied to one SEC at the same day) and is documented in Figure 2.23.

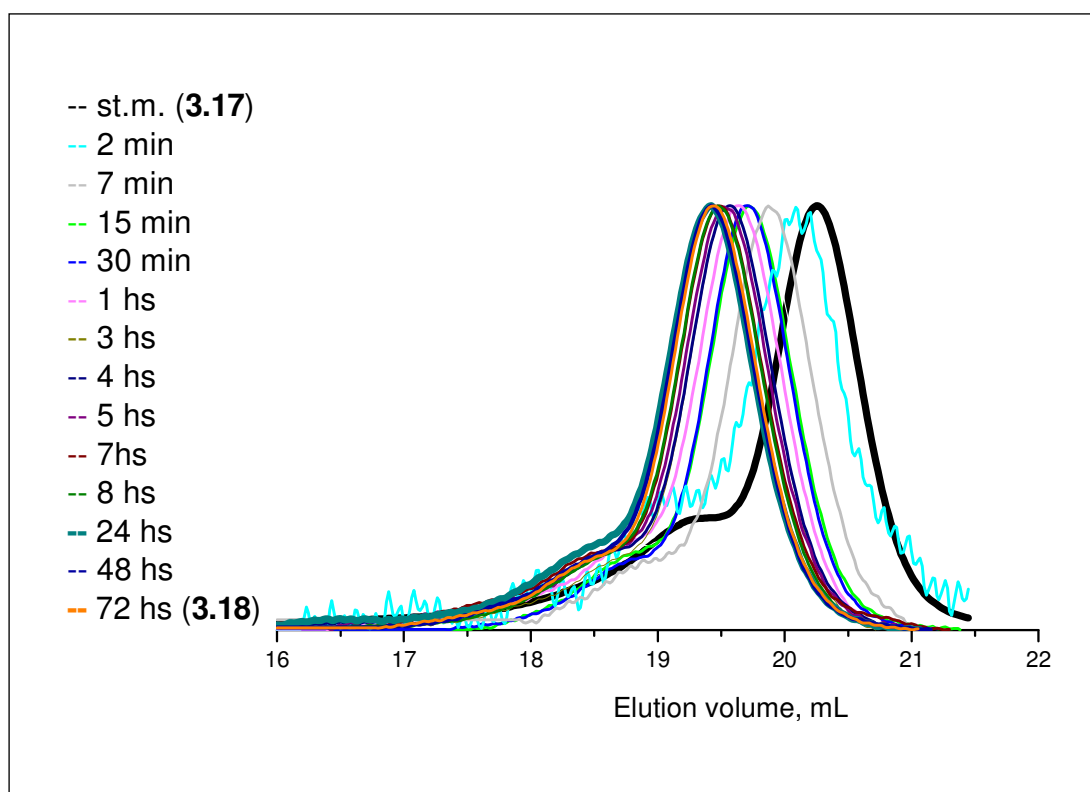


Figure 2.23: SEC control during the synthesis of G6 (**3.18**) from **3.17** in *o*-xylene, reflux.

Figure 2.23 showed that the product peak also quickly reached its final position after 40 hours. G6 (**3.18**) again displayed a shoulder at smaller elution volume (larger mass). Its shoulder was less intensive (Figure 2.24) than in the case of deprotected G5 (**3.17**) and slightly less than in the pre-deprotected dendrimer G5 (**3.16**).

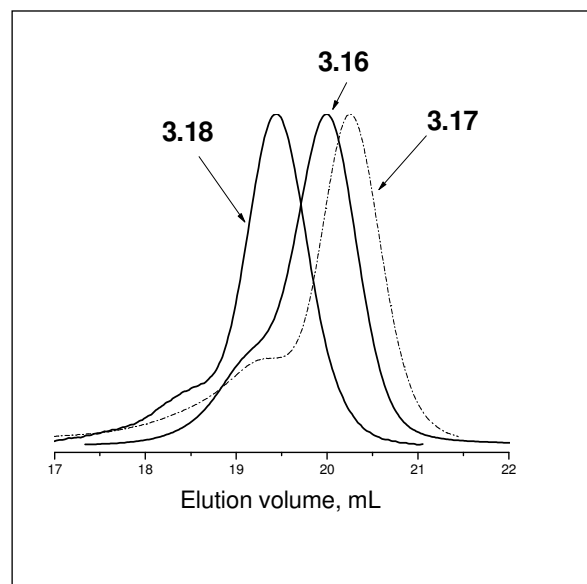


Figure 2.24: SEC of G5-G6 dendrimers (**3.16-3.18**) with shoulders.

Probably, the SEC technique is the most convenient method for the investigation of the rate of the Diels-Alder cycloaddition. In the case of PAMAM after the tenth generation, the rate drops suddenly and further reactions at the end groups cannot occur.^[20-21] In the general PDs case (where the branching unit **1.17** was used) the reaction rate for the growth of the fourth generation required one week for completion,^[37] while the reactions for the growth of both exploded G5 and G6 needed less than 50 hours. Their peaks shifted quickly within 8 hours, pointing to the fact that the majority of ethynyl groups had reacted after that time interval.

2.8 Multi-angle laser light scattering size exclusion chromatography

Multi-angle laser light scattering (MALLS) size exclusion chromatography (or MALLS-SEC) has been demonstrated to constitute a powerful technique for detailed analysis of the

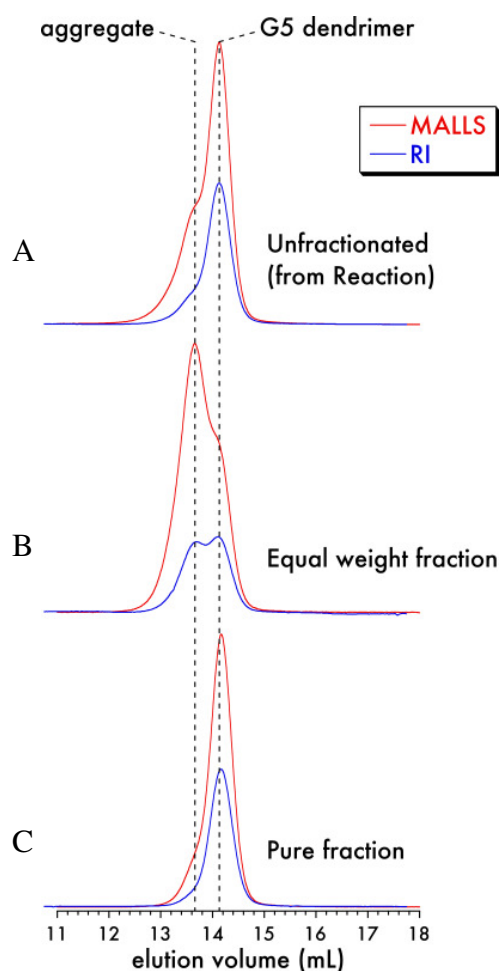


Figure 2.25: MALLS-SEC of **3.16** (see text).

multi-angle laser light scattering (MALLS) size exclusion chromatography (SEC) with RI detector and those from MALLS-SEC (red line). The compound **3.16** was fractionated by separation in SEC. One of the fractions contained two peaks with different elution volumes, but with similar compositional concentrations known from RI (Figure 2.25(B), blue line, the similar peak heights). In the light scattering signal these two peaks gave different heights (Figure 2.25(B), red line). As the height of the peak depends on the size of the macromolecule, the MALLS-SEC result indicated that the shoulder at higher molecular mass should be assigned to an aggregate rather than to the dendrimer **3.16** which is contaminated by material included in its cavities. This aggregate probably is to be a non-covalently interdigitated dimer or tetramer as was noticed in MALDI-TOF MS (Chapter 2.4).

molecular weight of various proteins, aggregates and minor components in protein products.^[38]

The MALLS- SEC method is based on the fact that light is more strongly scattered by large molecules than by small molecules. During a chromatographic run, the light scattering detector measures the degree of light scattering of a laser beam with detectors placed at different angles. The output of the light scattering detector is proportional to the product of concentration and molecular mass of macromolecules. It does not coincide with the refractive index (RI) signal in the classical SEC, because the RI detector signal is proportional to the concentration (g/L) only.

In the previous chapter it was mentioned, that the dendrimer sample G5-Td-(TiPS)₁₂₈ (**3.16**) displayed a shoulder in the region of higher molecular mass. Figure 2.25(A) shows a comparison of peaks obtained from classical

2.9 Vibrational spectroscopy (IR/Raman)

IR spectroscopy has been applied to check whether the branching unit **3.1** with a carbonyl group is actually present as an impurity in the dendrimer **3.16**. A hint is given by the colour of G5 (**3.16**) which is not purely colourless but has a slightly beige tint. The more cyclopentadienone **3.1** is used in the synthesis the more difficult it is to remove. Removal of the last trace of colour could be achieved either (1) by preparative SEC, which can not be scaled up easily, or (2) repeated precipitations of **3.16** which lowers the yields. However, after the removal of TiPS groups, the deprotected G5 (**3.17**) became colourless, which casts doubts on the contamination of **3.16** by included **3.1**.

In Figure 2.26 IR spectra of the branching unit **3.1**, the colourless second-generation dendrimer **3.10**, and the fifth-generation dendrimer **3.16** prior to purification by preparative SEC or re-precipitation are shown for comparison.

In Figure 2.26 IR spectra of branching unit **3.1**, the colourless second-generation dendrimer **3.10**, and the fifth-generation dendrimer **3.16** prior to purification by preparative SEC are shown for comparison.

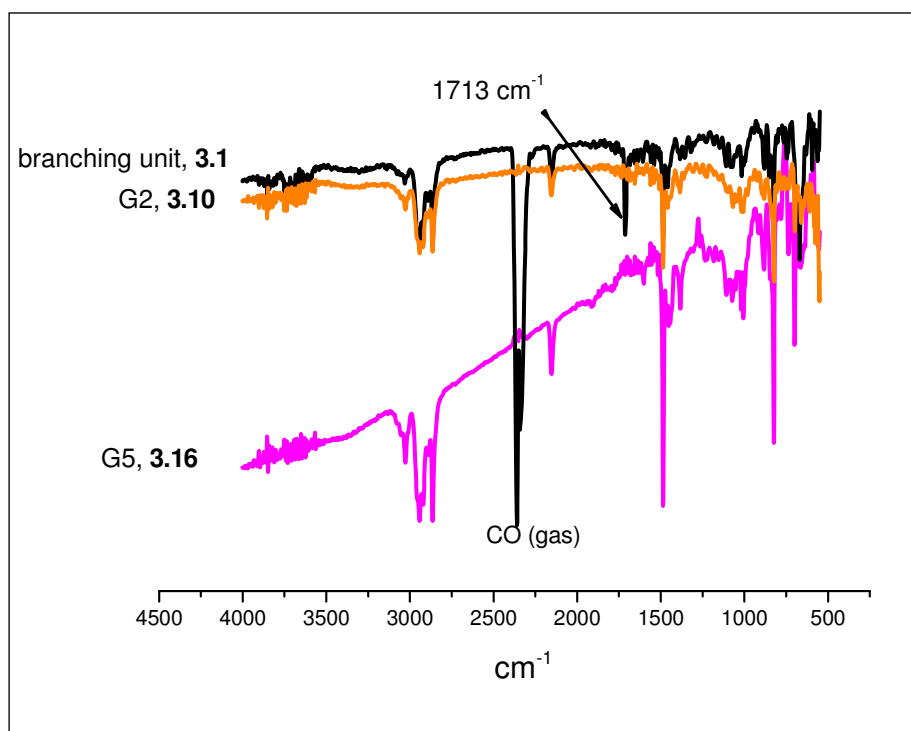


Figure 2.26: IR spectra of **3.1**, **3.10**, and **3.16**.

In the IR spectrum of the cyclopentadienone derivative **3.1** a band at 1713 cm^{-1} (pointing towards C=O stretching)^[39] is observed. This band is absent in both the dendrimers **3.10** and **3.16** spectra. The peaks at $2941\text{--}2862\text{ cm}^{-1}$ corresponds to C-H stretching of CH_3 group; 2154 cm^{-1} points to the C \equiv C stretching and $1489\text{--}826\text{ cm}^{-1}$ denotes C-H stretching in the aromatic region.

The two different dendrimers **3.10** and **3.16** show almost identical IR spectra. The ν_{CO} band for the branching unit **3.1** was not found in G5-Td-(TiPS)₁₂₈.

The IR result, in addition to NMR and FDMS/MALDI-TOF MS, showed that the branching unit **3.1** in **3.16** prior to purification by preparative SEC or re-precipitations had been almost exclusively removed.

2.10 Visualization of the exploded dendrimers by structural simulation

In order to demonstrate that the goal of this work has been reached, namely to generate large dendrimers which, because of the use of extended arms, display comparatively little steric crowding and the presence of cavities, the structures of the species G1-G4 (**3.8**, **3.10**, **3.12**, **3.14**) were simulated, employing PC Spartan Pro with the molecular force field MMFF.

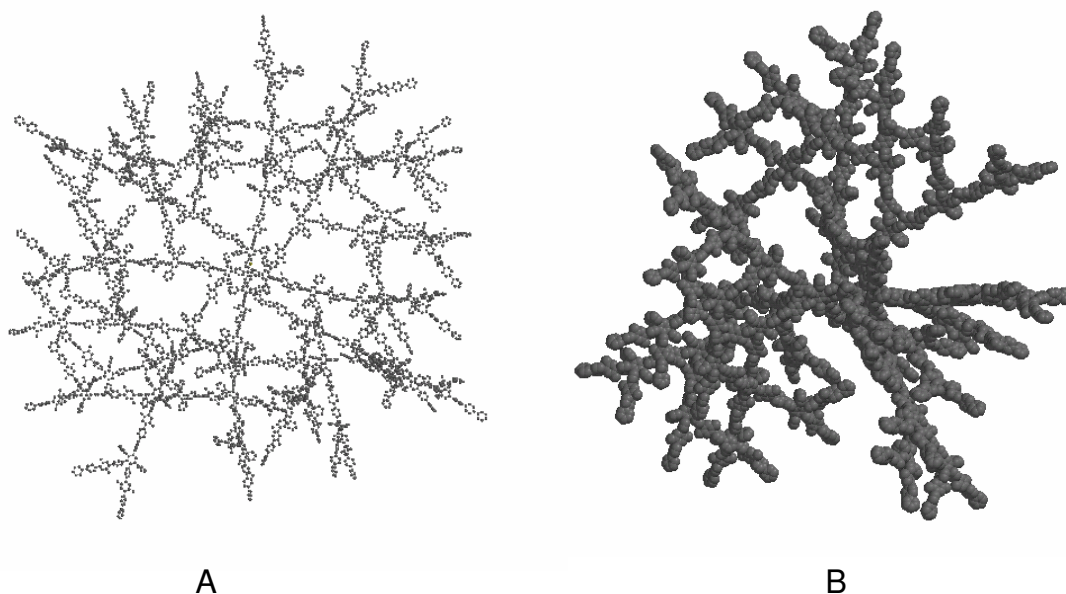


Figure 2.27: Visualization of the fourth-generation dendrimer **3.14**. **A** - ball and spoke model, **B** - space filling mode.

For G1-G4 dendrimers the structures of the tetrahedral core and dendrons (D-1, D-2, D-3, D-4) of G1-G4 respectively were optimized separately. Each generation bears 4 equivalent dendrons in the respective dendrimer. For any generation G1-G4 a combination of one single dendron with the tetrahedral core was minimized, to which the next dendron was subsequently attached for the following optimization. This was repeated until four dendrons had completed the structure of the dendrimer. The results of this endeavour are presented in Figure 2.38-A (Chapter 2.16) for **3.12** and Figure 2.27 for **3.14** (visualisations of **3.8** and **3.10** are not shown here, the ones of **3.16** and **3.18** were not generated). The maximal radii of G1-G6 are listed in Table 2.1 (Chapter 2.3). In the following paragraphs these calculated radii will be compared with experimentally measured radii obtained from the indirect method DLS, and direct methods such as TEM and AFM.

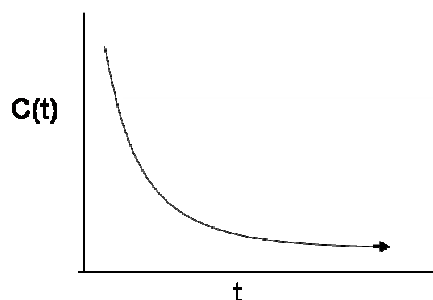
2.11 Dynamic light scattering (DLS)

In the light scattering experiment a monochromatic laser beam exposes the particles in a sample to oscillating dipoles. These dipoles serve as a source for scattered light waves which are recorded by a detector placed at different angles with respect to the transmitted beam. The molecules in the illuminated region perform Brownian motion; as a consequence the total scattered electric field at the detector will fluctuate in time.^[40]

Since the registration time of individual scattering intensities is long, relative to the time scale of translational motion, statistical analysis of the experimental data is called for. This takes the form of the intensity correlation function $C(t)$ of the light scattering data. The correlation function $C(t)$ is computed such that the intensity I_s of the scattered light at a time t_i is multiplied with the intensity at t_i+t_0 (t_0 delay time). This operation is repeated several times n at constant t_0 , the results are summed and divided by the number n of operations. The correlation function originates from varying t which may be expressed as $t = nt_0$.^[40]

$$C(t) = \frac{1}{n} \sum_{i=1}^n I_s(t_i) I_s(t_i+t_0).$$

For small t the correlation function $C(t)$ corresponds to the mean of the squared scattering intensity, $\langle I_s^2 \rangle$. For large t , $C(t)$ gives the square of the mean intensity $\langle I_s \rangle^2$. For short time intervals $t+t_0$, I_s is strongly time correlated, for long times $t+nt_0$ I_s ceases to be correlated. The results of the measurements are usually plotted as a function $C(t)$ which falls off with exponentially increasing time t .



The shape of this fall off contains information on the molecular translation rates which are, i.a., governed by the diffusion coefficient D . The experimentally obtained correlation function can often be approximated by an exponential series:

$$C(t) = A_1 + A_2 e^{-2DQ^2 t}$$

where $A_1, A_2 = \text{constants}$,

Q = relates to the wavelength of light and the scattering angle Θ

D = diffusion coefficient for translational molecular motion.

It should be noted in passing that analysis of experimental data via generation of a correlation function is not limited to light scattering but widespread in modern science whenever fast fluctuations of experimental observable must be treated (example: fluorescence correlation spectroscopy in Chapter 4). In the present case, the fluctuations in the intensity of the scattered light are related to the rate of diffusion of molecules in and out of the region being studied and the data are analyzed to give the diffusion coefficient of the particles causing the scattering. The relation between diffusion and particle size is based on the laws for Brownian motion of spherical particles. The Stokes (hydrodynamic) radius R_h can be obtained from Stokes-Einstein relation:^[40]

$$R_h = kT/(6\pi\eta D)$$

where k = Boltzmann constant, T = absolute temperature, and η = viscosity of the solvent.

DLS has been applied to the *TiPS*-protected dendrimers G1-G6 (**3.8**, **3.10**, **3.12**, **3.14**, **3.16**, and **3.18**). During these experiments it was observed that hydrodynamic radii of each dendrimer at different angles (60° , 90° , 120° , 150° for G1-G5, and 25° , 35° , 45° for G6) were similar in accordance with the spherical shape of the dendrimers being studied. The

dimensions derived therefrom nicely conform with the values taken from molecular models. The data are depicted graphically in Figure 2.28. They leave no doubt as to the identity of the new materials.

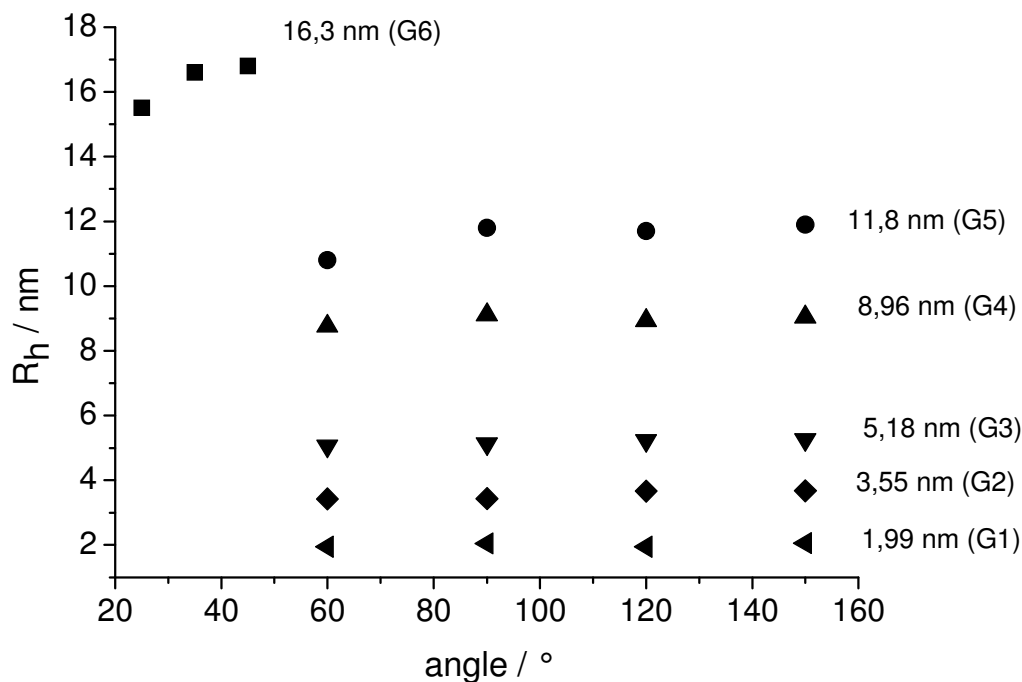


Figure 2.28: Hydrodynamic radii of extended dendrimers G1-G6 with TiPS groups (**3.8**, **3.10**, **3.12**, **3.14**, **3.16**, and **3.18**).

From the light scattering experiment the remarkable fact emerges, that G5 must be regarded as the largest spherically shaped monodisperse dendrimer ever produced, comprised of no less than 1368 benzene rings!

The hydrodynamic radius of G6 (**3.18**) obtained from DLS amounts to 16.3 nm; it is larger than the radius derived from molecular modelling. The latter for the linear array of 31 phenyl units present in each dendron of **3.18** gives an extension of 13.4 nm. The larger radius of **3.18** derived from the DLS experiment therefore suggests that this G6 dendrimer aggregates in solution.

2.12 Transmission electron microscopy (TEM)

The most direct way of checking the result of the synthetic efforts described above would be the creation of molecular images by means of electron microscopy. Techniques have now advanced to a stage where single molecule resolution is possible.

Since the dendrimers have dimensions of a few nm, optical microscopy is not suitable as an imaging method because the wavelength of light in the visible region amounts to 400-750 nm. If electron beams are used, wavelengths in the pm-range can be achieved. As the electron is a charged particle, it can easily be refracted in a magnetic field and accelerated by an electrical potential. The stronger the potential the faster the electron will move, the shorter the wavelength and the better is resolution due to the de Broglie relation: ^[41]

$$\lambda = \frac{h}{mv}$$

where h is Planck's constant, m and v the mass and the velocity of the electron respectively. ^[41]

The de Broglie relation makes it possible to use electrons, just as light, to produce images of objects. This can be achieved in a transmission electron microscopy (TEM). The TEM works much like a slide projector (Figure 2.29). In the TEM electrons are emitted from the cathode, made of tungsten wire, to which a negative high voltage is applied. The electrons are accelerated towards the anode. In order to prevent collisions with air (O_2 and N_2) molecules, the path in which the electrons travel must be in high vacuum. In the case of TEM, the acceleration voltage lies in the 60-200 kV range, which corresponds to wavelengths of the electron of 0.005-0.002 nm. The electron beam is guided by electromagnetic lenses which, like convex optical lenses, focus this beam. The latter passes through a two- or three-stage condenser lens and illuminates the sample (for example, a dendrimer molecule). The objective lens provides an image or diffraction pattern of the sample. The electron intensity distribution behind the specimen is magnified with a three- or four-stage lens system and viewed on a fluorescent screen or stored on a photographic film.

Because of the strong absorption and scattering of the electrons, in transmission electron microscopy a careful preparation of the sample is necessary. First of all, due to the strong interaction of the electron beam with materials, the thickness of the sample should be less than 100 nm, otherwise the electron beam would not be able to pass through the sample. Furthermore, the sample must display sufficient contrast for the electrons which eventually must be increased by the application of heavy metal compounds like OsO_4 which possess

strong scattering power. Another variant of sample preparation is the matrix replica process which is particularly suitable for the study of surface structures. Here by means of materials like cellulose nitrate a surface replica of the sample is generated which subsequently is investigated by means of electron microscopy. A surface replica can also be obtained by vapour deposition of Pt, W, C onto the surface of the sample. If vapour deposition is carried out at an inclined angle, a so-called topography contrast results, which can be used to estimate the size of the object.

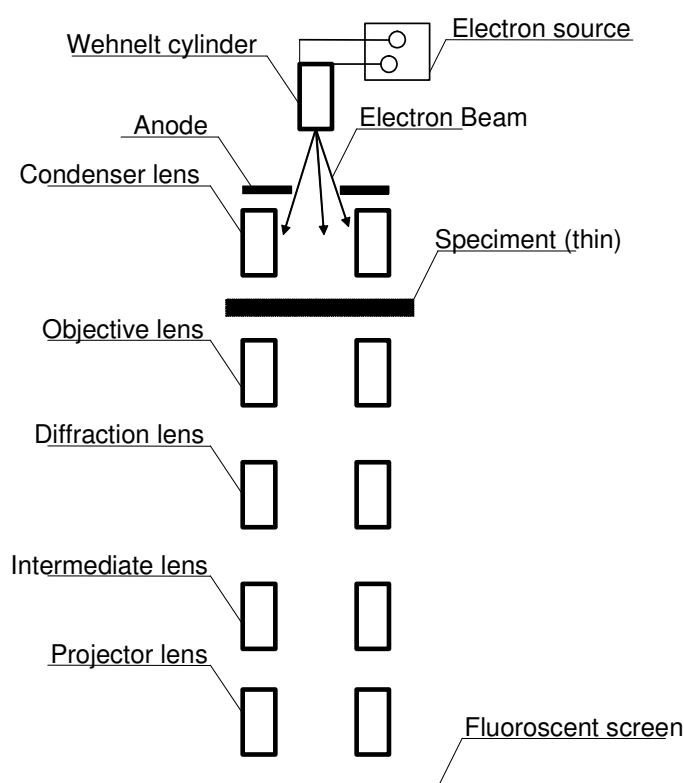


Figure 2.29: Schematic image of TEM.

Numerous dendrimers have been studied in the solid state by means of TEM. However, due to the small size, TEM pictures of isolated dendrimers are rare.^[7, 13, 15a, 20, 25a, 42]

For example, Jackson et al.^[25a] succeeded in differentiating individual dendrimer molecules of poly(amidoamine) (PAMAM), which were treated with sodiumphosphotungstate ($\text{Na}_3\text{PW}_{12}\text{O}_{40}$) as a contrast agent, from their environment. The dendrimers which could be visualized from the fifth generation up had diameter of 4.3 (G5) and 14.7 nm (G10). Other well separated polyphenylene dendrimers, based on biphenyl- and tetrahedral-cores, were

presented by Wiesler.^[7, 9a] These dendrimers could be well differentiated from their surrounding. Furthermore, third- and fourth-generation polyphenylene dendrimers with tetrahedral core (Td-G3 and Td-G4 respectively) were regarded as spherical objects with diameters of 5.2 and 6.1 nm respectively.

In collaboration with G. Lieser at the Max Planck Institute für Polymerforschung, Mainz, TEM measurements were performed in order to evaluate the size of the higher generation dendrimers G4 (**3.14**), G5 (**3.16**), and G6 (**3.18**), and direct visualisation by TEM was achieved. In order to picture single dendrimer molecules, solutions of the dendrimers G4-G6 in dichloromethane in the concentration range 10^{-8} - 10^{-9} mol/L were used for spin coating onto freshly cleaved mica. The coated mica platelets could subsequently be subjected to coating by vapour deposition in high vacuum by means of electron beam evaporation of a tungsten (W)/tantalum (Ta) alloy at angles of 30-45°, and finally of carbon vapour at an angle of 90° (perpendicular) relative to the sample surface. The choice of low volatile W/Ta alloy was dictated by the small size of only a few tenths of a nanometer of the metal grains formed during coating.^[43] Finally, the metal- and carbon film which contains the dendrimer molecules was made to float on a water surface and transferred to a 600 mesh copper net. In order to prevent corrosion, the samples were studied by TEM immediately or stored in high vacuum until measurement. The wavelength of the electron beam used for TEM study amounted to $\lambda = 4$ pm, corresponding to accelerating voltage of 80 kV.

The fourth-generation dendrimer **3.14** showed only film-like aggregation, however the fifth-generation dendrimer molecules **3.16** were well-separated (Figure 2.30-A). Although the individual molecules differ from hexagonal closest packing in that the intermolecular distances exceed the van der Waals contacts, they are distributed fairly regularly. A repetitive pattern cannot be spotted, however. As suggested by the simulation, the shape of the dendrimer molecules is in fact spherical.

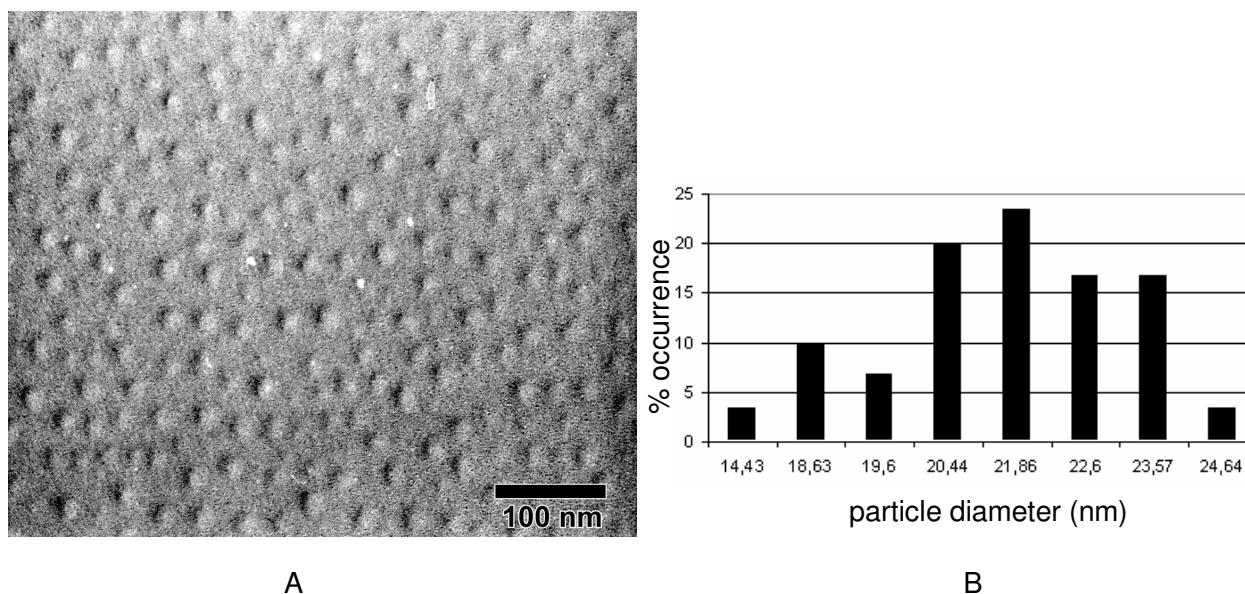


Figure 2.30: A - Transmission electron micrograph of tungsten/tantalum shadowed G5 (**3.16**); B - histograms of the particles size distributions are also shown (determined by counting at least 30 particles. Diameter from molecular modelling = 22.4 nm.

This conclusion is reinforced by the notion that, due to statistical orientations of the molecules, many different views are sampled which, however, all adhere to spherical shape. The size of the dendrimers is obtained from a statistical analysis of the circles which can be drawn around the images of the molecules. Figure 2.30-B shows a histogram for the measured diameters of the fifth generation-dendrimer **3.16**. The majority of the molecules possess identical diameters of 22 ± 2 nm, which is in good agreement with diameters from DLS and molecular modelling. Beyond doubt the fifth generation has actually been realized with the synthesis of **3.16** which is remarkable in view of the fact that the size of **3.16** approaches that of the biomolecule of γ -globulin ($M = 156$ kDa).^[44]

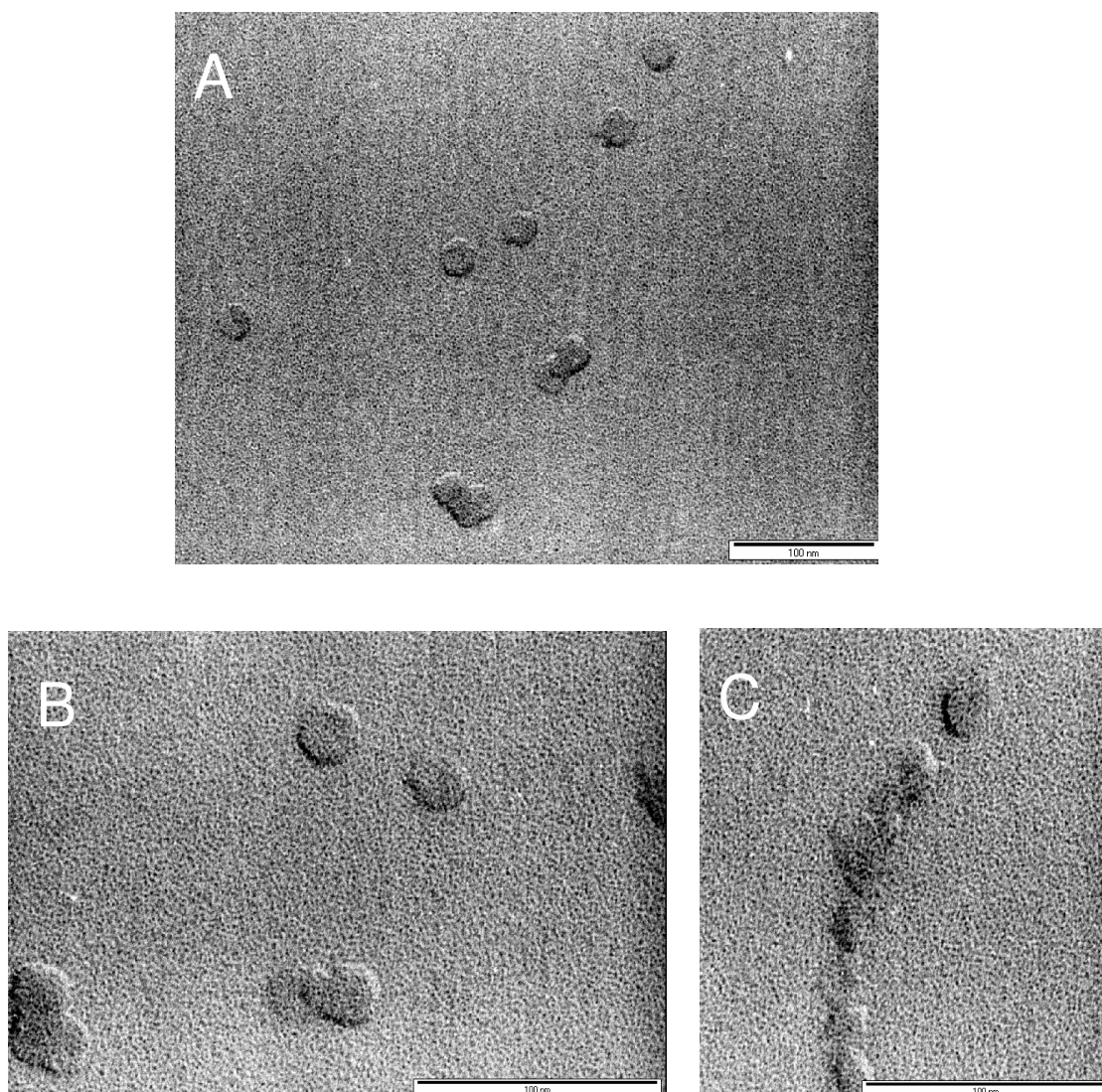


Figure 2.31: Transmission electron micrographs of tungsten/tantalum shadowed G6 (**3.18**).

TEM-picture of the sixth-generation dendrimer **3.18** showed only a few particles which were ordered randomly (Figure 2.31-A and Figure 2.31-B). However it completes the information about the progress of the Diels-Alder reaction from G5 to G6. One can see that these particles are well differentiated from their surrounding and may be regarded as spherical objects with diameters of about 27 nm, significantly bigger than the G5. The TEM pictures here also points to aggregation of two or three dendrimer molecules.

By way of summary, it can be stated that the size of the exploded dendrimer G5 can be derived in good agreement both by molecular mechanics calculation (radius 11 nm) and measurement of the diffusion coefficient (radius 11.8 nm). The radius of the G6 dendrimer (13.4 nm) illustrates the extension of the synthesis to even larger exploded dendrimers.

The diameter of the tenth-generation PAMAM-type is about 14 nm, it is much less than the size of the fifth-generation extended arm PD-type. The comparison of conventional dendrimers with branching unit **1.17**,^[7] exploded dendrimers and PAMAM-type dendrimers^[45, 25a] is shown in the Figure 2.32.

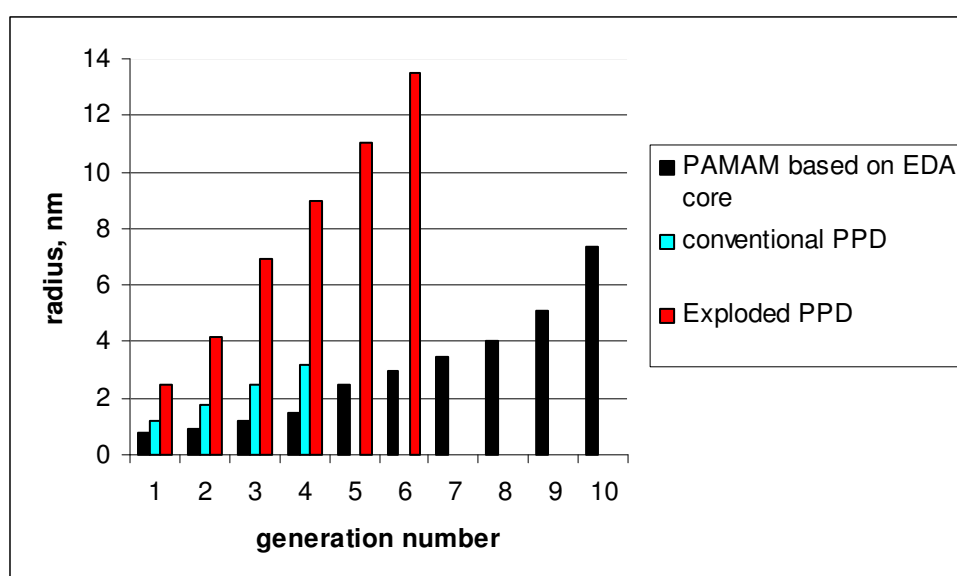


Figure 2.32: Comparison of theoretical size increase per generation for three different types of dendrimers.

Figure 2.32 demonstrates the enormous size increase which the new extended arm dendrimers **3.8-3.18** experience for each added generation. Interestingly, the third-generation extended arm polyphenylene dendrimers already matches in size the tenth-generation dendrimer of the PAMAM-type! Other example, a largest gold complex of polyphosphine dendrimer^[25b] (tenth generation) was observed to have diameter of 15 nm.^[25b] The designation "exploded" for the new type of dendrimers, made accessible in this work, therefore is fully justified.

Up to now, a combination of MALDI-TOF MS and ¹H NMR spectra, SEC, DLS and TEM confirmed the first stepwise chemical synthesis of the largest sixth-generation polyphenylene dendrimer (**3.18**) with diameter of more than 26 nm.

2.13. Atomic Force Microscopy (AFM).

Atomic force microscopy (AFM)^[46] is another tool to determine the size of dendrimers, since it is able to gauge the topography of a surface. Practically all materials are amenable to this technique, particularly as it is sensitive even to the ubiquitous van der Waals forces.

AFM measures interactions between the scanned tip and the surface such as electrostatic, van der Waals, frictional, capillary, and magnetic forces. The measurements typically cover areas of nanometer dimensions.^[47] The AFM image is a map of response obtained from each point on a surface. A deflection of the cantilever is recorded over each x,y coordinate (Figure 2.33) of the sample as it is scanned over the probe, a process which takes from several seconds to several minutes per image, depending on the scan area size, the surface roughness, and the resolution. The x,y -registered data are then assembled into a 2-D surface map. The image from the AFM is a map of forces detected over each point on the surface thereby furnishing its magnetic, electrostatic, or geometric topography.

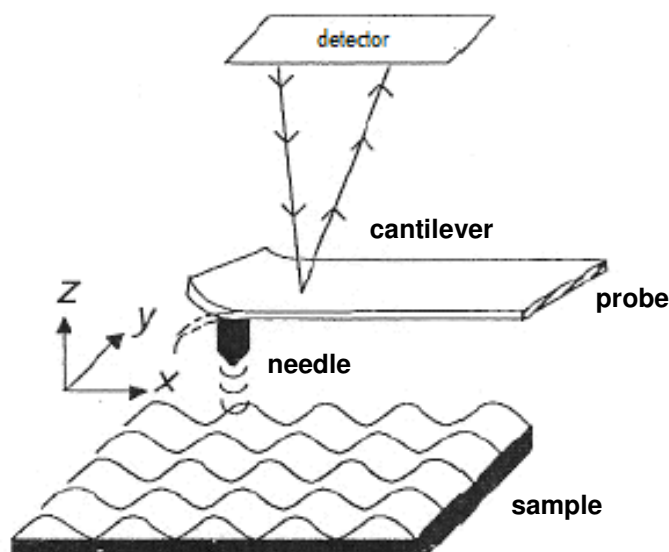


Figure 2.33: Principle of atomic force microscopy: a piezoceramic scanner moves the probe over the sample.^[47] The forces between needle and surface atoms cause deflections of the cantilever which are recorded by means of a laser beam.

AFM in its original version introduced in 1986^[48] utilized a sharp tip with an apex tens of nanometers in diameter which was in constant contact with the probe as the latter was scanned. It was realized soon, however, that soft materials such as biomolecules suffer mechanical damage under the impact of the needle which may lead to erroneous results with regards to the vertical dimensions. The introduction of the AFM tapping mode was a major step forward in the surface imaging of soft materials like biomolecules and polymers. In this variant rather than making permanent contact with the sample, the needle is located at a distance 2-20 nm above the sample surface and undergoes oscillation at its eigen-frequency. As the needle-surface distance decreases upon approach to an object on this surface, the tip-sample forces (essentially van der Waals forces) modify the resonance frequency and the vibrational amplitude of the cantilever. This change contains the surface topographic information. Contrary to the contact mode, during scanning tapping mode the probe comes only into intermittent contact with the sample surface and inelastic deformations of the object under study are practically eliminated. For scanner calibration, different lateral (x,y) and vertical (z) standards are used. Measurements of lateral dimension can then be performed with angstrom resolution and measurements of vertical dimension in favourable cases can even reach sub-angstrom resolution.^[46, 47] The contrast in an AFM topography image is based on an arbitrarily chosen grey scale to indicate the relative heights of features on a surface. High features are assigned light shades and low features dark shades. A scale bar is usually provided whose black/white gradation serves to define the altitudes above zero (the mica surface carrying the sample).

Using AFM, dendritic structures have been studied on a variety of surfaces, such as mica^[49-51] graphite,^[50-52] glass,^[50] and charged solid surface.^[53] For instance, the aggregation of a polyether third-generation dendrimer on a mica surface was observed, when the surface was rinsed with a benzene solution of the dendrimer.^[49] Aggregation of flexible-type dendrimers recorded by AFM have been observed in other cases.^[54] Sheiko studied the adsorption and aggregation of carbosiloxane dendrimers on mica, glass, and graphite surface by casting a dendrimer solution in hexane, wherefrom the height of a single dendrimer molecule was obtained.^[50] By tapping mode AFM, Huck et al. studied films of aggregated fifth-generation metallodendrimers on mica and graphite, prepared by spin coating a dendrimer solution in nitroethane. The value of the height was half that of the calculated dendrimer which was attributed to flattening of the spherical metallodendrimers on the surface.^[51] Flattenings were also found in other flexible-type dendrimers.^[13, 55-57] For instance, in the tapping mode AFM,

images of giant-silicon dendrimers on graphite showed that the height of the monolayers were slightly lower than those calculated up to G5, whereas the height corresponds to a double layer of even more flattened dendrimers from G6 to G9. A precise understanding of why double layers form for the last generations is not yet obvious at present.^[13] Individual molecules of core-shell tecto(dendrimers) on mica by tapping mode AFM have been observed,^[56, 57] where these dendrimers flattened to the shape of a spherical cap. Moreover, the reduced thickness of dendrimer layers on a solid surface could be observed with flexible-type PAMAM dendrimers.^[55]

The thickness of layers of rigid-type second-generation polyphenylene dendrimers with various locations of dodecyl chains on graphite were also investigated by AFM, where the polyphenylene dendrimers changed their shape when absorbing on the surface and were flattened as well.^[54] The measured thickness of dendrimer layers was in the range of 0.7-1.6 nm while the calculated diameter from the computer simulation is 5.5 nm. The position of the alkyl chains did not change the flattening of the molecule on the surface.^[58] The alkyl chain had a strong adsorption energy with the graphite surface and in addition each phenylene ring contributed to the adsorption energy. The high available energy of attraction could be sufficient to bend the oligophenylene chains. Besides, the structures of second-generation polyphenylene dendrimers with various lengths of alkyl chains on graphite were studied,^[59] for which three different types of packing structures were observed: 1) granular regions, where individual dendrimers could be identified in a glasslike phase, 2) diffuse, homogenous regions, and 3) nanorod regions consisting of parallel rows.

Another second-generation polyphenylene dendrimer with sixteen -COOH groups on the periphery was deposited on mica by spin coating with different concentrations. The AFM showed that it aggregates on the order of three to eight molecular layers.^[60] The molecules of the second-generation dendrimer with sixteen -COOH groups easily aggregates through the formation of hydrogen bonds.

The AFM result of the general fourth-generation polyphenylene dendrimer (**1.15**) was quite different. This dendrimer **1.15** possesses neither alkyl nor functional groups, thus reducing the absorption energy of the dendrimer with the surface and decreasing the aggregation accordingly. When it was absorbed on freshly cleaved mica by spin coating a 10^{-8} M CH_2Cl_2 solution (at higher concentration aggregates formed), individual molecules with height 4.9 nm were observed.^[60, 61] The structure of this dendrimer in solution is that of a tetrahedron characterized by the four branches A,B,C and D (Figure 2.35-A); the most probable conformation of a single dendrimer **1.15** is the conformation in which three of the four

branches (B,C, and D) were in contact with the mica. The fourth branch is pointing away from the mica surface (Figure 2.35-A). The height of the molecule (from the centre of BCD triangle to the top A) in this case is 4.9 nm, which is in perfect agreement with the experimentally determined value.^[61] This indicates that the dendrimer **1.15** is quite rigid.

Here, in the collaboration with C.G. Clark, Jr. in Max Planck Institute für Polymerforschung two extended dendrimers G4-Td-(TiPS)₆₄ (**3.14**) and G5-Td-(TiPS)₁₂₈ (**3.16**) were explored by a tapping-mode AFM. Dendrimer solutions diluted to concentrations 10⁻⁶-10⁻⁹ g/mol were spin-deposited on to freshly cleaved mica (10 µL of solution on 1 cm² of surface). Mica was chosen as a surface to minimize the interaction between the surface and the dendrimers, thereby reducing strong flatter and aggregations. The spin coating method was used to achieve well separated single particles in order to gain information about the structure of individual extended arm polyphenylene dendrimers.

Topographical images of **3.14** (G4) on mica from dichloromethane solution (10⁻⁸-10⁻⁹ g/mol) showed large aggregates with sizes of 100 nm (Figure not shown). The image of **3.16** (G5) on mica from dichloromethane solution (10⁻⁶-10⁻⁷ g/mol) also indicated the presence of aggregates with a total diameter of ca. 310 nm and height of 11 nm (Figure is not shown here). A more dilute dichloromethane solution (10⁻⁸-10⁻⁹ g/mol) over the whole area of mica showed globular structures (aggregates). Figure 2.34-A presents a topographical image of one of the aggregates which may be described as the superposition of six lobes, forming two layers.

It proved to be difficult to find optimal conditions to observe a single particle in the AFM-image of the extended G4 and G5 dendrimers (**3.14** and **3.16** respectively) on mica after spin coating from dichloromethane solution. However, from THF solution (10⁻⁸-10⁻⁹ g/mol) well separated dendrimer molecules of **3.16** (G5) were attainable. In this case, the image showed mostly single particles and a few aggregates only on the whole area of mica. Figure 2.34-B presents a single dendrimer molecule **3.16** adopting the shape of a spherical cap with diameter of 24 nm and height of less than 5 nm.

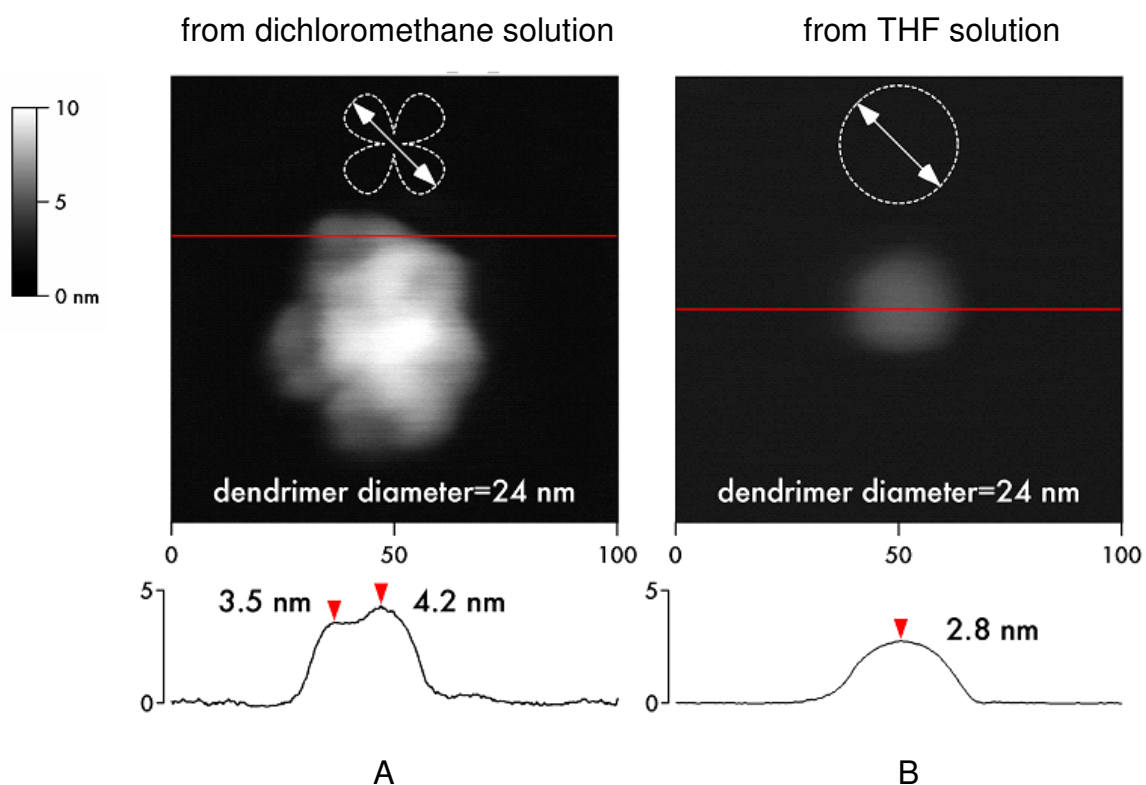


Figure 2.34: Tapping mode AFM image of **3.16** on mica after spin coating from highly diluted solutions in dichloromethane (**A**) and THF (**B**).

The interesting aspect of the AFM-image from dichloromethane solution (Figure 2.34-A) was that dendrimers **3.16** showed lobal shapes, which indicates that G5 on mica has the tendency to adopt a disposition of maximum contact with the surface, i.e. all four branching seem to be in contact with the mica (Figure 2.35-B). The absence of lobal shape in the AFM-image from THF solution suggests that the solvent influences the state of dendrimer in solution before spin coating onto the surface. Further investigations on this topic are in progress.

The diameter determined for **3.16** from THF solution (Figure 2.34-B) is in perfect agreement with the expected one (the radius of tip was 1 nm, the doubled radii for tip gave 2 nm, and the theoretical diameter of G5 is 22 nm, the sum generates the measured value 24 nm.). However, the height was found to be much smaller than the diameter, indicating that the dendrimer had a tendency to flatten on the surface.

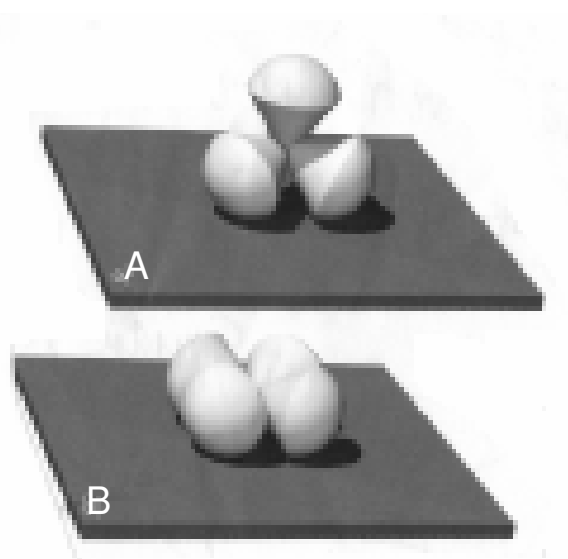


Figure 2.35: Cartoons of a general fourth-generation polyphenylene dendrimer (**1.15**) deposited on graphite (**A**), and the “exploded” fifth-generation polyphenylene dendrimer (**3.16**) on mica (**B**), (designed by C.G. Clark, Jr.)

This preliminary conclusion needs further support from future experimentation. Despite the aforementioned low density of exploded dendrimers, the conversion from spherical shape (fluid solution) to oblate shape with an axes ratio < 0.25 would require considerable internal rearrangement. While it is true that the flattened form depicted in Figure 2.35-B maximizes the number of benzene – supporting surface contact, this would call for a rehybridization of the core central carbon atom from tetrahedral to square planar. Tetracoordinate carbon of square planar coordination geometric is a much searched after goal which could only be reached under very special circumstances.^[62] With regards to the experimental evidence presented above it is surprising that the lateral diameter of **3.16** on mica matches that determined by other methods in fluid solution whereas the transition from spherical to oblate should engender an increase in this dimension. The precise determination of the vertical dimension of **3.16** on mica may suffer from the low material density at the surface of this exploded dendrimer. It should be recalled that in tapping mode AFM the response of the detecting system (the oscillating cantilever-tip combination) is governed by van der Waals forces between tip and sample. Since van der Waals forces correlate with the number of valence electrons present,^[46] the diluted state of matter at the surface of exploded dendrimers

possibly fakes a too small vertical dimension of the object under study. Flattening of adsorbed dendrimers has been observed repeatedly^[55, 63, 64] in the past although it rarely^[56, 57] reached the extent apparent from the AFM images of **3.16**. Admittedly in the previous cases the dendrimers possessed a normal material density at their surface with the result that the vertical dimension was traced more faithfully than in the case of the porous dendrimer **3.16**. Finally, the possibility of induced distortion of the dendrimer under study must be mentioned. Whereas this is held to be insignificant for tapping mode AFM, it may play a more important role for exploded dendrimer like **3.16** with very small interdendron steric hindrance.

Flattening of dendrimers upon adsorption has been previously predicted by Mansfield^[65] using Monte Carlo simulation where the analysis was based on the generation number (G) of dendrimers and the interaction strength (A) of the dendrimers with the surface. In any case, the sticky segments at or near the termini of the arms are more likely to be in contact than those near the core.^[65]

Since G5 (**3.16**) possess about 97% of free volume (density is 0.032 g/mL, see table in Chapter 5) its branching units have more space for the conformational movement. The porous structure and the attendant larger degree of conformational freedom of the exploded dendrimer **3.16** cause the adsorbed molecule to flatten as a result of van der Waals interaction. As was mentioned earlier, it is possible that the interaction between each branch in dendrimer **3.16** and the mica promotes flattening (Figure 2.35-B). It has been experimentally confirmed that the persistence length of single poly-*para*-phenylene with about 90 benzene rings in the chain is ca. 10 nm.^[66] Therefore, it is obvious that a certain bending of the dendrons in G5 could bring about maximum contact with the substrate. Although G5 is only slightly flexible locally, the large number of oligophenylene links cause small deformations to add up to a considerable extent over the molecule as a whole. Moreover, in this dendrimer, the reorganisation of tetraphenylbenzene groups^[67] and three-*para*-phenylene spacers may take place within the branching units, leading to more extensive flattening. However, the branched structure of the dendron does not allow bending as high as in the case of a single oligo-*para*-phenylene chain. This explains why the observed diameter of **3.16** is in agreement with theoretical one.

Open questions include the following: what is the effect of the solvent on the shape of dendrimers in the dissolved and the adsorbed state? Is the very extensive flattening, **3.16** experiences according to the result of AFM measurements, real? Can the tapping-mode induce deformations of the sample be confidently excluded?

Notwithstanding, whereas AFM analysis of the vertical dimension of absorbed **3.16** needs further refinement the lateral dimension determined for **3.16** nicely ties with the results of other methods of investigation.

2.14 Guest molecules and their monitoring by the quartz microbalance (QMB) technique

Host-guest chemistry involves the binding of a substrate molecule (guest) in a receptor molecule (host). Since dendrimers are macromolecules with very well-defined chemical structures, their cavities can be used as binding sites for small guest molecules, analogous to the way enzymes (natural catalysts) work in living organisms. The possibilities for encapsulating guest molecules in dendritic hosts were proposed by Maciejewski in 1982^[68] In 1990 Tomalia presented evidence for "unimolecular encapsulation" of guest molecules in dendrimers and pointed out that it was one of the possible future research areas in dendrimer chemistry.^[69]

Unlike linear polymers possessing random-coil structures the three-dimensional motif of dendrimers imparts to them unique structural features. Compared to the relatively open structures of lower generation dendrimers, at high generations they tend to adopt a spherical surface with pockets in the interior, thus acting as "unimolecular" micelles capable of guest inclusion.^[70] These empty spaces within the dendritic infrastructures may be envisioned as "dendritic voids."

Meijer and co-workers were the first to demonstrate physical encapsulation and release of guest molecules from a "dendritic box."^[61] Nowadays the inclusion of guest molecules into dendrimers, featuring flexible branching units, are studied widely.^[69, 72, 73]

The use of dendrimers as hosts or carriers of smaller guest molecules and the development of host-guest binding motifs in dendrimers aiming at biological applications have been extensively reviewed.^[74] However, the flexible dendrimers require a larger number of generations to possess a rigid, nonfluctuating core consisting of the stretched first few generations and in those all weak fluctuations take place at the outermost part of the molecule.^[75] The unique aspect of the rigid dendrimers is that they contain stable voids even at lower generation number. For instance, the investigation of the crystal structure of different polyphenylene dendrimers of the first generation has revealed that solvent molecules are readily trapped within these cavities.^[13, 76] As an other example, the iptycene dendrimer (**1.4**)

incorporates solvent molecules within its cavity, as was determined by X-ray structural analysis.^[77]

This property of polyphenylene dendrimers makes them attractive as selective layers for gravimetric sensors. Such sensors which are parts of the quartz microbalance (QMB)^[78] are widely used to monitor the concentration of various volatile organic compounds (VOCs) in different environments. Polyphenylene dendrimers are ideally suited as host molecules, since they contain stable cavities in their interior.^[79]

In the QMB technique, the dendrimer is dissolved in THF, accelerated by a high voltage through a thin capillary and sprayed onto the top electrode of the QMB. This leads to the formation of a homogeneous, rigid layer. The thickness of the layer is controlled *in situ* by simultaneously monitoring the frequency of the QMBs to be coated. The resulting thickness is standardized corresponding to a frequency reduction of 10 kHz, at which point the coating is stopped. According to Sauerbrey^[80] this offset is equal to a mass of 44 $\mu\text{g cm}^{-2}$ of the coating on a 10 MHz QMB.^[79, 81] A standardized thickness (or mass) of the host compound on the sensor is a prerequisite for comparing the sensitivity and selectivity of the coatings and to assure reproducible results. In QMB studies coated sensors have been sequentially exposed to different VOCs in a gas mixing chamber with N_2 at 30-50°C and at a highest possible concentration (400-1000 ppm). The associated lowering of the resonance frequencies of the QMBs caused by the reversible incorporation of the VOCs into the host compounds is termed the sensor response, $\Delta\nu$. The sensor responses are totally reversible and reproducible. The measurement of the frequency shift ($\Delta\nu$) allows the calculation of the number of guest molecules in the respective dendrimer (Table 2.5) with following formulas:^[79]

$$N_g = (\Delta\nu \cdot 4.4 \cdot 10^{-9} \cdot N_A) / M_A \quad (\text{eq. 2.1})$$

$$N_{\text{c.d.}} = (4.4 \cdot 10^4 \cdot N_A \cdot 10^{-9}) / M_d \quad (\text{eq. 2.2})$$

where N_g = number of guest molecules,

N_A = Avogadro's number ($6.024 \cdot 10^{23}$),

M_A = molecular mass of analyte (guest),

M_d = molecular mass of dendrimer (host), and

$N_{\text{c.d.}}$ = number of coating dendrimer molecules.

Using the general branching unit **1.7**, polyphenylene dendrimers with various cores, generation numbers and functional groups have been subjected to the QMB measurement.^[79]

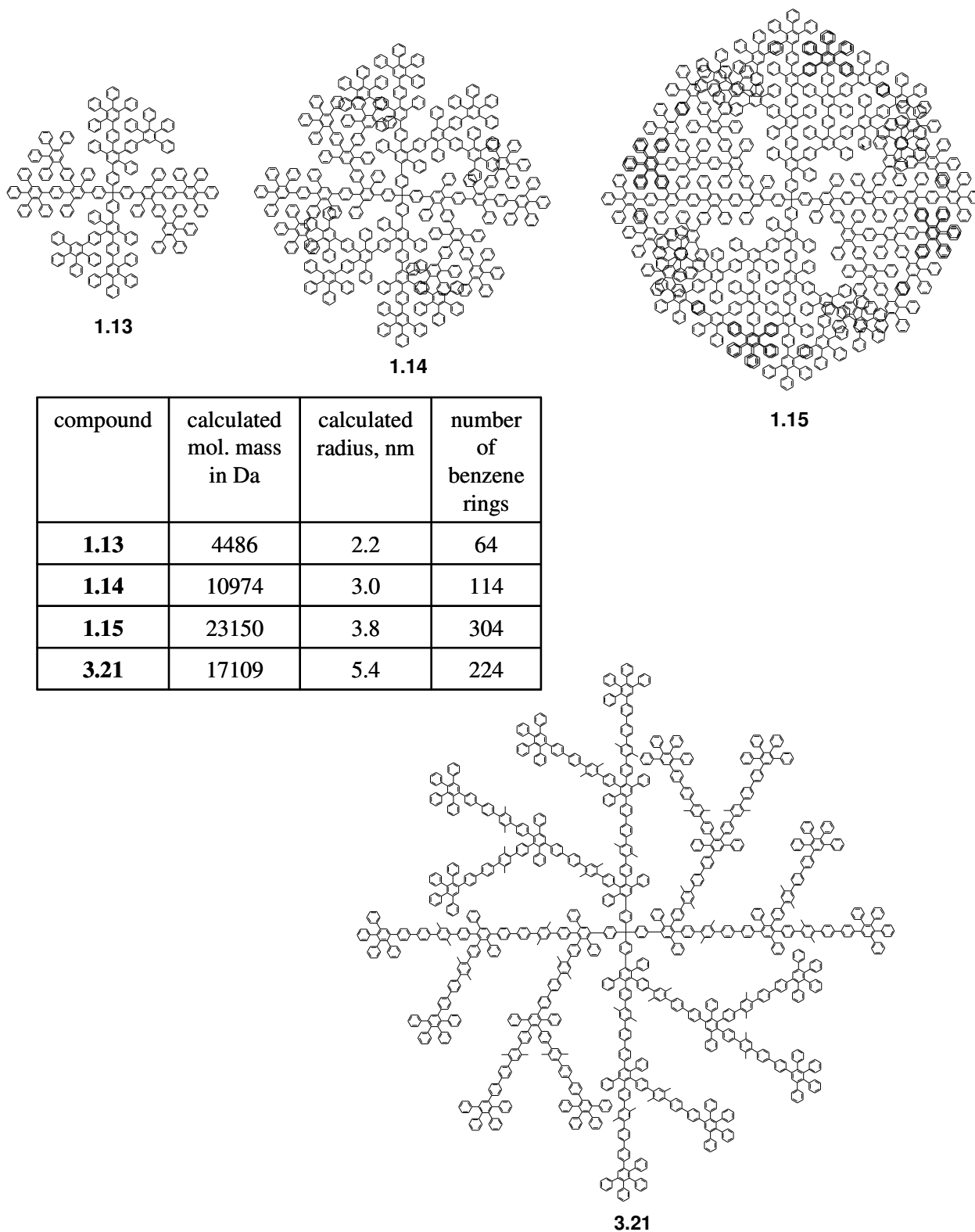
It was observed that the unsubstituted PDs responded selectively to polar aromatic VOCs,

such as acetophenone, aniline, benzaldehyde, benzonitrile, nitrobenzene, fluorobenzene, 2-methylbenzonitrile. The selectivity of PDs is attributed to their aromatic skeletons which can form π - π -electron-donor-acceptor complexes.^[79] In other words, the host-guest binding is assumed to be mediated through π - π interaction between the electron-rich polyphenylene of the dendrimers and the aromatic guests, which are electron-deficient because of the presence of electron withdrawing functional groups. This type of donor-acceptor stabilization is absent in the case of electron-rich aromatic substrate. In fact, in the case of electron-rich hosts and guests, mutual interactions would be limited to very weak van der Waals forces only.

In the present work it was of interest to compare the extended dendrimers with their shorter counterparts. Thus, the new extended third-generation dendrimer **3.21** (Scheme 2.9) was prepared, where the branching unit **3.1** was used for the synthesis of 1st and 2nd generations, and tetraphenylcyclopentadienone (**1.9**) for the last (3rd) generation. According to molecular modelling, the diameter of **3.21** is more than twice as large as that of previously described third-generation dendrimer **1.14**.

In collaboration with Ch. Kreutz in Bargon's group (Bonn University), the extended dendrimer **3.21** was subjected to QMB measurement with five chosen analytes: acetophenone, benzaldehyde, aniline, nitrobenzene and benzonitrile, and the results are depicted in Table 2.5 and Figure 2.36. Because of the lack of numerical data for the former PDs (**1.13**, **1.14**, and **1.15**) their values were derived approximately from Figures 35 and 37 of the Schlupp dissertation.^[81]

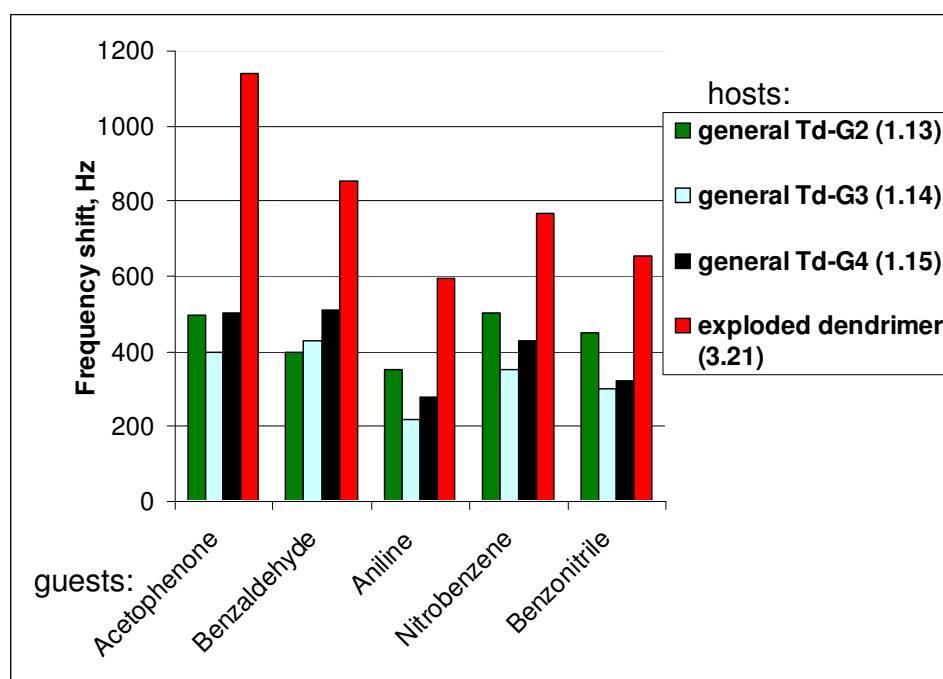
Comparing the two third-generation dendrimers **1.13** and **3.21** from Figure 2.36, the larger magnitude of the frequency shift indicates that the new dendrimer **3.21** incorporates far more guest molecules than **1.14**. It should be mentioned that for the coatings the same amount of dendrimer substance was used (standardization to a frequency reduction of 10 MHz, see page 71), and hence the number of molecules of the extended dendrimer **3.21** on the surface is less (Table 2.5). Nevertheless, the extended dendrimer coating absorbs more acetophenone molecules which formed from the short-arm counterpart **1.14**.



Scheme 2.9: Dendrimers used for QMB measurements of VOC incorporation.

Table 2.5.

Analyte its molecular mass in g/mol (its concentration in ppm)	Frequency shift, $\Delta\nu$, Hz		$N_{c.d.}$ Number of coating dendrimer molecules; units of 10^{12}		N_g Number of guest molecules; units of 10^{12}		ratio guests/hosts ($N_g / N_{c.d.}$)		ratio 3.21/ 1.14
	1.14	3.21	1.14	3.21	1.14	3.21	1.14	3.21	
Acetophenone 120.1 (400)	400	1141	2414	1550	8828	25181	3.66	16.25	4.44
Benzaldehyde 106.6 (800)	430	852			10742	21284	4.45	13.73	3.09
Aniline 93.1 (400)	220	595			6263	16940	2.60	10.93	4.21
Nitrobenzene 123.1 (200)	350	766			7536	16493	3.12	10.64	3.41
Benzonitrile 103.1 (700)	300	655			7716	16839	3.20	10.86	3.40

Figure 2.36: Comparison of the sensor responses of four host compounds **1.13**, **1.14**, **1.15**, and **3.1** to selected guests.

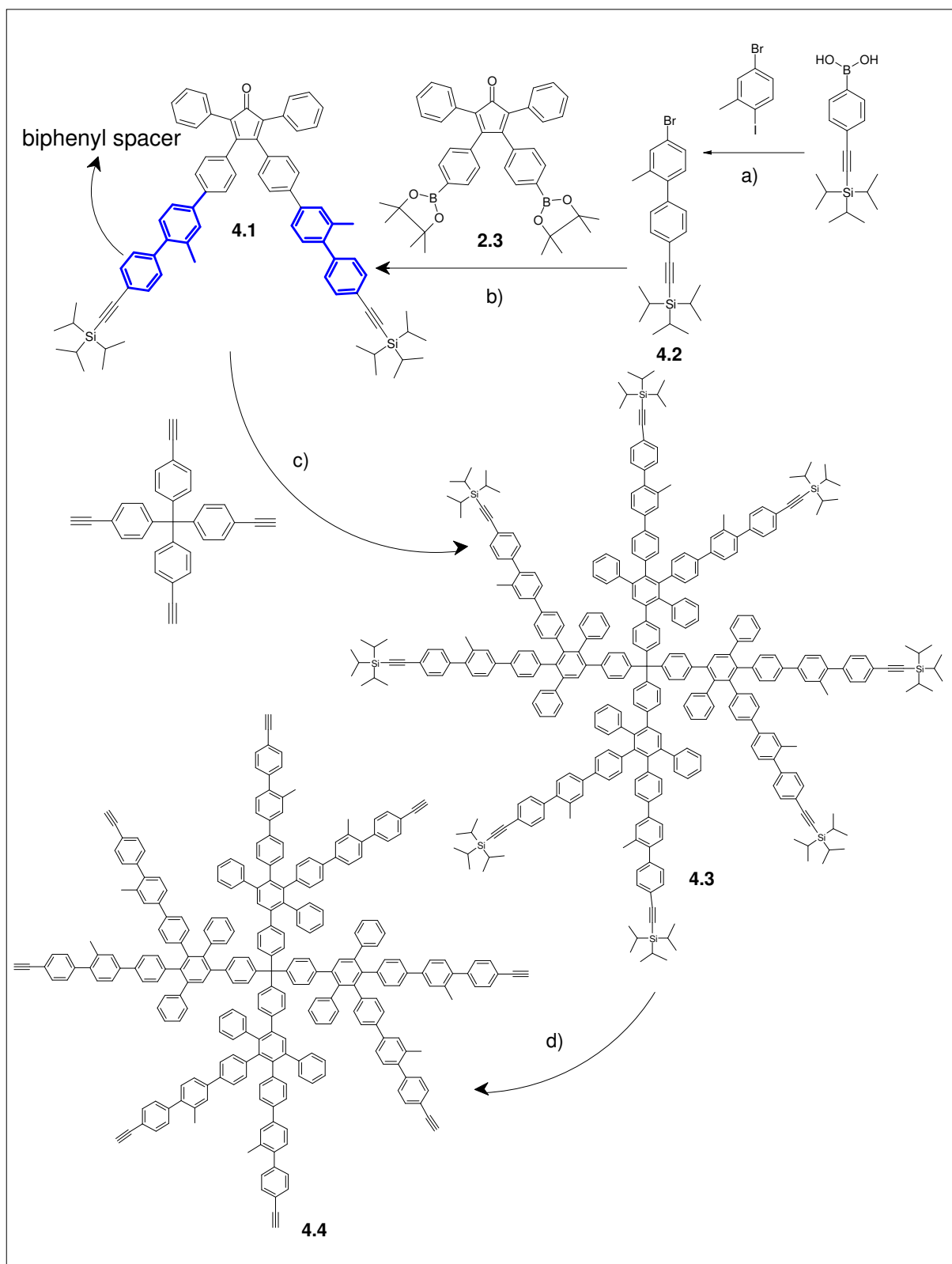
From the results compiled in Table 2.5 and the representation in Figure 2.36 it is seen that, although the ratio of molecular masses of the exploded dendrimer **3.21** to that of the short-arm dendrimer **1.14** amounts to 1.5 and the ratio of benzene rings present takes the value of 2.0, the number of incorporated guests per exploded host molecule exceeds that of the short-arm host by a factor 3.7. In a crude manner, this number may be equated to the ratio of accessible voids in both types of hosts. The pictorial representation in Figure 2.36 lends plausibility to this notion. Interestingly, and contrary to expectation, the number of incorporated guest per host appears to be nearly independent of the nature of the guest. Thus, the number of guests per host in case of **1.14** as a host amounts to 2.6 for aniline and 3.1 for nitrobenzene. For **3.21** as a host the respective numbers are 10.9 for aniline and 10.6 for nitrobenzene. Therefore, electron-donating and electron-withdrawing substituents do not markedly affect the tendency of a benzene derivative to be incorporated into the dendrimer scavenger. Admittedly, selectivity for guest molecules with strongly deviating electron density in the arene part would not have been expected from hosts which feature hydrocarbon framework devoid of polar functional groups.

The results also indicate that the guest molecules adopt positions inside the dendrimer rather than at the periphery. This is because for equal masses of adsorbed dendrimer the relation $N_{c,d}(\mathbf{3.21}) < N_{c,d}(\mathbf{1.14})$ holds. Therefore adsorbed **3.21** exposes a smaller surface than **1.14** to arriving VOCs. Nevertheless, the gradation $N_g(\mathbf{3.21}) > N_g(\mathbf{1.14})$ is observed, which requires guests to be bonded in the interior rather than at the periphery of the host dendrimer **3.21**.

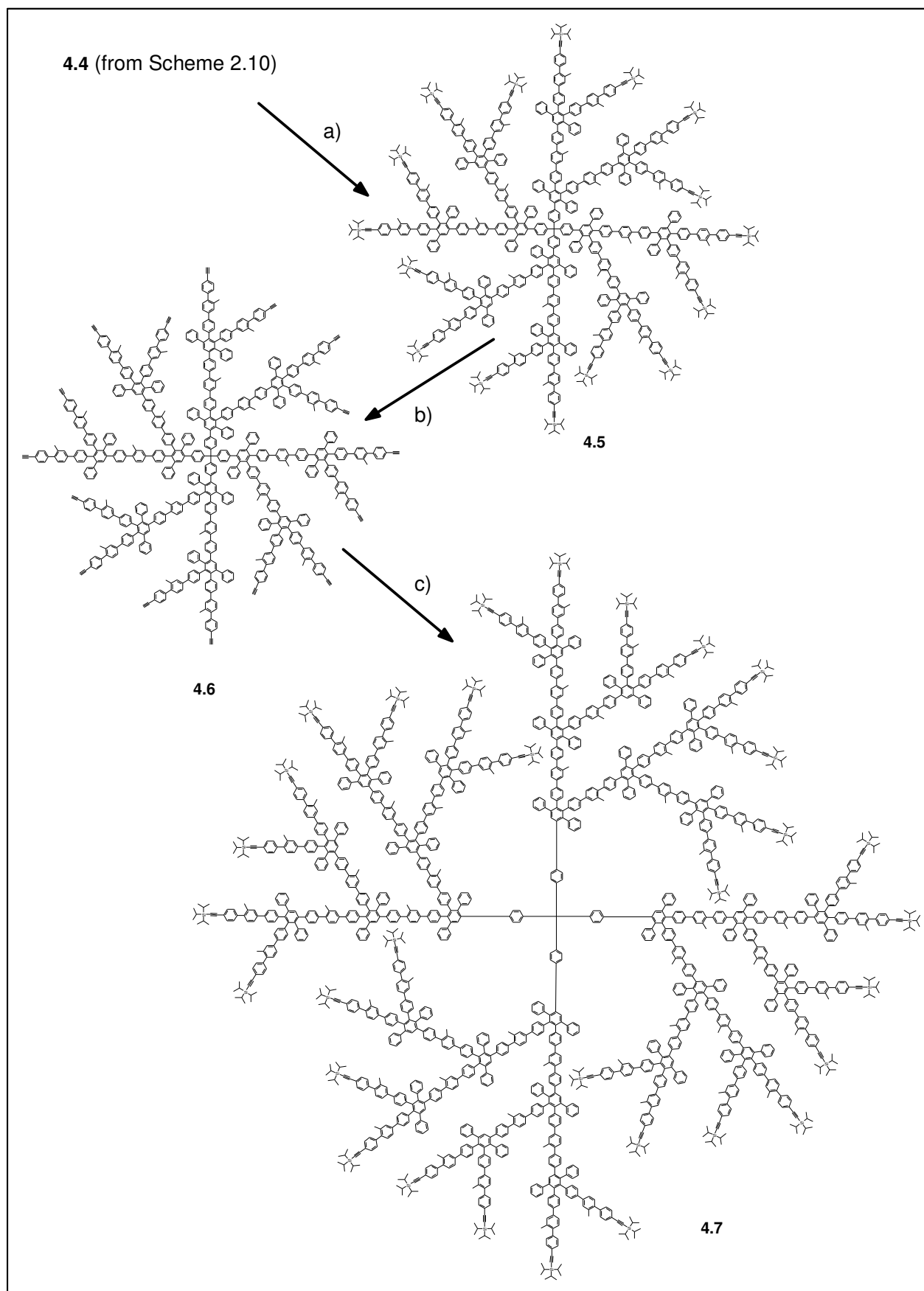
2.15 Shortening the arms slightly: “semi-extended” dendrimers bearing a biphenyl-instead of a terphenyl spacer

Judging from the results presented in Section 2.14, the application of the extended polyphenylene dendrimers (PDs) at low generations (**3.10**, **3.12**) appears promising for the field of host-guest chemistry. This is because the extended dendrimer **3.21** incorporates significantly more guest molecules than the general PDs with branching unit **1.7**. However, the synthesis of the *para*-terphenylene spacer (branching unit **3.1**) for this application is tedious and its scaling up would be very expensive. With this in mind the extended building block **3.1** should be modified. For this, a new building block **4.1** which has a biphenyl spacer (Scheme 2.10) is proposed. The “semi-extended” dendrimers with unit **4.1** could mimic the physical properties of those containing the unit **3.1** at low generations (**3.10** and **3.12**).

The synthesis of **4.1** required a few steps only. As starting material in this route serves inexpensive commercially available 2-iodo-5-bromotoluene (Scheme 2.10). It couples to (4-triisopropyl-silylethynyl)-phenylboronic acid^[82] via a Suzuki reaction analogously to the literature procedure,^[83] forming the new arm **4.2**, which is now ready for the synthesis of the branching unit **4.1**. All spectra of **4.1** confirmed its high purity. At the time of writing, **4.1** has been used for Diels-Alder cycloadditions to grow dendrimers up to the third generation (Scheme 2.11) analogously to the syntheses of the "exploded dendrimers". During this exploratory stage, 1 g of the branching unit **4.1** has been prepared (Experimental section); the protocol can readily be scaled up as demonstrated by ongoing work in this laboratory which supplied 20 g of **4.1**.^[84]



Scheme 2.10: Synthesis of the branching unit **4.1** and the first-generation semi-extended dendrimers with biphenyl spacers; a) $\text{Pd}(\text{OAc})_2$, PPh_3 , Na_2CO_3 , acetone, water, 53%; b) K_2CO_3 , $\text{Pd}(\text{PPh}_3)_4$, toluene, water, EtOH, reflux, 53%; c) *o*-xylene, reflux, 84%; d) tetrabutylammonium fluoride trihydrate, THF, r.t. 80%.



Scheme 2.11: Synthesis of the second- and third-generation dendrimers with biphenyl spacers; a) *o*-xylene, **4.1**, reflux, 88%; b) tetrabutylammonium fluoride trihydrate, THF, r.t., 81%; c) *o*-xylene, **4.1**, reflux, 84%.

2.16 Characterization of the dendrimers with biphenyl spacer

All methods of characterization, such as MALDI-TOF, SEC, ^1H and ^{13}C NMR spectroscopy, of the 1st-3rd generation dendrimers with biphenyl spacers (**4.3-4.7**) showed their monodispersity and purity. Their data are presented in the Experimental part.

Most importantly, the MALDI-TOF mass spectrum for the protected second-generation dendrimer **4.5** with biphenyl spacers (Figure 2.37-A) in addition the molecular peak M^+ (Calcd. 11744; found 11709) also showed peaks pointing to the presence of oligomers, just as in the case of **3.10** (Figure 2.5-B, Chapter 2.5). The combination of MALDI-TOF MS and SEC confirmed its monodispersity.

MALDI-TOF MS of the third-generation dendrimer **4.7** (Figure 2.37-B) gave a single peak, where its molecular mass (26064 Da) is in good agreement with the theoretical one (26055 Da).

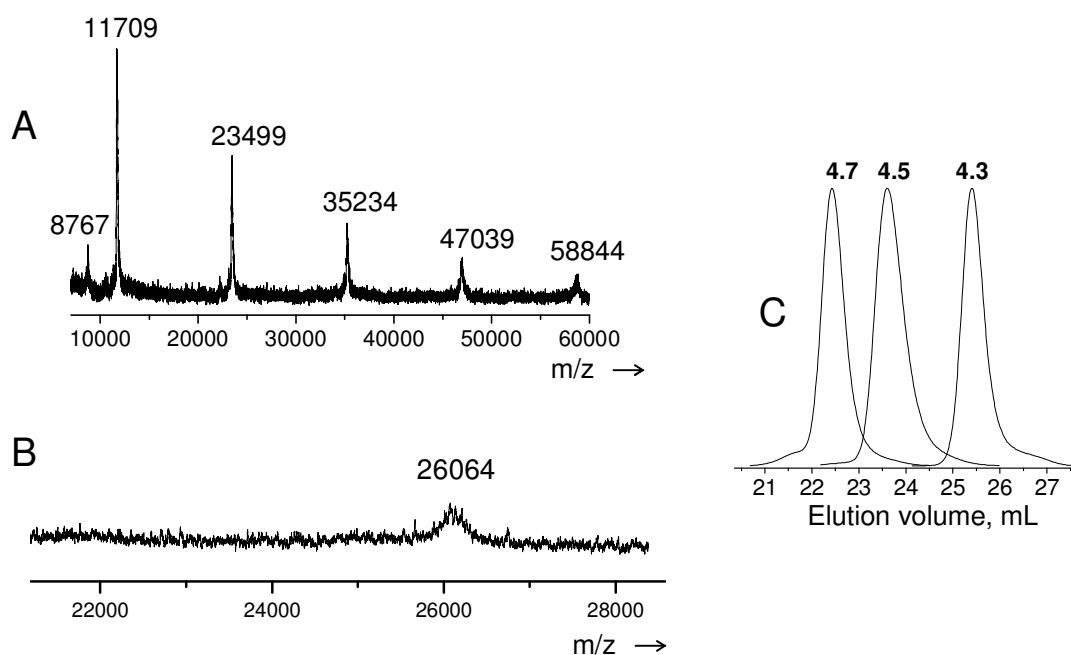


Figure 2.37: **A** - MALDI-TOF MS of the second-generation dendrimer with a biphenyl spacer (**4.5**), linear mode, dithranol, without salt; **B** - MALDI-TOF MS of the third-generation dendrimer with biphenyl spacer (**4.7**), linear mode, dithranol, without salt; **C** - SEC of G1-G3 dendrimers with biphenyl spacers (**4.3**, **4.5**, and **4.7**).

The hydrodynamic radii (from DLC) of dendrimers with biphenyl spacers up to generation three (**4.3**, **4.5**, and **4.7**) were also determined; they are quite similar those with *para*-terphenyl spacers (Figure 2.38-B). Molecular models of the third-generation dendrimers with various branching units (**3.1**, **4.1** and **1.7**) are compared in Figure 2.38-A, which again shows that the dendrimers **4.7** and **3.12** have a more porous structure than **1.14**.

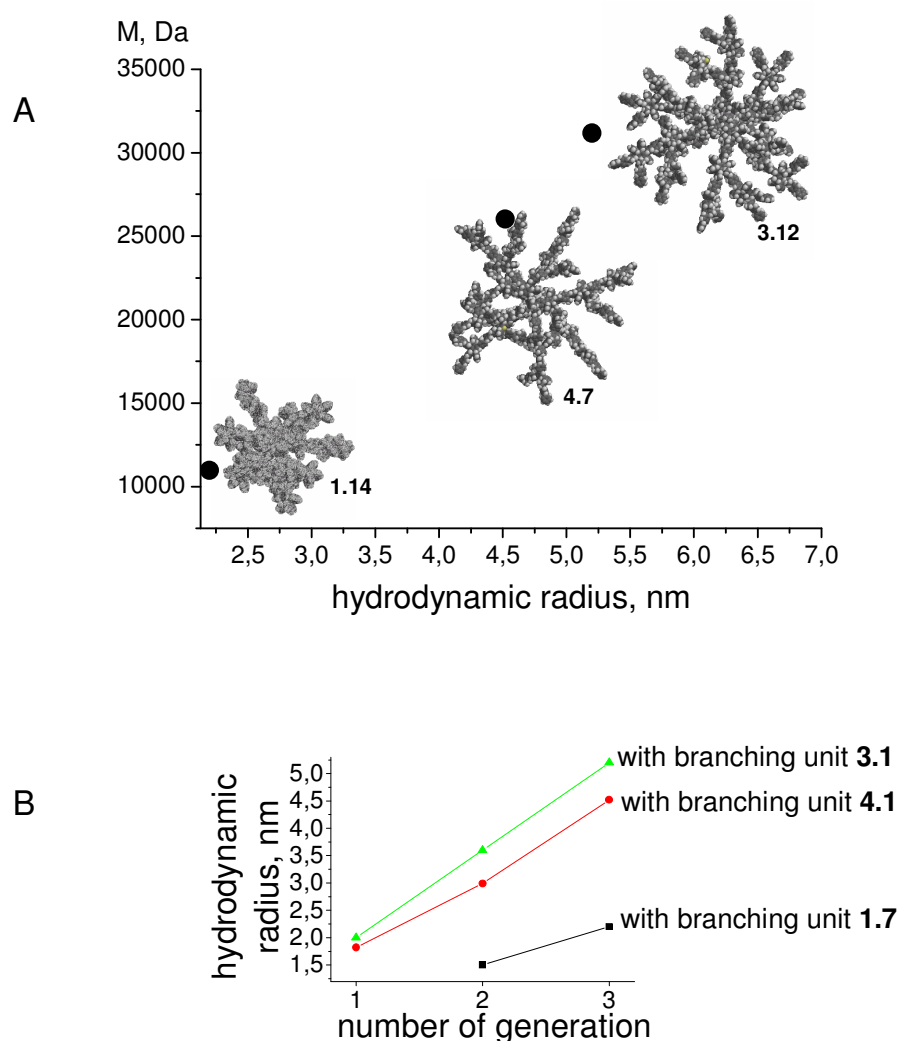


Figure 2.38: **A** – Space filling molecular models of the three third-generation dendrimers **1.14**, **4.7**, and **3.12** with different branching units, their comparison in term of molecular masses and hydrodynamic radii; **B** – Comparison of size for **1.14**, **4.7**, and **3.12** based on DLS results.

Thus, the dendrimers with biphenyl spacers which have been synthesized up to the third generation appear not to differ strongly from those with terphenyl spacers. The much greater

ease of synthesis renders the biphenyl-spacered, “semi-extended” dendrimers attractive for future applications.

2.17 Outlook: dendrimers with biphenyl spacers for future applications

To put the size of the new giant dendrimers into perspective, it is instructive to compare them with some objects which can be easily realized (Figure 2.39). The diameters of a human hair, seen by the unarmored eye, is 0.1 mm, the length of a bacterium (1 μm) and the length of most viruses (100 nm) vary by factors of ten. The wavelength of visible light (400-700 nm) lies between the latter two entities, and bacteria can be observed with light microscopy while viral particles cannot. Most cellular proteins (diameter), for example, cytochrome (4 nm), hemoglobin and immunoglobulin (5.5 nm), prealbumin (6.7 nm), hemerythrin (8 nm), DNA 2.4 nm, histone 10 nm^[57, 85] are ten times smaller than a virus.

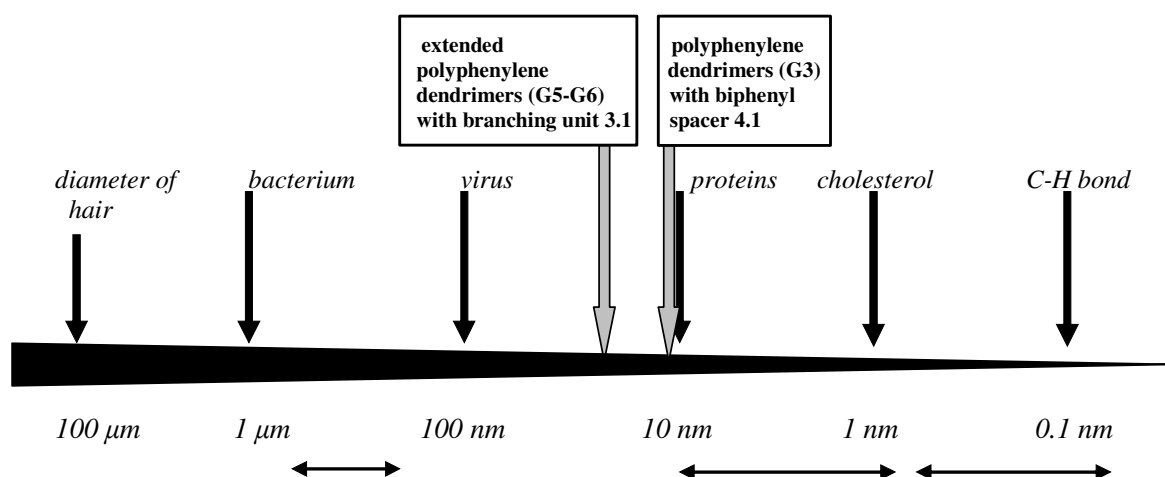


Figure 2.39: Size comparison of dendrimers with biological molecules (taken from ref.^[85]).

The size of most organic molecules that are synthesized in the laboratory do not exceed 1 nm. The length of a carbon-hydrogen bond is 0.1 nm. Dendrimers typically fall in the range of 3-10 nm in diameter. Therefore, dendrimers are sometimes referred to as artificial proteins and they led many researchers to engineer protein-like function into these molecules,^[85] including catalysis (enzyme-like catalysis,^[86] light harvesting,^[87] drug delivery,^[88] surface engineering^[89]).

The extended sixth-generation polyphenylene dendrimer (**3.18**) with diameter of 26 nm exceeds the size of most proteins and the size of all known giant dendrimers. The third generation dendrimer (**3.12**) with branching unit **3.1** has some nice aspects:

- its calculated diameter (14 nm) reaches that of the eighth- and tenth-generation dendrimer of the PAMAM-type (Figure 2.32),
- larger cavities are present than in the general PDs with branching unit **1.7** (Chapter 2.14).

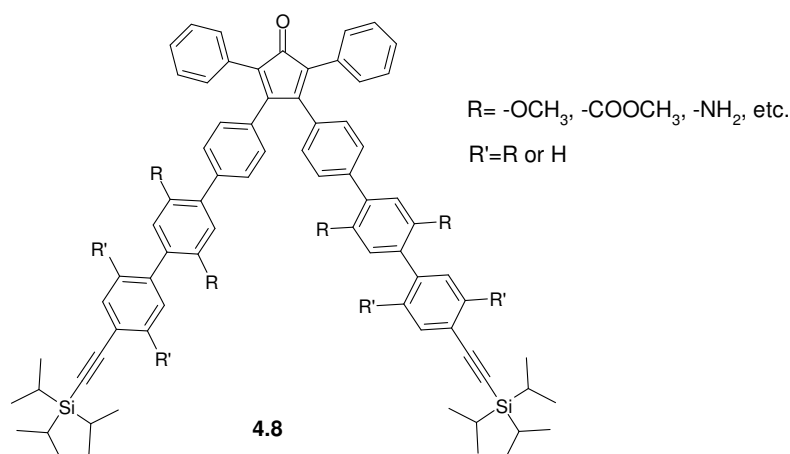
The use of exploded dendrimers could be interesting; however as was stressed above, their synthesis is demanding and costly. On the other side, more economical third-generation dendrimers with biphenyl spacer could seriously be considered for practical use, since the diameter of **4.7** (11 nm) is similar to that of **3.12** (14 nm).

The applications alluded to above must take into account the specific features of the novel extended arm dendrimers reported in this work, namely their hydrocarbon-based nature, shape persistence, content of large internal cavities with diameter in the 2-3 nm range and their surface porosity. The latter property suggests that de Gennes dense packing, which usually furnishes giant dendrimers with an impermeable surface, in the present case is absent, thereby allowing transfer of material into and out of these dendrimers. Therefore it is conceivable that they can incorporate, transport and release large guest molecules. For this process, considerable size selectivity may be envisaged. This can be derived from the fact that the enthalpic contribution to host-guest binding will be small, essentially arising from weak van der Waals and π - π interactions. More important is the entropic contribution which favors the incorporation per cavity of one large size-adapted molecule over that of several small molecules.

The preparation of functionalized dendrimers is a key step towards various applications. Depending on the particular purpose, functional groups are introduced at the core, at the periphery or both. For general polyphenylene dendrimers (with branching unit **1.7**) major functional groups have been attached to their periphery such as bromo-, cyano-, amino-, lithium-, carboxyl-, methoxyl-, and chromophore- groups. The latter type is also known as a core, resulting in topological isolation of the chromophore and therefore its protection from the environment.^[90]

However, the specific incorporation of functional groups at the interior regions of dendrimer represents a considerable synthetic problem.^[91] Just a few PDs with functional groups at the interior^[92-94] have been obtained. For instance, a second-generation dendrimer with eight inner

benzophenone functional groups could be synthesized and the chemical transformation of the keto groups into triphenylmethanol- or diphenylpyrenylmethanol- derivatives, using organolithium reagent with high yields has been performed.^[92] Other polyphenylene dendrimers up to the second generation with internal $-\text{COOCH}_3$ groups^[93] were easily converted into $-\text{COOH}$ and removed by CuO .^[93] The installation of a sugar bearing protective groups inside the rigid dendrimers and their conversion into active groups was achieved.^[94] All these PDs showed that there is little steric hindrance for internal chemical reactions. From molecular modeling (Figure 2.38-A), it is seen that the third-generation dendrimer with biphenyl spacer (**4.7**) has a more open structure and contains more cavities than the standard PDs with branching unit **1.7**. It is promising to explore the chemical reactivity inside the new extended dendrimer with biphenyl spacer. For that purpose a new branching unit **4.8** (Scheme 2.12) with biphenyl spacer, containing functional groups at phenyl rings, may be envisaged, since aromatic boron derivative, used in the synthesis of these branching units, are tolerant towards many functional groups.



Scheme 2.12: A potential new branching unit with a substituted biphenyl spacer bearing various functional groups for specific applications.

The new building block **4.8** is designed as $\text{AB}_2\text{RR}'$, where R and R' are functional groups. In this case, the number of functional groups can be controlled. Internal functionalization can dramatically increase the degree of complexity that can be implemented into a dendrimer macromolecule, and therefore, promises to lead to “smart” materials for future use in bio- and nanotechnologies.^[92]

In general, dendrimers, bearing interior functional groups and cavities are expected to bind guest molecule selectively, depending on the nature of the guest, its size, and the structure and chemical composition of the terminal groups. The driving force for guest encapsulation within dendrimers can be based on electrostatic interaction, covalent bonding, steric confinement, various types of weaker forces (van der Waals, hydrogen bonding, the hydrophobic force etc.), and combinations therefrom.^[73]

The presence of -OH or -NH₂ groups inside the polyphenylene dendrimers is expected to form hydrogen bonds with a guest molecule. In this case selective incorporation of guest molecules should be possible.

2.18 Literature for Chapter 2

1. T. Weil; U.-M. Wiesler; A. Herrmann; R. Bauer; J. Hofkens; F. C. De Schryver; K. Müllen. *J. Am. Chem. Soc.* **2001**, *123*, 8101-8108.
2. a) X. Watanabe; N. Miyaura; A. Suzuki. *Synlett.* **1992**, 207-210; b) K.A. Smith; E.M. Campi; W.R. Jackson; S. Marcuccio; C.G.M. Naeslund; G.B. Deacon. *Synlett.* **1997**, 131-132.
3. a) A. Godt. *Org. Chem.* **1997**, *62*, 747; b) O. Lavastre; P. Ollivier; P.H. Dixneuf; *Tetrahedron.* **1996**, *52*, 15, 5495; c) S. Ito; M. Wehmeier; J.D. Brand; C. Kübel; R. Epsch; J.P. Rabe; K. Müllen. *J. Chem. Eur.* **2000**, *6*, 23, 4327; d) A. Fechtenkötter; N. Tchegotareva; M. Watson; K. Müllen. *Tetrahedron.* **2001**, *57*, 3769.
4. a) P. Liess; V. Hensel; A.-D. Schlüter. *Liebigs Ann.* **1996**, 1037-1040; b) V. Hensel; A.-D. Schlüter. *J. Chem. Eur.* **1999**, *5*, 421-429; c) G. W. Gray; M. Hird; D. Lacey; K.J. Toyne. *J. Chem. Soc. Perkin Transactions II.* **1989**, 2041-2053; d) G. Manickam, A.-D. Schlüter. *J. Org. Chem.* **2000**, 3475-3481.
5. B.C. Berris; G.H. Hovakeemian; Y.-H. Lai; H. Mestdagh; K.P.C. Vollhardt. *J. Am. Chem. Soc.* **1985**, *107*, 5670-5687.
6. J. Peterson; V. Allikmaa; J. Subbi; T. Pehk; M. Lopp. *European Polymer Journal.* **2003**, *39*, 33-42.
7. U.-M. Wiesler; A.J. Berresheim; F. Morgenroth, G. Lieser; K. Müllen. *Macromolecules.* **2001**, *34*, 187-199.
8. K.L. Walker; M.S. Kahr; C.L. Wilkins; Z. Xu, J.S. Moore. *J. Am. Soc. Mass Spectrom.* **1994**, *5*, 731-739.

9. a) U.-W. Wiesler. Ph-D dissertation, University of Mainz, **2000**; b) T. Weil. Ph-D dissertation, University of Mainz, **2002**; c) S. Bernhardt. Ph-D dissertation, University of Mainz, **2005**.
10. L. Ulmer; J. Mattay; G. Torres-Garcia; H. Luftmann. *Eur. J. Mass. Spectrom.* **2000**, 6, 49-52.
11. K. Takagi; T. Hattori; H. Kunisada; Y. Yuki. *J. Polym. Science: Part. A: Polymer Chemistry.* **2000**, 38, 4385-4395.
12. J.C. Blais; C.O. Turrin; A.M. Caminade; J.P. Majoral. *Anal. Chem.* **2000**, 72, 5097-5105.
13. J. Ruiz; G. Lafuente; S. Marcen; C. Ornelas; S. Lazare; E. Cloutet; J.-C. Blais; D. Astruc. *J. Am. Chem. Soc.* **2003**, 125, 7250-7257.
14. F. Sournies; F. Crasnier; M. Graffeuil; J.-P. Faucher; R. Lahana; M.-C. Labarre; J.-F. Labarre. *Angew. Chem., Int. Ed. Engl.* **1995**, 34, 5, 578-579.
15. a) D.A. Tomalia; H. Baker; J. Dewald; M. Hall; G. Kallos; S. Martin; J. Ryder; P. Smith. *Macromolecules.* **1986**, 19, 9. b) B.L. Schwartz; A.L. Rockwood; R.D. Smith; D.A. Tomalia; R. Spindler. *Rapid Comm. In Mass Spectrometry.* **1995**, 9, 1552-1555. c) L.P. Tolic; G.A. Anderson; R.D. Smith; H.M. Brothers II; R. Spindler; D.A. Tomalia. *Int. J. Mass Spect. And Ion Processes.* **1997**, 165/166, 405-418.
16. J.-P. Majoral; A.-M. Caminade. *Chem. Rev.* **1999**, 99, 845-880
17. M.-L. Lartigue; B. Donnadiou; C. Galliot; A.-M. Caminade; J.-P. Majoral; J.-P. Fayet. *Macromolecules.* **1997**, 30, 7335-7337.
18. M. Frank; S.E. Labov; G. Wesrmacott, W.H. Benner. *Mass Spectrometry Reviews.* **1999**, 18, 155-186.
19. R.J. Wenzel; U. Matter; L. Schultheis; R. Zenobi. *Anal. Chem.* **2005**, 77, 4329-4337.
20. D.A. Tomalia; A.M. Naylor; W.A. Goddard. *Angew. Chem., Int. Ed. Engl.* **1990**, 29, 138-175.
21. B. Klajnert; M. Bryszewska. *Acta Biochimica Polonica.* **2001**, 48, 1, 199-208.
22. G.R. Newkome; C.N. Moorefield; F. Vögtle. *Dendrimers and dendrons.* **2001**, Wiley-VCH.
23. H.F. Chow; Z.Y. Wang; Y.F. Lau. *Tetrahedron.* **1998**, 54 (45), 13813-13824.
24. a) V. Percec; W.-D. Cho; M. Möller; S.A. Prokhorova; G. Ungar; D.J.P. Yeardley. *J. Am. Chem. Soc.* **2000**, 122, 4249-4250; b) V.S.K. Balagurusamy; G. Ungar; V. Percec; G. Johansson. *J. Am. Chem. Soc.* **1997**, 119, 1539-1555.

25. a) C. L. Jackson; H. D. Chanzy; F. P. Booy; B. J. Drake; D. A. Tomalia; B. J. Bauer; E. J. Amis. *Macromolecules* **1998**, *31*, 6259-6265; b) M. Slany; M. Bardaji; M.-J. Casanove; A.-M. Caminade; J.-P. Majoral; B. Chaudret, *J. Am. Chem. Soc.* **1995**, *117*, 9764-9765.
26. C. Ornelas; D. Mery; J.-C. Blais; E. Cloutet; J.R. Aranzaes; D. Astruc. *Ang. Chem., Int. Ed. Engl.* **2005**, *117*, 7565-7570.
27. S.M. Aharoni; C.R. Crosby III; E.K. Walsh. *Macromolecules*. **1982**, *15*, 1093-1098.
28. C.J. Hawker; J.M.J. Frechet. *J. Am. Chem. Soc.* **1990**, *112*, 7638-7647.
29. T.P. Bender; Y. Qi; P. Desjardins; Z.Y. Wang. *Can. J. Chem.* **1999**, *77*, 1444-1452.
30. M.E. Piotti; F. Rivera; R. Bond; C.J. Hawker; J.M.J. Frechet. *J. Am. Chem. Soc.* **1999**, *121*, 9471.
31. I. Sendijarevic; A.J. McHugh. *Macromolecules*. **2000**, *33*, 590.
32. P. Moschogianni; S. Pispas; N. Hadjichristidis. *J. Polym. Sci.* **2001**, *39*, 650.
33. S.M. Waybright; K. McAlpine; M. Laskoski; M.D. Smith; U.H.F. Bunz. *J. Am. Chem. Soc.* **2002**, *124*, 8661-8666.
34. a) T.P. Bender; Y. Qi; P. Desjardins; Z.Y. Wang. *Can. J. Chem.* **1999**, *77*, 1444-1452; b) S. Li; D.V. McGrath. *J. Am. Chem. Soc.* **2000**, *122*, 6795-6796; c) D.-S. Choi; Y.S. Chong; D. Whitehead; K.D. Shimizu. *Org. Letts.* **2001**, *3*, 23, 3757-3760.
35. E.M. Harth; S. Hecht; B. Helms; E.E. Malmstrom; J.M.J. Frechet, C.J. Hawker. *J. Am. Chem. Soc.* **2002**, *124*, 3926-3938.
36. G. Mihov; I. Scheppelmann; K. Müllen. *J. Org. Chem.* **2004**, *69*, 8029-8037.
37. U.-M. Wiesler; T. Weil; K. Müllen. *Topics in Current Chemistry*. Vol. 212; Springer-Verlag Berlin Heidelberg **2001**.
38. a) T. Wang; J.A. Lucey. *J. Dairy Sci.* **2003**, *86* (10), 3090-3101; b) A. Oliva; M. Llabres; J.B. Farina. *Current Drug Discovery Technologies*, **2004**, Vol. 1, 229-242.
39. L.J. Bellamy. *The Infra-red Spectra of Complex Molecule*. **1975**, Chapman and Hall, London, 3 Ed.
40. a) B.J. Berne; R. Pecora. *Dynamic Light Scattering*. **1976**, Wiley, N.Y.; b) R. Pecora. *Dynamic Light Scattering-Applications of Photon Correlation Spectroscopy*. **1985**, Plenum Press, N.Y.; c) K.S. Schmitz. *An Introduction to Dynamic Light Scattering by Macromolecules*. **1990**, Academic Press, Boston; d) R. Winter; F. Noll. *Methoden der Biophysikalischen Chemie*. **1998**, B.G.Teubner Stuttgart.
41. a) L. Reimer. *Transmission electron microscopy*. **1989**, Springer Verlag; b) J.P. Eberhart. *Structural and chemical analysis of materials*. **1995**, John Willey & Sons.

42. a) M. Higuchi; S. Shiki; K. Ariga; K. Yamamoto. *J. Am. Chem. Soc.* **2001**, 123, 4414-4420; b) G. Newkome; C.N. Moorefield; G.R. Baker; M.J. Grossman. *Angew. Chem., Int. Ed. Engl.* **1991**, 30, 1178.
43. The choice of low volatile W/Ta alloy was dictated by the small size of only a few tenths of a nanometer of the metal grains formed during coating. R. Abermann; L. Bachmann. *Naturwissenschaften.* **1969**, 56, 324.
44. L.P. Eberhart. *Structural and chemical Analysis of materials*, Wiley, New York, **1991**, Part five.
45. P.K Maiti; T. Cagin; G. Wang; W.A. Goddard III. *Macromolecules.* **2004**, 37, 6236-6254.
46. S.N. Magonov. *Encyclopedia of Analytical Chemistry*. Atomic Force Microscopy in Analysis of Polymers. **2000**, John Wiley & Sons Ltd, Chichester, 7432-7491.
47. J. Frommer. *Angew. Chem., Int. Ed. Engl.* **1992**, 31, 1298-1328.
48. G. Binning; H. Rohrer. *Ang. Chem., Int. Ed. Engl.* **1987**, 26, 606.
49. J. Hellmann; M. Hamano; O. Karthaus; K. Ijio; M. Shimomura; M. Irie. *Japan. J. Appl. Phys.* **1998**, 37, L816.
50. a) S.S. Sheiko; G. Eckert; G. Ignat'eva; A.M. Muzafarov; J. Spickermann; H.J. Räder; M. Möller. *Macromol. Rapid Commun.* **1996**, 17, 283.
51. W.T.S. Huck; F.C.J.M. van Veggel; S.S. Sheiko; M. Möller; D.N. Reinhoudt. *J. Phys. Org. Chem.* **1998**, 11, 540.
52. W. Stocker; B. Karakaya; B.L. Schürmann; J.P. Rabe; A.D. Schlüter. *J. Am. Chem. Soc.* **1998**, 120, 7691.
53. a) V.N. Bliznyuk; F. Rinderspracher; V.V. Tsukruk. *Polymer*, **1998**, 39, 5249; b) V.V. Tsukruk; F. Rinderspracher; V.N. Blinyuk. *Langmuir*, **1997**, 13, 2171.
54. a) S.S. Sheiko; M. Gautheir; M. Möller. *Macromolecules.* **1997**, 30, 2343-2349; b) D.J. Diaz; G.D. Storrier; S. Bernhard; K. Takada; H.D. Abruna. *Langmuir.* **1999**, 15, 7351-7354; c) M. Sano; J. Okamura; A. Ikeda; S. Shinkai. *Langmuir.* **2001**, 17, 1807-1810.
55. A. Hierlemann; J.K. Campbell; L.A. Baker; R.M. Crooks; A.J. Ricco. *J. Am. Chem. Soc.* **1998**, 120, 5323-5324.
56. J. Li; D.R. Swanson; D. Qin; H.M. Brothers; L.T. Piehler; D. Tomalia; D.J. Meier. *Langmuir.* **1999**, 15, 7347-7350.
57. J.M.J. Frechet; D.A. Tomalia. *Dendrimers and other dendritic polymers.* **2001**, John Wiley & Sons, Ltd.

58. S. Loi; U.-M. Wiesler; H.-J. Butt; K. Müllen. *Macromolecules*. **2001**, 34, 366-3671.
59. S. Loi; H.-J. Butt; C. Hampel, R. Bauer; U.-M. Wiesler; K. Müllen. *Langmuir*. **2002**, 18, 2398-2405.
60. H. Zhang; P.C.M. Grim; T. Vosch; U.-M. Wiesler; A.J. Berresheim; K. Müllen; F.C. De Schryver. *Langmuir*, **2000**, 16, 9294-9298.
61. H. Zhang; P.C.M. Grim; P. Foubert; T. Vosch; P. Vanoppen; U.-M. Wiesler; A.J. Berresheim; K. Müllen; F.C. De Schryver. *Langmuir*, **2000**, 16, 9009-9014.
62. W. Siebert; A. Gunale. *Chem. Soc. Rev.* **1999**, 28, 367.
63. J. Li; L.T. Piehler; D. Qin; J.R. Baker, Jr.; D.A. Tomalia; D.J. Meier. *Langmuir*, **2000**, 16, 5613.
64. J. R. Aranzaes; C. Belin; D. Astruc. *Angew. Chem.* **2006**, 118, 138.
65. M.L. Mansfield. *Polymer*. **1996**, 17, 3835-3841.
66. U.B. Steiner; M. Rehahn; W.R. Caseri; U.W. Suter. *Macromolecules*, **1994**, 27, 1983-1984.
67. P. Brocorens; E. Zojer; J. Cornil; Z. Shuai; G. Leising; K. Müllen; J.L. Bredas. *Synthetic metals*. **1999**, 100, 141-162.
68. M.J. Maciejewski. *J. Macromol. Sci.-Chem.* **1990**, A17, 689.
69. a) D.A. Tomalia; A.M. Naylor; W.A. Goddard III. *Angew. Chem., Int. Ed. Engl.* **1990**, 29, 138; b) A.M. Naylor; W.A. Goddard III; D.A. Tomalia. *Angew. Chem., Int. Ed. Engl.* **1989**, 111, 2339.
70. G.R. Newkome; Y.-Q. Yao; G.R. Baker; V.K. Gupta. *J. Org. Chem.* **1985**, 50, 2003.
71. a) J.F.G.A. Jansen; E.M.M. de Brabander-van den Berg; E.W. Meijer. *Science*, **1994**, 266, 1226; b) J.F.G.A. Jansen; E.M.M. de Brabander-van den Berg; E.W. Meijer. *J. Am. Chem. Soc.* **1995**, 117, 4417-4418.)
72. a) S.M. Grayson; J.M.J. Frechet. *Chem.Rev.* **2001**, 101, 3819-3867; b) J.M.J. Frechet. *Science*. **1994**, 263, 1710; c) J.F.G.A. Jansen; E.M.M. de Brabander-van den Berg; E.W. Meijer. *J. Am. Chem. Soc.* **1995**, 117, 4417-4418; d) G.R. Newkome; C.N. Moorefield; J.M. Keith; G.R. Baker; G.H. Escamilla. *Angew. Chem., Int. Ed. Engl.* **1994**, 33, 666; e) V.V. Naraynan; G.R. Newkome. *Supramolecular Chemistry within Dendritic Structures. Topics in Current Chemistry*. Vol. 197, Springer Verlag Berlin Heidelberg, **1998**.
73. R.M. Crooks; B.I. Lemon III; L. Sun; L.K. Yeung; M. Zhao. *Topics in Current Chemistry*. Vol. 212; Springer-Verlag Berlin Heidelberg **2001**.

74. a) F. Zeng; S.C. Zimmermann. *Chem. Rev.* **1997**, 97, 1681-1712; b) R. Esfand; D.A. Tomalia. *Drug Discovery Today*. **2001**, 6, 427-436; c) A.K. Patri; I.J. Majoros, J.R. Baker. *Curr. Opin. Chem. Biol.* **2002**, 6, 466-471; d) U. Boas; P.M.H. Heegaard. *Chem. Soc. Rev.* **2004**, 33, 43-63.
75. I.O. Götze; C.N. Likos. *Macromolecules*. **2003**, 36, 8189-8197.
76. A.J. Berresheim. Ph-D dissertation, University of Mainz, **2000**.
77. a) A. Bashir-Hasheimi; H. Hart; D.L. Ward. *J. Am. Chem. Soc.* **1986**, 108, 6675-6679; b) P. Venugopalan; H.-B. Bürgi; N.L. Frank; K.K. Baldrige; J.S. Siegel. *Tetrahedron Letter*. **1995**, 36, 2419-2422.
78. a) A. Janshoff; H.J. Galla; C. Seinem. *Ang. Chem., Int. Ed.* **2000**, 39, 4004-4032; b) C.K. O'Sullivan; G.G. Guilbault. *Biosens. Bioelectron.* **1999**, 14, 663-670; c) F.L. Dicer; H. Stathopoulos; M. Reif. *Adv. Mater.* **1996**, 8, 525-529.
79. M. Schlupp; T. Weil; A.J. Berresheim; U.-M. Wiesler; J. Bargon; K. Müllen. *Angew. Chem., Int. Ed. Engl.* **2001**, 40, N 21, 4011-4015.
80. G. Sauerbrey. *Z. Phys.* **1959**, 155, 206-222.
81. Martin Schlupp. Ph-D Thesis, Mathematisch-Naturwissenschaftlichen Fakultät der Rheinisch Friedrich-Wilhelms-Universität Bonn (Bonn), **2001**.
82. A. Godt; Ö. Ünsal; M. Roos. *J. Org. Chem.* **2000**, 65, 2837-2842.
83. a) M.J. Fray; R.P. Dickinson; J.P. Huggins; N.L. Occleston. *J. Med. Chem.* **2003**, 46 (16), 3514-3525; b) T. Jeffery. *Tetrahedron Lett.* **1991**, 32, 1212.
84. Ding-Ding He. MPI für Polymerforschung, Mainz. Personal communication.
85. E.E. Simanek; S.O. Gonzalez. *J. Chem. Education*. **2002**, 79, 1222-1231.
86. M.E. Piotti; F. Rivera; R. Bond; C.J. Hawker; J.M.J. Frechet. *Am. Chem. Soc.* **1999**, 121, 9471.
87. A. Andronov; J.M.J. Frechet. *Chem. Comm.* **2000**, 1701.
88. M. Liu; J.M.J. Frechet. *Pharmaceut. Sci. Technol. Today*. **1999**, 2, 393.
89. D.C. Tully; J.M.J. Frechet. *Chem. Comm.* **2001**, 1229.
90. a) A. Herrmann. Ph-D dissertation, University of Mainz, **2000**; b) J. Qu. Ph-D dissertation, University of Mainz, **2000**.
91. S. Hecht. *J. of Polymer Science*. **2003**, 41, 1047-1058.
92. a) S. Bernhardt; M. Baumgarten; M. Wagner; K. Müllen. *J. Am. Chem. Soc.* **2005**, 127, 12392-12399; b) S. Bernhardt. Ph-D dissertation, University of Mainz, **2005**.
93. R. Bauer. Ph-D dissertation, University of Mainz, **2005**.
94. J. Sakamoto; K. Müllen. *Org. Letters*. **2004**, 6, 23, 4277-4280.

3 Synthesis and Hydrogenation of Dendrimers possessing internal $-C\equiv C-$ Triple bonds

3.1 Introduction

The ideal extended arm in the construction of ‘‘exploded’’ dendrimers would be the oligoalkyne unit $(-C\equiv C-)_n$ because of rigidity^[1] and small steric demand. Oligoalkynes have gained reputation as models for ‘‘molecular wires’’.^[1-2] However, their limited stability^[1, 2-a,b] and difficult access render their incorporation into dendrimers problematic at present.

Yet, even single alkyne units as part of dendrons have many interesting aspects to offer. Typically, links of the conjugated and more rigid composition $(-C_6H_4-C\equiv C-)_n$ in which arene- and alkyne units alternate, are widely used as spacers in studies of intramolecular communication.^[3-4] It therefore was logical to incorporate this type of segment into dendrimers as well.

Of particular appeal is the possibility to convert these alkyne units into alkane segments by means of hydrogenation of the respective dendrimers. There are two sides to this medal:

- on the one side it was an open question whether internal alkyne units are accessible at all to homogeneously or heterogeneously catalysed hydrogenation. This uncertainty stems from the considerable steric shielding of internal alkyne segments in the target dendrimers.
- on the other side, if hydrogenation would be successful, comparisons of the spectral properties of pre- and post- hydrogenation dendrimers as well as their relative propensity to act as hosts for guest molecules could be revealing.

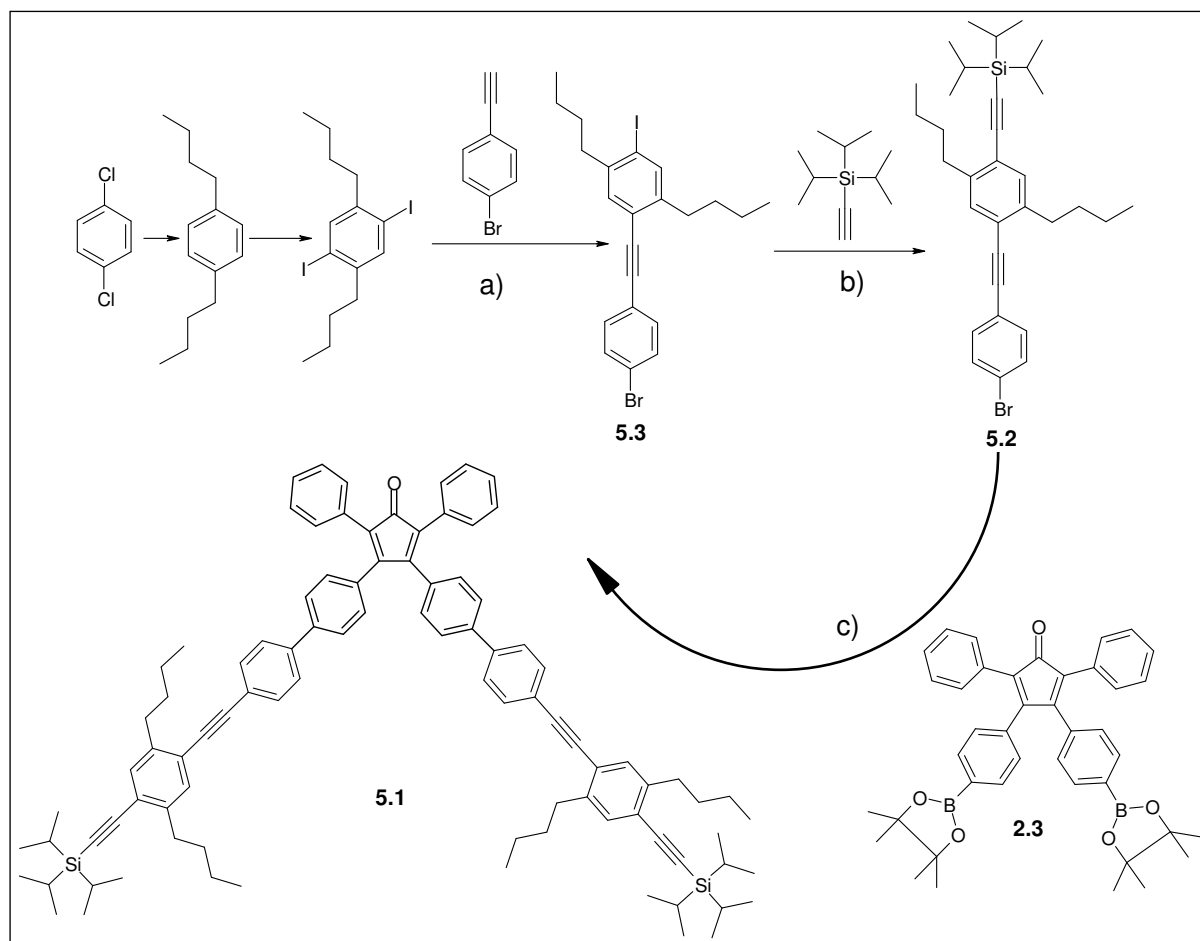
In the following, results of studies along these lines will be described, based on two representative examples.

3.2 Synthesis of a new cyclopentadienone branching unit bearing the *para*-phenylene ethynylene arms (5.1)

In Chapter 2.2 it was pointed out, that the purification of the cyclopentadienone **2.1**, containing tris-*para*-phenylene ethynylene arms, failed due to its strong interaction with silica in column chromatography. To remedy this problem, the idea arose to shorten the tris-*para*-

phenylene ethynylene arm, which could allow the purification of a new branching unit **5.1** (Scheme 3.1).

The synthesis started from 1,4-di-*n*-butyl-2,5-di-iodobenzene,^[5] which via Sonogashira-Hagihara reaction coupled to commercially available *para*-bromophenylacetylene generating the new compound **5.3** in 44% yield. The following Sonogashira-Hagihara coupling of **5.3** to tris-*iso*-propylsilylacetylene produced the arm **5.2** quantitatively. The Sonogashira-Hagihara reaction selectively proceeded at the C-I than at the C-Br position.^[6] Butyl chains in the phenyls were introduced to improve the solubility of **5.2** during the Suzuki coupling to 3,4-bis(4-(4,4,5,5-tetramethyl-1,3,2-dioxaborolan-2-yl)phenyl)-2,5-diphenylcyclopentadienone (**2.3**) in a two phase system (water and toluene) to generate the branching unit **5.1** in a yield of 33%.



Scheme 3.1: Synthesis of branching unit **5.1**, a) THF, piperidine, r.t, CuI, Pd(PPh₃)₂Cl₂, 44%; b) THF, Et₃N, 0 °C, CuI, Pd(PPh₃)₂Cl₂, 95.5%; c) K₂CO₃, Pd(PPh₃)₄, toluene, water, reflux, 33%.

Physical data (FD MS, ^1H and ^{13}C NMR spectra, elementary analysis) confirmed the high purity of the branching unit **5.1**. The ^{13}C NMR spectrum was the most convenient method to confirm the identity of the new branching unit bearing two pairs of equivalent triple bonds, where four signals from $-\underline{\text{C}}\equiv\underline{\text{C}}-\text{TIPS}$ and $-\text{C}_6\text{H}_4-\underline{\text{C}}\equiv\underline{\text{C}}-\text{C}_6\text{H}_4-$ at $\delta=105.80, 95.96, 94.04$ and 89.94 ppm were observed. Moreover, two $-\text{CH}_2-$ and two $-\text{CH}_3-$ segments of the butyl groups, connected to the terminal benzene rings, had shifts at $\delta=34.43, 34.20, 14.42$ and 14.38 ppm (Figure 3.1), indicating that they were nonequivalent.

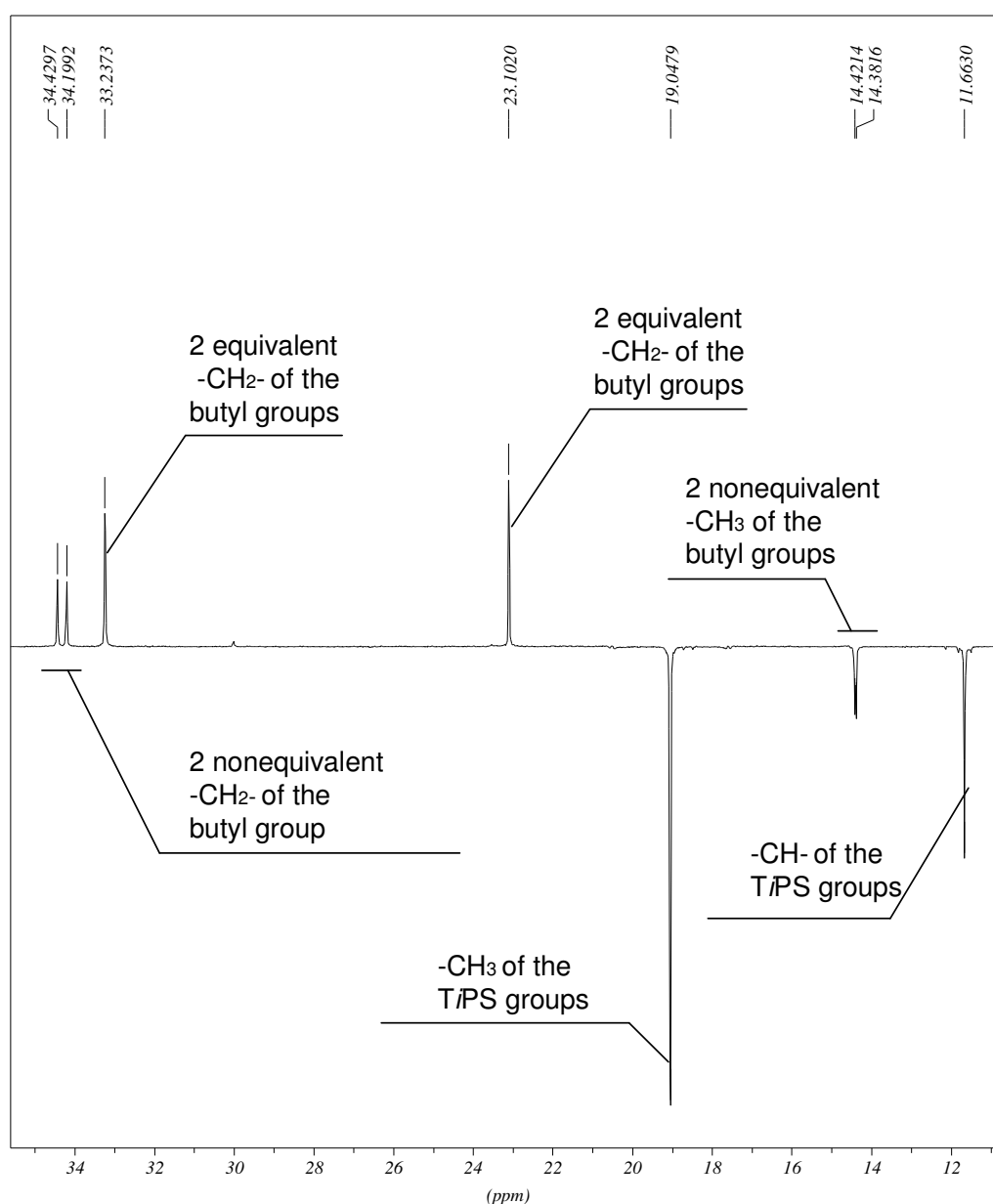


Figure 3.1: Spin echo ^{13}C NMR spectrum of the new branching unit **5.1** in the alkyl range (175 MHz, r.t., $\text{C}_2\text{D}_2\text{Cl}_4$).

3.3 Synthesis of the first-generation dendrimer with branching unit 5.1

Dendrimer synthesis utilizing the Diels-Alder reaction consists of the Diels-Alder reaction between an alkyne- and the diene unit of the substituted cyclopentadienone.^[7] The branching unit **5.1** contains two pairs of inequivalent $-C\equiv C-$ triple bonds, one of which being subjected to deprotection during the reaction sequence. A third type of $C\equiv C$ triple bond is present in the core **1.10** which is used in the primary step. Therefore, in order to avoid product spread, chemoselectivity of the Diels-Alder step must be ascertained.

In general the Diels-Alder reaction, like all pericyclic reaction, can be rationalized in terms of the π -molecular orbitals of the reactants.^[8] For the prototypical Diels-Alder reaction, between butadiene and ethylene (ethyne), there are two requirements:

- 1) one molecule must donate electrons, from its highest occupied molecular orbital (HOMO) to the lowest unoccupied molecular orbitals (LUMO) of the other, and
- 2) the two interacting orbitals must have identical symmetry (the phases of the terminal π -orbitals of each MO must match).^[8]

Figure 3.2 shows two possible ways for the [4+2]-cycloaddition reaction of the HOMO of the diene combining with the LUMO of the dienophile, and the LUMO of the diene with the HOMO of the dienophile.

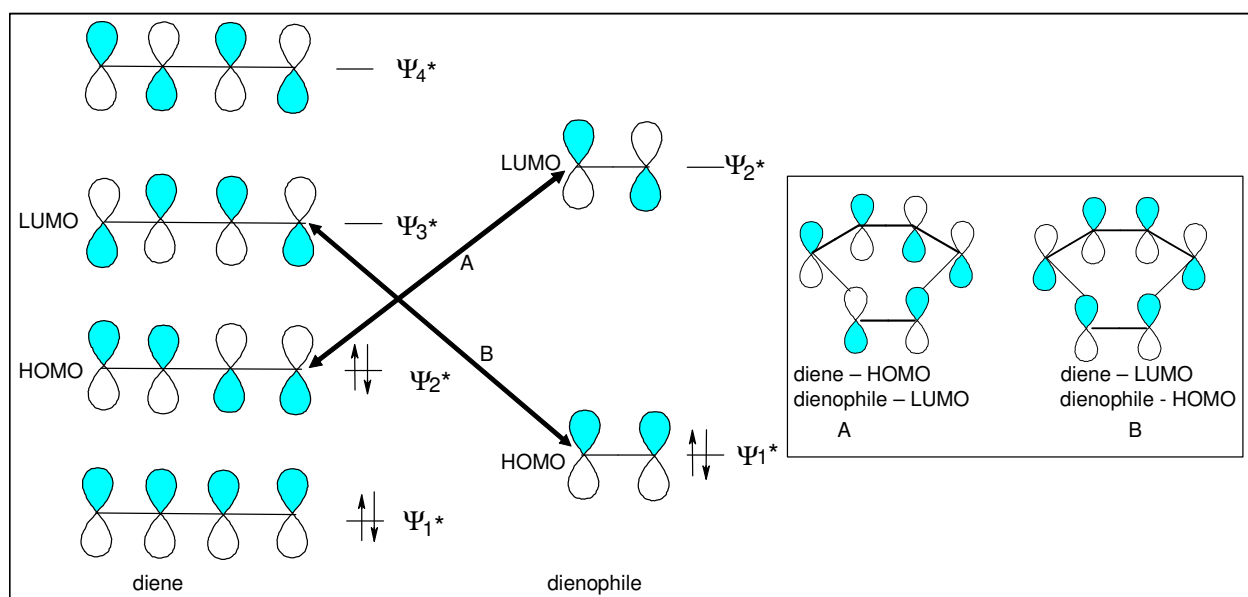


Figure 3.2: Correlation diagram for Diels-Alder cycloaddition.

A Diels-Alder reaction takes place well when the diene is electron rich and the dienophile is electron poor or vice versa.^[8b] In the present case (Dilthey reaction) the cyclopentadienone constitutes the electron-poor and the alkyne the electron-rich component of the cycloaddition. The group adjacent to the triple bond (double bond) has steric and electronic influence on the rate of [4+2]-cycloaddition reaction.

The HOMO/LUMO gap (ΔE) increases from tolane to phenylacetylene (Figure 3.3).

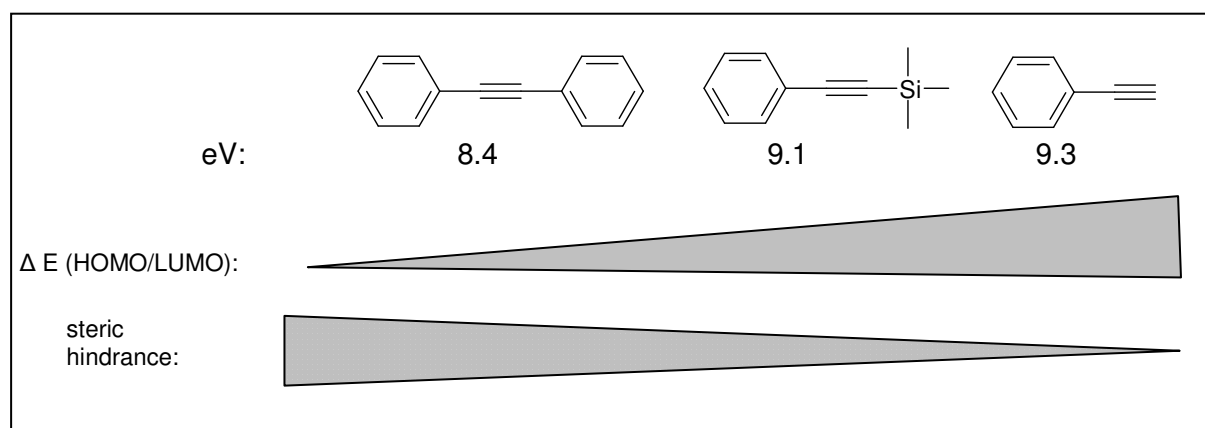
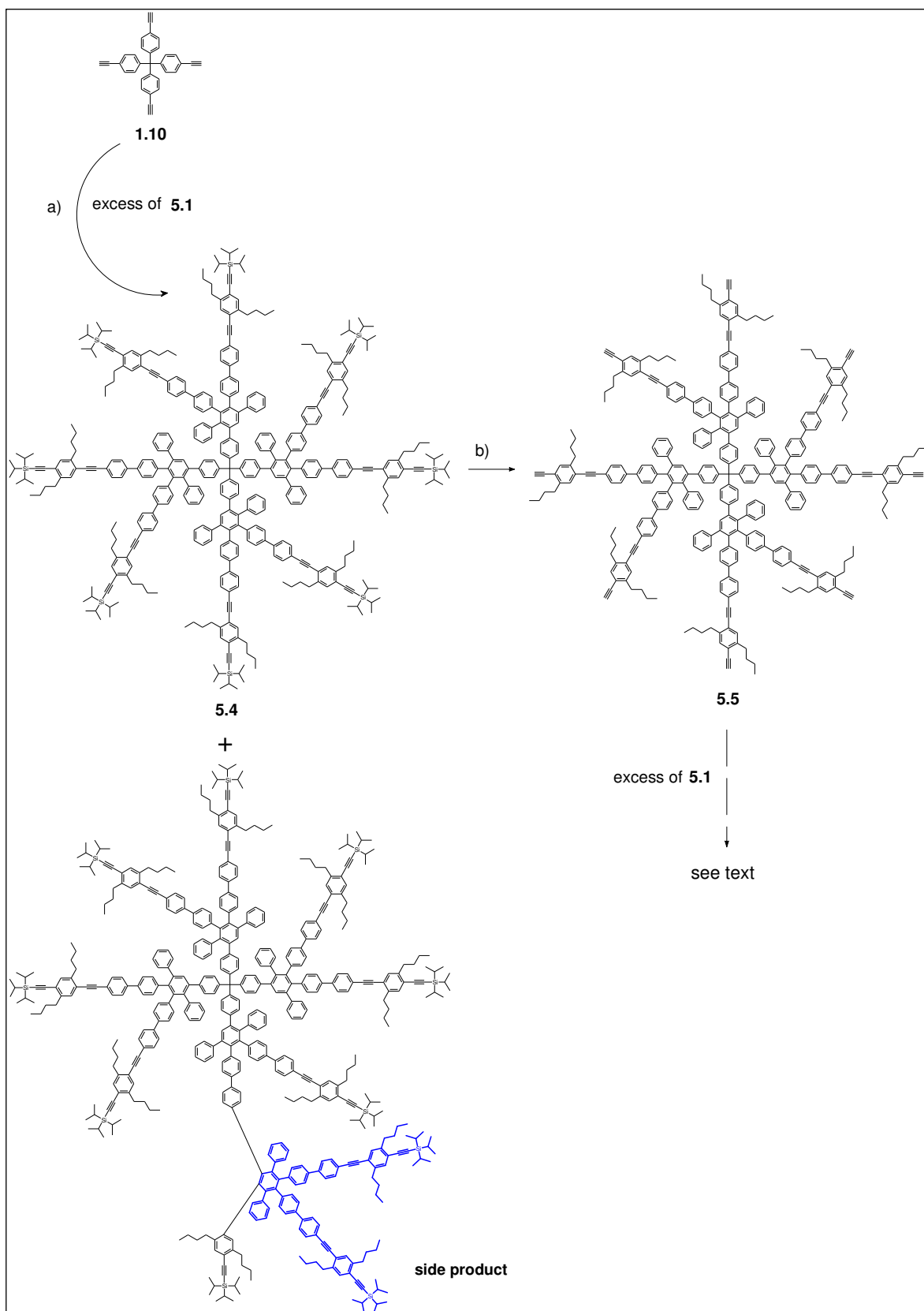


Figure 3.3: Comparison of tolane, trimethylsilyl-phenylacetylene and phenylacetylene with regard to the HOMO/LUMO gap ΔE (calculated by means of program PC Spartan Pro with AM 1) and steric hindrance.

Electronically in the Diels-Alder reaction the triple bond located between phenyl groups should be more reactive compared to phenylacetylene in the Diels-Alder reaction. However, the present work showed that for the steric reasons the outer phenylacetylene units react more readily with the cyclopentadienones than the interior tolanes. Therefore steric hindrance to the Diels-Alder cycloaddition is more important than the orbital control in the present case. It is also known from previous experience^[7] that a triple bond in diphenylacetylenes undergoes Diels-Alder cycloaddition only at higher temperature (220 °C).

Subsequently the less reactive $-C\equiv C-$ triple bonds of the internal tolane segments would also react with excessive branching unit **5.1** giving rise to undesired side product (Scheme 3.2).

Scheme 3.2: Synthesis of the first generation dendrimers **5.4** and **5.5** with branching unit **5.1**:a) *o*-xylene, reflux, 66%; b) tetrabutylammonium fluoride trihydrate, THF, r.t., 85%.

To generate a first-generation dendrimer **5.4** (Scheme 3.2) via the Diels-Alder cycloaddition in *o*-xylene (142 °C), it is important to limit the excess of branching unit **5.1** (1.06-1.08 equivalent of cyclopentadienone **5.1** pro 1 ethynyl group) to decrease the amount of side products of the type shown in Scheme 3.2.

Purification of the first-generation dendrimer **5.4** from a small amount of side product can be achieved by column flash chromatography on silica gel, collecting the first fraction of the product in 66% yield. The new dendrimer **5.4** was characterized by MALDI TOF MS (Figure 3.4-A), where in addition to the molecular ion (calcd. for $[M+Ag^+]$ 5701 Da, found 5700 Da), a fragmentation at the core was also observed (calcd. for $[^3/4 M^+]$ 4195 Da, found 4198 Da). The MALDI-TOF and SEC (Figure 3.4-B) results confirmed the purity and monodispersity of compound **5.4**.

After removal of the TiPS protecting group in **5.4**, the dendrimer **5.5** was obtained which lends itself to build-up of higher generation dendrimers via subsequent Diels-Alder coupling.

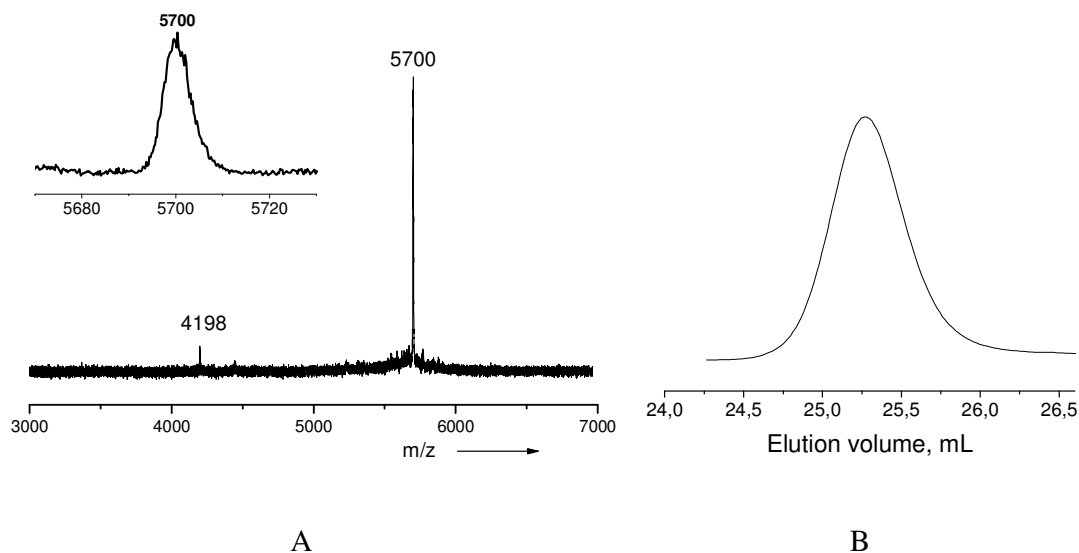


Figure 3.4: **A** - MALDI-TOF spectrum (reflector mode, dithranol, Ag^+) of **5.4**; **B** - SEC of **5.4**.

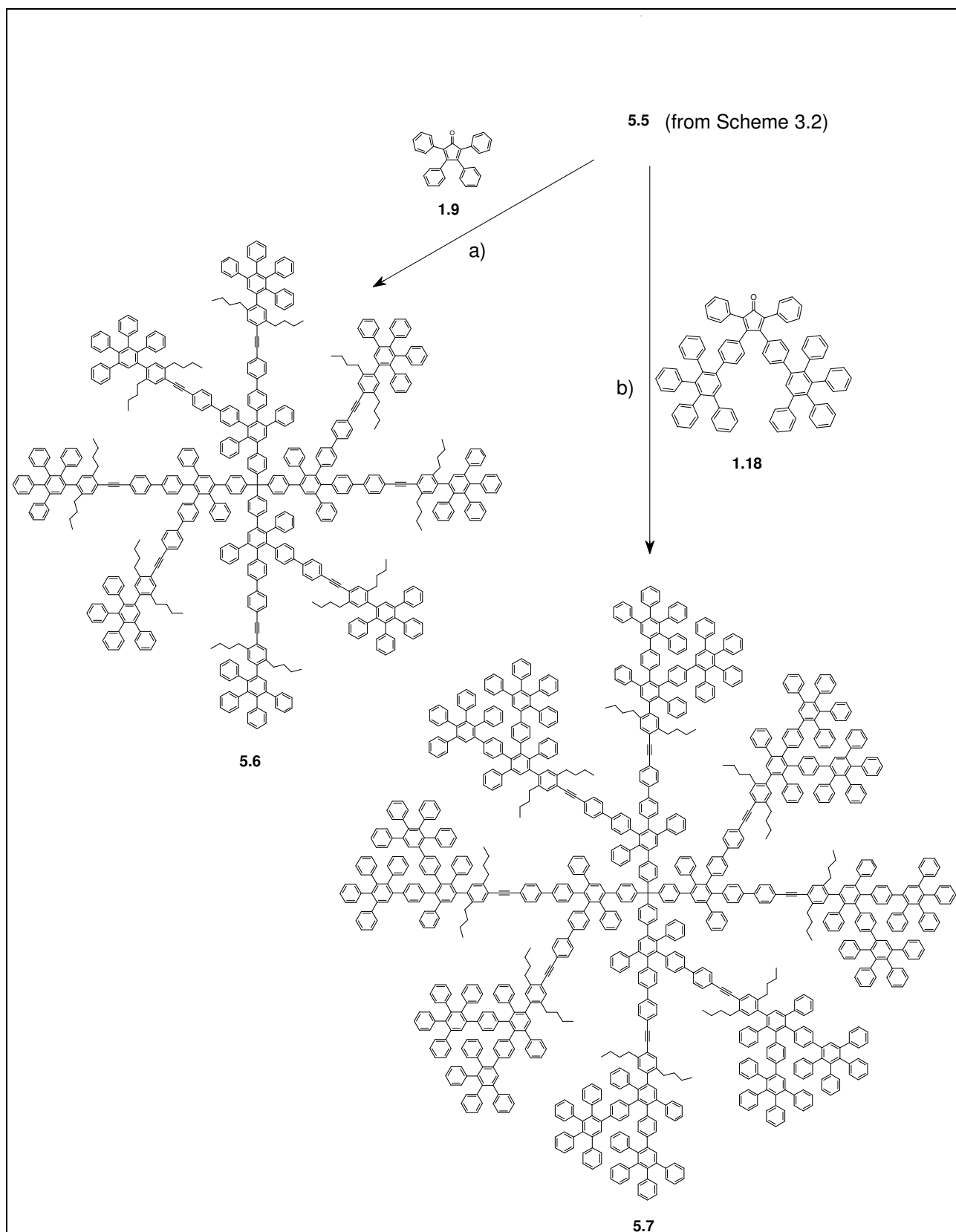
3.4 Synthesis of the second- and third-generation dendrimers bearing eight internal triple bonds

The new dendrimer **5.5** which bears eight external $-C\equiv CH$ and eight internal $-C\equiv C-$ units initially appeared to be an ideal substrate for the synthesis of higher-generation dendrimers featuring a large number of internal $-C\equiv C-$ triple bonds. This was thought to be accomplished by reacting **5.5** with the branching unit **5.1**, deprotection and repeating these steps. It turned out, however, that the use of branching unit **5.1** is limited up to the first generation: when **5.1** is used in high excess on **5.5** for the synthesis of second-generation dendrimer, separation of the target molecule from side products of the type shown in Scheme 3.2 was impossible. In fact, only the simple branching units **1.9** and **1.18**, which are devoid of internal $C\equiv C$ triple bonds were found to be suitable for higher-generation dendrimer formation, starting from **5.5** (Scheme 3.3).

The Diels-Alder cycloaddition of **5.5** with the branching unit **1.9**, taken in slight excess (1.25 eq. of **1.9** per 1 eq. of **5.5**) was carried out in *o*-xylene at 130 °C for 3 days to generate a second-generation dendrimer **5.6** in a yield of 70%. MALDI-TOF (Figure 3.5-A, calcd. for $[M+Ag]^+$ 7302.86, found 7307) and SEC (Figure 3.5-C) confirmed its monodispersity.

In the case of the reaction of the more bulky dendron **1.18** with **5.5** (1.3 eq. of **1.18** per 1 eq. of **5.5**), the higher boiling solvent diphenyl ether was applied, and the reaction mixture was heated to 190 °C for 3 days to form the third-generation dendrimer **5.7** in 75% yield.

The MALDI-TOF spectrum (calcd for $[M+K]^+$ 13320.76, found 13319; calcd. for dimer 26550, found 26587) and the SEC trace of **5.7** are presented in Figure 3.5-B and Figure 3.5-C respectively. Both SEC, where a small peak appears on the wing at about twice the molecular mass, and MALDI-TOF MS, where a second peak indicates a dimer, suggests that the third-generation dendrimer **5.7** tends to form an aggregate. For the second-generation dendrimer **5.6** neither a shoulder in SEC nor a second peak in MALDI-TOF MS was observed. Possibly, a dimer only forms when the dendrimer is more crowded and the large number of peripheral benzene rings favours dimerization by means of π/π stacking interaction.^[9]



Scheme 3.3: Synthesis of the second- and third-generation dendrimers **5.6** and **5.7** bearing eight internal triple bonds: a) *o*-xylene, 130 °C; 3 days, 70%; b) Ph₂O, 190 °C, 3 days, 75%.

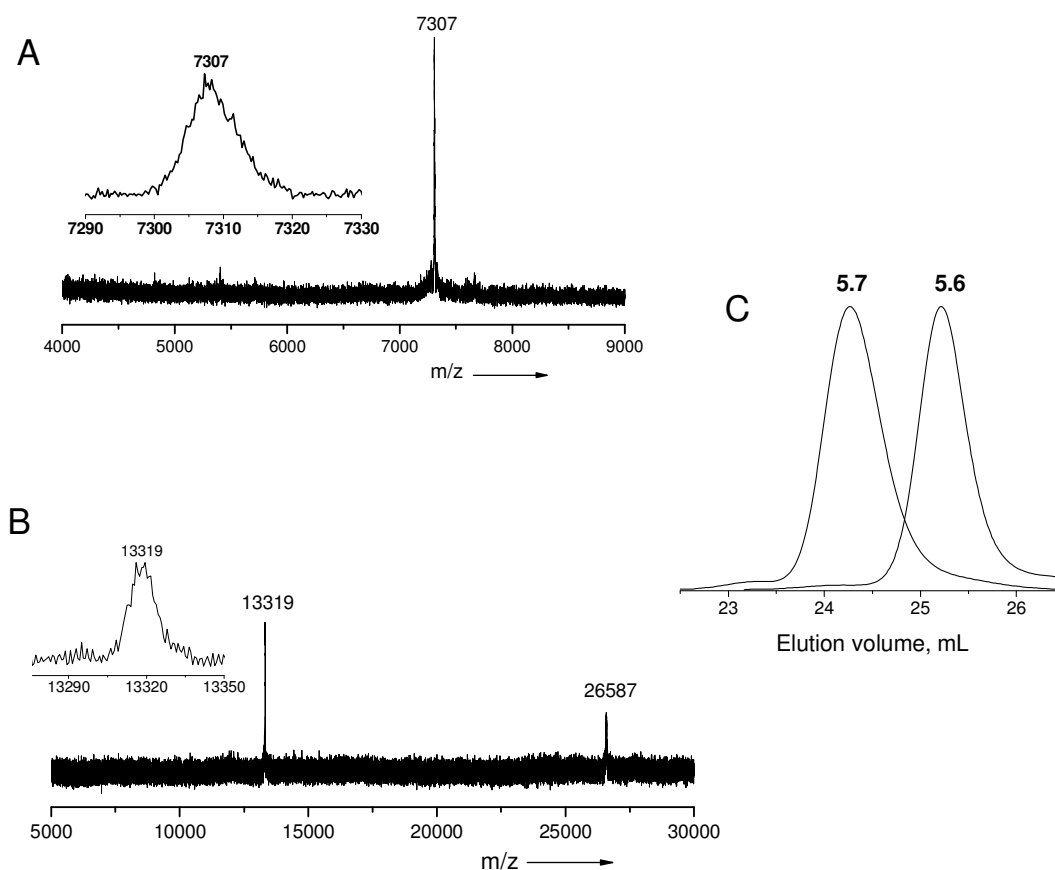


Figure 3.5: **A** - MALDI-TOF mass spectrum of **5.6** (reflector mode, dithranol, Ag⁺); **B** - MALDI-TOF spectrum of **5.7** (reflector mode, dithranol, K⁺), and **C** - SEC eluograms for **5.6** and **5.7** in THF.

The new dendrimers **5.6** and **5.7** thus possess eight internal $C\equiv C$ triple bonds. Hydrogenation is expected to change the dimension of the inner cavities in these dendrimers as well as flexibility of the dendrons. Both features should modify the access to the cavities for substrates.

3.5 Heterogeneous catalysis of hydrogenation: some principal considerations

Hydrogenation of carbon-carbon multiple bonds is an exothermic reaction.^[10] Hydrogenation reactions usually have high free energies of activation which can be reduced by using catalysts such as platinum, palladium, rhodium, or nickel.^[10b] The most commonly used catalysts for this reaction serve to chemisorb hydrogen molecules on their surface whereby the

H-H bond is weakened (Figure 3.6-a). At the surface of the catalyst, adsorbed organic molecules (Figure 3.6-b) react with individual atoms of hydrogen via a half-hydrogenated intermediate (Figures 3.6-c and 3.5-d).^[10a] This process is aided by C=C bond weakening which is effected by coordination of the alkene or alkyne to metal atoms of the catalyst surface.

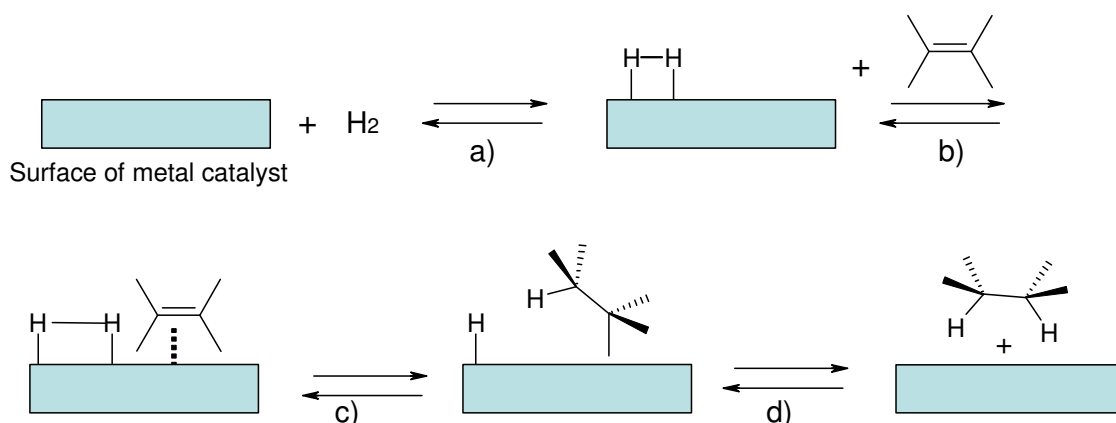
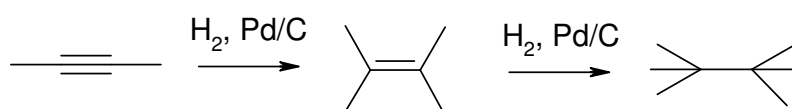
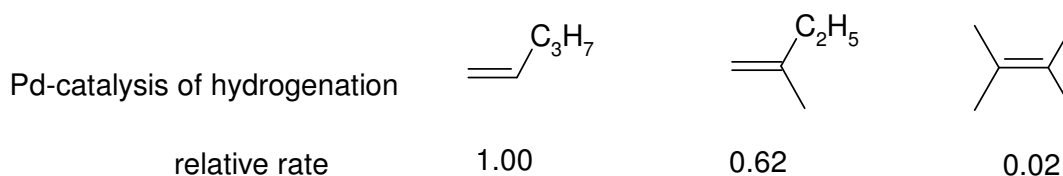


Figure 3.6: The mechanism for the hydrogenation of an alkene as catalyzed by finely divided platinum metal. Both hydrogen atoms add from the same side of the double bond (taken from ref.^[10a]).

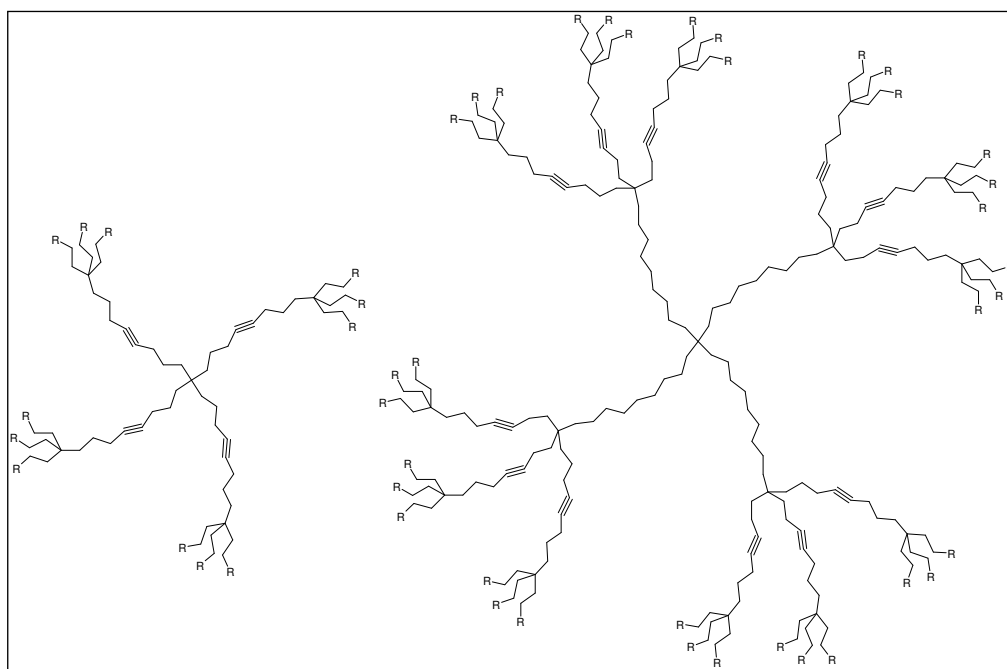
Hydrogenation of the triple bond proceeds in 2 steps: first the triple bond converts into the double one, which in its turn into a single bond:



These conversions obviously require access of the multiple bonds to the catalyst surface. Therefore the outcome of the hydrogenation experiment involving the dendrimers **5.6** and **5.7** was not a priori clear since in these substrates the $-C\equiv C-$ triple bonds are subject to extensive steric shielding. The sensitivity of the rate of hydrogenation to steric effect can be read from the following gradation:^[11]



Dendrimer literature contains a limited number of reports that deal with species bearing triple bonds, such as dendrimers with polyphenylacetylene building blocks,^[4-c-k, 12] y-enyne dendrimers,^[13] silylacetylene dendrimers,^[14] acetylene-terminated dendrimers,^[15] and a few others.^[16] The chemistry of these dendrimers with triple bonds was not studied in detail, however, except for Newkome-type dendrimers, where triple bonds in the flexible aliphatic backbones (Scheme 3.4) could be hydrogenated (4 atm. H_2 , Pd/C, 60°C, 4 days),^[17] and even reacted with bulky decaborane as a reducing agent.^[18]



Scheme 3.4: Newkome-type dendrimers bearing internal triple bonds.

However, these flexible dendrimers contain long alkyl chains, which create large space between the arms. Therefore the palladium catalyst has access to the triple bonds more easily than in the case of polyphenylene dendrimers. The two new rigid dendrimers **5.6** and **5.7** (Schemes 3.3) contain eight internal triple bonds. Each triple bond is part of a tolane segment, which subsequently is surrounded by polyphenyl units in both directions. Additionally, two butyl chains were attached to one of the benzene rings adjacent to the triple bond. This significantly increases the steric shielding of the $C\equiv C$ triple bond and the rate of hydrogenation should differ considerably compared to simple tolane.

To get an idea how the Pd catalyst can enter the inner region of the substrates **5.6** and **5.7** to be hydrogenated, molecular modelling was performed by employing the program PC Spartan

Pro with molecular force field MMFF (Figure 3.7) in the same way as presented in Chapter 2.10. From the molecular modelling, it is seen that whereas there is free space between the 4 dendrons, so that an appropriately sized of Pd/C particle can approach the triple bonded segments, the microenvironment of the triple bond is extensively shielded to the effect that molecular bonding contact of the $-C\equiv C-$ triple bond with the catalyst surface should be severely hindered. Unfortunately, there is no information about the size distribution of particles present in the commercially available catalysts Pd/C. Admittedly, these catalysts are structurally very heterogeneous and reactions probably proceed at kinks and tips of the catalyst surface where coordinatively unsaturated Pd atoms are thought to reside. The alternative homogeneously catalyzed hydrogenation employing Wilkinson-type catalyst will be briefly touched on in section 3.8.1.

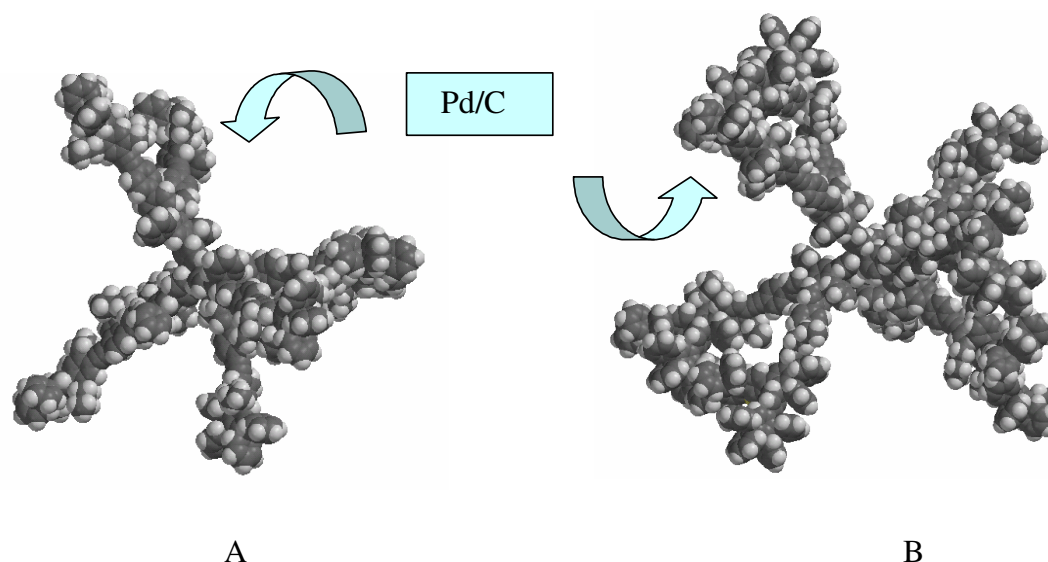


Figure 3.7: Space filling molecular modelling of pre-hydrogenated dendrimers **5.6** (A) and **5.7** (B).

3.6 Hydrogenation of the second-generation dendrimer **5.6**

Before giving experimental details, it is worth to keep in mind, that high pressure hydrogenation (as performed for the Newkome-type dendrimers) could effect hydrogenation of the benzene rings^[19] in addition to alkyne hydrogenation.

Therefore the conversion of the alkyne into alkane function of **5.6** was carried out at atmospheric pressure using palladium on carbon (10% Pd/C) as a catalyst and dihydrogen gas from a balloon at practically atmosphere pressure. The hydrogenation of **5.6** in chloroform

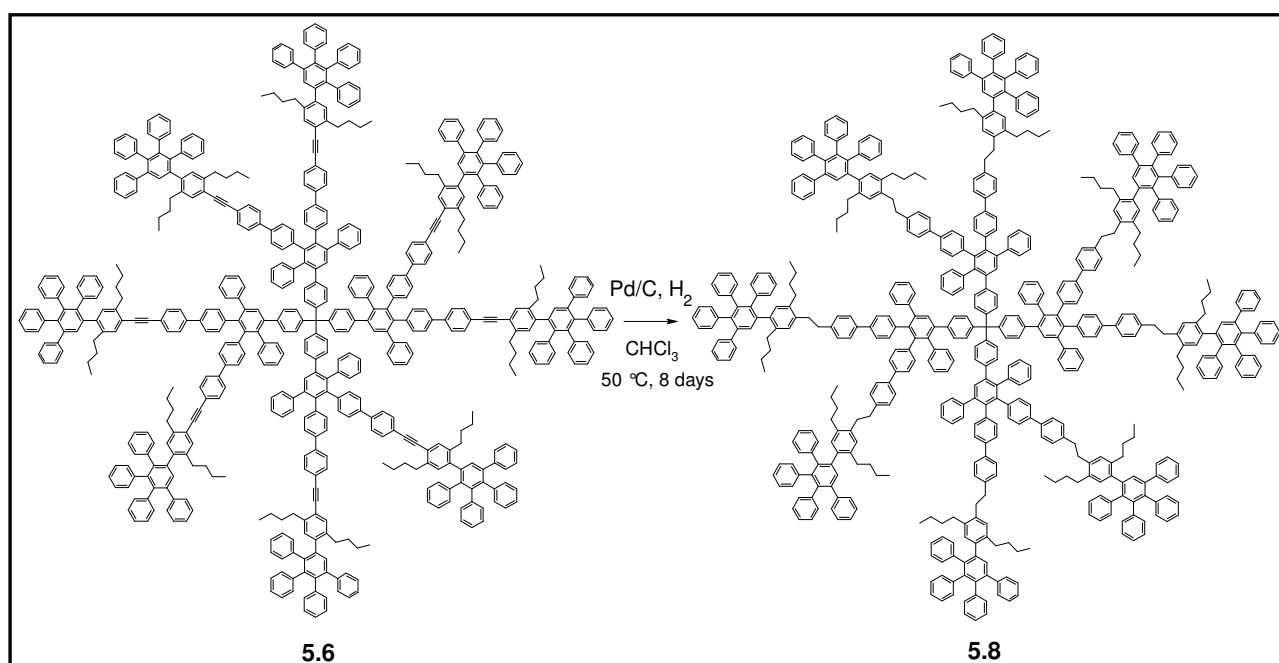
was allowed to proceed at 50 °C for 8 days to generate **5.8** (Scheme 3.5). After separation from the catalyst, the hydrogenated dendrimer **5.8** was characterized as follows.

From the MALDI-TOF measurement, it is difficult to infer completeness of hydrogenation, as the molecular mass of pre-hydrogenated molecule **5.6** and that of hydrogenated molecule **5.8** differ by 32 Da only, while the width of MW peak of **5.6** is about 20 Da (Figure 3.5-A) to 35 Da (Figure not shown here), depending on the sample preparation. Fortunately, there are other methods which can attest to the progress of the hydrogenation reaction.

^1H NMR and ^{13}C NMR spectra confirm completeness of the hydrogenation reaction.

Therefore the heterogeneous nature and particle size of the catalyst Pd/C do not prevent the reaction of the dendrimer **5.6**.

The ^1H NMR spectra (Figure 3.8) demonstrate, that the benzylic protons of the dendrimer **5.6** prior to hydrogenation are nonequivalent, they give rise to four proton signals at $\delta=2.76$, 2.58, 2.44, and 2.35 ppm of correct intensity. Hydrogenation causes a decrease of the chemical shift difference, and the hydrogenation creates an additional signal ($\delta=2.77$ ppm) in the benzylic region which indicates the newly formed $-\text{CH}_2-\text{CH}_2-$ unit in **5.8**.



Scheme 3.5: Hydrogenation of the second-generation dendrimer **5.6**.

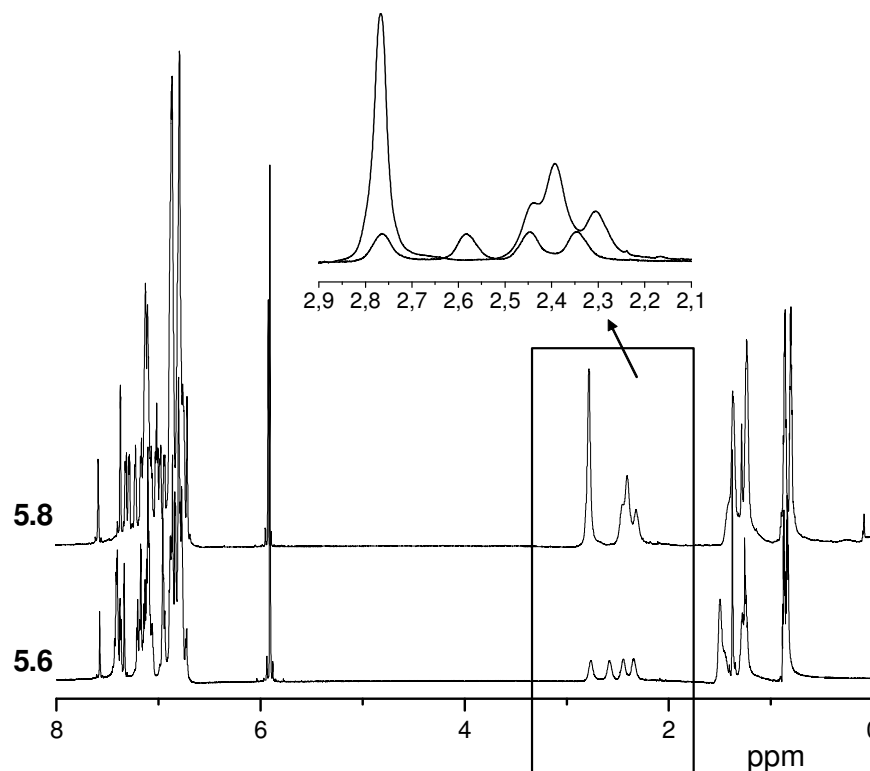


Figure 3.8: Comparison of ^1H NMR spectra (700 MHz, $\text{C}_2\text{D}_2\text{Cl}_4$, 370 K) of second-generation dendrimers before (**5.6**) and after (**5.8**) hydrogenation.

^{13}C NMR spectroscopy was the most convenient method for analysis; after the hydrogenation new signals appeared at 37.32 and 34.48 ppm pointing to the new segments $\text{CH}_2\text{-CH}_2$ (Figure 3.9-A). Moreover, the pre-hydrogenated dendrimer **5.6** exhibits three resonances from $-\underline{\text{C}}\text{C}\equiv\text{C}\underline{\text{C}}-$ at 122.86, 122.80 and 121.18 ppm (intensity 1:1:2) and two signals from the triple bond carbon atoms at 92.55 and 90.12 ppm (Figure is not shown here). After the hydrogenation all these signals were absent. Interestingly, the addition of 32 H atoms to **5.6**, that is the small increase in molecular mass from 7195 (**5.6**) to 7227 (**5.8**) clearly increased the elution volume in size exclusion chromatography (Figure 3.9-B). This indicates, that hydrogenation of the internal triple bonds causes a sizeable decrease in effective volume of the dendrimer which governs the retention characteristics in the SEC experiments. The increased conformational flexibility imposed by the alkyne \rightarrow alkane conversion certainly must be considered as a main contributor to this effect as it facilitates the entry of the hydrogenated dendrimer **5.8** into the pores of the stationary phase. The more rigid dendrimer **5.6**, on the other hand, is less prone to be incorporated into the stationary-phase voids.

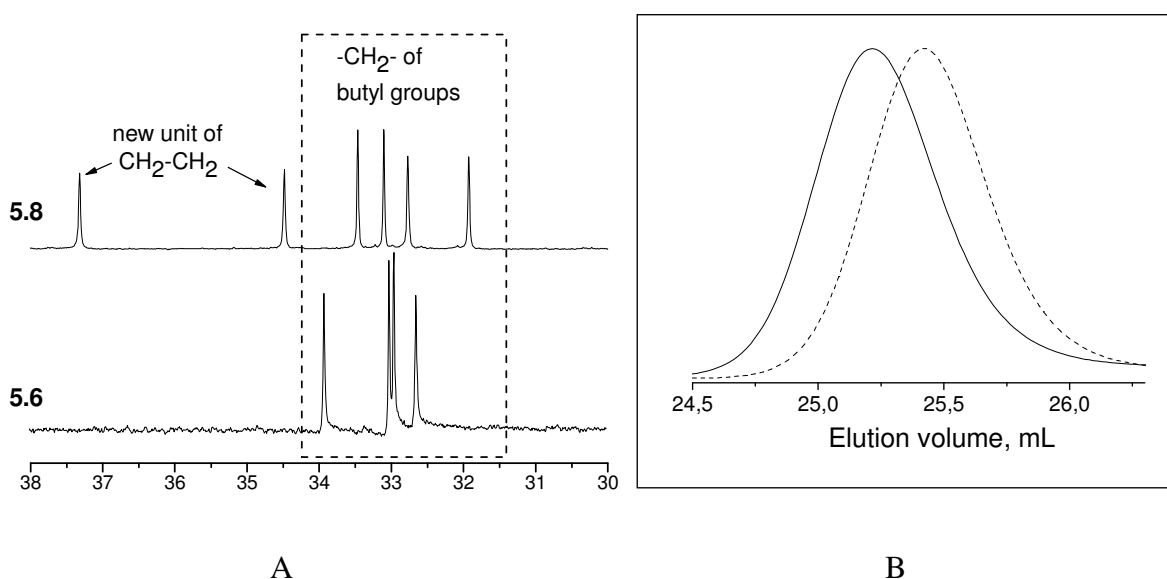


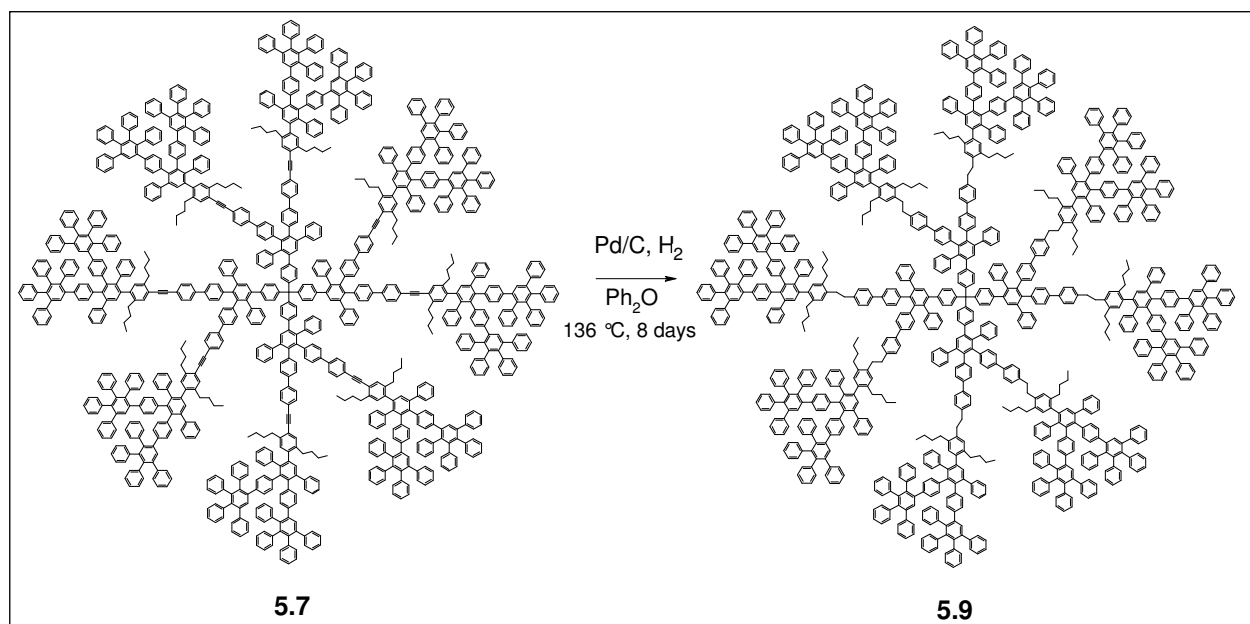
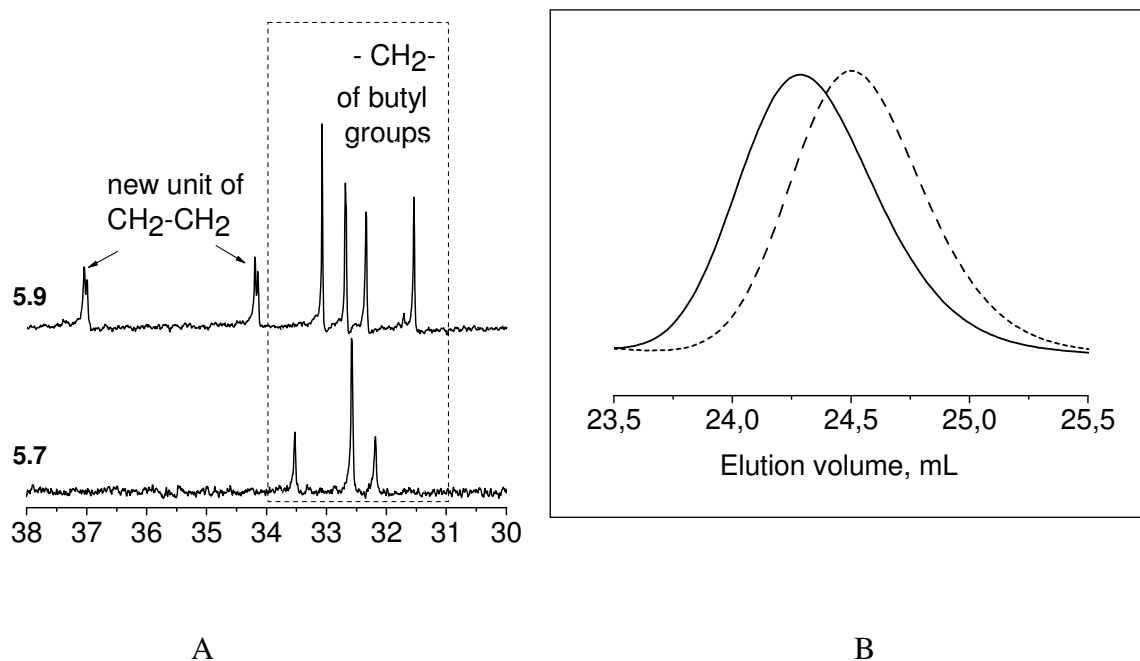
Figure 3.9: **A** - Comparison of ^{13}C NMR spectra (175 MHz, $\text{C}_2\text{D}_2\text{Cl}_4$, 370 K) in the benzylic region of pre- and after- hydrogenated second generation dendrimers **5.6** and **5.8** respectively, **B** - SEC comparison of **5.6** (solid line) and **5.8** (dotted).

3.7 Hydrogenation of the third-generation dendrimer 5.7

In **5.6**, the alkyne groups obviously can make contact with the catalyst surface, steric hindrance is not prohibitive. In order to assess the influence of steric shielding on the hydrogenation, the more bulky dendrimer **5.7** was studied.

Under mild condition (1 atm, 50 °C, Pd/C) hydrogenation of the third-generation dendrimer **5.7** did not occur. Therefore, a higher boiling solvent diphenylether was applied; the reaction mixture was heated to 136 °C for 8 days to produce the hydrogenated molecule **5.9** (Scheme 3.6).

The difference of the dendrimers before and after hydrogenation (**5.7** and **5.9** respectively) in the ^1H NMR spectra corresponds to that of **5.6** and **5.8**. Analogously to Figure 3.8, the chemical shift differences of four benzylic protons at $\delta=2.75$, 2.57, 2.39, and 2.29 ppm of **5.7** are changed by hydrogenation. The new peak at $\delta=2.74$ ppm of the hydrogenated dendrimer **5.9** indicates a newly formed $\text{CH}_2\text{-CH}_2$ unit.

Scheme 3.6: Hydrogenation of the third-generation dendrimer **5.7**.Figure 3.10: **A** - Comparison of ^{13}C NMR spectra (175 MHz, $\text{C}_2\text{D}_2\text{Cl}_4$, 370 K) in the benzylic region of third-generation dendrimers before (**5.7**) and after (**5.9**) hydrogenation. **B** - SEC comparison of **5.7** (solid line) and **5.9** (dotted).

The hydrogenation of the triple bonds is also indicated in the ^{13}C NMR spectrum by the disappearance of resonances assigned to the alkyne carbon atoms ($\delta=92.53$ and 90.14 ppm) and to $-\underline{\text{C}}\text{C}\equiv\text{C}\underline{\text{C}}-$ atoms ($\delta=122.84$ and 121.11 ppm), as well as the appearance of doublets at $\delta=37.40$ and 37.36 , 34.55 and 34.51 ppm (Figure 3.10-A). Their SEC results (Figure 3.10-B) were analogous to those of compounds **5.6** and **5.8** and the same reasoning may be put forward as an explanation.

3.8 Further effects caused by hydrogenation of internal $-C\equiv C-$ triple bonds

3.8.1 UV-Vis absorption of the second- and third-generation dendrimers

The UV-Vis spectra (Figure 3.11) showed that prior to hydrogenation the dendrimers **5.6** and **5.7** have absorption maxima around 320 nm. Hydrogenation induces strong hypsochromic shifts (compounds **5.8** and **5.9**) as expected from the disruption of conjugation upon elimination of the $-C\equiv C-$ triple bonds.

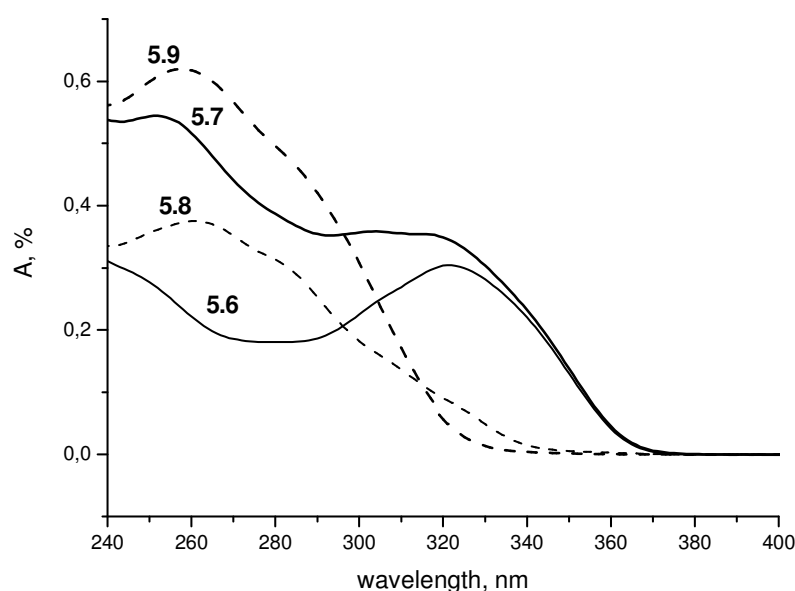


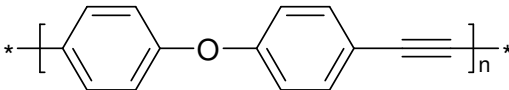
Figure 3.11: UV-vis spectra of before (solid line) and after (dotted) hydrogenation (**5.6-5.9**) in dichloromethane, $c=0.68 \times 10^{-6}$ mg/mmol.

UV-vis spectroscopy may be the most convenient method to monitor the progress of dendrimer hydrogenation. In this way, reaction conditions could be optimized. Conceivable variants include the use of heterogeneous catalysts such Lindlar, Pd on carbon or on Al_2O_3 , SiO_2 or SiO_2 /tetraethylene-glycol/Pd.^[20] Maybe in the future it would be interesting to use the nearly monodisperse palladium nanoparticles, prepared within the interiors of PAMAM dendrimers^[21] where the size of the palladium is controlled in order to study the rate of hydrogenation inside the PDs dendrimers bearing triple bonds.

Homogeneous catalysis effected by Wilkinson-type catalysts $(Ar_3P)_3RhCl$ also comes to mind. An interesting aspect would be the use of Wilkinson catalysts under variation of the size of the phosphane ligands in $(Ar_3P)_3RhCl$. In this way the steric limitations with regard to accessibility of the internal $-C\equiv C-$ triple bonds by the catalyst could be tested. It is anticipated that for each dendrimer a critical size of the phosphane ligands exists beyond which homogeneous hydrogenation will fail because the entry of the catalyst into the inner regions of the dendrimers and approach of the unsaturated reaction site is impossible.

3.8.2 Raman spectroscopy of the third-generation dendrimers 5.7 and 5.9

Raman spectroscopy rather than IR spectroscopy is usually employed as a powerful tool to detect the triple bond.

For example, as applied to the polymer  Raman

spectroscopy clearly showed its specific sensitivity for apolar bonds such as the $C\equiv C$ triple bond at 2200 cm^{-1} . No corresponding IR absorption band was visible.^[22]

Thus, in the present work, toluene as a model, and the alkyne- containing dendrimers before and after hydrogenation were subjected to Raman spectroscopy (Figure 3.12). The spectra supply information about the presence or absence of $-C\equiv C-$ triple bonds in these molecules in a fingerprint fashion.

From these spectra it is seen that characteristic vibrational frequencies of toluene and the pre-hydrogenated dendrimer **5.7** amount to 2220 cm^{-1} and 2208 cm^{-1} respectively. The elimination of the triple bonds in the dendrimer **5.9** was confirmed by the absence of a signal in the region of the alkyne groups. All other spectral features are virtually unchanged since the oligophenylene and alkyl units are unaffected by alkyne hydrogenation.

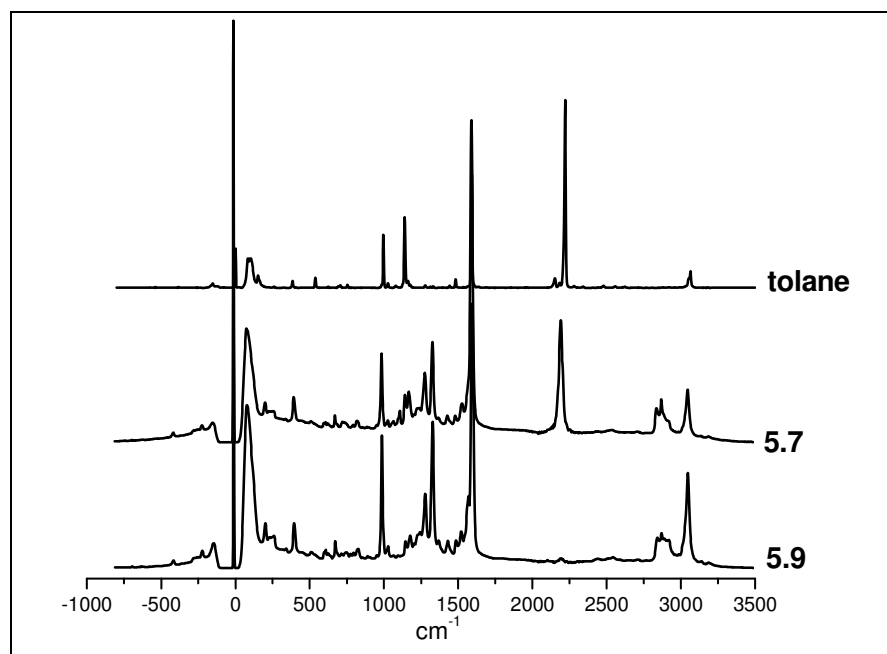


Figure 3.12: Raman spectra of the reference tolane, the dendrimer **5.7** and its hydrogenation product **5.9**.

3.8.3 Diffusion-ordered 2D NMR (DOSY) of the third-generation dendrimers **5.7** and **5.9**

DOSY has been developed for the analysis of mixtures in order to simultaneously characterize the sizes of simple and aggregated structural units present. The results of these experiments are plotted as chemical shifts in one dimension and diffusion coefficients in the other. This experiment complements existing analytical methods and provides a global view of particle sizes in the sample. It is effective at detecting impurities and aggregates.^[23, 24] Thus, diffusion ordered NMR was applied to the third-generation dendrimers **5.7** and **5.9**.

The DOSY NMR spectrum is obtained by the use of pulsed magnetic field gradient spin-echo NMR according to different diffusion of the components in the mixture. Diffusion behaviour is governed by the translational motion of a molecule. According to the Debye-Einstein equation, it is related to the size, shape of individual molecules and specific effects such as aggregation.^[25] DOSY measurements are acquired by means of either gradients in the main magnetic field or gradients in radio frequency fields. The signal contribution of each component from the DOSY experiment is described by formula:^[25]

$$I(i, g^2) = I_0(i) \exp[-D(i) (\Delta - \delta/3) (g\gamma\delta)^2],$$

where $I(i)$ is the signal amplitude of component i , $I_0(i)$ the amplitude with no gradient applied, Δ the diffusion time (s), δ the duration of gradient pulses (s), g the gradient strength (T), γ the gyro-magnetic ratio of the ^1H nucleus ($\text{rads}^{-1}\text{T}^{-1}$), and $D(i)$ the diffusion coefficient of i -th component (m^2/s). If Δ and δ are experimental variables, the signals of a DOSY NMR experiment depend on the gradient strength and diffusion coefficient. Thus, it leads to two dimensions of DOSY NMR (Figure 3.13).

In the DOSY NMR experiment, a dimer of **5.7** in solution was not observed. The diffusion coefficients of the two components **5.7** and **5.9** are very similar. Therefore these dendrimers in solution behave more or less identically and their shapes adopted in the solution appear to be very similar. This contrasts with the SEC experiment (Figure 3.10-A) which showed that hydrogenation of the $\text{C}\equiv\text{C}$ triple bonds has considerable influence on the retention properties.

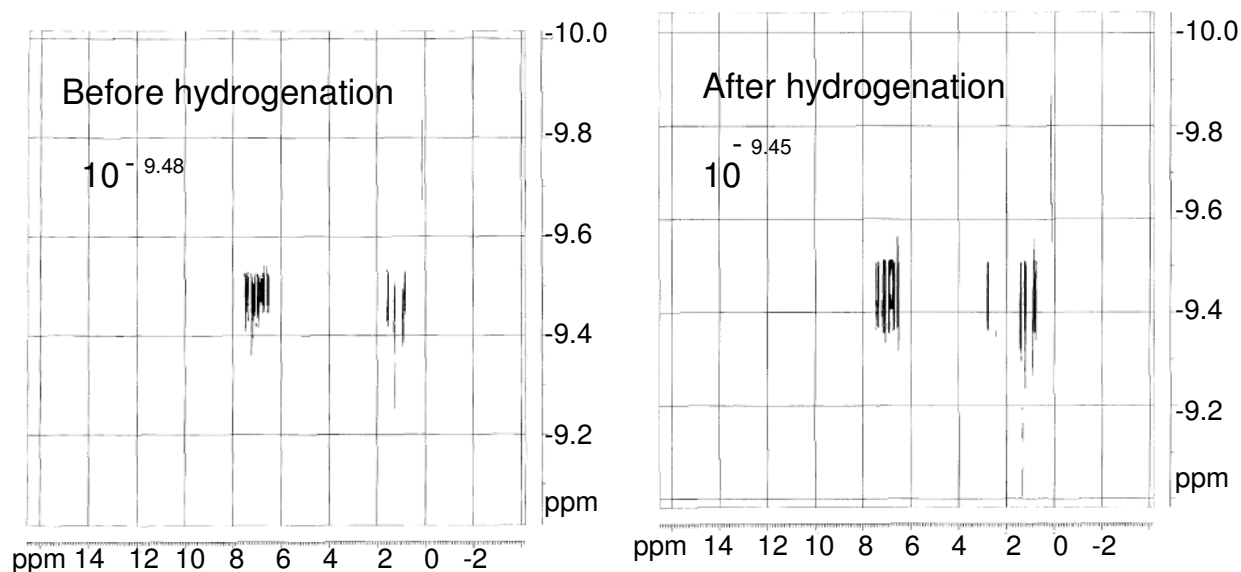


Figure 3.13: DOSY NMR for the pre- (**5.7**) and post- (**5.9**) hydrogenated dendrimers.

3.8.4 Incorporation of guest molecules

In Chapter 2.14 the incorporation of guest molecules into dendrimers serving as hosts and the detection by the quartz microbalance (QMB) was addressed. The compounds **5.7** and **5.9** were also subjected to QMB measurement. Figure 3.14 shows that the rigid pre-hydrogenation dendrimer **5.7** incorporate the guest molecules about 30% times more readily than the more flexible post-hydrogenation dendrimer **5.9**.

This initially surprising result can be interpreted as follows: whereas for the rigid-arm dendrimer **5.7** intramolecular interactions between the arms are limited if not impossible, the flexibility of the arms in the hydrogenated dendrimer **5.9** favors intramolecular bonding between the benzene rings of adjacent structural units. These interactions compete with the bonding of guest molecules whose incorporation is therefore attenuated compared to the rigid dendrimer **5.7**. In this context a comparison of the softness (=mechanical deformability) of **5.7** and **5.9** would be of interest. Therefore, pulsed atom force microscopy experiments are in progress in collaboration with the de Feyter groups.

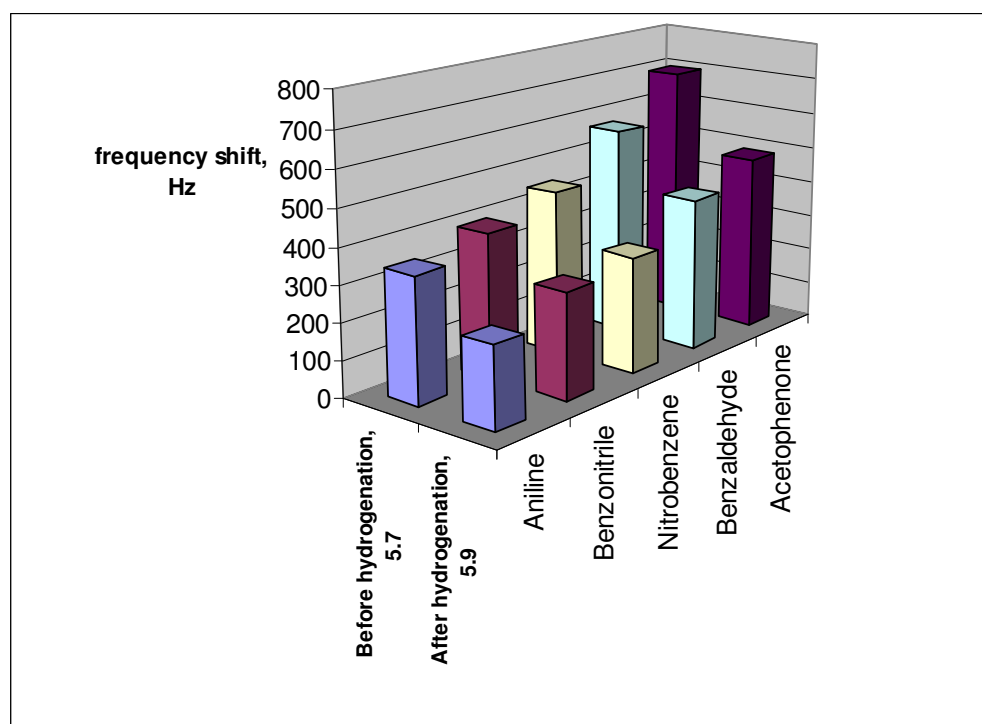


Figure 3.14: Comparison of **5.7** and **5.9** in QMB measurement.

3.9 Literature for Chapter 3

1. W. Mohr; J. Stahl; F. Hampel; J.A. Gladysz. *Chem. Eur. J.* **2003**, 9, 3324-3340.
2. a) R. Dembinski; T. Bartik; B. Bartik; M. Jaeger; J.A. Gladysz. *J. Am. Chem. Soc.* **2000**, 122, 810-812; b) R. Schennach; D.G. Naugle; D. Cocke; R. Dembinski; J.A. Gladysz. *Vacuum.* **2000**, 56, 115-121; c) L.M. Tolbert; X. Zhao; Y. Ding; L.A. Bottomley. *J. Am. Chem. Soc.* **1995**, 117, 12891-12892; d) F. Coat; C. Lapinte. *Organometallics.* **1996**, 15, 2, 477-479.
3. J. K. Young; J.C. Nelson; J.S. Moore. *J. Am. Chem. Soc.* **1994**, 116, 10841-10842, and references herein.
4. See examples: a) F.R.F. Fan; R.Y. Lai; J. Corni; Y. Karzazi; J.L. Bredas; L. Cai; L. Cheng; Y. Yao; D.W. Price, Jr.; S.M. Dirk; J.M. Tour; A.J. Bard. *J. Am. Chem. Soc.* **2004**, 126, 2568-2573; b) P. Wautelet; J.L. Moigne; V. Videva; P. Turek. *J. Org. Chem.* **2003**, 68, 8025-8036; c) C. Devadoss; P. Bharathi; J.S. Moore. *J. Am. Chem. Soc.* **1996**, 118, 9635-9644; d) R. Kopelman; M. Shortreed; Z.-Y. Shi; W. Tan; Z. Xu; J.S. Moore; A. Bar-Haim; J. Klasta. *The Am. Phys. Soc.* **1997**, 78, 1239-1242; e) Z. Xu; J.S. Moore. *Acta Polymer.* **1994**, 45, 83-87; f) E. Atas; Z. Peng; V.D. Kleiman. *J. Phys. Chem. B.* **2005**, 109, 13553-13560.
5. W.Y. Huang; W. Gao; T.K. Kwei, Y. Okamoto. *Macromolecules.* **2001**, 34, 1570-1578.
6. a) A. Godt. *Org. Chem.* **1997**, 62, 747; b) A. Fechtenkötter; N. Tchebotareva; M. Watson; K. Müllen. *Tetrahedron.* **2001**, 57, 3769.
7. a) W. Dilthey; W. Schommer; H. Dierichs; O. Trösken. *Chem. Berichte.* **1933**, 66, 1627; b) W. Dilthey; G. Hurtig. *Chem. Berichte.* **1934**, 67, 2004.
8. N.S. Isaacs. Physical organic chemistry. **1995**, Longam; b) Organikum. **2000**, 22 Auf, VEB Deutscher Verlag der Wissenschaften, Berlin.
9. See examples: a) J. Portilla; J. Quiroga; J. Cobo; M. Nogueras; J.N. Low; C. Glidewell. *Acta Cryst.* **2005**, C61, o398-o403; b) J.J. Apperloo; R.A.J. Janssen; P.R.L. Malenfant; J.M.J. Frechet. *Macromolecules.* **2002**, 33, 7038-7043.
10. a) T.W. Graham Solomons. Organic chemistry. **1992**, John Wiley & Sons; b) J. Horiuti; M. Polanyi. *Trans. Faraday Soc.* **1934**, 30, 1164.
11. a) M. Hudlický. Reductions in Organic Chemistry. **1996**, ACS Monograph 188, Am. Chem. Society, Washington, DC; b) Brown. *J. Org. Chem.* **1970**, 35, 1900.

12. a) Z. Xu; J.S. Moore. *Angew. Chem., Int. Ed. Engl.* **1993**, 32, 246-248; b) Z. Xu; J.S. Moore. *Angew. Chem., Int. Ed. Engl.* **1993**, 32, 1354-1357; c) K.M. Gaab; A.L. Thompson; J. Xu; T.J. Martinez; C.J. Bardeen. *J. Am. Chem. Soc.* **2003**, 125, 9288-9289; d) M. Lu; Y. Pan; Z. Peng. *Tetrahedron Letters.* **2002**, 43, 7903-7906.
13. B.R. Kaafarani; B. Wex; F. Wang; O. Catanescu; L.C. Chien; D.C. Neckers. *J. Org. Chem.* **2003**, 68, 5377-5380.
14. T. Matsuo; K. Uchida; A. Sekiguchi. *Chem. Commun.* **1999**, 1799-1800.
15. M. Malkoch; K. Schleicher; E. Drockenmuller; C.J. Hawker; T.P. Russel; P. Wu; V.V. Fokin. *Macromolecules.* **2005**, 38, 3663-3678.
16. a) S. Leininger; P.J. Stang. *Organometallics.* **1998**, 17, 3981-3987; b) F. Zeng; S.C. Zimmerman. *J. Am. Chem. Soc.* **1996**, 118, 5326-5327.
17. G.R. Newkome, C.N. Moorefield, J.M. Keith; G.R. Baker; A.L. Johnson; R.K. Behera. *Angew. Chem., Int. Ed. Engl.* **1991**, 30, 1176-1177.
18. G.R. Newkome, C.N. Moorefield, J.M. Keith; G.R. Baker; G.H. Escamilla. *Angew. Chem., Int. Ed. Engl.* **1994**, 33, 2666-668.
19. F. Zymalkowski. Howbel-Weyl. 4. Aufl. Band 4/1c. Reduction I.
20. N. Kim; M.S. Kwon; C.M. Park; J. Park. *Tetrahedron Letters.* **2004**, 45, 7057-7059.
21. a) Y. Niu; L.K. Yeung; R. Crooks. *J. Am. Chem. Soc.* **2001**, 123, 6840-6846; b) M. Zhao; R.M. Crooks. *Angew. Chem., Int. Ed. Engl.* **1999**, 38, 3, 364-366.
22. a) A. Mank. *Philips Research, Material Analysis.* **2004**, Technical Note 10, September; b) <http://www.pww.natlab.research.philips.com:25222> and <http://www.philips.com/materialsanalysis>.
23. K.F. Morris; C.S. Johnson, Jr. *J. Am. Chem. Soc.* **1992**, 114, 3139-3141.
24. K.F. Morris; C.S. Johnson, Jr. *J. Am. Chem. Soc.* **1993**, 115, 4291-4299.
25. R. Huo; R. Wehrens; J. van Duynhoven; L.M.C. Buydens. *Analytica Chimica Acta*, **2003**, 490, 231-251.

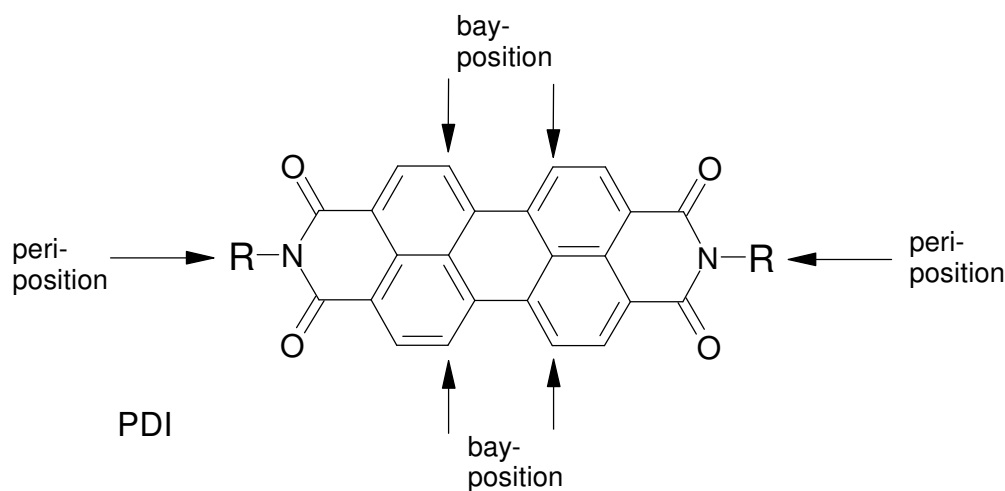
4 Dendronization of a Chromophore Core by means of the New Extended Arm 3.1

4.1 Introduction

Rylene derivatives are an important class of components in dyes and pigments, extensively employed in modern technology. In addition to their standard use as colorants in paints and lacquers, they are also encountered in reprographic processes,^[1a] optical switches,^[1b, 1c] fluorescent solar collectors^[1d] and dye lasers.^[1e, 1f] Fundamental research on the respective molecules is therefore fully justified.

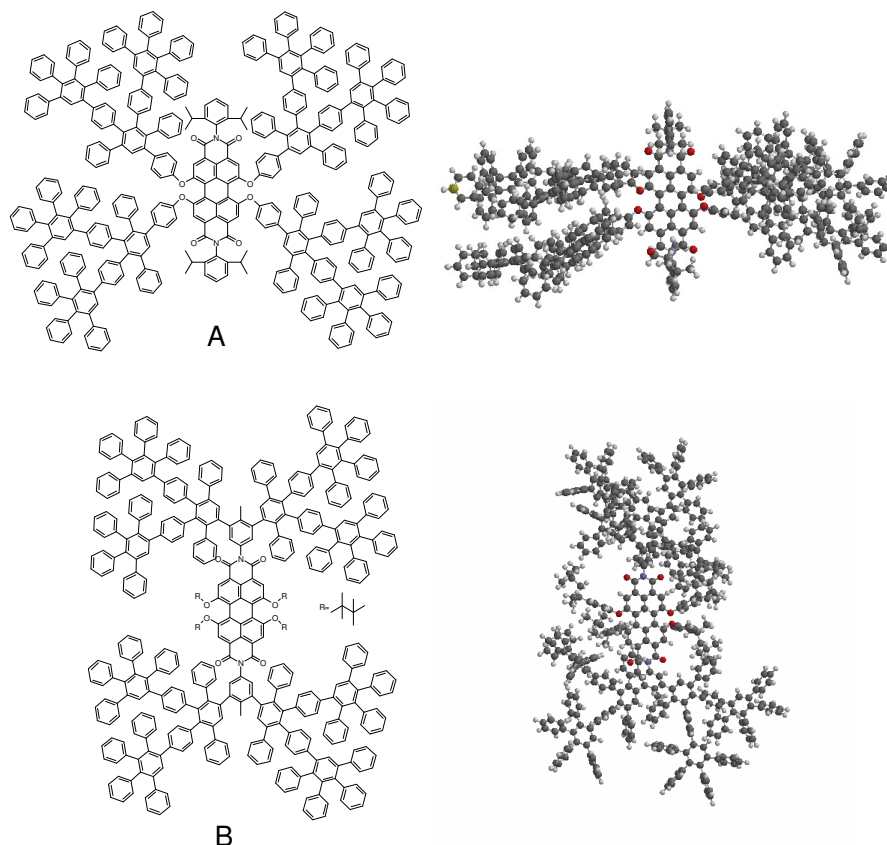
The term “rylene” derives from the structure which consists of two or more naphthalene units linked in the peri-positions (perylene, terylene, quaterylene etc.).

The most commonly employed unit is perylene-3,4,9,10-tetracarboxdiimide (PDI) which has been derivatized in multifarious ways in order to serve particular purposes.



A recurring theme has been the modification of optical properties brought about by using the PDI structure as a core in dendrimers. Dendronization may be divided into the *peri*-variant in which the branches are connected to the N atom of the carboxdiimide function (i.e. they constitute the substituent R) and the *bay*-variant where the branches are directly linked to the naphthalene units, namely in positions *ortho*- to the perylene inter-naphthalene bonds. Two examples are shown in Scheme 4.1. In view of the differing disposition of the dendrimer

branches relative to the perylene chromophore, the effect of dendronization on the optical properties should differ significantly in the two classes. This has been confirmed in that the more direct dendronization at the *bay*-position has a stronger impact than that at the more remote *peri*-carboxydiimide functionality.^[2]



Scheme 4.1: Two alternative ways of dendronizing the PDI core: **A** (*bay*-variant)^[3] and **B** (*peri*-variant)^[4] with the respective ball-and-stick models.

Another variable, at constant degree of dendronization, is the nature of the branches connected to the chromophore. Up to now, most work has been performed by attaching Müllen-type polyphenylene dendrimer branches (in the following called “general”) to the *peri*- and *bay*-positions. In order to achieve particular properties (water solubility, Broenstedt basicity) these branches have occasionally been decorated with hydrophilic groups, amino acid- and oligopeptide residues or diphenylamino groups.^[5]

Since the new extended arm dendrons prepared in the present work (Chapter 2) had led to remarkable observations with regard to achieving high generation numbers and unparalleled hydrocarbon based dendrimer extension (“exploded” dendrimers), in a side project the arm

3.1 was also connected to the perylene core. In the following, synthesis and characterization will be reported, full physico-chemical study being left to future investigations.

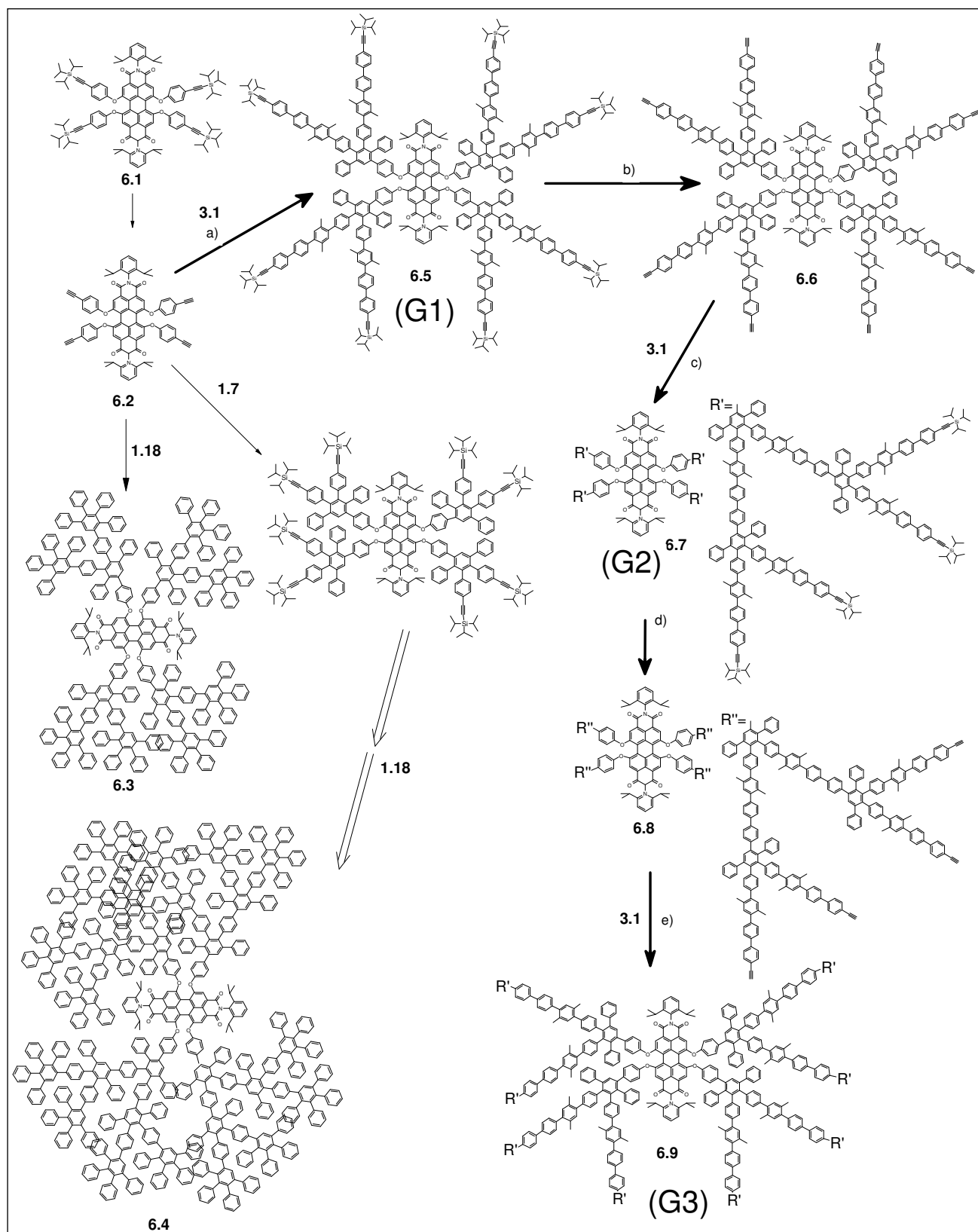
Nevertheless, at this place a few considerations will be presented with regards to the effects expected from the perylene-cored exploded dendrimers compared to the general ones. This is intended to demonstrate why the synthetic endeavour is justified:

- 1) Furnishing the perylene core with dendrons has steric as well as electronic effects. The former should be governed by the bulkiness of the arms in that the extended arms generate a much lower benzene ring density in the perylene environment. Therefore, quencher molecules have easier access to the chromophore in the extended arm, compared to the regular polyphenylene arm (**1.7**) configuration. This should influence the fluorescence properties.
- 2) The less encumbering extended arms **3.1** which generate considerable free space between them, allow extensive interpenetration of the dendronized perylene molecules. This is expected to lead to increased aggregation behavior of the “exploded” perylene-core dendrimers and properties derived therefrom.
- 3) The reduced inter-dendron steric hindrance in the extended-arm perylene dendrimers correlates with higher conformational mobility within the arms. Therefore, momentary conformations relevant to π -conjugation are expected to be more frequent. Consequently, extended arms could exert stronger mesomeric effects on the perylene core to be gleaned from shifts in the UV-vis absorption maxima. Furthermore, extended arm dendrons are expected to be more effective in energy- and electron transfer processes.

4.2 Synthesis of dendronized perylene dyes using the branching unit **3.1**

The synthesis of the extended arm modified perylenetetracarboxydiimides is shown in Scheme 4.2, where the starting material is the luminescent core **6.2**.^[6]

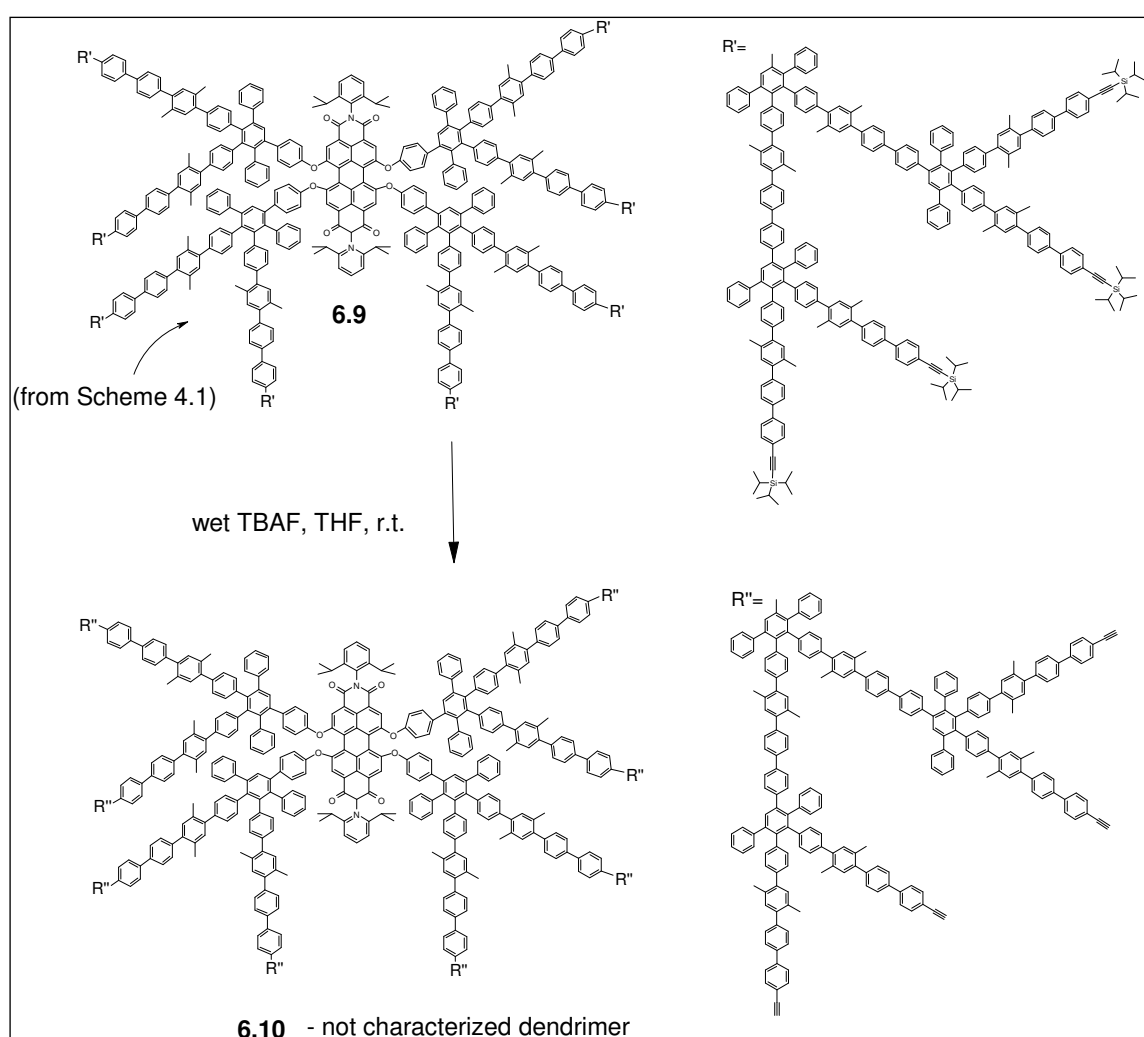
By means of iterative Diels-Alder cycloaddition the first-, second- and third-generation dendrimers (**6.5-6.9**) were synthesized in moderate yield. Since an excess of the branching unit **3.1** was employed in the Diels-Alder reaction, the first-generation dendrimer **6.5** had to be purified by column chromatography, while the second- and third-generation dendrimers (**6.7** and **6.9** respectively) were isolated in the same way as described for **3.10-3.16**.



Scheme 4.2: Synthesis of the new dendrimers **6.5-6.9** with the extended arm branching unit **3.1** based on the perylene chromophore core **6.2**, a), c), e) *o*-xylene, reflux; b), d) THF, TBAF, r.t. a) 62%, b) 80%, c) 72%, d) 89%, e) 74%. Synthesis of the corresponding short-arm dendrimers^[2] **6.3** and **6.4** is shown for comparison.

The removal of the TiPS groups by tetrabutylammoniumfluoride trihydrate (TBAF) gave the dendrimers **6.6** and **6.8**. All dendrimers **6.5-6.9** are soluble in dichloromethane, tetrachloromethane and THF. Their solubility allowed them to be characterized by spectroscopy as described in the next paragraph.

Deprotection by removal of the 32 TiPS groups in **6.9** was performed in order to obtain a new dendrimer **6.10** with 32 peripheral ethynyl groups (Scheme 4.3). Unfortunately, the compound **6.10** is insoluble in common solvents (THF, dichloromethane) as well as at elevated temperature in solvents such as toluene, tetrachloromethane or o-xylene, which limits its identification.



Scheme 4.3: Attempted deprotection of the third-generation dendronized perylene dye dendrimer **6.9**.

4.3 Characterization of dendronized chromophore dendrimers 6.5-6.10

The dendrimers **6.5-6.9** were characterized by MALDI-TOF MS, SEC, and NMR spectrometry. The MALDI-TOF MS of the second-generation dendrimer **6.7** (Figure 4.1-A) (as well as the one of **6.8**, not shown here) gave peaks pointing to oligomers (from monomer to tetramer), just like in the case of the second-generation polyphenylene dendrimers based on the tetraphenylmethane core with ter- and biphenylene spacers (**3.10**, **3.11**, and **4.5**, **4.6** in Chapter 2). SEC of **6.7** confirmed its monodispersity. The MALDI TOF MS of **6.9** (Figure 4.1-B) pointed to the molecular ion (calcd. 31853 Da, found 32063 Da), and a fragmentation at the core (calcd. for $[1/4 M^+]$ 7953 Da, found 7840 Da), their oligomers in MALDI-TOF MS with multichannel plates (Chapter 2.5) were not observed. The combination of MALDI-TOF MS and SEC (Figure 4.1) demonstrated the monodispersity of **6.9**.

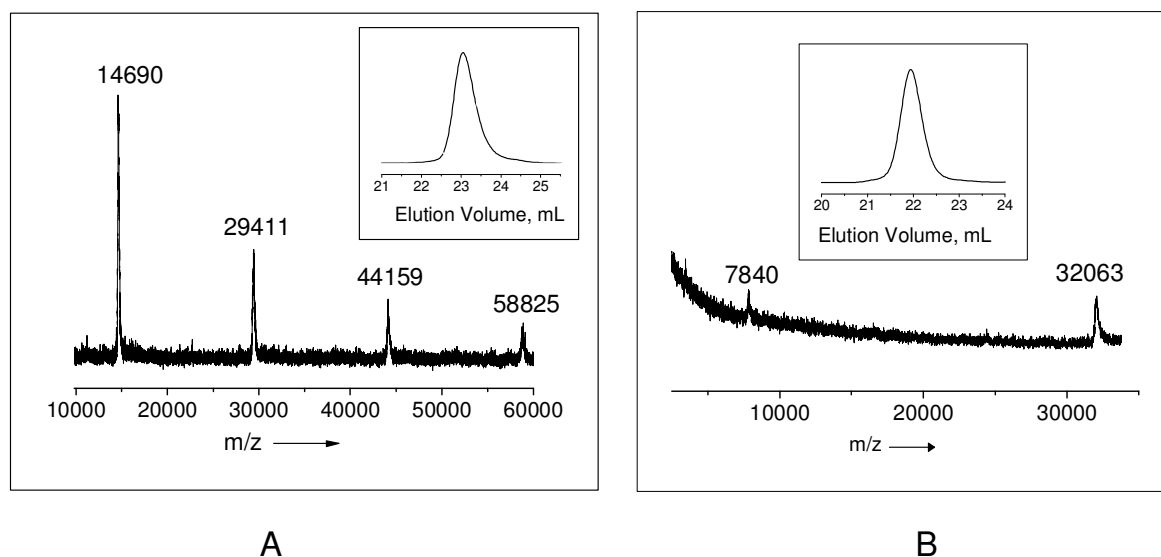
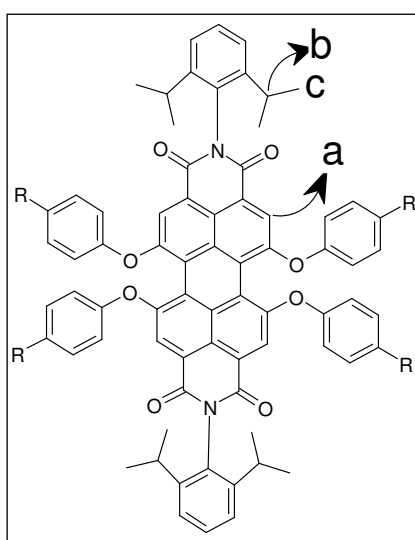


Figure 4.1: **A** - MALDI-TOF MS (dithranol, linear mode, Ag^+) and SEC of the PDI-cored second-generation dendrimer **6.7**; **B** - MALDI-TOF MS (dithranol, linear mode, K^+) and SEC of the PDI-core third-generation dendrimer **6.9**.

Compound **6.10**, the deprotected form of **6.9**, evaded full characterization (NMR spectra and SEC) because of lack of solubility in all common solvents. MALDI-TOF MS in the solid state showed no peaks. From the highly porous structure of **6.10** it is anticipated, though, that this dendrimer will show a high propensity for aggregation which may explain its low solubility.

In the ^1H NMR spectra the aromatic protons of the core and those of the dendrons cannot be distinguished due to an overlap of the signals. As the number of generation increases with the number of generation, the peaks become more unstructured in the aromatic region (unresolved signals multiplicity). Moreover, the relative signal intensity for the protons in the core position H^a , H^b and H^c (Scheme 4.4) became weaker with increasing generation number; for **6.9** (G3) peaks from H^b (Figure 4.2) and from H^a (Figure 4.3) ceased to be observable at their expected positions because of low number of H atoms (4 H^a and 4 H^b). However the intensity ratios of the aromatic protons to those of the methyl groups or of the TiPS groups agreed perfectly with the theoretically expected values.



Scheme 4.4: Designation of protons in PDI-cored dendrimers G1-G3 (**6.5-6.9**)

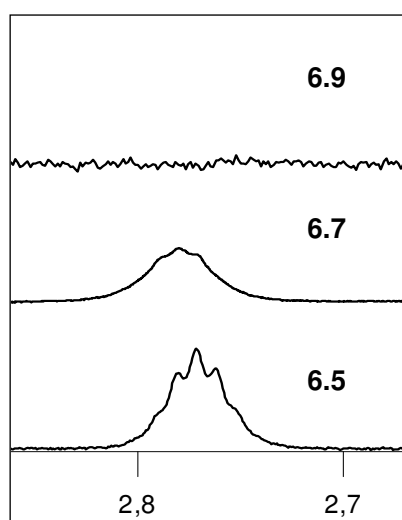


Figure 4.2: ^1H NMR signal for proton H^b (500 MHz, CD_2Cl_2 for **6.5**, 700 MHz, CD_2Cl_2 for **6.7**, and 700 MHz, $\text{C}_2\text{D}_2\text{Cl}_4$, 370 K for **6.9**).

Moreover, ^{13}C NMR spectra, as an additional tool, gave signals for C^{a} and C^{b} . NMR spectra confirmed the formation of dendrimers **6.5-6.9**.

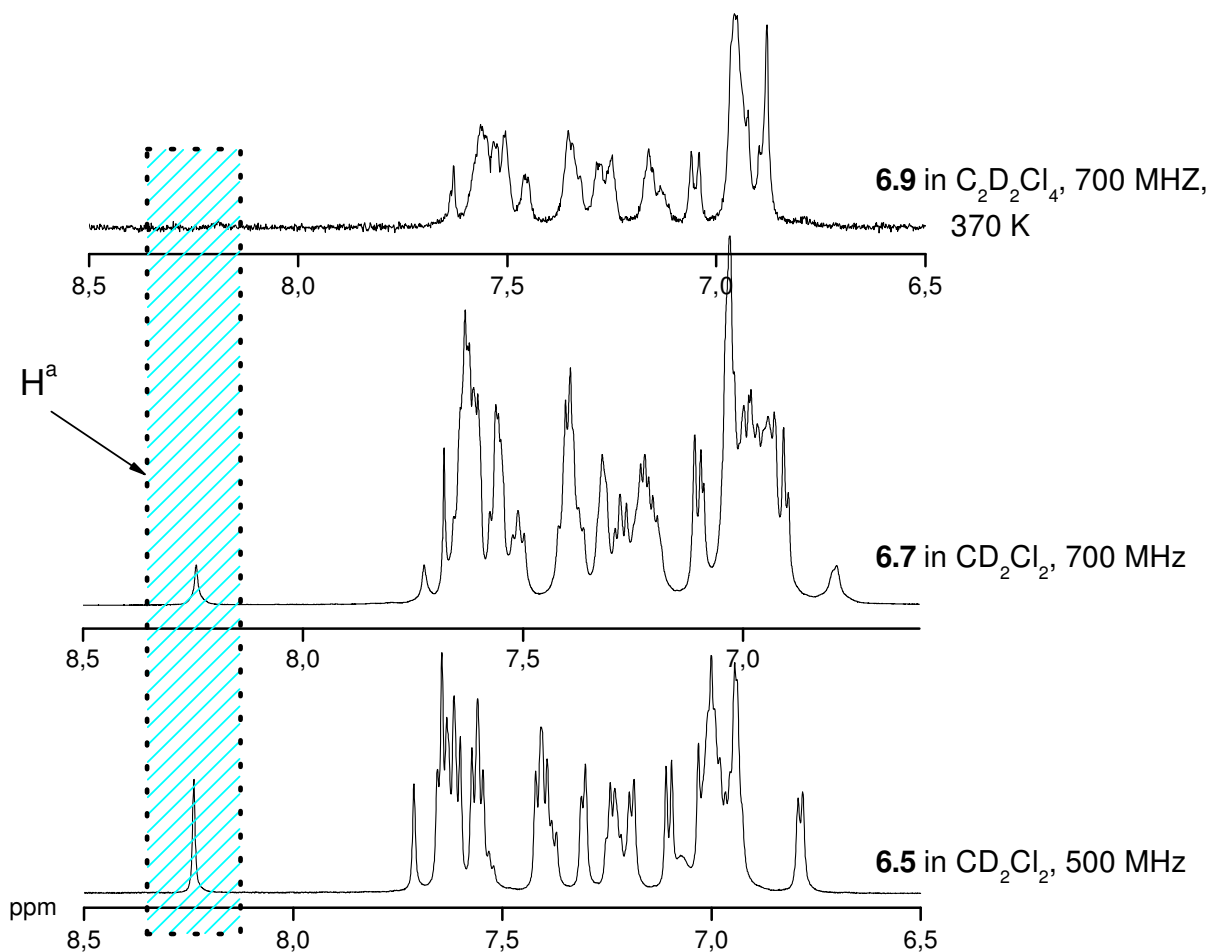


Figure 4.3: ^1H NMR spectra in the aromatic region of the first-, second- and third-generation PDI-cored dendrimers (**6.5**, **6.7**, and **6.9**).

4.4. Optical properties.

4.4.1 Absorption and emission

In order to determine the effect of the new dendritic shell on the PDI chromophore, the optical properties of dendrimers **6.5-6.9** and of core **6.1** were investigated.

The absorption spectra of dendrimers **6.5-6.9** in toluene exhibit three main bands, in the ranges 287-349 nm, 400-490 nm, and 480-615 nm (Figure 4.4). The absorption band in the UV region (287-349 nm) is assigned to the dendritic framework, which consists of strongly

twisted chains of benzene rings. The absorptions in the visible range are due to the central PDI chromophore. The intensity ratio of the dendron absorption to that of the core increases with increasing generation number. The dramatic rise in the intensity of the dendron absorption (with maxima ca 304 nm) relative to that of the perylene diimide absorption (with maxima at 449, 538, and 580 nm) is as expected from the composition of the molecules **6.5-6.9**: in **6.5** (G1) four dendrons contain 44 benzene rings, whereas the species **6.7** (G2) and **6.9** (G3) carry 132 and 308 benzene rings, respectively, in their dendrons.

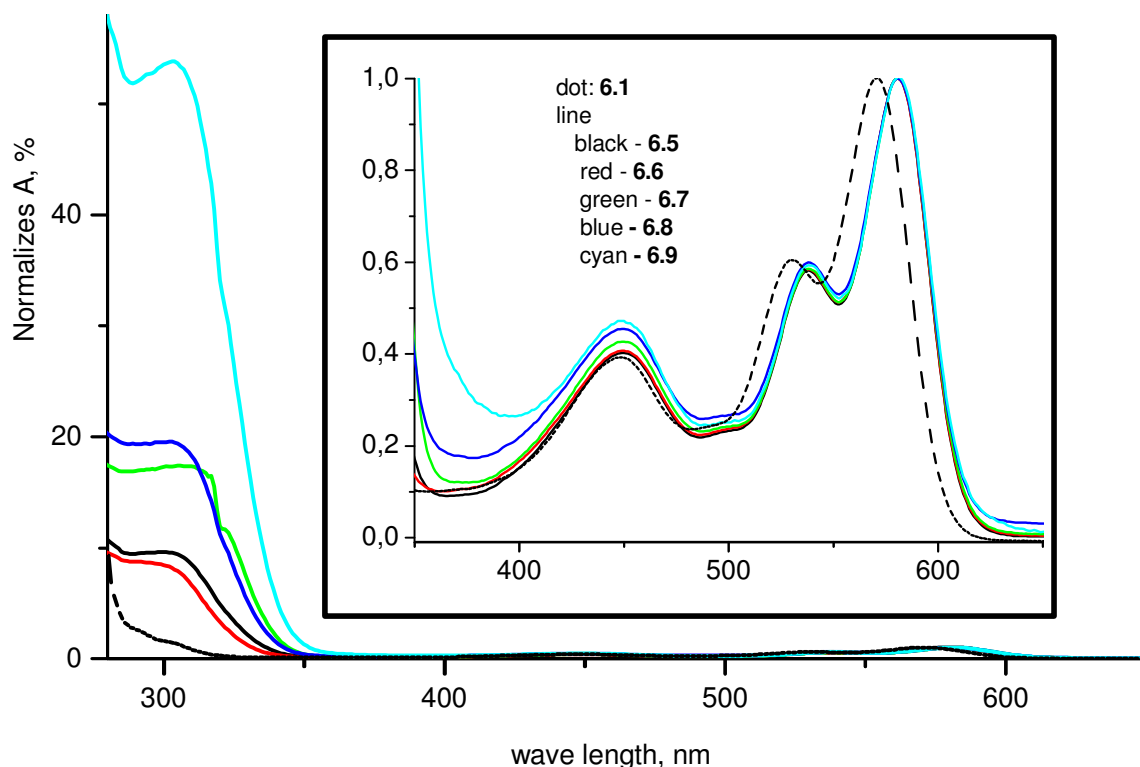


Figure 4.4: UV-vis spectra of **6.1**, **6.5-6.9** in toluene ($c=10^{-5}$ g/mL).

With regard to the assignment of the absorption spectrum of the core **6.1**, the structured strong band between 500 and 600 nm belongs to the S_0-S_1 transition, the vibronic states 0,1 and 2 being discernable. The S_0-S_1 (0-0) absorption peak lies at ≈ 570 nm and the S_0-S_1 (0-1) peak at ≈ 530 nm, they display a pronounced solvent dependence.^[7] There is even indication for the S_0-S_1 (0-2) transition at ≈ 490 nm. The band at 448 nm is assigned to the S_0-S_2 transition.^[7] These characteristics are also found in the UV-vis spectra of the new PDI-cored dendrimers **6.5-6.9**. As can be gleaned from Figure 4.4, dendronization of the core **6.1** leads to bathochromic shift of 10 nm for the components of the S_0-S_1 band but no shift for the S_0-S_2 band. Bathochromic shifts of this magnitude were also observed for the general dendrimers **6.3-6.4**^[2, 3] and other polyphenylene dendronized chromophors.^[5, 8] Apparently, the

substituent effects exerted by the dendrons are very similar for the S_0 - and S_2 electronic states leaving the HOMO/LUMO gap unaffected whereas they differ for S_0 and S_1 .

Table 4.1: UV-vis data for the PDI core **6.1** and the derived dendrimers **6.5-6.9** in toluene.

	6.1 λ_{\max}/nm	6.5-6.9 λ_{\max}/nm
S_0 - S_1 (0-0)	570	580
S_0 - S_1 (0-1)	530	538
S_0 - S_1 (0-2)	485	496
S_0 - S_2 (0-0)	448	448

Interestingly, the bathochromic shift caused by the replacement of a *para*-alkynyl group (**6.1**) for a 2,3,4,5-tetraarylphenyl substituent (**6.5-6.9**) is independent of the nature of the aryl groups since all dendrimers **6.5-6.9** display identical spectra in the visible region. In other words: the electronic structure of the PDI core is measurably affected only by the short-distance influence of the tetraarylphenyl substituents, further modifications of the dendron like proceeding to higher generations being undetectable. This means that the impact of increasing dendronization on optical properties of the core will not be governed by intramolecular electronic effects. Instead it is more likely that the variations of steric effects, which accompanies the build-up of higher generation PDI-cored dendrimers, plays the dominating role, as it controls access to the core in bimolecular processes, such as collision induced quenching.

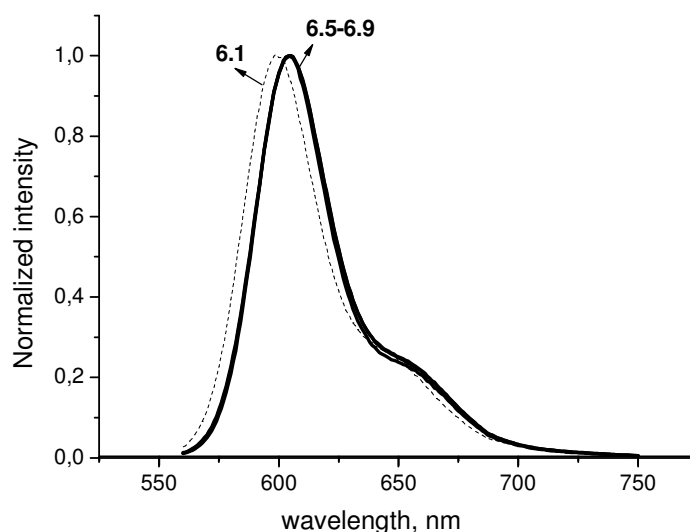


Figure 4.5: Emission spectra of core **6.1** (dot) and dendrimers (**6.5-6.9**) (solid) in toluene (with excitation at 550 nm).

The fluorescence emission spectra of the dendrimers **6.5-6.9** (Figure 4.5) appear as mirror images of the S_0-S_1 (0-0) absorption, the Stokes shift amounting to 23 nm.

As for the absorption spectra, the fluorescence spectra of the dendrimers **6.5-6.9** display identical bathochromic shifts relatively to the core **6.1**; compared to absorption these bathochromic shifts (7 nm) are somewhat smaller. Again the decisive role is played by the initial replacement of alkynyl for tetraarylphenyl and further dendronization does not significantly affect the fluorescence trace in the visible region.

4.4.2 Fluorescence quenching experiment

Study of fluorescence quenching can provide information regarding structural characteristics of dendrimers,^[9-11] since it is the nature and extension of the dendrons which governs access of the quencher molecules to the central fluorophore. For example, in the case of pyrene-labeled flexible dendrimers up to the third generations^[10] or rigid polyphenylene dendrimers based on the pyrene core^[11] up to fourth generations with variable quenchers, the Stern-Volmer quenching constant (K_{sv}) decreased with increasing generation number. These findings are explained in terms of a blocking of the pyrene fluorophore by the growing dendrimer network. The results of fluorescence quenching experiments are frequently presented as a Stern-Volmer plot.^[12]

In the Stern-Volmer equation

$$F_0/F = 1 + K_{sv}[Q] = 1 + k_q\tau_s[Q] \quad (\text{eq. 4.1})$$

F_0 and F are the fluorescence intensity in the absence and presence of the quencher, K_{sv} is the Stern-Volmer quenching constant which is the product of the bimolecular quenching rate constant (k_q) and the life time τ_s of the fluorescent species in the absence of the quencher, $[Q]$ is the concentration of the quencher.

If F_0/F is plotted versus $[Q]$ a straight line will be obtained if a single type of fluorophore is present. The Stern-Volmer quenching constant $K_{SV} = k_q\tau_s$ constitutes the slope of the line, it is characteristic for the system under study. K_{SV} among others depends on the access which the quencher molecules have to the fluorophore. Since an aim of this preliminary study was to explore whether the new extended arm dendrons differ fundamentally from the more conventional shorter ones in affecting the fluorescence properties of the PDI core, Stern-Volmer plots were drawn for the series **6.5**, **6.7**, **6.9** (Figure 4.6). As quenchers, N-benzylethylaniline and triphenylamine were employed. The quenching mechanism presumably consists of electron transfer from the amine to the lower singly occupied MO of electronically excited perylene.

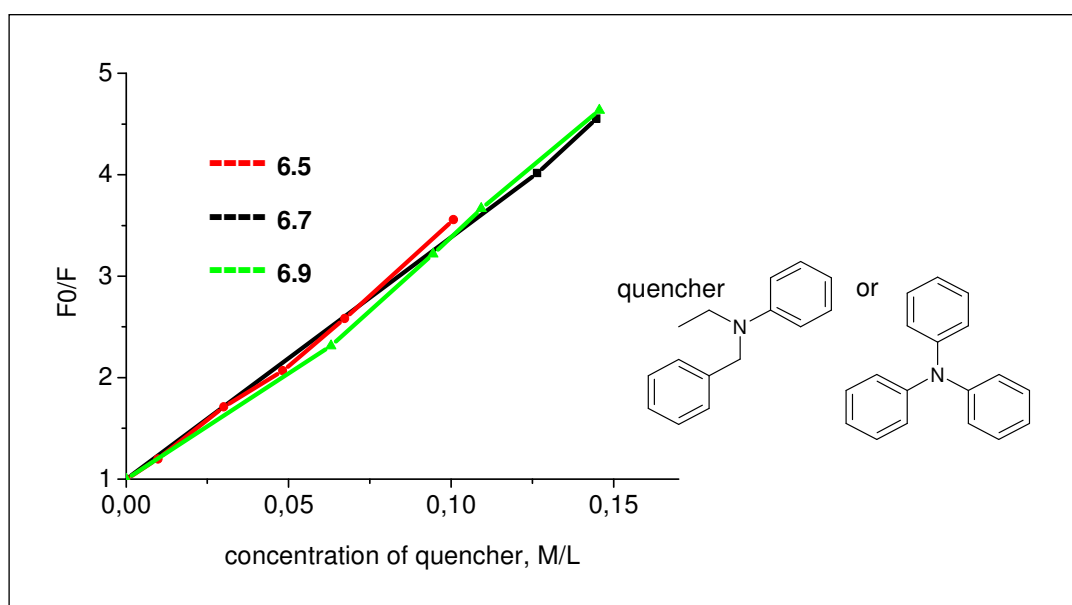


Figure 4.6: Stern-Volmer plot of the dendrimers **6.5**, **6.7**, and **6.9** in toluene.

As can be inferred from Figure 4.6 the dendrimers **6.5**, **6.7**, **6.9** share the same quenching constant $K_{SV} = 25.82 \pm 0.3 \text{ mol}^{-1}$ and no specific effect results from extending the arms in these PDI-cored dendrimers. In other words, there is no discrimination with regards to the case of collisional encounter effected by dendron variation - at least concerning the small quenchers used. A systematic study of the influence of quencher dimension on fluorescent behaviour of the new PDI-cored extended arm dendrimers reported here is in progress (C.G. Clark, Jr., personal communication). The distinction between static and dynamic quenching will have to be established by checking for possible dependence on temperature and viscosity and lifetime measurements could also be revealing.

It is worth mentioning, that apart from the quenching studies, fluorescence quantum yields also suggest that there is nothing extraordinary about extended-arm dendronization of the PDI fluorophore.

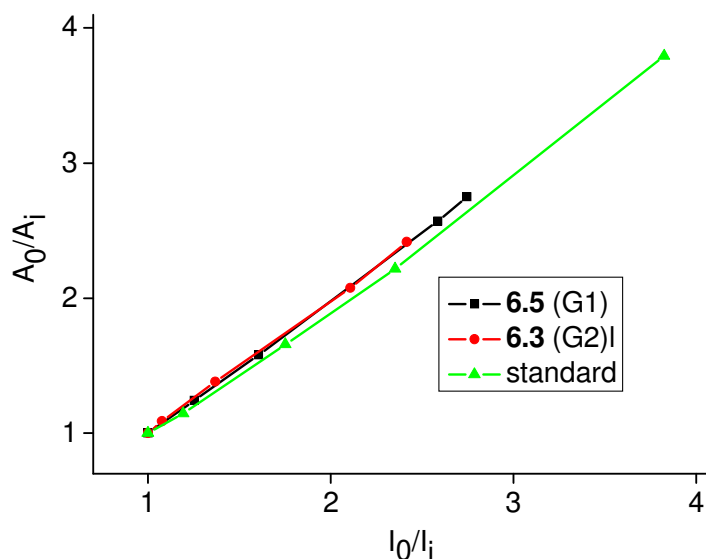


Figure 4.7: Experimental data for the determination of fluorescence quantum yields (Q_{fl}) for **6.3** and **6.5**.

In Figure 4.7 the experimental data for the determination of fluorescence quantum yields (Q_{fl}) are plotted. From the slopes, the quantum yields Q_{fl} (9,10-diphenylanthracene, standard) = 0.94 in cyclohexane and $Q_{fl}(\mathbf{6.3}) = Q_{fl}(\mathbf{6.5}) = 0.98$ in toluene are obtained in agreement with the literature value for the standard and for parent perylene.^[13] Therefore, neither the general dendron present in **6.3** (G2) nor the extended arm dendron of **6.5** (G1) notably modify the fluorescence behaviour of the PDI core.

4.4.3 Fluorescence correlation spectroscopy

Since its inception by Magde, Elson and Webb in 1972,^[14] fluorescence correlation spectroscopy (FCS) has become a well-established and powerful tool for the measurement of low particle concentrations, diffusion coefficients and kinetic parameters. Furthermore, via use of the diffusion law, hydrodynamic radii are also accessible from FCS experiments.^[14]

In view of the importance of diffusional behaviour in macromolecular chemistry in general and in the FCS technique in particular, it seems appropriate to recall a few fundamental

aspects of diffusion before discussing FCS applications to the new PDI-cored dendrimers **6.5**, **6.7**, and **6.9**.

Molecules in solution move from regions of high concentration to those of low concentration until concentration equilibration has been reached. Herein, the particle flux J is proportional to the concentration gradient:

$$J = - D \left(\frac{dc}{dx} \right) \quad \text{Fick's First Law} \quad (\text{eq. 4.2})$$

The diffusion coefficient D (m^2s^{-1}) is specific for a certain molecule, describing its mobility in fluid solution. As the concentration gradient decreases during equilibration, a time dependence of diffusion must also be introduced:

$$\left(\frac{\partial c}{\partial t} \right)_x = D \left(\frac{\partial^2 c}{\partial x^2} \right)_t \quad \text{Fick's Second Law} \quad (\text{eq. 4.3})$$

Diffusion coefficients may be determined

- from the temporal change of the concentration gradient according to

$$\left(\frac{dc}{dx} \right)_t = - \frac{c_0}{2\sqrt{\pi Dt}} e^{-x^2 / (4Dt)} \quad (\text{eq. 4.4})$$

- from dynamic light scattering (DLS) experiments (Chapter 2.11)
- by means of fluorescence correlation spectroscopy (FCS).

The latter method deals with diffusional behaviour in a system at equilibrium. Apart from size and mass, other molecule inherent features such as polarity and surface porosity also govern the magnitude of D and an a priori calculation would be extremely difficult.^[14] This justifies the elaborate methods of experimental determination of D . As has already been mentioned (Chapter 2.11), diffusion coefficients can also serve for the calculation of the Stokes-radius R_s of the diffusing molecules by means of the Stokes-Einstein relation:

$$D = - k_B T / (6\pi\eta R_s), \quad (\text{eq. 4.5})$$

where η is the coefficient of solvent viscosity. The Stokes radius is not necessary identical with the molecular dimension since it describes the radius of the moving particle as a whole, which in general travels together with its solvation shell. Therefore, R_s is usually larger than the value suggested by molecular structure. For the particular case of the solvent water, R_s is

also called the hydrodynamic radius. For species deviating from spherical symmetry, the denominator in the Stokes-Einstein relation must be modified; fairly complicated expressions for rod- and disc-shaped molecules have been given.^[15] Even these formulae are only crude approximation to real molecular shape.

At this point we return to the autocorrelation technique, already alluded to in the case of dynamic light scattering. Emphasis will be placed on the determination of the diffusion coefficients D for the new PDI-cored dendrimers **6.5**, **6.7**, and **6.9** which bear extended arms and their comparison with the general dendrimers **6.4** and **6.5**.

In fluorescence correlation spectroscopy (FCS) the spatial and temporal evolution of the fluctuations of fluorescence signal intensity is subjected to statistical analysis. This furnishes information on the behaviour of individual molecules because the number of molecules in the observation volume is very small. In a typical FCS experiment, a femtoliter quantity of a nanomolar solution is investigated, which corresponds to a one digit number of molecules in the observation volume. Under these conditions every molecule contributes to the observed signal. The fluctuations arise from the fact, that the molecules diffuse into and out of the focal volume (see experimental considerations). Therefore, the temporal pattern by which fluorescence fluctuations arise and decay carries information about the molecular dynamics. Statistical analysis in FCS consist in the experimental determination of the autocorrelation function $G(\tau)$ and its simulation based on the underlying molecular process. (Apart from diffusion, this process may also be a chemical reaction in which case kinetic parameters rather than the diffusion coefficients are obtained.) The autocorrelation function takes the following form:

$$G(\tau) = \frac{\langle \delta F(t) \cdot \delta F(t+\tau) \rangle}{\langle F(t) \rangle^2}, \quad (\text{eq. 4.6})$$

where $\langle \rangle$ is a temporal average

$F(t)$ = intensity of fluctuating fluorescence signal at time t

$\delta F(t) = F(t) - \langle F(t) \rangle$ = deviation at time t from temporal average

$\delta F(t+\tau) - \langle F(t) \rangle$ = deviation at time $(t+\tau)$ from temporal average

τ is a time lag between two measurements (correlation time).

The autocorrelation function experimentally determined for the dye Rhodamin green is shown in Figure 4.8.^[16]

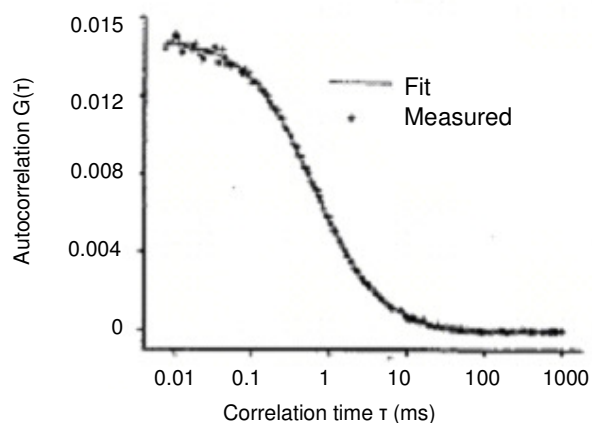


Figure 4.8: Autocorrelation function for Rhodamin green, $\lambda_x=488$ nm.

It has been stated that “autocorrelation analysis provides a measure for the self-similarity of a time series signal and therefore describes the persistence of information carried by it”.^[17] Referring to Figure 4.8 this may be interpreted as the fact, that for small time lags τ , successive measurements yield similar results (strong correlation of signals) whereas for large time lags τ correlation is lost ($G(\tau) = 0$). Of interest is not the correlation function itself but its interpretation with the aim of extracting quantitative information on the physical process which gives rise to its shape. For a single type of species diffusing into and out of a prolate ellipsoidal observation volume, the following analytical form applies:

$$G(\tau) = \frac{1}{\langle N \rangle} \frac{1}{1 + \frac{\tau}{\tau_0}} \frac{1}{\sqrt{1 + \left(\frac{w_z}{w_{xy}}\right)^2 \frac{\tau}{\tau_D}}} \quad (\text{eq. 4.7})$$

$$\text{with } \tau_D = \frac{w_{xy}^2}{4D} \quad (\text{diffusion time}) \quad (\text{eq. 4.8})$$

where $\langle N \rangle$ = mean number of molecules in the observation volume

w_z = axial waist of prolate ellipsoidal observation volume

w_{xy} = lateral waist of prolate ellipsoidal observation volume

(w_z and w_{xy} are properties of the experimental set up).

Fitting this expression to the experimental correlation function yields the diffusion time τ_D and therefrom the diffusion coefficient D of the fluorescent species. Alternatively, if the diffusion coefficient is known, the concentration can be determined from the value of $\langle N \rangle$ and the observation volume. The latter variant is important for biochemical application, for example the determination of concentration in the interior of cells.

The experimental setup for obtaining the correlation functions will be described only briefly, Figure 4.9 illustrates the essential components.

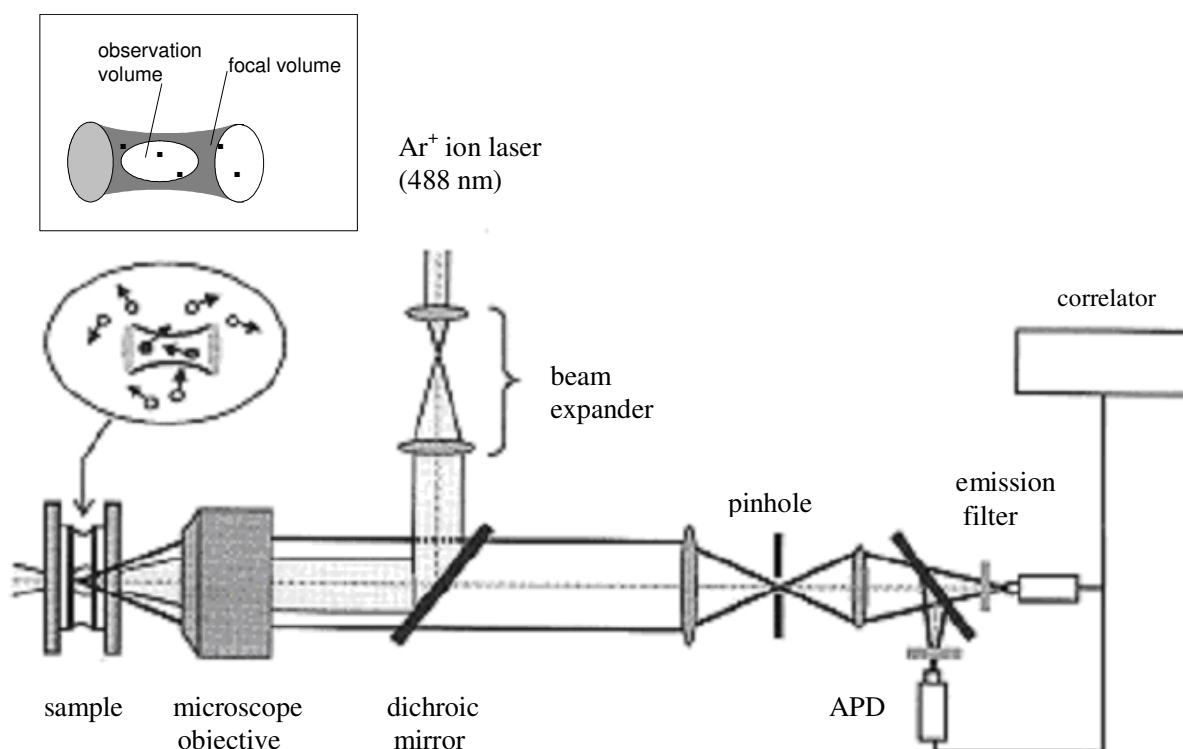


Figure 4.9: Sketch of FCS instrumentation (taken from ref.^[18]). The prolate ellipsoidal observation is defined by the axial waist w_z and the lateral waist w_{xy} .

Key to the FCS experiment is the generation of a minute observation volume. This is achieved by strongly focusing the incoming laser beam to a diffraction limited spot. The waist of the beam in the objective focal plane therefore is similar to the illumination wavelength which typically is about 500 nm. In order to limit the detection volume in axial direction as well, a pinhole is introduced in the image plane which blocks all light not coming from the focal region of the sample. Only the small numbers of fluorophores within the illuminated region are excited and give rise to fluorescence signals. Confocal detection is applied in that the

fluorescent light is collected through the same microscope objective. A dichroic mirror separates the fluorescence light from the excitation light, taking advantage of the fact that, because of the Stokes shift, the emitted fluorescence occurs at longer wavelength than the excitation. Detection is preferably performed by means of an avalanche photodiode (APD).

The fluorescence intensity signal is computer-processed by a correlator which can handle varying sampling and delay times; the latter can range from less than a microsecond to several minutes. For more details see references.^[16-19] The normalized autocorrelation functions for the general Müllen-type dendrimers **6.3** (G2) and **6.4** (G3) are depicted in Figure 4.10-A, those for the core **6.1** (G0) and for new extended arm dendrimers **6.5** (G1), **6.7** (G2), and **6.9** (G3) are presented in Figure 4.10-B

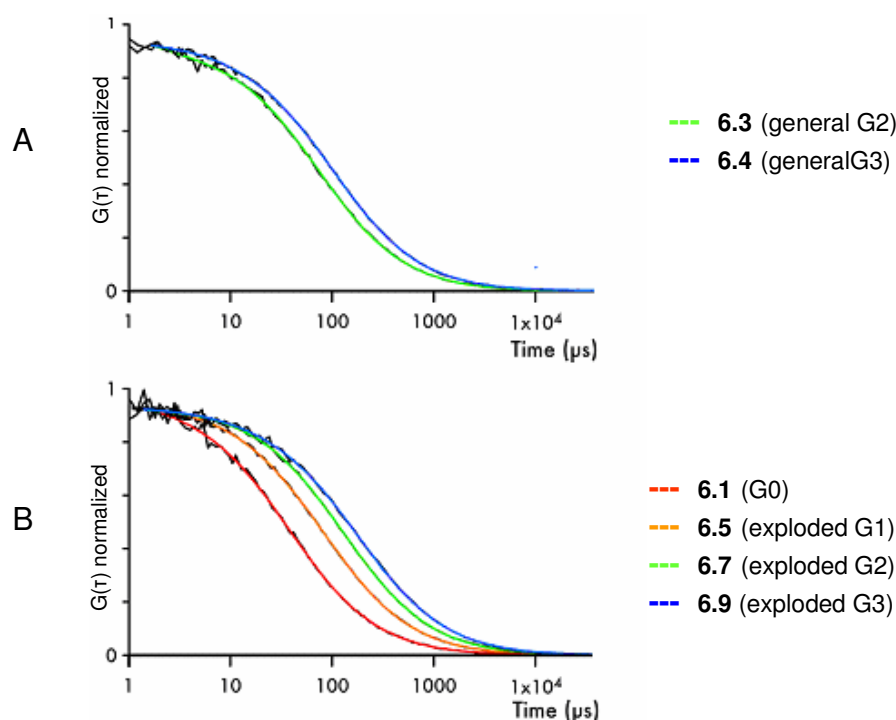


Figure 4.10: Normalized fluorescence autocorrelation curves: **A** for general (**6.3**, **6.4**), **B** for “exploded” (**6.5**, **6.7**, **6.9**) PDI-cored dendrimers. The curve for the core **6.1** is also shown.

The excitation light was provided by a He/Ne laser (2.5 mW, $\lambda=543$ nm) and an adjustable pinhole (90 μm) and an emission filter (543 nm) were used. Solutions were prepared from HPLC grade toluene at concentrations ca 10^{-8} mol/L which corresponds to about one particle in the observation volume.

Application of equations 4.7 and 4.8 requires knowledge of w_{xy} , the lateral dimension of the observation volume. Since w_{xy} is not known a priori, it must be determined by means of standards with known diffusion coefficients D . For this purpose, the dendrimers **6.3** and **6.4** can be employed whose D values have been derived independently from dynamic light scattering DLS (Table 4.2).

Table 4.2: Standardization of the FCS experiment, using diffusion coefficients $D(\mathbf{6.3})$ and $D(\mathbf{6.4})$ obtained from DLS. Toluene was used as a solvent.

	DLS	FCS			
	$D/10^{-10} \text{ m}^2 \text{ s}^{-1}$	$w_{xy}/\mu\text{m}$	$w_z/\mu\text{m}$	diffusion time $\tau_D/\mu\text{s}$	Stokes radius R_S/nm
6.3	2.36	0.246	2.06	63.7	1.58
6.4	1.69	0.247	2.07	89.8	2.23

The lateral radius $w_{xy} = 246 \text{ nm}$ determined in this way agrees with the notion mentioned above that the dimension of the waist of the observation volume resembles the wavelength of the excitation beam ($543 \sim 2 \times 246 \text{ nm}$ in the present experiments). The diffusion coefficients D deduced from the experimental autocorrelation functions are listed in Table 4.3.

Table 4.3: Values for the diffusion time τ_D , the diffusion coefficient D , and the Stokes radius R_S , obtained from the respective autocorrelation function making use of eq. 4.7 and 4.8. $\langle N \rangle$ is known from the concentrations of the samples and w_{xy} has been determined by standardization. Toluene was used as a solvent. The Stokes radii R_S were calculated with eq. 4.5.

	FCS		
	$D/10^{-10} \text{ m}^2 \text{ s}^{-1}$	$\tau_D/\mu\text{s}$	R_S/nm
6.1	4	37.8	0.94
6.5	1.83	82.8	2.06
6.7	1.17	129.7	3.22
6.9	0.84	180.1	4.48

Since molecular dimension is a major factor governing the magnitude of D , in Figure 4.11, D is plotted against R_{\max} which represents the largest extension of the respective dendrimers taken from molecular models (Spartan Pro with the molecular force field MMFF). These models deviate grossly from spherical symmetry and a single Stokes radius cannot be defined; rather, molecular shape should be approximated by an ellipsoid which would require consideration of three orthogonal axes differing in magnitude. Yet, for dendrimers which feature a highly porous surface this approach is unrealistic because diffusional behaviour is controlled by the dimension of the solvated molecule rather than by naked species. Therefore, the effective Stokes radius will be considerably larger than the radius derived from a model or from a precise structure determination.

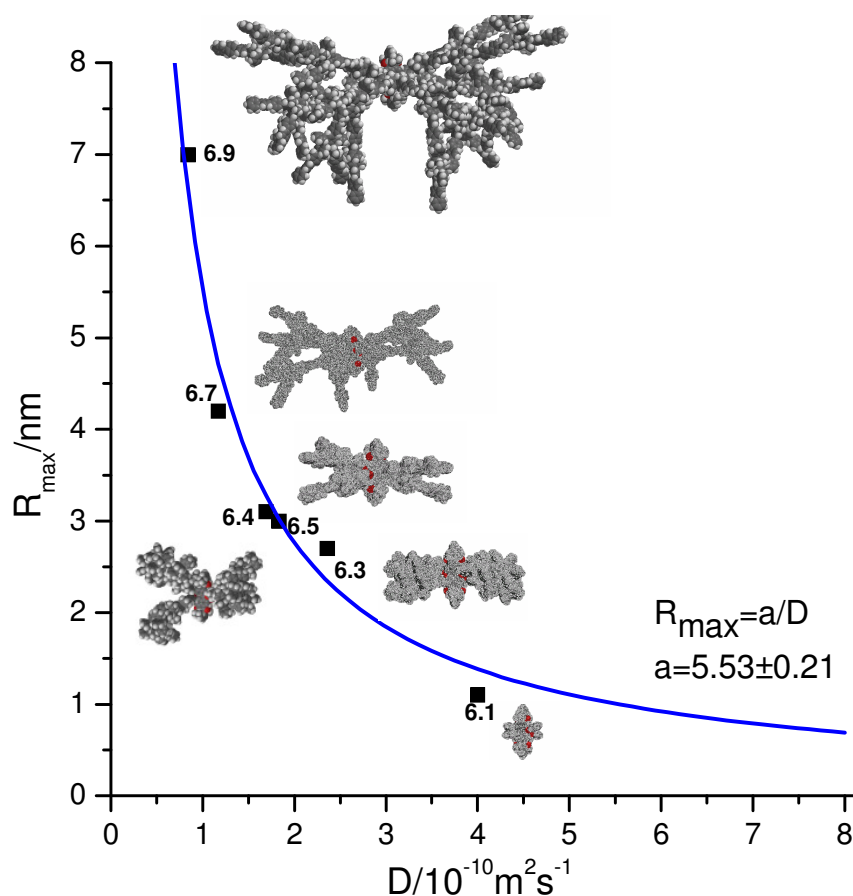


Figure 4.11: Plot of molecular size represented by the largest extension R_{\max} taken from molecular models against diffusion coefficient D determined by means of FCS.

It is the more surprising that the plot of D versus R_{\max} nicely approximates a hyperbolic shape thereby implying proportionality between R_{\max} and D^{-1} . Importantly, this proportionality

includes the more dense “surface-closed” general dendrimers (**6.3**, **6.4**), and the less dense, more porous extended arm dendrimers (**6.5**, **6.7**, **6.9**, and the core **6.1** (G0) itself). This is exemplified by **6.4** (G3) and **6.5** (G1) which share the same R_{\max} value and possess nearly identical diffusion coefficients despite largely differing mass. Significant differences would be expected at higher concentrations because then, the cleft extended arm dendrimers **6.5**, **6.7**, and **6.9** would be more prone to aggregation than the more rounded general dendrimers **6.3** and **6.4**. Concentrated solutions are, however, out of the realm of fluorescence correlation spectroscopy.

4.5. Literature for Chapter 4

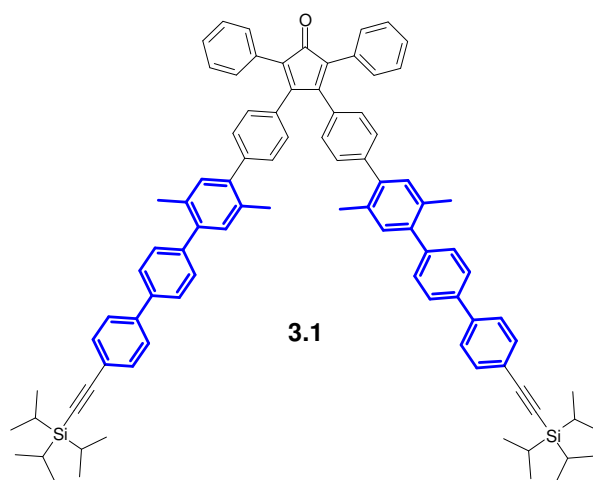
1. a) H.O. Loufty; A. M. Hor; P. Kazmaler; M. Tarn. *J. Imaging Sci.* **1989**, 33, 151; b) M.P. O’Neil; M.P. Niemczyk; W.A. Svec; D. Gosztola; G.L. Gaines; M.R. Wasielewski. *Science*. **1992**, 257, 63; c) S. Tasch; E.J.W. List; O. Ekstrom; W. Graupner; G. Leising; P. schlichting; U. Rohr; Y. Geerts; U. Scherf; K. Mull. *Appl. Phys. Lett.* **1997**, 71, 2883; d) G. Seybold; G. Wagenblast. *Dyes Pigm.* **1989**, 11, 303; e) R. Gvishi; R. Reisfeld; Z. Burshtein. *Chem. Phys. Lett.* **1993**, 213, 338; f) M Sadrai; L. Hadel; R.R. Sauer; S. Husain; K. Krogh-Jespersen; J.D. Westbrook; G.R. Bird. *J. Phys. Chem.* **1992**, 96, 7988.
2. D. Liu; S.De Feyter; M. Cotler; A. Stefan; U.-M. Wiesler; A. Hermann; D. Grebel-Koehler; J. Qu; K. Müllen; F.C. De Schryver. *Macromolecules*. **2003**, 36, 5918-5925.
3. D. Grebel-Koehler. Ph-D dissertation, University of Mainz, **2004**.
4. A. Hermann; T. Weil; V Sinigersky; U.-M. Wiesler; T. Vosch; J. Hofkens; F.C. De Schryver; K. Müllen. *J. Chem. Eur.* **2001**, 7, 22, 4844.
5. a) C. Kohl; T. Weil; J. Qu; K. Müllen. *Chem. Eur. J.* **2004**, 10, 5297-5310; b) J. Qu. Ph-D dissertation, University of Mainz, **2004**; c) C. Kohl. Ph-D dissertation, University of Mainz, **2004**.
6. a) J. Qu; N.G. Pschirer; D. Liu; A. Stefan; F.C. De Schryver; K. Müllen. *Chem. Eur. J.* **2004**, 10, 528.
7. R. Gvislu; R. Reisfeld; Z. Burshtein. *Chem. Phys. Letters.* **1993**, 213, 338.
8. J. Qu; J. Zhang; A.C. Grimsdale; K. Müllen; F. Jaiser; X. Yang; D. Neher. *Macromolecules*. **2004**, 37; 8297.

9. a) S. Glazier; J.A. Barron; N. Morales; A.M. Ruschak; P.L. Houston; H.D. Abruna. *Macromolecules*. **2003**, 36, 1272-1278; b) A.C.H. Ng; X. Li; D.K.P. Ng. *Macromolecules*. **1999**, 32, 5292-5298.
10. C.M. Cardona; T. Wilkes; W. Ong; A.E. Kaifer; T.D. McCarley; S. Pandey; G.A. Baker; M.N. Kane; S.N. Baker; F.V. Bright. *J. Phys. Chem. B*. **2002**, 106, 8649-8656;
11. a) S. Bernhardt; M. Kastler; V. Enkelmann; M. Baumgarten; K. Müllen. Submitted, **2006**; b) S. Bernhardt. Ph-D dissertation, University of Mainz, **2005**.
12. a) M.W. Legenza; C.J. Marzocco. *J. Chem. Education*. **1977**, 54, 3, 183; b) W. R. Ware; H.P. Richter. *J. Chem. Physics*. **1968**, 18, 4, 1595.
13. a) E. Clar; B.A. McAndrew; M. Zander. *Tetrahedron*, **1967**, 23, 985; b) M. Zander. *Polycyclische Aromaten*, **1995**, Teubner, Stuttgart.
14. D. Magde; E. Elson, W.W.W. Webb. *Phys. Rev. Lett.* **1972**, 29, 705.
15. R. Winter; F. Noll. *Methoden der Biophysikalischen Chemie*. **1998**, Teubner, Stuttgart, 91.
16. S.T. Hess; S. Huang; A.H. Heikal; W.W. Webb. *Biochemistry*. **2002**, 41, 697.
17. a) P. Schwillw; E. Haustein. Fluorescence correlation spectroscopy, an introduction to its concepts and applications, www.biophysics.org/education/schwille.pdf.
18. L. Wawrezinieck; P.-F. Lenne; D. Marguet; H. Rigneault. *Biophysical J.* **2005**, 89(6), 4029-4042.
19. a) E.L. Elson; D. Magde. *Biopolymers*. **1974**, 13, 1; b) D. Magde; E.L. Elson. *Biopolymers*. **1974**, 13, 29.

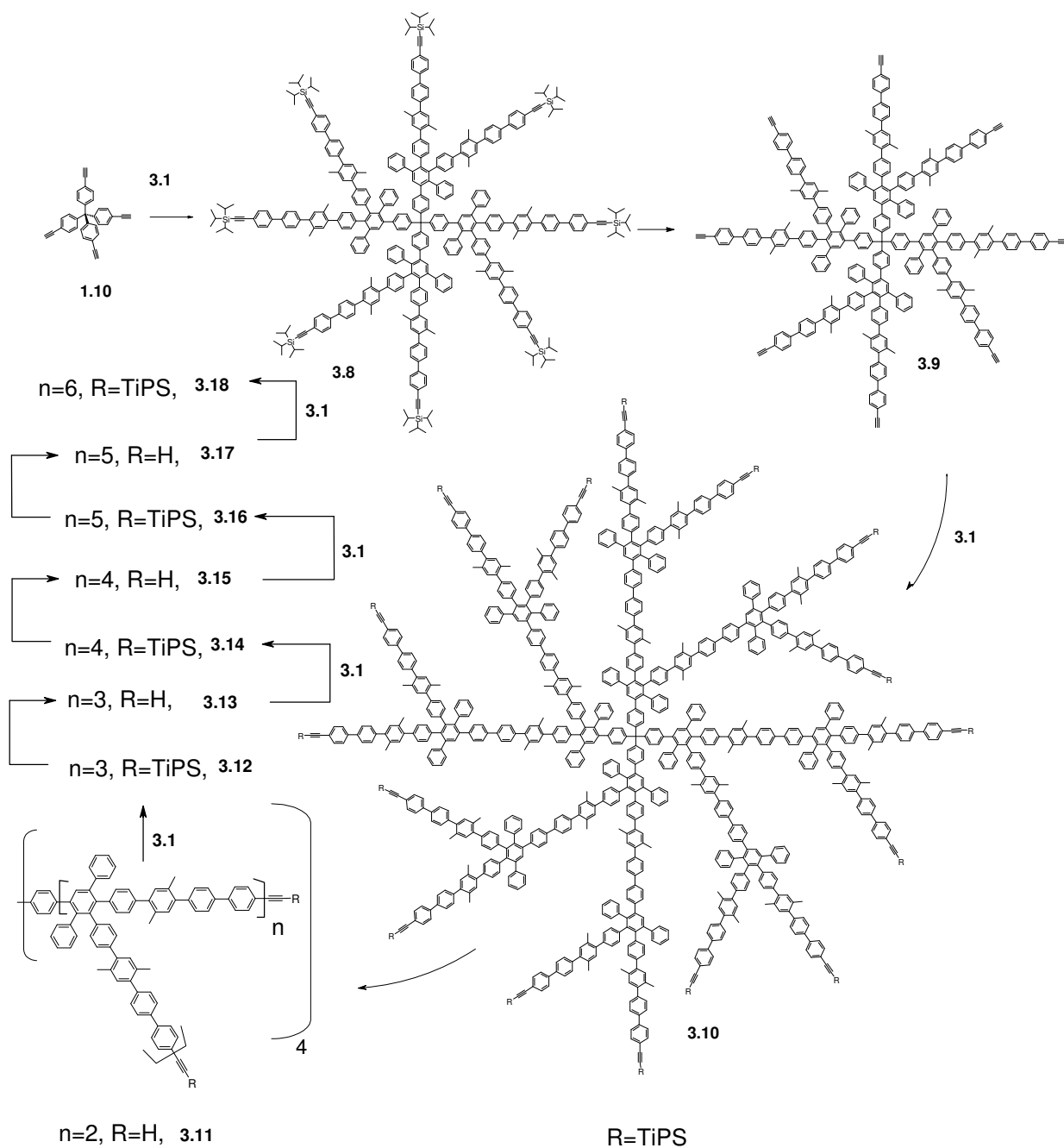
5 Summary

Dendrimers, a new class of macromolecular compounds, complement conventional polymers in that they display monodispersity and, accordingly, control over structural features and related physical and chemical properties. Therefore, since the 1970's they have become the object of intense investigation. A rough division into (a) heteroatom containing and (b) hydrocarbon based representatives can be made. Whereas the former, depending on the type of functionalities they contain, display specific chemical properties, for the latter structural features such as flexibility versus rigidity, and the number, size and shape of internal cavities are of foremost concern. Work described in the present dissertation deals with the second category only. In particular, the polyphenylene principle of dendronization is put to work with the aim of increasing the number of generations beyond G4, starting from the premise that extended arms should result in less steric hindrance, a factor which usually limits the attainable maximal generation number.

Chapter 2, in which *Extended Arm Polyphenylene Dendrimers* are explored, constitutes the core of the present dissertation. Since the Dilthey reaction, which had proved to be highly successful in the synthesis of polyphenylene dendrimers, was selected as the synthetic strategy, preparation of an extended arm branching unit was called for. This was accomplished in the seven-step synthesis of unit **3.1**.



The new branching unit **3.1** proved to be applicable in the preparation of dendrimers up to the sixth generation (G6) starting from the tetrahedral core **1.10**.



MALDI-TOF techniques play an important role in the identification of the new dendrimers up to G4 (**3.14**, $M = 65495$ Da, comparable to human hemoglobin!). M^+ peaks could be recorded in the linear mode of operation; in this technique oligomers were frequently observed, up to M_9^+ in the case of **3.10** (G2), which point to clustering in the gas phase. For the G5- and G6 extended arm dendrimers we had to resort to the newly developed technique MALDI-TOF STJ which, thanks to the use of a superconducting tunnel-junction detector, is capable of detecting molecular ions M^+ with $M > 250$ kDa. Again, clustering was present to the extent that for **3.14** (G4) M^+ and the following oligomers M_n^+ ($n = 2,3,4$) appeared in comparable intensity, while for **3.16** (G5) and **3.18** (G6) oligomers only were detectable, M^+ evading observation. For **3.18** (G6), the highest observable peak pointed to a hexamer $(\mathbf{3.18})_6^+$ which places this species in the 1.5 MDa range. Apart from these details it must be stated that MALDI-TOF MS confirmed success of the extended arm approach to increase the attainable generation number, since the use of the general dendron (**1.7**) in the past only permitted dendrimer synthesis up to G4.

Whereas, due to the self-similarity of successive shells in higher generation dendrimers, NMR techniques were not particularly revealing, size exclusion chromatography (SEC) constitutes an important technique for gathering approximate molecular masses of the new dendrimers.

SEC elution profiles for **3.8** (G1) to **3.18** (G6) provided unequivocal proof for the gradual build-up of higher generations and good monodispersity of the individual dendrimers. With regard to only fair numerical agreement between calculated and SEC-derived molecular masses, it must be stressed that SEC standardization is based on linear polystyrene molecules whose shape radically differs from that of dendrimers. For **3.16** (G5) and **3.18** (G6) shoulders towards low elution volumes may be traced to aggregation. That the lower elution volume shoulders, observed for **3.16** and **3.18**, can really be attributed to species of increased size rather than to higher mass particles formed by inclusion of material into the dendrimer cavities was proved by multi-angle laser light scattering size exclusion chromatography (MALLS-SEC).

Whereas the estimation of size by means of SEC is very approximate, more precise information could be gained from dynamic light scattering (DLS). In fact, the hydrodynamic radii of the dendrimers **3.8** (G1)-**3.16** (G5) nicely conform to those, taken from molecular models. The larger hydrodynamic radius determined for **3.18** (G6) by DLS again points to aggregation.

Direct visualization of the new extended arm dendrimers **3.16** (G5) and **3.18** (G6) was achieved by transmission electron microscopy (TEM). These studies confirmed the spherical

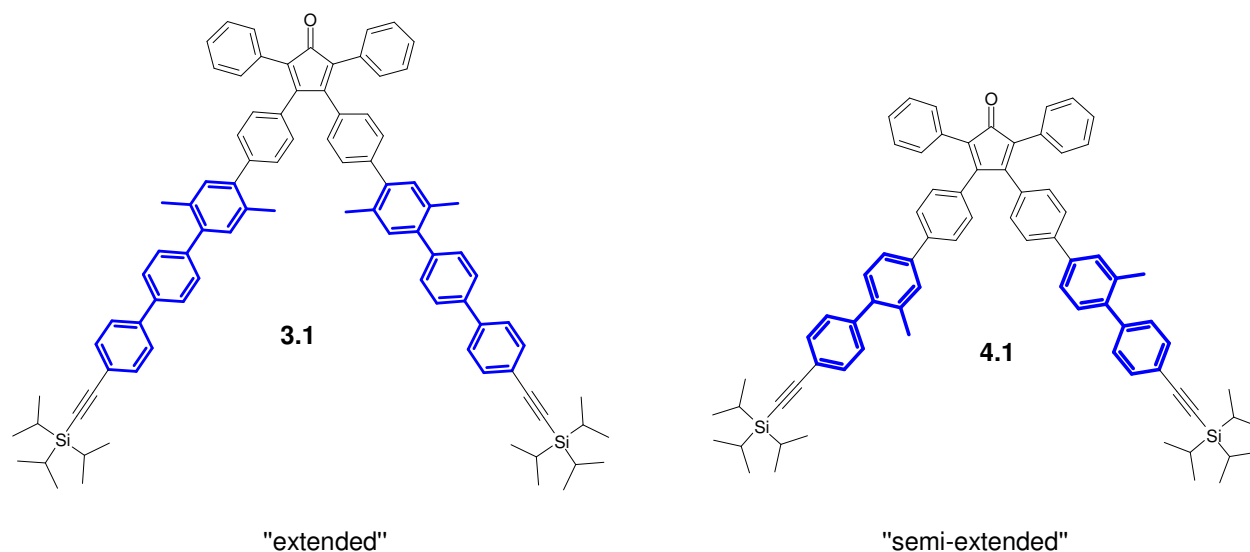
shape of the particles and the histograms of particle size distribution led to diameters in good agreement with those obtained from molecular modeling. The enormous increase in size per added generation is demonstrated by the fact that G3 for extended arm polyphenylene dendrimers matches in size G10 in the class of polyaminoamine (PAMAM) dendrimers, both radii being in the 7 nm range. Furthermore, the G5 (extended arm) dimension approaches that of γ -globulin (radius = 12 nm).

Atomic force microscopy (AFM), performed in the non-invasive tapping mode, also furnished images of the single extended arm dendrimer **3.16** (G5) in sufficiently diluted solutions in THF where spin-coated onto mica. Under these conditions only few aggregates were discernible. Whereas the lateral diameter of 24 nm for **3.16** (G5) agrees well with expectation, the (vertical) height of about 3 nm indicated pronounced flattening upon adsorption on mica.

A different result was obtained from dichloromethane as a solvent in that two-layered aggregates were seen. Flattening is a well known phenomenon in AFM study of dendrimers; it is made plausible by the tendency to maximize interfacial contact of the substrate with the supporting surface with attendant gain in energy of adsorption. However, it must also be kept in mind that the “exploded” dendrimers studied here constitute low density solids exposing a highly porous surface to the measuring device of AFM. Therefore, it is arguable whether this technique, which relies on van der Waals forces, faithfully reproduces the vertical dimension of absorbed “exploded” dendrimers.

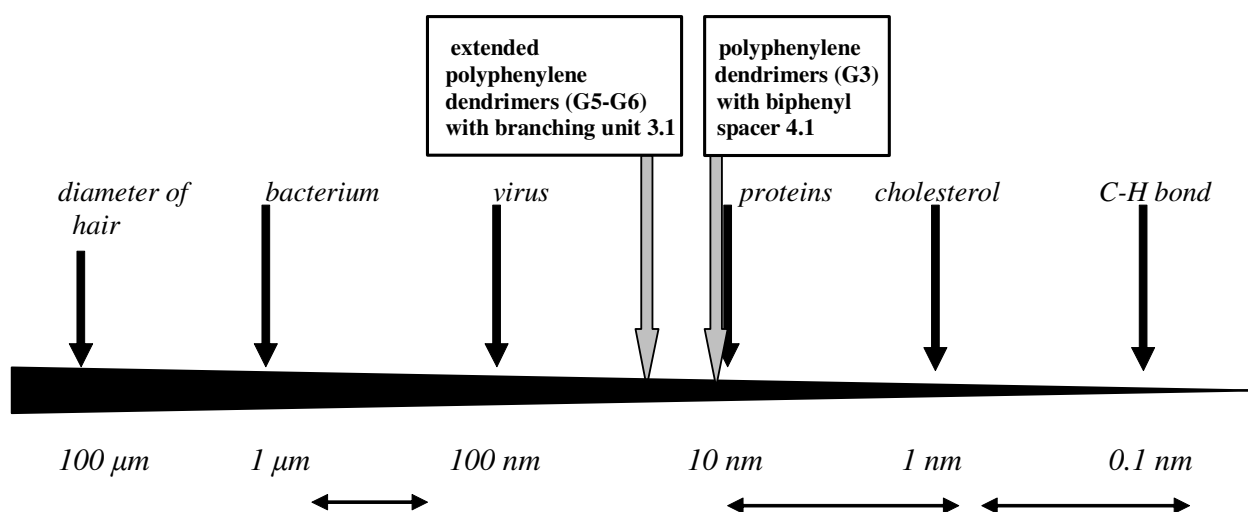
In response to the initial question as to whether extended arm dendrimers lend themselves particularly well to the incorporation of guest molecules in their internal cavities, measurements with the quartz microbalance (QMB) were performed. Competition experiments revealed that the extended arm type dendrimer is much more apt to incorporate guest molecules than the general type.

Although the new exploded dendrimers show interesting properties, also in view of potential applications, the fairly difficult access to the extended arm branching unit **3.1** should not be overlooked. Therefore the synthesis and characterization of “semi-extended” dendrimers was carried out. The name implies that the spacer between the tetraphenylcyclopentadienone and the alkynyl groups in the arm is a biphenyl rather than a terphenyl unit.



The branching unit **4.1** could be obtained more simply and economically than **3.1**, it was subsequently converted into semi-extended dendrimers up to G3, using the same methods of synthesis and characterization as for the extended analogs. Importantly, the hydrodynamic radii and the surface porosity show the gradation: general \ll semi-extended \sim extended. Therefore, the semi-extended dendrimers are promising materials for exploratory studies on practical applications.

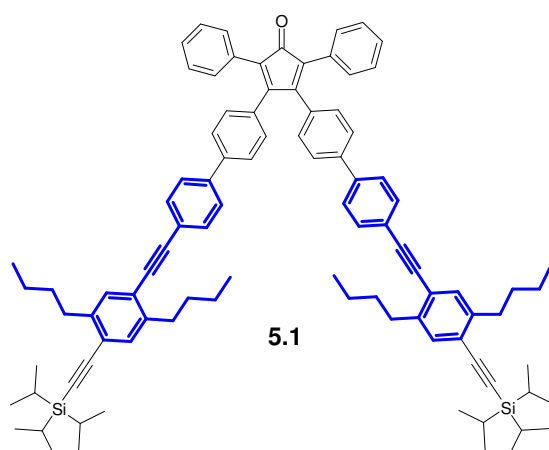
The summary of the central Chapter 2 should not be ended without placing the dimension of the new extended arm dendrimers in perspective:



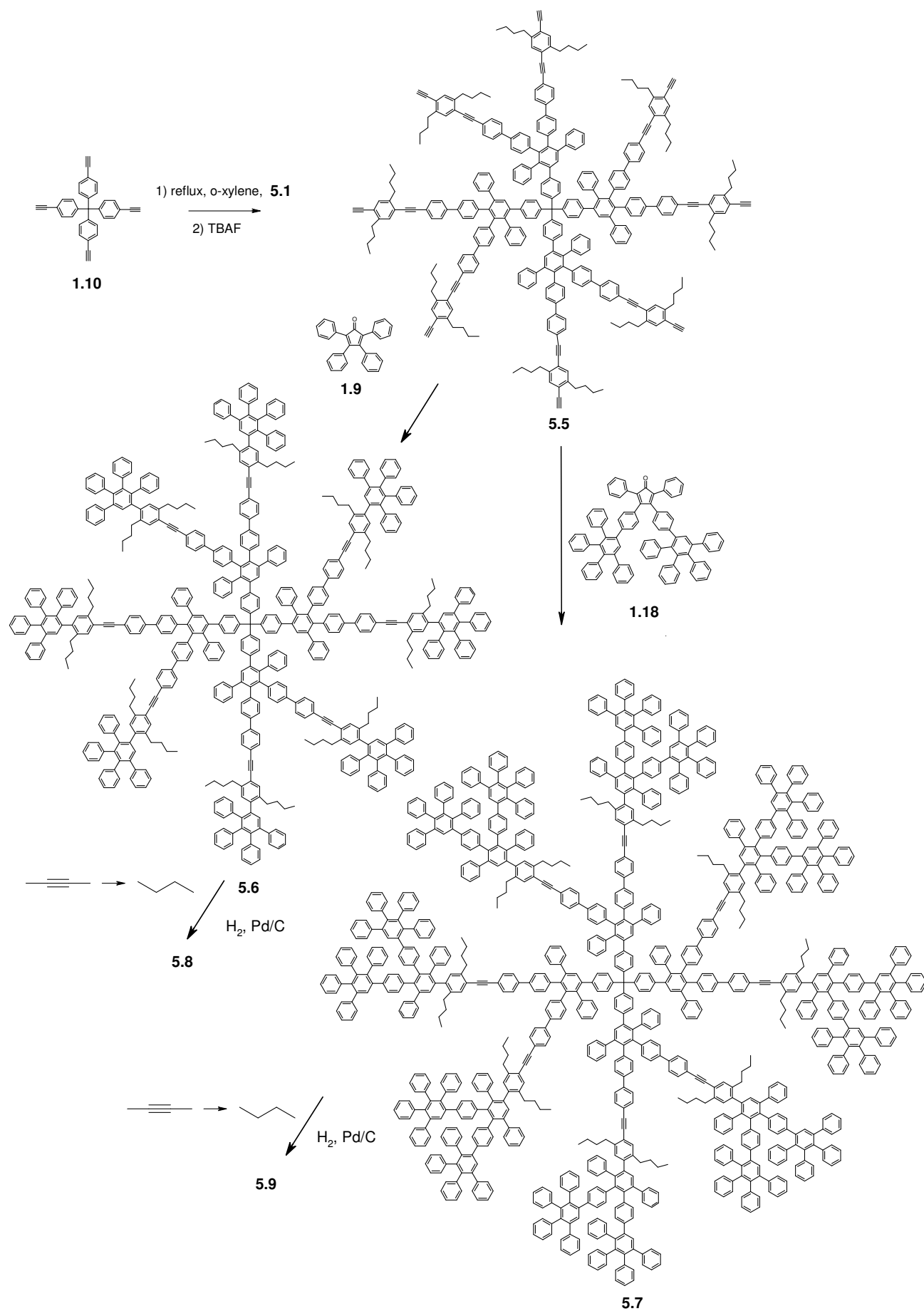
While it is true, that many other macromolecules in the 0.1 – 1 MDa mass range have been prepared in the laboratory and by industry (e.g. polyolefins), synthetic high generation dendrimers stand out for their monodispersity. Because of the latter property, they qualify as

carriers for functional groups in applications where control over size and structure of the matrix is essential. The fairly easy access to semi-extended branching units and their decoration with functionalities render them particularly promising as dendrimer building blocks.

Chapter 3, Synthesis and Hydrogenation of Dendrimers possessing internal Triple Bonds, takes up the concept mentioned before namely that of carrying out chemical reactions in the interior of a dendrimer. Whereas the synthesis of exploded dendrimers containing oligo(*para*-phenylene ethynylene) spacers had failed (Chapter 2.2), incorporation of a single $\text{-C}\equiv\text{C-}$ triple bond into each arm was successful. This was achieved through the synthesis of the new branching unit **5.1** that bears a diphenylacetylene segment in the spacer. Fortunately, dienophilicity of the terminal (deprotected) $\text{-C}\equiv\text{C-}$ triple bond strongly dominated over that of the internal tolane segment. Therefore, product spread from competing Diels-Alder reactions did not create problems.



The novel dendrimers **5.6** and **5.7** possess eight inner $\text{-C}\equiv\text{C-}$ triple bonds which are shielded by first- and second-generation dendrons. Nevertheless, hydrogenation of the dendrimers **5.6** (G2) and **5.7** (G3) proceeds readily [Pd/C; 1 bar H_2 , 55 °C (**5.6**), 136 °C (**5.7**)] to yield the products **5.7** and **5.9** in which the $\text{-C}\equiv\text{C-}$ triple bonds have been quantitatively converted into $\text{-CH}_2\text{-CH}_2\text{-}$ units. In view of the sensitivity of heterogeneous hydrogenation to steric effects, these relatively mild conditions are surprising.



Size exclusion chromatography SEC points to significant shrinkage of the dendrimers **5.6** and **5.7** brought about by hydrogenation. Yet, this contraction is too small to measurably affect the DOSY (diffusion-ordered 2D NMR) spectra. According to quartz microbalance (QMB) studies, the rigid pre-hydrogenation dendrimer **5.7** incorporates guest molecules about 30 % more readily than the more flexible post-hydrogenation dendrimer **5.9**. This finding may be rationalized by inter-dendron interactions in the more flexible dendrimer which compete with guest-molecule binding.

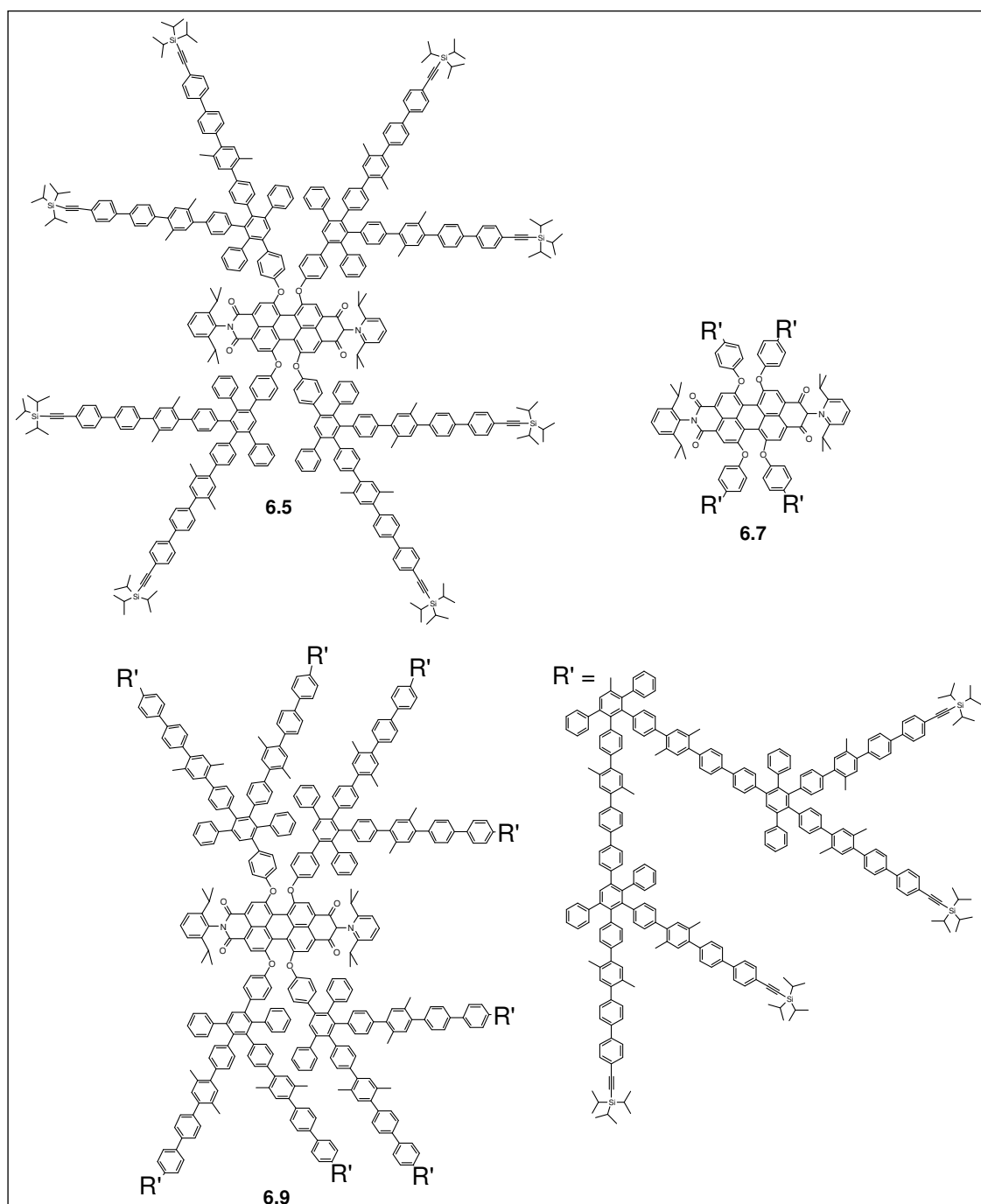
In the following table relevant data for the newly prepared extended dendrimers are compiled. For comparison, some general Müllen-type dendrimers are also included.

Compilation of characteristic data for the new extended arm dendrimers with branching units **3.1**, **4.1**, **5.1**, and the hydrogen end-capped general polyphenylene dendrimers:

	polyphenylene dendrimers													
	with <i>para</i> -terphenylene spacers branching unit (3.1)						with <i>para</i> - biphenyl spacers branching unit (4.1)			with general branching unit (1.7 / 1.9)			with branching unit (5.1) and (1.9/1.18)	
	<i>G1</i>	<i>G2</i>	<i>G3</i>	<i>G4</i>	<i>G5</i>	<i>G6</i>	<i>G1</i>	<i>G2</i>	<i>G3</i>	<i>G2</i>	<i>G3</i>	<i>G4</i>	<i>G2</i>	<i>G3</i>
	3.8	3.10	3.12	3.14	3.16	3.18	4.3	4.5	4.7	1.13	1.14	1.15	5.6	5.7
Molecular formula	$C_{393}H_{388}Si_8$	$C_{1041}H_{964}Si_{16}$	$C_{2337}H_{2116}Si_{32}$	$C_{4929}H_{4420}Si_{64}$	$C_{10113}H_{9028}Si_{128}$	$C_{20481}H_{18244}Si_{256}$	$C_{337}H_{340}Si_8$	$C_{873}H_{820}Si_{16}$	$C_{1945}H_{1780}Si_{32}$	$C_{385}H_{260}$	$C_{865}H_{580}$	$C_{1825}H_{1220}$	$C_{561}H_{452}$	$C_{1041}H_{772}$
Aryl rings	48	136	312	664	1368	2776	40	112	256	64	144	304	80	160
Chain ends	8	16	32	64	128	256	8	16	32	16	32	64	16	32
Molecular mass, g/mol	5336	13924	31101	65454	134162	271577	4615	11762	26023	4886	10974	23150	7195	13283
SEC M_p (g/mol) based on PS standards	8000	22000	38900	83200	114200	136711	7062	17854	32440	3900	7900	13800	9582	15578
SEC PDI	1.04	1.05	1.03	1.05	1.10	1.46	1.05	1.04	1.03	1.04	1.03	1.05	1.05	1.06
Theor.radius (nm)	2.7	4.8	6.9	9.1	11.2	13.4	2.2	3.8	5.62	2.2	3.0	3.8	3.3	4.1
Radius from DLS, nm	2.0	3.6	5.2	9.0	11.8	16.3	1.82	2.99	4.52	1.5	2.2	2.9	2.48	3
Radius from TEM, nm	-	-	-	-	11	13	-	-	-	-	2.6	3.0	-	-
Radius from AFM, nm	-	-	-	-	11	-	-	-	-	-	-	-	-	-
Dendrimer density (g/mL)	0.26	0.12	0.09	0.04	0.032	0.025	0.3	0.17	0.12	0.57	0.41	0.38	0.19	0.20

Chapter 4, Dendronization of a Chromophore Core by means of the New Extended Arm 3.1, was triggered by the question whether the more porous structure of “exploded” dendrimers would have an impact on optical properties - fluorescence in particular - of a rylene-type core.

Perylene-3,4,9,10-tetracarboxdiimide (PDI) was therefore dendronized at the *bay*-positions to yield the first, second and third generation dendrimers **6.5** (G1), **6.7** (G2), and **6.9** (G3).



Whereas **6.5** and **6.7** and their deprotected form **6.6** and **6.8** could be fully characterized, deprotection of **6.9** yielded a product which, due to its insolubility in all common solvents, evaded complete identification. MALDI-TOF of **6.7** attests to extensive aggregation in that peaks starting from mono-, di-, tri-, and tetramers are discernible. This probably results from the fairly open surface of extended arm dendrimers which permits intermolecular dendron penetration. In fluid solution, however, SEC points to the absence of aggregation.

UV-vis spectroscopy reveals, that dendronization of the PDI core at the *bay*-positions causes a bathochromic shift (10 nm) for the components of the S_0 - S_1 band whereas the S_0 - S_2 band is virtually unaffected. The size of the dendron plays a minor role since the UV-vis spectra of the G2- and G3- species in the visible region are identical. This also applies to the emission spectra which all show the same Stokes shift (23 nm).

Fluorescence quenching experiments revealed, that the species **6.5**, **6.7**, and **6.9** possess the same Stern-Volmer quenching constant $K_{SV} = 25.8 \text{ mol}^{-1}$. Extending the arms within these PDI-cored dendrimers therefore demonstrates, that successive generations do not exhibit increased hindrance of access of the central chromophore for quencher molecules. This contrasts with the general Müllen-type dendronized PDI derivatives for which an increase in generation number is accompanied by decreasing K_{SV} values. Fluorescence quantum yields Q_{fl} point in the same direction in that general as well as extended arm PDI-cored dendrimers exhibit the value $Q_{fl} = 0.98$.

The emissive property of the PDI-cored dendrimers can be used for determining their diffusion coefficients D by means of fluorescence correlation spectroscopy (FCS). It is gratifying to note, that the obtained D values correlate well with $1/R_{max}$ (R_{max} is the largest extension of the respective dendrimer taken from molecular models) in accordance with the Stokes-Einstein relation. Notably, the proportionality $R_{max} \cdot D = \text{constant}$ includes the PDI core, its general and its exploded dendrimers and nicely illustrates that bulk rather than mass governs diffusional behavior.

6 Experimental Part

6.1 Reagents and solvents

The following compounds were commercially available:

-reagents: 1,4-dibromobenzene, *n*-BuLi 1.6 M solution (in hexane), 1,2-diiodoethane, 4-trimethylsilylphenylboronic acid, ICl 1 M solution (in CH₂Cl₂), triisopropylsilylacetylene, tetrabutylammonium fluoride trihydrate, 1-bromo-4-iodobenzene, 2-iodo-5-bromotoluene, *n*-butylbromid, I₂, magnesium, *p*-dichlorobenzene, periodic acid H₅IO₆, 1-bromo-4-ethynylbenzene, tetraphenylcyclopentadienone, water.

-catalysts: dichlorobis(triphenylphosphine)nickel(II) NiCl₂(dpe), dichlorobis(triphenylphosphine)palladium Pd(PPh₃)₂Cl₂, tetra(triphenylphosphine)palladium Pd(PPh₃)₄, palladium acetate (II) (Pd(OAc)₂), and palladium on carbon (10% Pd/C),

-solvents: tetrachloromethane, piperidine, ethanol, toluene, dichloromethane, petroleum ether, acetone, methanol, hexane, diphenylether and dried solvents: Et₂O, THF, *o*-xylene. Dichloromethane was dried by distillation from P₂O₅, and CCl₄ was dried over 4 Å molecular sieves.

All of them were purchased from companies: ABCR, Acros, Aldrich, Avocado, Lancaster, Fluka, Merck.

The following compounds were synthesized according to the literature method indicated:

1-Bromo-4-iodo-2,5-dimethylbenzene was synthesized analogously to the literature^[1] and identified^[2] by ¹H NMR spectroscopy and EI mass spectrometry. *n*-Butyl magnesium bromide,^[3] 1,4-di-*n*-butylbenzene,^[4] 3,4-bis(4-(4,4,5,5-tetramethyl-1,3,2-dioxaborolan-2-yl)phenyl)-2,5-diphenylcyclopentadienone,^[5] second generation cyclopentadienone dendron,^[6] tetra(4-ethynylphenyl)methane,^[7] 4-(triisopropylsilylethynyl)-phenylboronic acid,^[8] and 1,6,7,12-tetra-(*p*-ethynylphenoxy)-*N,N'*-(2,6-diisopropylphenyl)-perylene-3,4,9,10-tetracarboxdiimides,^[9] 2,5-di-*n*-butyl-1,4-diiodobenzene^[10] were synthesized and characterized as described in the literature.

6.2 Instruments and analysis

Nuclear magnetic resonance-spectroscopy: ^1H and ^{13}C NMR spectra were recorded on Bruker AMX250, AC300, AMX500, and AMX700 NMR spectrometers.

Mass spectrometry:

-Field desorption mass spectra (FDMS) were obtained from a VG-Instrument ZAB 2-SE-FDP using 8 kV accelerating voltage.

-Electron impact (EI) ionization mass spectrometry was performed on a VG Instruments TRIO 2000 mass spectrometer.

-MALDI-TOF mass spectra were measured using a Bruker Reflex II, calibrated against poly(ethylene glycol) (3,000 g/mol). Samples for MALDI-TOF MS were prepared by mixing the analyte with the matrix (dithranol) in THF in a ratio of 1:250. Cationization was performed by mixing the matrix with potassium trifluoroacetate (K) or silver trifluoroacetate (Ag). Theoretical, average masses were calculated using iMass (Urs Roethlisberger). All reported MALDI-TOF MS measurements were within the experimental error inherent in the technique.

-MALDI-TOF MS with STJ detector (Comet AG, Flamatt, Switzerland).

Elemental analysis (EA): Elemental analyses were performed by the Microanalytical Laboratory of Johannes Gutenberg University. The nature of the porosity of the dendrimers, as hosts for small quantities of solvent impurities as well as incomplete combustion limit the effectiveness of elemental analyses for polyphenylene dendrimer samples.

SEC analyses: Size exclusion chromatography (SEC) was performed in THF at room temperature using a 515 pump (Waters), 717plus injector (Waters), 10 μm guard column, and SDV GPC columns with 500 Å, 10^4 Å, and 10^6 Å porosities (PSS, Mainz), UV S-3702 (SOMA) (at 254 nm) and RI ERC 7512 refractive index (ERMA Inc.) detectors. SEC data analysis was performed using the software PSS-WinGPC (PSS, Mainz).

Temperature: Melting points were measured using a Büchi Melting Point Apparatus B545. Thermogravimetric Analyses (TGA) was measured by Mettler TG 50 and Differential calorimetry by Mettler DSC 30 with heating rate 10 K/min.

UV/vis and fluorescence spectroscopy: UV/vis absorbance spectra were recorded on a Perkin Elmer Lambda 25 spectrophotometer and fluorescence spectra on a SPEX Fluorolog 2 spectrometer.

Raman spectroscopy: FT-Raman spectra were recorded on a Bruker RFS-100/S spectrometer with a liquid-nitrogen cooled Ge detector. An air-cooled Nd:YAG (1064 nm) was used as excitation source.

IR spectroscopy: Nicolet FT-IR 320.

Transmission electron microscopy: Samples for transmission electron microscopy (TEM) were prepared and characterized according to a literature procedure.^[11]

Atom force microscopy: Veeco Instrument Multimode equipment with a 100 μm x 100 μm (J) scanner and Nanoscope IIIa controller. Olympus OMCL-AC160TS silicon cantilevers (resonance frequency: 300 kHz and spin constant: 42 N/nm)

Dynamic light scattering for dendrimers with tetraphenylmethane core: Dynamic light scattering (DLS) was performed at 25 °C at the MPI für Polymerforschung in Mainz using a krypton ion laser (647.1 nm) (Spectra Physics), a toluene filled index matching bath, an SP-125 goniometer, optical fiber detection system and an ALV-500 correlator, all from ALV and detected at 60, 90, 120, and 150 degrees with respect to the incident beam. Sample solutions for DLS were prepared in THF at 0.2 g/L and were filtered through 0.2 μm porosity PTFE filters.

Dynamic light scattering for dendrimers with chromophore core: DLS was performed at 25 °C with a custom PDDLs/Batch+ (Precision Detector) equipped with a diode laser (70 mW, 810 nm), 90° dynamic light scattering optics, single aperture (17 μm) fiber optic cable, integrated photon counting module, and autocorrelator. Sample solutions for DLS were prepared in toluene at 2-5 mg/mL.

Fluorescence Correlation Spectroscopy (FCS) measurements were acquired at 22 °C using a Confocor II FCS (Zeiss) equipped with a HeNe laser (2.5 mW, 543 nm), acousto-optical filter (10% transmission), single-mode optical fiber, LP560 long pass dichromatic filter, 40x

Plan Neofluar 0.9 NA Multi Immersion objective with the correction ring set to “oil”, refractive index matching oil, quartz microplate strip with 8 wells (3 mm diameter wells, 0.17 mm coverslip thickness) (Hellma) sealed against leaking with a PDMS gasket (PDMS swells over time, but not on the time scale of the measurement) and a glass plate, adjustable pinhole (90 μm), emission filter (543 nm), avalanche photodiode, and autocorrelator. Data collection was made with the focus placed 100 μm above the quartz surface. Fifteen data sets of 30 sec data acquisition time each were preceded by a 3 sec bleach time and averaged. An increase in the laser power from 2% transmission to 10% resulted in a net increased fluorescence but less triplet excitation population. Fits were made from 2 μs and above, accounting for triplet excitation which was in most cases less than 5% and in all cases less than 10%. Solutions were prepared from freshly procured HPLC grade toluene at concentrations with less than or equal to one particle in the focal volume on average (ca. 10^{-8} M).

6.3 General procedures

Suzuki coupling: The respective bromo- or iodo- derivatives and boronic derivative were dissolved in toluene or acetone. The solution was degassed and flushed with argon repeatedly. A solution of K_2CO_3 or Na_2CO_3 in H_2O was added. In some cases a transfer solvent EtOH was added. The system was again degassed and $\text{Pd}(\text{PPh}_3)_4$ (or other suitable palladium catalyst) was added. The mixture was refluxed one day with vigorous stirring. Then the mixture was allowed to cool to room temperature, the layers were separated, the aqueous phase was washed a few times with organic solvents. The organic layer was dried (MgSO_4). The solvent was removed and crude material was purified by means of column chromatography on silica gel.

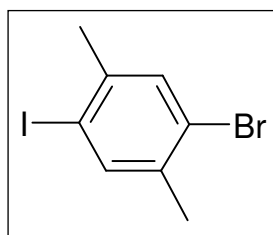
General procedure for TMS/I conversion: The respective trimethylsilylbenzene derivative was dissolved in dry CCl_4 or CH_2Cl_2 and at 0°C a solution of 1 M ICl in CH_2Cl_2 was added slowly under Argon. The mixture was allowed to reach r.t. and stirred 1 hour more. A 1 M solution of sodium disulphide was added. The layers were separated, the aqueous layer was washed with dichloromethane and the combined organic layers were washed with water. The organic phase was dried over MgSO_4 . Chromatographic filtration through silica gel with hexane and evaporation of solvent gave the pure product.

Diels-Alder reaction: A degassed mixture of the appropriate ethynyl derivative and cyclopentadienone type with excess in the suitable solvent was heated at the appropriated temperature for 24-48 hours under argon. The product was purified either by silica gel column or by slow precipitation.

Deprotection of TIPS groups: To a solution of the respective TIPS derivative in THF under argon was added an excess of $n\text{-Bu}_4\text{NF}\cdot 3\text{H}_2\text{O}$ in THF and the mixture was stirred at r.t. for 20-60 min. After quenching with H_2O the majority of solvent was evaporated and the reduced volume was slowly dropped into the mixture of methanol with water (4:1) and stirred 20-60 minutes. The precipitate was collected by filtration and dried *in vacuo* yielded a colored solid.

6.4 Syntheses of the Extended Arm Polyphenylene Dendrimers (for Chapter 2)

1-Bromo-4-iodo-2,5-dimethylbenzene (3.2)



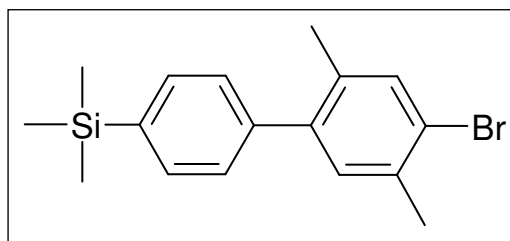
1,4-Dibromobenzene (20 g, 76 mmol) was dissolved in dry THF (296 mL) and cooled to $-90\text{ }^\circ\text{C}$ under argon. $n\text{-BuLi}$ in hexane (1.6 M, 47.3 mL, 76 mmol) was added dropwise, keeping the temperature of the reaction mixture below $-80\text{ }^\circ\text{C}$. The solution was transferred *via* cannula to a solution of 1,2-diiodoethane (22.8 g, 81 mmol) in dry THF (148 mL) at $-60\text{ }^\circ\text{C}$. After the addition was complete, the reaction mixture was allowed to warm to room temperature and stirred for 30 min, commensurate with a change in color from yellow to brown. The reaction was quenched with sat. $\text{Na}_2\text{S}_2\text{O}_3(\text{aq})$. The aqueous phase was extracted 3 times with diethyl ether, the combined organic phases were dried over MgSO_4 , and the solvent was removed *in vacuo*. The residue was recrystallized from methanol to give a colorless solid (15.45 g, 65%), mp: $75.5\text{-}76.6\text{ }^\circ\text{C}$.

^1H NMR (250 MHz, CD_2Cl_2): δ = 7.66 (s, 1, Ar), 7.38 (s, 1, Ar), 2.32 (s, 3 H), and 2.27 (s, 3 H) ppm.

^{13}C NMR (62.5 MHz, CD_2Cl_2): δ =141.09, 140.72, 137.52, 133.16, 125.03 (C-Br), 99.36 (C-I), 27.32, and 21.95 ppm.

EI: m/z [ue^{-1}] 309.7 (100%), 311.8 (100%), [M^+]; calcd. 309.89, 311.88.

Anal. Calcd. for $\text{C}_8\text{H}_8\text{BrI}$: C, 30.90, H, 2.59. Found: C, 31.35, H, 2.98.

4-Bromo-2,5-dimethyl-4'-trimethylsilylbiphenyl (3.3)

1-Bromo-4-iodo-2,5-dimethylbenzene **3.2** (10.55 g, 34 mmol) and 4-trimethylsilylphenylboronic acid (7.57 g, 39 mmol) were dissolved in toluene (160 mL). The mixture was degassed, purged with argon, and a solution of K_2CO_3 (8.08 g, 58.5 mmol) in deionized water (40 mL) was added. The system was degassed again and $Pd(PPh_3)_4$ (1.96 g, 1.7 mmol) was added. The reaction mixture was stirred at reflux for 24 h. After cooling to room temperature, the layers were separated, the aqueous phase extracted twice with toluene, and the combined organic layers washed with water. The organic layer was dried over $MgSO_4$, and the solvent was removed *in vacuo*. The crude product was purified by means of column chromatography on silica using hexane as eluent ($R_F = 0.25$). Evaporation of the solvent gave a waxy solid (7.14 g, 62%), mp: 67.4-67.8 °C.

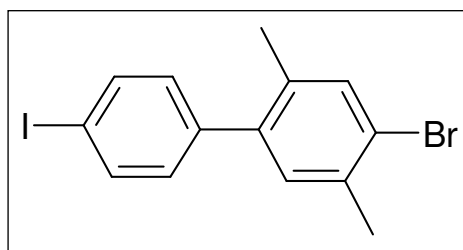
1H NMR (250 MHz, CD_2Cl_2 , 300 K): δ =7.58 (d, 2 H, Ar, $^3J = 7.9$ Hz), 7.45 (s, 1 H, Ar), 7.28 (d, 2 H, Ar, $^3J=8.21$ Hz), 7.10 (s, 1 H, Ar), 2.38 (s, 3 H, CH_3), 2.21 (s, 3 H, CH_3), and 0.31 (s, 9 H, Si- CH_3) ppm.

^{13}C NMR (75 MHz, CD_2Cl_2 , 300 K): δ =141.66, 141.50, 139.47, 135.40, 135.14, 134.04, 133.58, 132.42, 128.68, 123.67, 22.39, 19.86, and -1.05 ppm.

EI ($C_{17}H_{21}BrSi$): m/z [ue^{-1}] 331.8 (100%), 333.9 (100%), [M^+]; calcd: 332.06, 333.34.

4-Bromo-4'-iodo-2,5-dimethylbiphenyl (3.4)

A 1 M solution of ICl in CH_2Cl_2 (27.3 mL, 27.0 mmol) was added dropwise to a solution of 4-bromo-2,5-dimethyl-4'-trimethylsilylbiphenyl (**3.3**) (7.0 g, 21 mmol) in dry CCl_4 (40 mL) at 0 °C under argon atmosphere.



The reaction mixture was allowed to warm to room temperature and stirred for 1 h. A solution of sodium disulphide was added, and the layers were separated. The aqueous layer was extracted with dichloromethane, and the combined organic phases were washed with water. The organic phase was dried over $MgSO_4$, and chromatographic filtration through silica with hexane as eluent ($R_F = 0.26$) gave a colorless solid (7.86 g, 96%), mp: 70.7-70.8 °C.

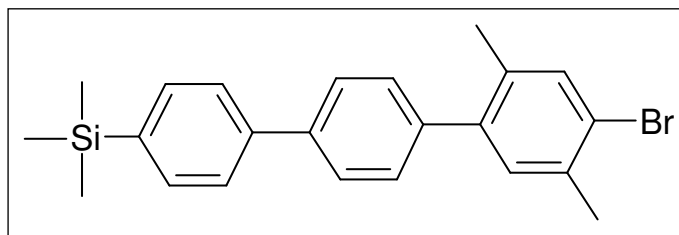
1H NMR (250 MHz, CD_2Cl_2 , 300 K): δ =7.75 (d, 2 H, $^3J=8.53$ Hz), 7.44 (s, 1 H, Ar), 7.07-7.03 (m, 3 H, Ar), 2.37 (s, 3 H, CH_3), and 2.18 (s, 3 H, CH_3) ppm.

^{13}C NMR (75 MHz, CD_2Cl_2 , 300 K): δ =140.84, 140.32, 137.67, 135.57, 134.99, 134.15, 132.10, 131.37, 124.05, 92.96, 22.38, and 19.76 ppm.

FDMS: m/z [ue^{-1}] 386.0 (100%), 388.3 (100%), [M^+]; calcd: 385.9, 387.1.

Anal.: Calcd for $\text{C}_{14}\text{H}_{12}\text{BrI}$: C, 43.44; H, 3.13. Found: C, 43.55; H, 3.21.

4-Bromo-4'-trimethylsilyl-2,5-dimethyl-1,1':4',1''-terphenyl (3.5)



4-Bromo-4'-iodo-2,5-dimethylbiphenyl (3.4) (7 g, 18 mmol) and 4-trimethylsilylphenylboronic acid (3.5 g, 18.0 mmol) were dissolved in toluene (160 mL). The mixture was purged

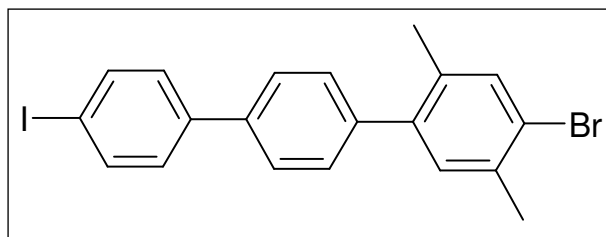
with argon, and a solution of K_2CO_3 (3.73 g, 27 mmol) in deionized water (30 mL) was added. The system was purged with argon again and $\text{Pd}(\text{PPh}_3)_4$ (0.62 g, 0.54 mmol) and ethanol (4 mL) were added. After a final argon purge, the reaction mixture was stirred at reflux for 24 h. After cooling to room temperature, the layers were separated, the aqueous phase extracted twice with toluene, and the combined organic layers washed with water. The organic layer was dried over MgSO_4 , and the solvent was removed *in vacuo*. The crude product was purified by means of column chromatography on silica using hexane as eluent ($R_F = 0.14$). Evaporation of the solvent gave a colorless solid (6.15, 83%), mp: 108.8-110.2 °C.

^1H NMR (250 MHz, CD_2Cl_2 , 300 K): δ =7.68-7.65 (m, 6 H, Ar), 7.48 (s, 1 H, Ar), 7.38 (d, 2 H, Ar, $^3J=8.22$ Hz), 7.15 (s, 1 H, Ar), 2.40 (s, 3 H, CH_3), 2.26 (s, 3 H, CH_3), and 0.32 (s, 9 H, Si- CH_3) ppm.

^{13}C NMR (75 MHz, CD_2Cl_2 , 300 K): δ =141.32, 141.11, 140.40, 140.11, 139.90, 135.47, 135.22, 134.30, 134.11, 132.41, 129.89, 127.16, 126.62, 123.77, 22.42, 19.93, and -1.05 ppm.

FDMS: m/z [ue^{-1}] 408.8 (100%), 411.1 (100%), [M^+]; calcd: 408.09, 409.44.

Anal. Calcd for $\text{C}_{23}\text{H}_{25}\text{BrSi}$: C, 67.47; H, 6.15. Found: C, 67.48; H, 6.18.

4-Bromo-4''-iodo-2,5-dimethyl-1,1':4',1''-terphenyl (3.6)

A 1 M solution of ICl in CH₂Cl₂ (20 mL, 19.5 mmol) was added dropwise to a solution of 4-bromo-4''-trimethylsilyl-2,5-dimethyl-1,1':4',1''-terphenyl (**3.5**) (6.1 g, 14.8 mmol) in 30 mL of dry CH₂Cl₂ at 0 °C under argon.

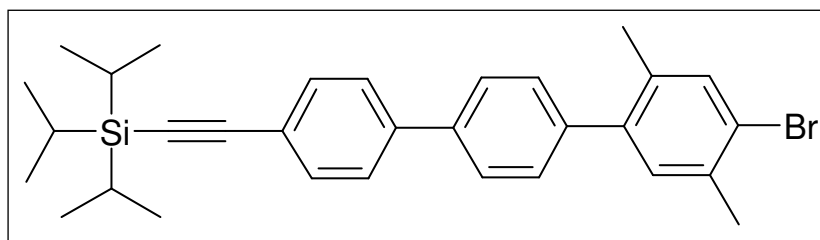
The reaction mixture was warmed to room temperature and stirred for 1 h. Thereafter, a solution of sodium disulphide was added, and the layers were separated. The aqueous layer was extracted with dichloromethane, and the combined organic phases were washed with water. The organic phase was dried over MgSO₄, and chromatographic filtration through silica with hexane as eluent ($R_F = 0.16$) gave a colorless solid (6 g, 87%). The product was recrystallized from dichloromethane, before the next reaction step took place, mp: 168.8-170 °C.

¹H NMR (250 MHz, CD₂Cl₂, 300 K): δ =7.81 (d, 2 H, ³J=8.53 Hz, Ar), 7.63 (d, 2 H, Ar, ³J=8.53 Hz), 7.47 (s, 1 H, Ar), 7.43-7.36 (m, 4 H, Ar), 7.14 (s, 1 H, Ar), 2.39 (s, 3 H, CH₃), and 2.24 (s, 3 H, CH₃) ppm.

¹³C NMR (75 MHz, CD₂Cl₂, 300 K): δ =140.76, 140.57, 138.93, 138.30, 135.47, 135.16, 134.10, 132.32, 129.98, 129.22, 126.93, 123.81, 93.30, 22.39, and 19.87 ppm.

FDMS: m/z [ue⁻¹] 462.3 (100%), 464.2 (100%), [M⁺]; calcd: 461.95, 463.16.

Anal.Calcd for C₂₀H₁₆BrI: C, 51.87; H, 3.48. Found: C, 51.91; H, 3.21.

4-Bromo-4''-triisopropylsilylethynyl-2,5-dimethyl-1,1':4',1''-terphenyl (3.7)

CuI (0.18 g, 0.93 mmol), PPh₃ (0.24 g, 0.93 mmol), Pd(PPh₃)₂Cl₂ (0.33 g, 0.46 mmol) were added to a degassed solution of 4-

bromo-4''-iodo-2,5-dimethyl-1,1':4',1''-terphenyl (**3.6**) (4.3 g, 9.3 mmol) in dry CH₂Cl₂ (50 mL) and Et₃N (70 mL). Triisopropylsilylacetylene (2.3 mL, 10.2 mmol) was added dropwise to maintain the reaction mixture at room temperature. The reaction was stirred overnight, and dichloromethane and water were added. The two phases were separated, the organic layer was washed with sat. NH₄Cl (aq), cold HCl (1 N), 10% NaHCO₃ (aq), dried over MgSO₄, and concentrated *in vacuo*. The crude material was purified by means of column chromatography

using hexane as eluent ($R_F = 0.16$). Upon evaporation of the solvent, a colorless oil was obtained (3.84 g, 80%).

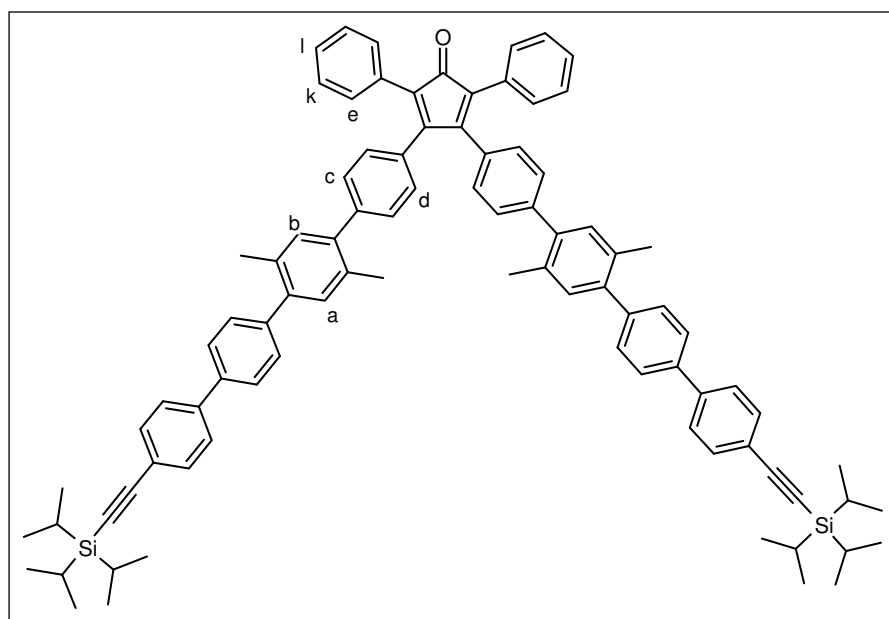
^1H NMR (250 MHz, CD_2Cl_2 , 300 K): $\delta=7.68\text{--}7.55$ (m, 6 H, Ar), 7.47 (s, 1 H, Ar), 7.38 (d, 2 H, Ar, $^3J=8.22$ Hz), 7.14 (s, 1 H, Ar), 2.39 (s, 3 H, CH_3), 2.25 (s, 3 H, CH_3), and 1.15 (s, 21 H, TiPS) ppm.

^{13}C NMR (75 MHz, CD_2Cl_2 , 300 K): $\delta=141.00$, 140.92, 140.75, 139.26, 135.50, 135.20, 134.13, 132.81, 132.36, 129.98, 127.15, 127.08, 132.85, 122.92, 107.31, 91.86, 22.42, 19.92, 18.86, and 11.78 ppm.

FDMS: m/z [ue^{-1}] 516.2 (100%), 518.1 (100%), [M^+]; calcd: 516.18, 517.62.

3,4-Bis-{2',5'-dimethyl-4''-triisopropylsilylethynyl-1,1':4',1'':4'',1'''-quaterphenyl-4-yl}-2,5-diphenyl-cyclopentadienone (3.1)

A mixture of 4-bromo-4''-triisopropylsilylethynyl-2,5-dimethyl-1,1':4',1''-terphenyl (**3.7**) (3.84 g, 7.44 mmol) and 3,4-bis(4-(4,4,5,5-tetramethyl-1,3,2-dioxaborolan-2-yl)phenyl)-2,5-diphenylcyclopentadienone (1.18 g, 1.90 mmol) were dissolved in toluene (20 mL). The



solution was purged with argon. K_2CO_3 (1.03 g, 7.44 mmol) in H_2O (5 mL) and EtOH (3 mL) was added, and the system was degassed again. After the addition of $\text{Pd}(\text{PPh}_3)_4$ (0.43 g, 0.37 mmol), the reaction mixture was heated to 80°C and stirred overnight. The reaction

mixture was allowed to cool to room temperature, the layers separated, and the aqueous phase was extracted with CH_2Cl_2 . The combined organic layers were dried over MgSO_4 , and the solvent was removed *in vacuo*. The crude product was purified by means of column chromatography with silica using petroleum ether/ CH_2Cl_2 (2:1) as eluent (TLC(1.5:1 PE: CH_2Cl_2): $R_F = 0.55$) to give a dark red powder (1.12 g, 48%), $T_{\text{dec}} > 200^\circ\text{C}$.

^1H NMR (CD_2Cl_2 , 700 MHz, 300 K): $\delta=7.68$ (d, 4 H, Ar, $^3J=8.37$ Hz), 7.64 (d, 4 H, Ar, $^3J=7.7$ Hz), 7.58 (d, 4 H, Ar, $^3J=7.69$ Hz), 7.45 (d, 4 H, Ar, $^3J=8.55$ Hz), 7.37-7.28 (m, 10 $\text{H}^{\text{c,d,e,k,l}}$, Ar), 7.24 (d, 4 H, Ar, $^3J=8.54$ Hz), 7.18 (d, 4 $\text{H}^{\text{a,b}}$, Ar, $J=6.84$ Hz), 7.09 (d, 4H, Ar, $^3J=8.55$ Hz), 2.32 (s, 6 H, CH_3), 2.26 (s, 6 H, CH_3), and 1.18 (s, 42 H, iPr_3Si) ppm.

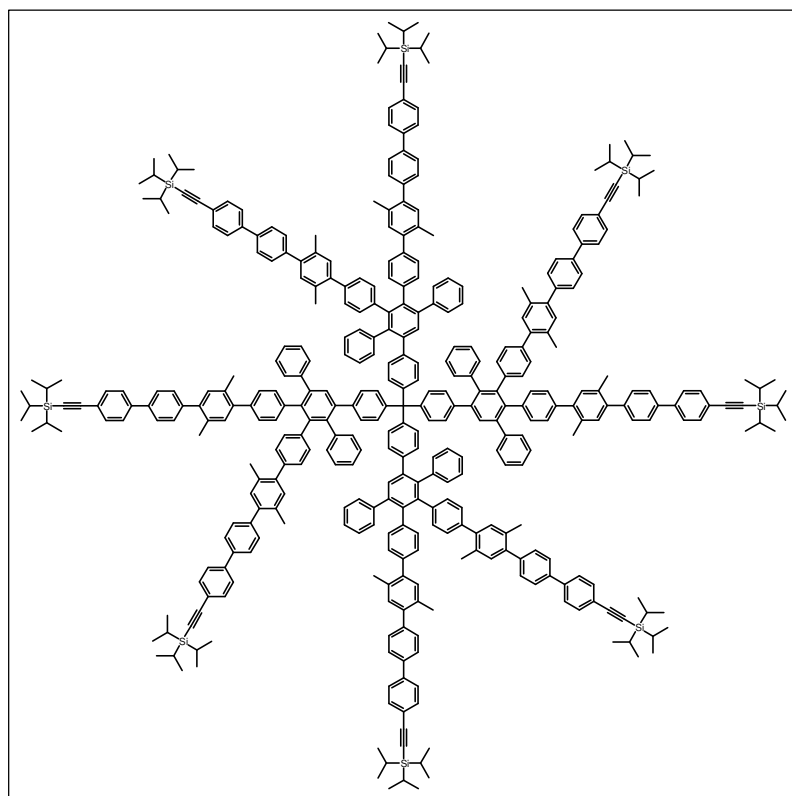
^{13}C NMR (175 MHz, CD_2Cl_2 , 300 K): $\delta=200.68$, 154.99, 142.33, 141.45, 140.99, 140.84, 140.65, 139.01, 133.08, 133.02, 132.80, 132.18, 132.13, 132.02, 131.49, 130.60, 130.11, 129.62, 129.17, 128.42, 127.89, 127.13, 127.01, 125.77, 122.82, 107.31, 91.81, 20.14, 20.11, 20.05, 20.01, 18.87, 18.84, 18.82, and 11.76 ppm.

FDMS: m/z [ue^{-1}] 1257.9 (100%), [M^+]; calcd: for $\text{C}_{91}\text{H}_{92}\text{OSi}_2$:1257.92.

Anal. Calcd for $\text{C}_{91}\text{H}_{92}\text{OSi}_2$: C, 86.89; H, 7.37. Found: C, 86.90; H, 7.30.

G1-Td-(TiPS) $_8$ (3.8)

A mixture of tetra(4-ethynylphenyl)methane (22 mg, 0.05 mmol) and 3,4-bis-{2',5'-dimethyl-4'''-triisopropylsilylethynyl-1,1':4',1'':4'',1'''-quaterphenyl-4-yl}-2,5-diphenyl-



cyclopentadienone (**3.1**) (345 mg, 0.27 mmol) in *o*-xylene (5 mL) was heated to reflux for 24 h under argon. After cooling to room temperature, the solvent was removed *in vacuo*. The residue was purified by means of column chromatography using petroleum ether/ CH_2Cl_2 (2/1) was eluent. Upon evaporation of the solvent, a colorless solid was obtained (238 mg, 85%), $T_{\text{dec}} > 300$ °C.

^1H NMR (500 MHz, CD_2Cl_2 , 273 K): $\delta=7.72$ -6.83 (m, 172 H, Ar), 2.29, 2.28, 2.13, 2.10 (4 s, 48 H, CH_3), and 1.19 (s, 168 H, iPr_3Si) ppm.

^{13}C NMR (125 MHz, CD_2Cl_2 , 273 K): $\delta=145.07$, 142.25, 142.16, 141.69, 141.31, 141.22, 141.09, 140.63, 140.46, 140.41, 141.12, 140.07, 139.81, 139.61, 139.53, 139.26, 138.95,

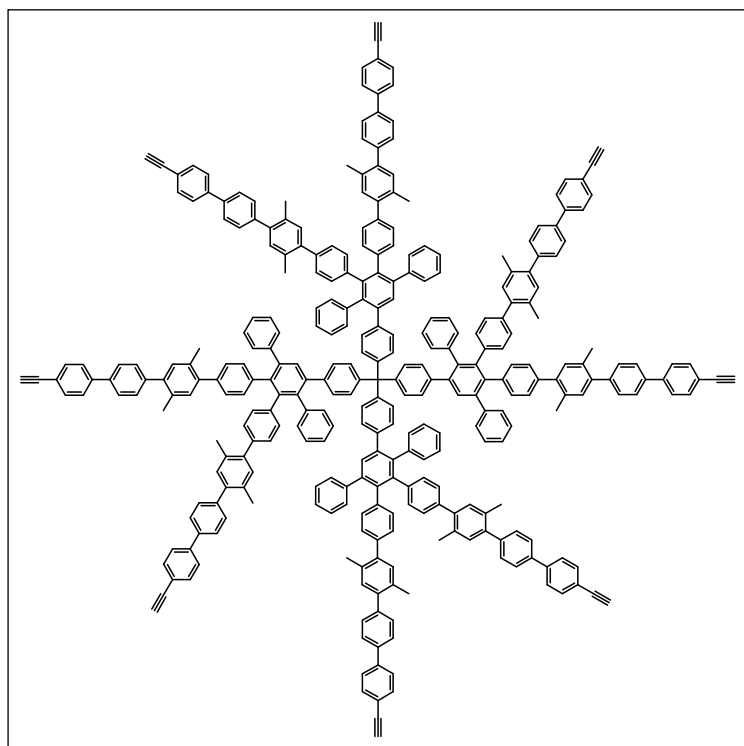
133.16, 132.82, 132.26, 131.93, 131.85, 131.34, 130.86, 130.56, 130.16, 129.30, 128.21, 128.10, 127.93, 127.32, 127.16, 127.00, 126.81, 126.07, 122.85, 107.41, 91.82, 20.08, 19.98, 18.89, and 11.82 ppm.

MALDI-TOF (dithranol): exact mass calcd for $[M+Ag]^+$ $C_{393}H_{388}Si_8Ag$: 5443.95 found 5443.

Anal. Calcd for $C_{393}H_{388}Si_8$: C, 88.46; H, 7.33. Found: C, 86.63; H, 7.29.

G1-Td-(ethyne)₈ (3.9)

To an argon purged mixture of G1-Td-(TiPS)₈ (3.8) (0.140 g, 0.026 mmol) in THF (3 mL)



was added a solution of tetrabutylammonium fluoride trihydrate (TBAF) (66 mg, 0.21 mmol) in THF (3 mL). The reaction mixture was stirred at room temperature for 20 min. After quenching with H₂O (1 mL), the mixture was concentrated *in vacuo*, a minimum amount of THF added, and precipitated into a methanol/water mixture (4/1). The product was collected by filtration and was dried *in vacuo* to yield a colorless

solid (81 mg, 76%), $T_{dec} > 300$ °C.

¹H NMR (CD₂Cl₂, 500 MHz, 273 K): δ =7.71-6.82 (m, 172 H, Ar), 3.20 (s, 8H, C≡C-H), 2.28, 2.27, 2.13, and 2.09 (4 s, 48 H, CH₃) ppm.

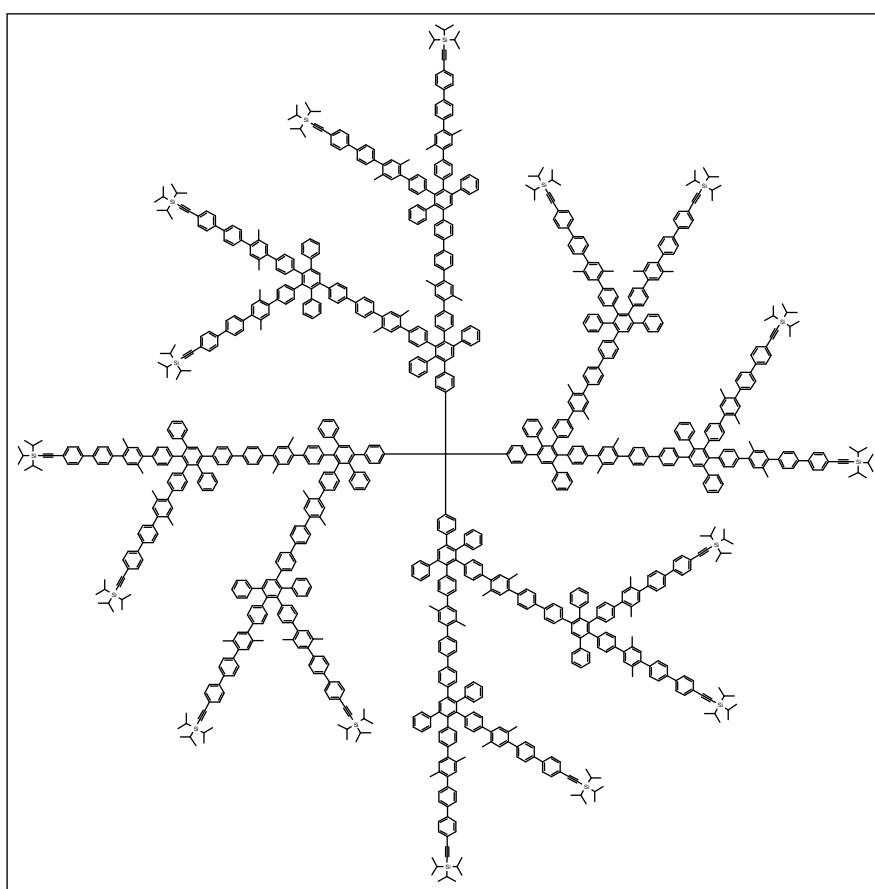
¹³C NMR (CD₂Cl₂, 125 MHz, 273 K): δ =145.08, 142.25, 142.15, 141.80, 141.61, 141.32, 141.22, 140.63, 140.42, 140.38, 140.13, 140.06, 139.80, 139.62, 139.52, 139.25, 138.83, 133.18, 132.98, 132.81, 131.77, 132.26, 131.94, 131.85, 131.34, 130.87, 130.56, 130.19, 129.32, 128.21, 128.10, 127.93, 127.29, 127.04, 126.81, 126.07, 121.40, 83.81, 78.14, 20.08, and 19.99 ppm.

MALDI-TOF (dithranol): exact mass calcd for $[M+K]^+$ $C_{321}H_{228}K$: 4124 found 4125.

G2-Td-(TiPS)₁₆ (3.10)

A mixture of **3.9** (79 mg, 0.02 mmol) and **3.1** (290 mg, 0.24 mmol) was heated to reflux in *o*-xylene (5 mL) under argon for 24 h. After cooling to room temperature, the reaction mixture was concentrated *in vacuo*, precipitated into acetone, and filtered. The precipitate was loaded onto a plug of silica and washed with acetone until the elution remained colourless.

The stationary phase was dried and extracted with THF. The THF solution was concentrated to a viscous solution (1-2 mL) and reprecipitated in acetone. After filtration, the solid washed with acetone and dried *in vacuo* to yield the product as a colorless solid (258 mg, 95.6%), $T_{\text{dec}} > 300\text{ }^{\circ}\text{C}$.



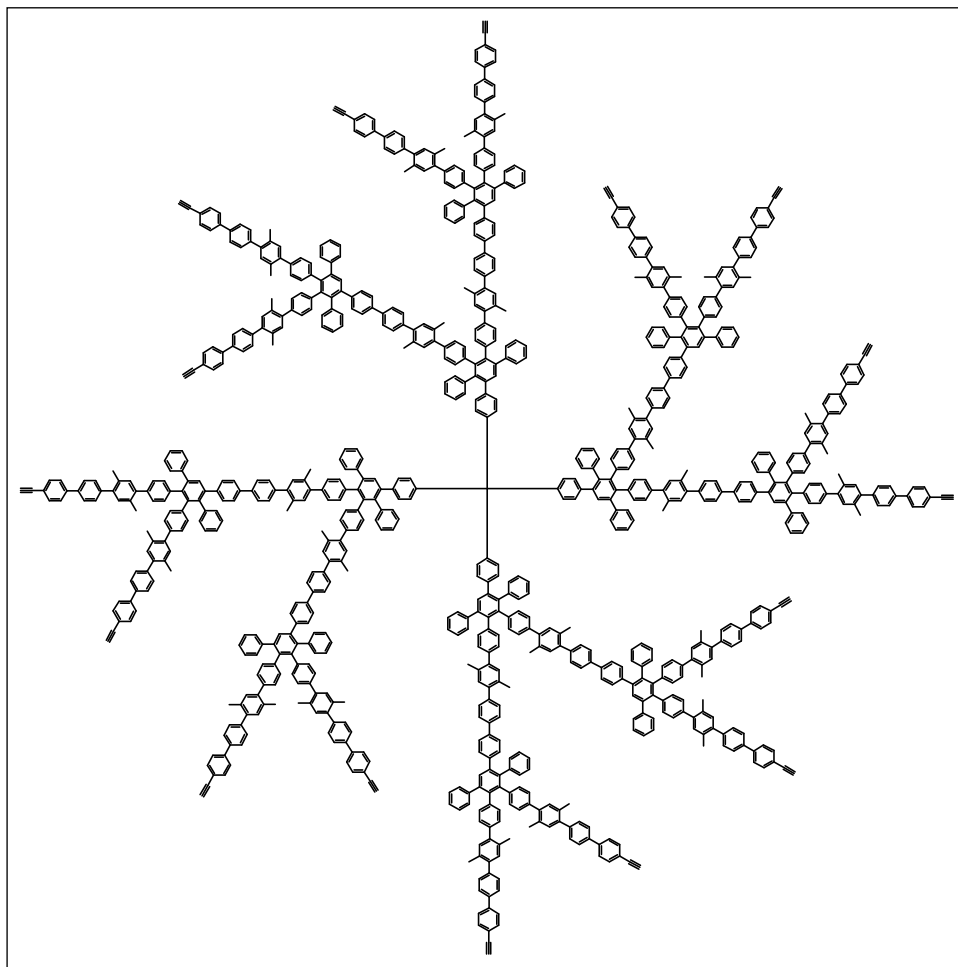
^1H NMR (700 MHz, CD_2Cl_2 , 273 K): $\delta=7.69\text{--}6.82$ (m, 484 H, Ar), 2.26, 2.11, 2.08 (3 s, br, 144 H, CH_3), and 1.18 (s, 336 H, iPr_3Si) ppm.

^{13}C NMR (175 MHz, CD_2Cl_2 , 273 K): $\delta=142.49$, 142.47, 142.25, 142.20, 141.15, 141.69, 141.34, 141.09, 140.82, 140.64, 140.41, 139.86, 139.60, 139.21, 138.94, 133.17, 132.82, 132.75, 132.15, 131.94, 131.81, 130.96, 130.52, 130.15, 128.17, 128.09, 127.87, 127.50, 127.15, 126.99, 126.88, 126.53, 122.85, 107.42, 91.83, 20.09, 19.97, 18.89, and 11.82 ppm.

MALDI-TOF (dithranol): exact mass calcd for $[\text{M}+\text{K}]^+ \text{C}_{1041}\text{H}_{964}\text{Si}_{16}\text{K}$: 13924, found 13935.

G2-Td-(ethyne)₁₆ (3.11)

To an argon purged mixture of G2-Td-(TiPS)₁₆ (**3.10**) (251 mg, 0.020 mmol) in THF (7 mL) was added a solution of tetrabutylammonium fluoride trihydrate (91 mg, 0.29 mmol) in THF (3 mL). The reaction mixture was stirred for 1 h, worked up as described for **8**, and yielded a colorless solid (150 mg, 75%), $T_{\text{dec}} > 300\text{ }^{\circ}\text{C}$.



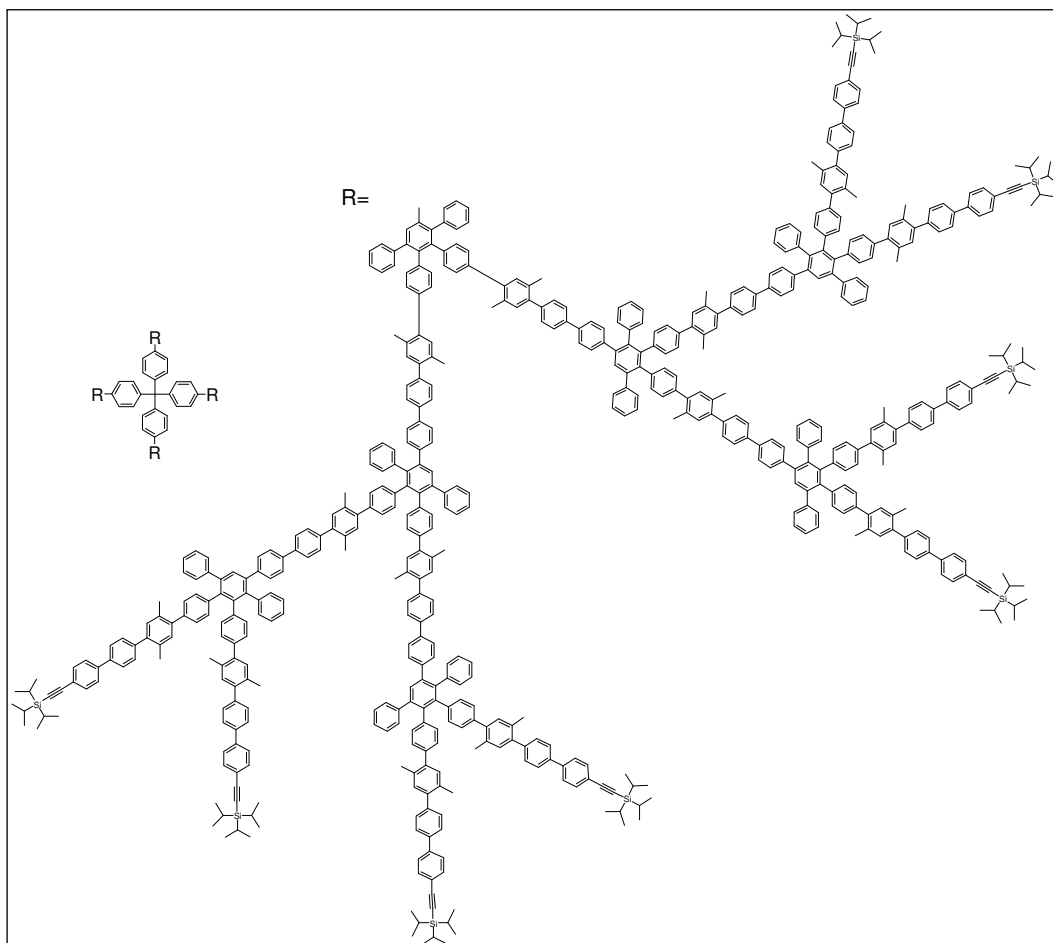
^1H NMR (700 MHz, CD_2Cl_2 , 306 K): δ =7.68-6.81 (m, 484 H, Ar), 3.20, 3.19, 3.18 (3 s, 16H, $\text{C}\equiv\text{CH}$), 2.25, 2.10, and 2.06 (3 s, br, 144 H, CH_3) ppm.

^{13}C NMR (CD_2Cl_2 , 175 MHz, 306 K): δ =142.47, 142.18, 141.78, 141.59, 141.34, 140.80, 140.61, 140.36, 139.85, 139.59, 139.49, 139.20, 138.95, 138.79, 133.17, 132.97, 132.78, 132.74, 132.13, 131.97, 131.92, 131.79, 130.95, 130.51, 130.17, 130.07, 128.16, 128.07, 127.86, 127.48, 127.27, 127.02, 126.87, 126.52, 126.20, 121.38, 83.80, 78.12, 20.07, and 19.95 ppm.

MALDI-TOF (dithranol): exact mass calcd for $[\text{M}+\text{H}]^+ \text{C}_{897}\text{H}_{645}$: 11409, found 11410.

G3-Td-(TiPS)₃₂ (3.12)

A mixture of **3.11** (145 mg, 0.013 mmol) and the branching unit **3.1** (540 mg, 0.43 mmol) in *o*-xylene (10 mL) was heated at reflux under argon for 36 h. The reaction was worked up as described for **3.10** and yielded a colorless solid (338 mg, 87%), $T_{\text{dec}} > 300$ °C.



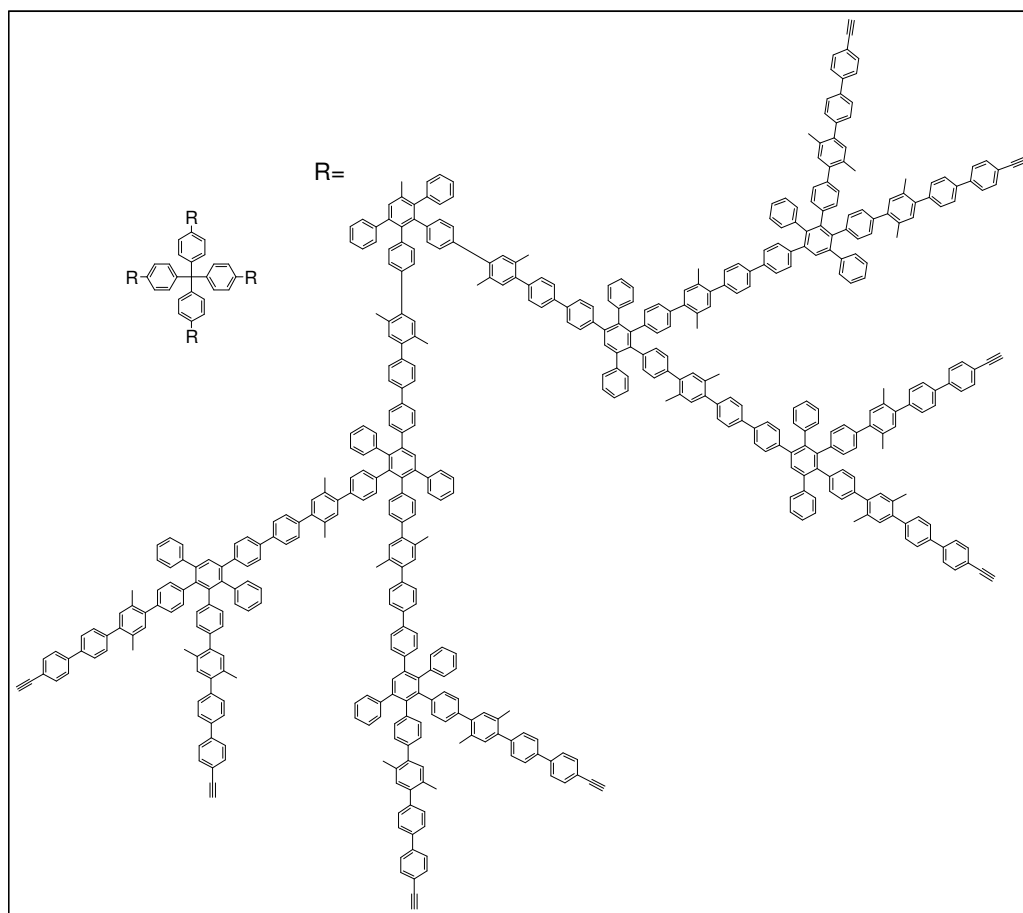
¹H NMR (700 MHz, C₂D₂Cl₄, 393 K): δ =7.65-6.83 (m, 1108 H, Ar), 2.24, 2.10, 2.05 (3 s, br, 336 H, CH₃), and 1.16 (s, br, 672 H, iPr₃Si) ppm.

¹³C NMR (175 MHz, C₂D₂Cl₄, 393 K): δ =142.27, 142.20, 141.69, 141.30, 141.25, 141.08, 140.54, 140.51, 140.44, 140.32, 140.27, 139.82, 139.76, 139.47, 139.31, 139.16, 139.01, 138.86, 138.72, 132.87, 132.84, 132.65, 132.49, 132.44, 131.98, 131.77, 131.63, 131.59, 131.20, 130.72, 130.35, 129.92, 129.81, 127.95, 127.71, 127.65, 127.12, 126.91, 126.73, 126.62, 126.45, 126.19, 125.85, 122.98, 107.59, 91.97, 19.92, 19.75, 18.87, and 11.86 ppm.

MALDI-TOF (dithranol): exact mass calcd for [M+H]⁺ C₂₃₃₇H₂₁₁₇Si₃₂ 31102, found 31168.

G3-Td-(ethyne)₃₂ (3.13)

To an argon purged mixture of G3-Td-(TiPS)₃₂ (**3.12**) (190 mg, 0.006 mmol) in THF (15 mL) was added a solution of tetrabutylammonium fluoride (73 mg, 0.23 mmol) in THF (2 mL). The reaction mixture was stirred for 1 h, worked up as described for **3.9**, and yielded a colorless solid (120 mg, 75%).



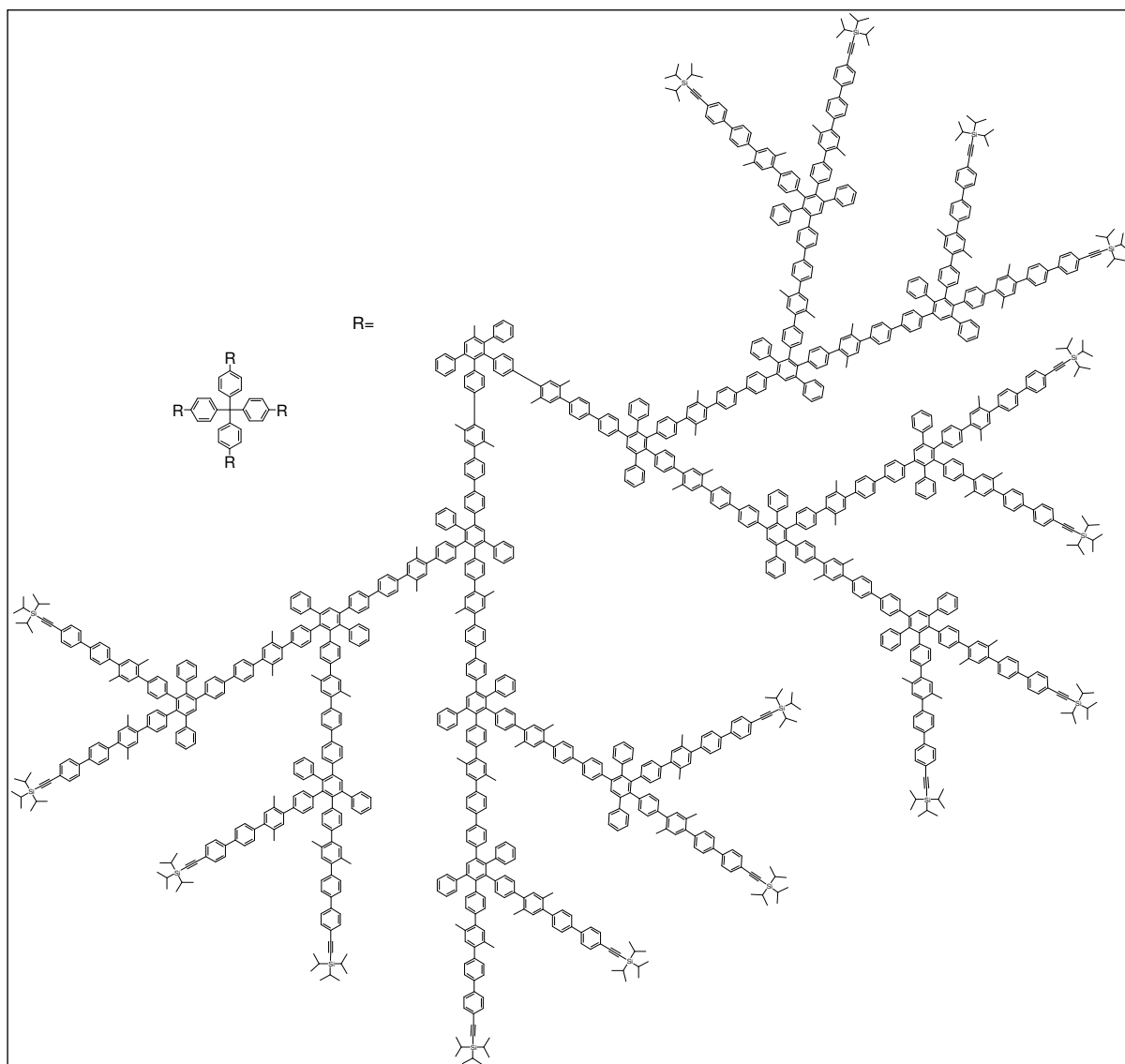
¹H NMR (700 MHz, C₂D₂Cl₄, 393 K): δ=7.65-6.83 (m, 1108 H, Ar), 3.10, 3.09, 3.08 (3 s, 32 H, C≡CH), 2.24, 2.10, and 2.05 (3 s, br, 336 H, CH₃) ppm.

¹³C NMR (175 MHz, C₂D₂Cl₄, 393 K): δ=142.26, 142.20, 141.87, 141.83, 141.57, 141.35, 141.28, 141.20, 141.12, 140.59, 140.57, 140.53, 140.28, 140.23, 139.84, 139.76, 139.49, 139.33, 139.30, 139.15, 139.02, 138.68, 132.90, 132.50, 132.44, 131.98, 131.78, 131.63, 130.45, 130.06, 129.87, 127.94, 127.65, 127.13, 127.02, 121.45, 84.17, 78.05, 19.94, 19.91, 19.76, and 19.73 ppm.

MALDI-TOF (dithranol): exact mass calcd for [M+K]⁺ C₂₀₄₉H₁₄₇₆K: 26137, found 26164.

G4-Td-(TiPS)₆₄ (3.14)

A mixture of **3.13** (62 mg, 0.0023 mmol) and the branching unit **3.1** (260 mg, 0.21 mmol) in *o*-xylene (5 mL) was heated to reflux for 36 h. The reaction was worked up as described for **3.10** and yielded a colorless (117 mg, 75%).



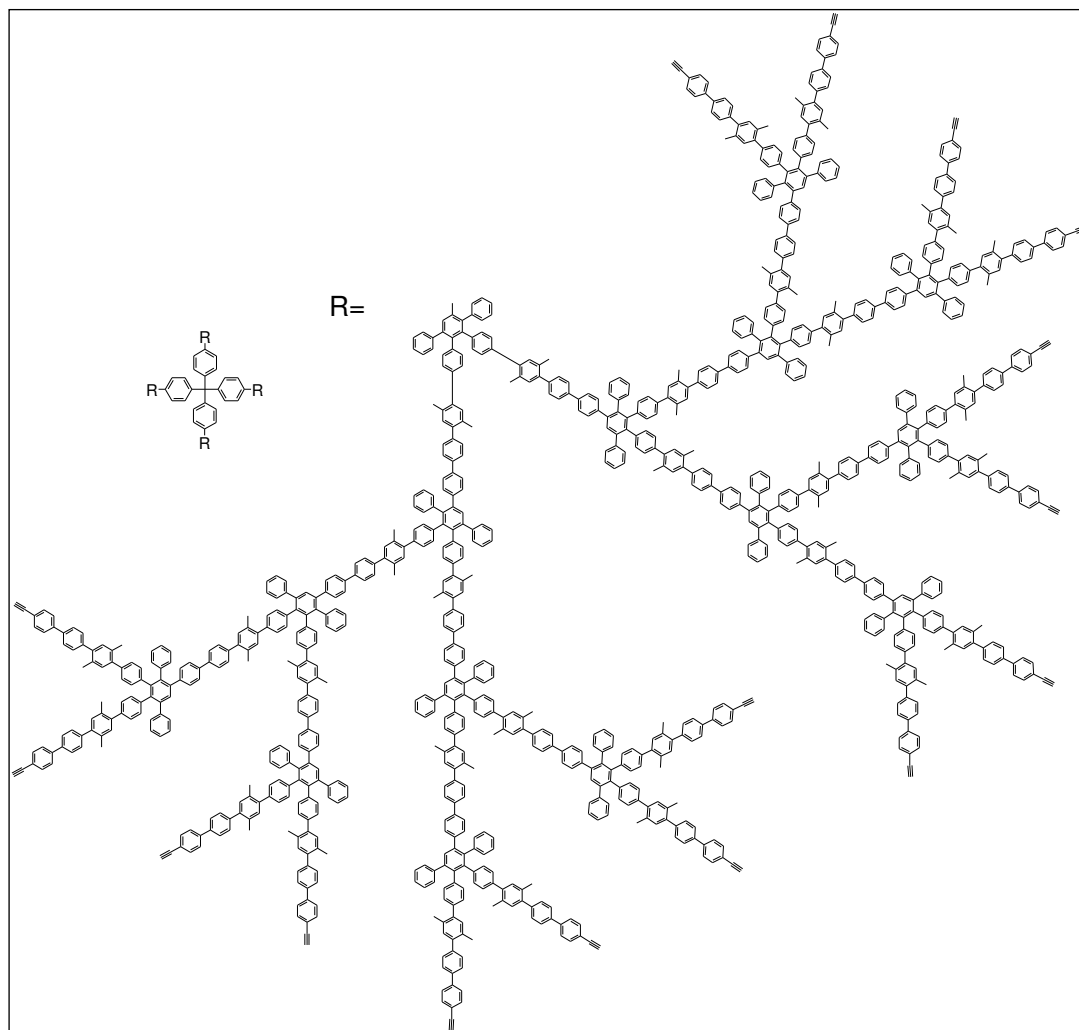
¹H NMR (700 MHz, C₂D₂Cl₄, 393 K): δ=7.63-6.89 (m, 2356 H, Ar), 2.23, 2.08, 2.03 (3 s, br, 720 H, CH₃), and 1.15 (s, br, 1344 H, iPr₃Si) ppm.

¹³C NMR (175 MHz, C₂D₂Cl₄, 393 K): δ=142.11, 142.03, 141.42, 141.10, 140.90, 140.31, 140.06, 139.62, 139.39, 138.89, 138.64, 138.53, 132.98, 132.82, 132.64, 132.60, 132.01, 131.93, 131.63, 130.83, 130.41, 130.03, 129.96, 128.07, 127.87, 127.75, 126.98, 126.86, 126.67, 126.24, 122.78, 107.20, 91.93, 20.27, 20.14, 19.02, and 11.69 ppm.

MALDI-TOF (dithranol): exact mass calcd for [M+K]⁺ C₄₉₂₉H₄₄₂₀Si₆₄K 65454, found 65430.

G4-Td-(ethyne)₆₄ (3.15)

To an argon purged mixture of G4-Td-(TiPS)₆₄ (**3.14**) (100 mg, 0.0017 mmol) in THF (10 mL) was added a solution of tetrabutylammonium (42 mg, 0.13 mmol) in THF (2 mL). The reaction mixture was stirred for 1 h, worked up as described for **3.9**, and yielded a colorless solid (78 mg, 86%).



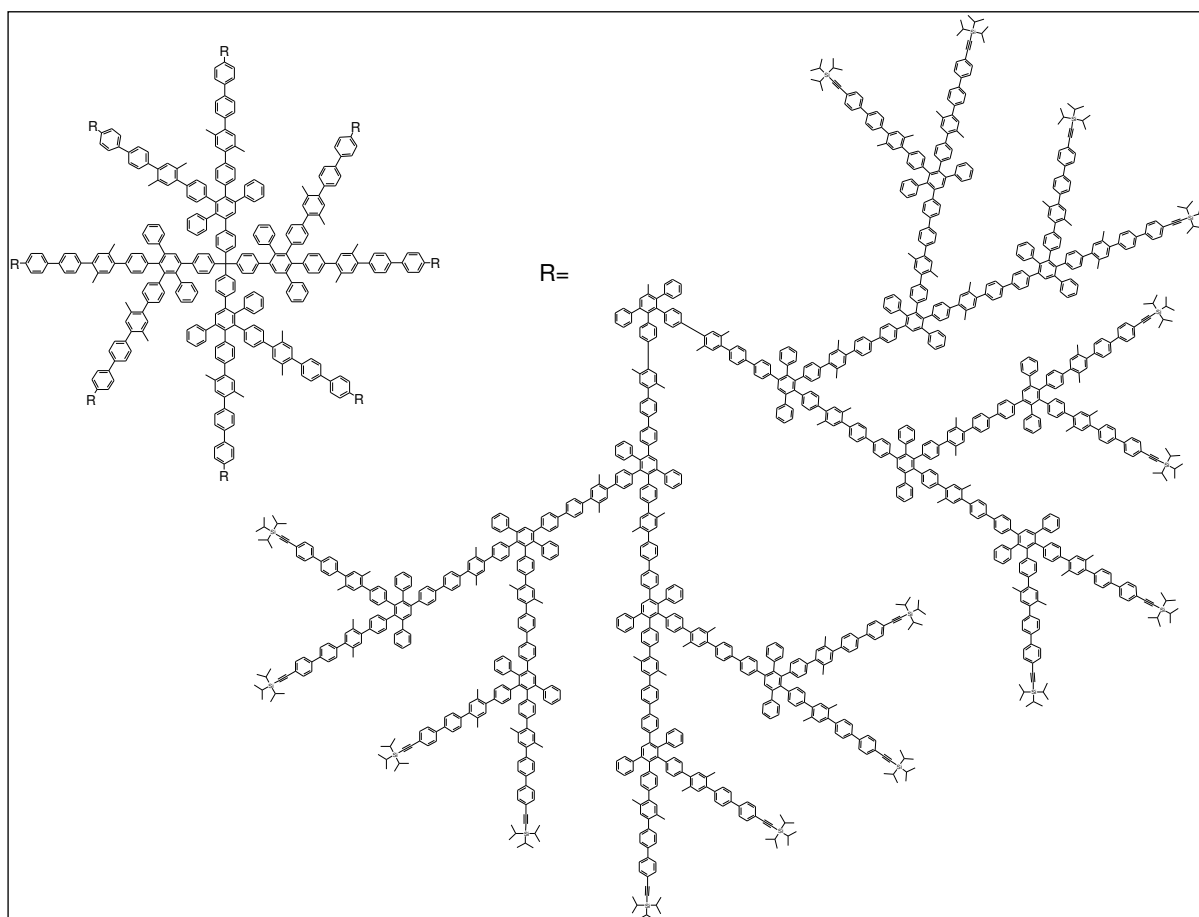
¹H NMR (700 MHz, C₂D₂Cl₄, 393 K): δ=7.63-6.89 (m, 2356 H, Ar), 3.09 (s, br, 64H, C≡CH), 2.22, 2.08, and 2.03 (3 s, 720 H, CH₃) ppm.

¹³C NMR (175 MHz, C₂D₂Cl₄, 398 K): δ=142.26, 142.20, 141.82, 141.56, 141.33, 141.26, 141.11, 140.54, 141.51, 140.42, 140.27, 140.23, 139.82, 139.74, 139.48, 139.15, 139.01, 138.71, 138.66, 132.88, 132.85, 132.48, 132.43, 131.98, 131.75, 131.63, 131.59, 130.71, 130.35, 130.02, 129.85, 127.94, 127.71, 127.64, 127.28, 127.12, 127.01, 126.73, 126.45, 126.28, 125.85, 121.45, 84.16, 78.03, 19.90, and 19.75 ppm.

MALDI-TOF (dithranol): exact mass calcd for [M+H]⁺ C₄₃₅₃H₃₁₄₁: 55450, found 55539.

G5-Td-(TiPS)₁₂₈ (3.16)

A mixture of **3.15** (75 mg, 0.00135 mmol) and the extended branching unit **3.1** (365 mg, 0.29 mmol) in *o*-xylene (7 mL) was heated to reflux for 50 h. The reaction mixture was worked up as described for **3.10** to yield a slightly beige solid (117 mg, 65%) which was subjected to analytical characterization. The slight coloration can be removed by SEC.



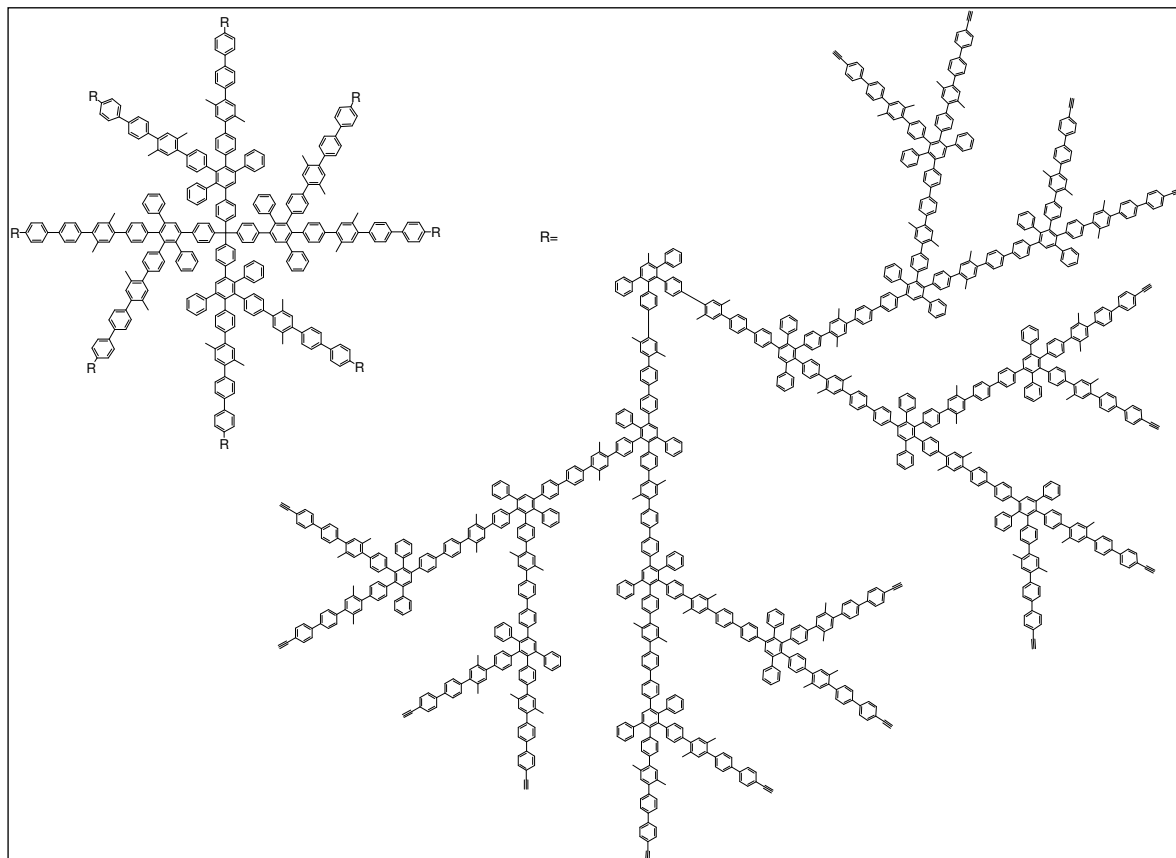
¹H NMR (700 MHz, C₂D₂Cl₄, 393 K): δ=7.63-6.90 (m, 4852 H, Ar), 2.22, 2.07, 2.03 (3 s, br, 1488 H, CH₃), and 1.15 (s, br, 2688 H, iPr₃Si) ppm.

¹³C NMR (175 MHz, C₂D₂Cl₄, 393 K): δ=142.23, 142.15, 141.62, 141.24, 141.18, 141.05, 141.02, 140.83, 140.50, 140.21, 139.76, 139.69, 139.45, 139.10, 138.90, 138.79, 132.89, 132.86, 132.70, 132.68, 132.52, 132.47, 131.81, 131.62, 131.58, 130.02, 129.86, 127.96, 127.75, 127.72, 127.67, 127.18, 126.94, 126.90, 126.72, 126.50, 125.88, 122.93, 107.50, 91.94, 20.01, 19.85, 18.91, and 11.81 ppm.

MALDI-TOF (Luftmann): exact mass calcd for [M]⁺C₁₀₁₁₃H₉₀₂₈Si₁₂₈: 134162, found 135290.

G5-Td-(ethyne)₁₂₈ (3.17)

To an argon purged mixture of G5-Td-(TiPS)₁₂₈ (**3.16**) (100 mg, 0.7×10^{-3} mmol) in THF (20 mL) was added a solution of tetrabutylammonium (32 mg, 0.102 mmol) in THF (2 mL). The reaction mixture was stirred for 1 h, worked up as described for **3.9**, and yielded a colorless solid (49 mg, 58%).



¹H NMR (700 MHz, C₂D₂Cl₄, 373 K): δ =7.62-6.87 (m, 4852 H, Ar), 3.08 (s, br, 128 H), 2.20, 2.06, and 2.02 (3 s, br, 1488 H, CH₃) ppm.

G6-Td-(TiPS)₂₅₆ (3.18)

A mixture of **3.17** (37 mg, 32.4×10^{-5} mmol) and the branching unit **3.1** (209 mg, 0.166 mmol) in *o*-xylene (4 mL) was heated to reflux for 50 h. The reaction mixture was worked up as described for **3.9** to yield a slightly beige solid (57 mg, 75%) which was subjected to analytical characterization. The slight coloration can be removed by SEC.

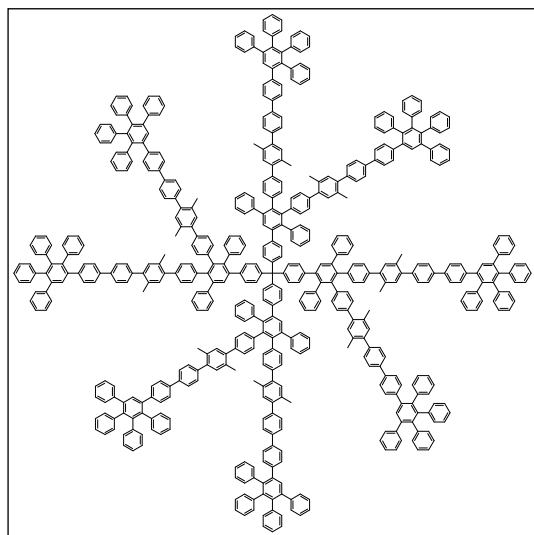
¹H NMR (700 MHz, C₂D₂Cl₄, 373 K): δ =7.62-6.86 (m, 9844 H, Ar), 2.20, 2.06, 2.02 (3 s, br, 3024 H, CH₃), and 1.12 (s, br, 5376 H, *i*Pr₃Si) ppm.

¹³C NMR (125 MHz, C₂D₂Cl₄, 360 K): δ =142.25, 142.14, 141.63, 141.20, 140.46, 140.22, 139.78, 139.47, 139.10, 138.81, 132.84, 132.66, 132.48, 132.44, 132.41, 131.90, 131.78, 131.60, 131.28, 130.72, 130.34, 129.91, 129.80, 127.94, 127.71, 127.16, 126.90, 126.73, 126.63, 126.18, 122.93, 128.93, 107.51, 91.95, 19.95, 19.78, 18.88, and 11.83 ppm.

Compound 3.19 see Chapter 6.5.

Compound 3.20

A mixture of dendrimer **3.9** (50 mg, 0.015 mmol) and tetraphenylcyclopentadienone (75 mg, 0.019 mmol) in *o*-xylene (2 mL) was heated to reflux for 24 h under argon. After cooling to room temperature, the solvent was removed *in vacuo*. The reaction mixture was purified by means of the short silica column chromatography (PE/CH₂Cl₂:2/1) to collect the branching unit, then dichloromethane to collect the product yielding colorless solid (69 mg, 81%).



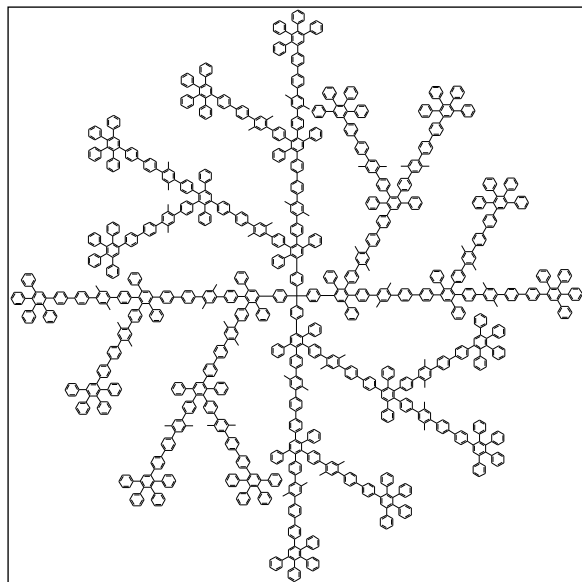
¹H NMR (500 MHz, CD₂Cl₂, 300 K): δ =7.59-6.70 (m, 340 H, Ar), 2.25, 2.24 (2 s, 24 H, CH₃), 2.10, and 2.06 (2 s, 24 H, CH₃) ppm.

¹³C NMR (125 MHz, CD₂Cl₂, 273 K): δ =145.06, 142.36, 142.27, 142.21, 141.31, 141.25, 140.95, 140.73, 140.61, 140.52, 139.88, 139.78, 139.27, 139.20, 138.90, 131.96, 131.90, 131.64, 130.87, 130.36, 130.05, 127.98, 127.25, 126.97, 126.84, 126.70, 126.43, 126.11, 125.74, and 19.94 ppm.

MALDI-TOF (dithranol): exact mass calcd for [M+Na]⁺: C₅₄₅H₃₈₈Na: 6960.24, found 6959.

Compound 3.21

A mixture of C(Ph([G2](ethyne)₄)₄) (3.11) (46 mg, 4.38 x 10⁻³ mmol) and tetraphenylcyclopentadienone (45 mg, 0.126 mmol) in *o*-xylene (2 mL) was heated at reflux



under argon for 24 h. The reaction was worked up as described for 3.10 and yielded a colorless solid (59 mg, 85%).

¹H NMR (500 MHz, CD₂Cl₂, 300 K): δ=7.69-6.80 (m, 820 H, Ar), 2.26-2.22 (m, 72 H, CH₃), and 2.11-2.05 (m, 72 H, CH₃) ppm.

¹³C NMR (125 MHz, CD₂Cl₂, 300 K): δ=142.60, 142.45, 142.37, 141.41, 141.37, 141.05, 140.82, 140.70, 140.63, 139.98, 139.88, 139.66, 139.33, 139.06, 139.01, 133.20, 132.87, 132.82, 132.22, 132.04,

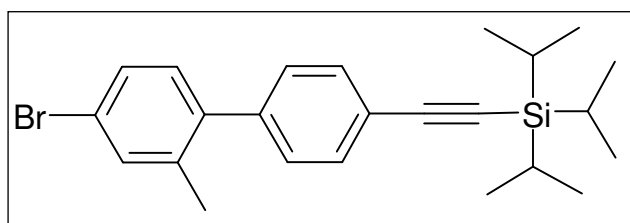
131.99, 131.68, 131.01, 130.93, 130.58, 130.43, 130.10, 128.25, 128.13, 128.03, 127.94, 127.52, 127.42, 127.30, 127.02, 126.90, 126.74, 126.57, 126.50, 126.17, 126.08, 125.80, 20.08, and 19.97 ppm.

MALDI-TOF (dithranol): exact mass calcd for [M+Ag]⁺ C₁₃₄₅H₉₆₄Ag: 17235, found 17240.

6.5 Syntheses of the semi-extended arm polyphenylene dendrimers (for Chapter 2)

(4'-Bromo-2'-methyl-biphenyl-4-yl-ethynyl)-triisopropyl-silane (4.2)

A degassed mixture of 4-(triisopropylsilylethynyl)phenyl-boronic acid (5 g, 16.41 mmol) and



5-bromo-2-iodo-toluene (3.50 g, 11.72 mmol), Pd(OAc)₂ (133 mg, 0.59 mmol), PPh₃ (306 mg, 1.17 mmol), Na₂CO₃ (2.76 g, 26 mmol) in water (10 mL), and acetone (45 mL) were refluxed overnight. The reaction

mixture was allowed to cool to room temperature, CH₂Cl₂ was added and the phases were separated. The organic phase was dried over MgSO₄, the solvent was removed *in vacuo*. The crude product was purified by means of column chromatography on silica gel using hexane as eluent (R_F = 0.42) to give slowly solidifying oil (2.7 g, 53%), mp: 68.3-68.8 °C.

^1H NMR (250 MHz, CD_2Cl_2 , 300 K): δ =7.53 (d, 2 H, Ar, 3J =8.21 Hz), 7.44-7.36 (m, 2 H, Ar), 7.25 (d, 2 H, Ar, 3J = 8.22 Hz), 7.08 (d, 1 H, Ar, 3J =7.89 Hz), 2.23 (s, 3 H, CH_3), and 1.15 (s, 21 H, $i\text{Pr}_3\text{Si}$) ppm.

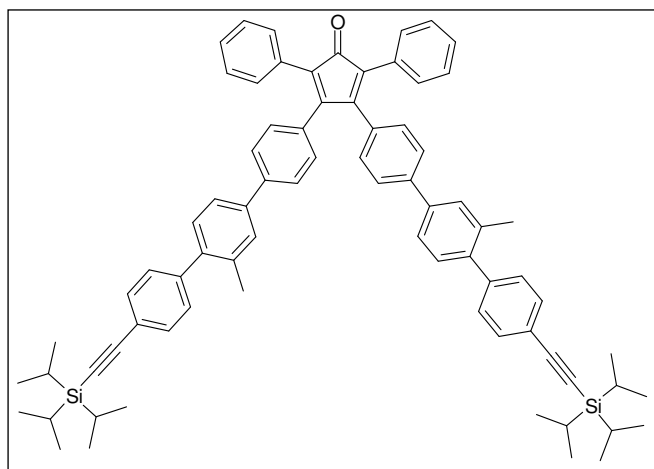
^{13}C NMR (62.5 MHz, CD_2Cl_2 , 300 K): δ =141.23, 140.60, 138.12, 133.44, 132.15, 131.50, 129.40, 129.20, 128.57, 122.68, 121.59, 107.18, 91.50, 20.43, 18.82, and 11.72 ppm.

FDMS: m/z [ue^{-1}] 426.5 (100%), 428.5 (100%) [M^+]; calcd: 427.50, 429.50.

Anal.Calcd for $\text{C}_{24}\text{H}_{31}\text{BrSi}$: C, 67.43; H, 7.31. Found: C, 67.31; H, 7.30.

3,4-Bis-{2'-methyl-1'-[(4''-triisopropylsilylethynyl)-phenyl]-biphenyl}-2,5-diphenyl-cyclopentadienone (4.1)

A mixture of (4'-bromo-2'-methyl-biphenyl-4-yl-ethynyl)-triisopropyl-silane (**4.2**) (2.47 g, 5.8 mmol) and 3,4-bis(4-(4,4,5,5-tetramethyl-1,3,2-dioxaborolan-2-yl)phenyl)-2,5-diphenyl-cyclopentadienone (1.23 g, 1.90 mmol) were dissolved in toluene (25 mL). The solution was



purged with argon. K_2CO_3 (1.06 g, 8.00 mmol) in H_2O (20 mL), and EtOH (3 mL) were added, and the system was degassed again. After the addition of $\text{Pd}(\text{PPh}_3)_4$ (0.67 g, 0.67 mmol), the reaction mixture was heated to 80 °C and stirred overnight. The reaction mixture was allowed to cool to room temperature, the layers separated, and the aqueous phase was extracted with CH_2Cl_2 . The combined organic layers were dried over MgSO_4 , and the solvent was removed *in*

vacuo. The crude product was purified by means of column chromatography in silica gel using petroleum ether/ CH_2Cl_2 (2:1) as eluent to give a dark red powder (1.13 g, 53 %), $T_{\text{dec}} > 300$ °C.

^1H NMR (700 MHz, CD_2Cl_2 , 300 K): δ =7.54-7.52 (m, 10 H, Ar), 7.48, 7.47 (dd, 2 H, Ar, J =7.75, 1.8 Hz), 7.32-7.26 (m, 16 H, Ar), 7.10 (d, 4 H, Ar, 3J =8.3 Hz), 2.32 (s, 6 H, CH_3), and 1.16 (s, 42 H, $i\text{Pr}_3\text{Si}$) ppm.

^{13}C NMR (175 MHz, $\text{C}_2\text{D}_2\text{Cl}_4$, 300 K): δ =200.77, 154.47, 141.70, 140.96, 140.54, 139.27, 136.84, 136.17, 132.24, 132.20, 131.12, 130.55, 130.50, 130.36, 129.94, 129.35, 129.11,

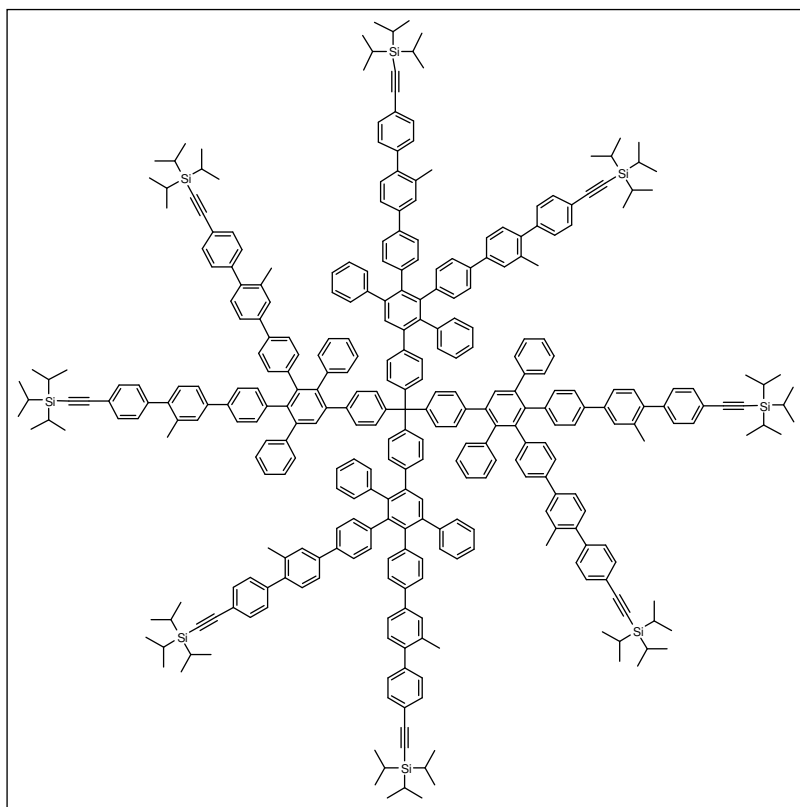
128.45, 127.87, 126.57, 126.16, 125.75, 124.65, 122.45, 107.15, 91.58, 20.94, 19.04, and 11.65 ppm.

FDMS: m/z [ue^{-1}] 1076 (100%) [M^+]; calcd: 1077.67.

Anal. Calcd for $C_{77}H_{80}OSi_2$: C, 85.82; H, 7.48. Found: C, 85.82; H, 7.67.

First-generation dendrimer with eight TiPS protective groups (4.3)

A mixture of the core tetra(4-ethynylphenyl)methane (30 mg, 0.07 mmol) and the branching unit (4.1) (373 mg, 0.35 mmol) in *o*-xylene (5 mL) was heated to reflux for 24 h under argon. After cooling to room temperature, the solvent was removed *in vacuo*. The residue was purified by means of column chromatography on SiO_2 using petroleum ether/ CH_2Cl_2 (2/1) as eluent. Upon evaporation of the solvent, a colorless solid was obtained (278 mg, 84%), $T_{dec} > 300$ °C.

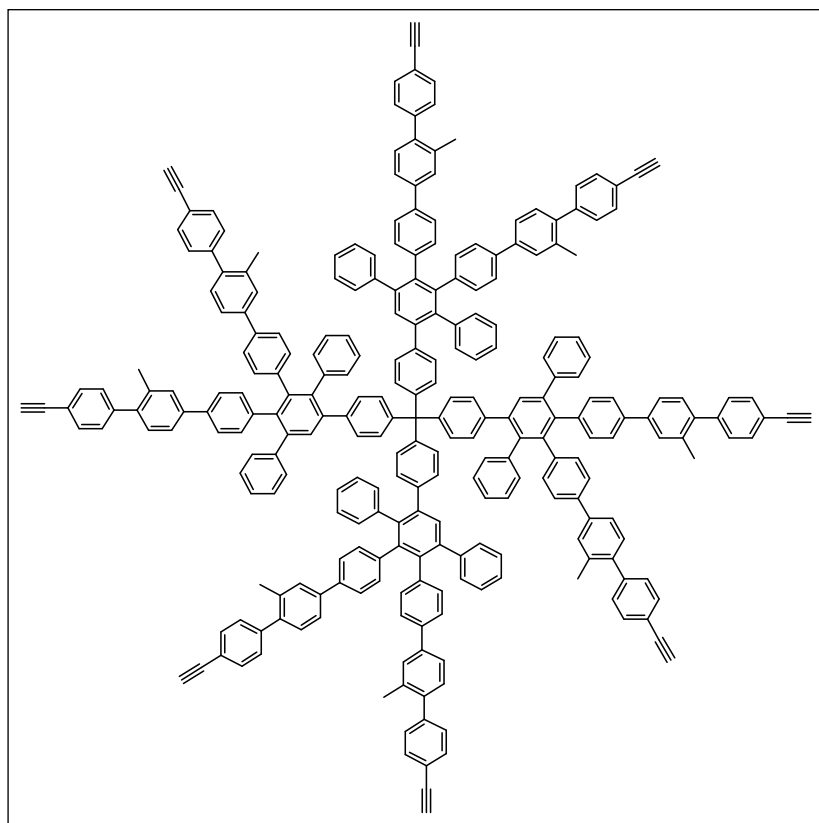


1H NMR (500 MHz, CD_2Cl_2 , 273 K): δ =7.66 (s, 4 H, Ar), 7.52-7.51 (m, 14 H, Ar), 7.40-7.17 (m, 78 H, Ar), 7.04-6.93 (m, 44 H, Ar), 6.77, 6.76 (2 s, 8 H, Ar), 2.26, 2.25 (2 s, 24 H, CH_3), and 1.16 (s, 168 H, iPr_3Si) ppm.

^{13}C NMR (125 MHz, CD_2Cl_2 , 273 °K): δ =145.08, 142.34, 142.28, 141.80, 141.41, 141.37, 140.63, 140.55, 140.50, 140.21, 140.05, 139.86, 139.51, 138.15,

137.88, 136.03, 136.00, 132.58, 132.55, 132.18, 132.10, 131.48, 130.82, 130.48, 130.34, 129.58, 129.25, 129.14, 129.10, 128.14, 127.35, 126.82, 126.10, 125.78, 125.51, 124.52, 124.48, 122.43, 107.53, 91.33, 20.70, 18.90, and 11.86 ppm.

MALDI-TOF (dithranol): exact mass calcd for $[M+Ag]^+ C_{337}H_{340}Si_8Ag$: 4726.16, found 4724.

First-generation dendrimer with eight ethynyl groups (4.4)

To **4.3** (200 mg, 0.043 mmol) in THF (5 mL) was added a solution of tetrabutylammonium fluoride trihydrate (60 mg, 0.19 mmol) in THF (2 mL). The reaction mixture was stirred under argon at room temperature for 20 min. After quenching with H₂O (1 mL), the mixture was concentrated *in vacuo*, a minimum amount of THF was added, precipitation was effected by dropping the solution into

methanol/water mixture (4/1). The product was collected by filtration and was dried *in vacuo* to yield a colorless solid (117.3 mg, 80%), T_{dec} > 300 °C.

¹H NMR (500 MHz, C₂D₂Cl₄, 273 K): δ=7.60 (s, 4 H, Ar), 7.48-7.46 (m, 14 H, Ar), 7.37-7.08 (m, 78 H, Ar), 6.94-6.80 (m, 44 H, Ar), 6.70, 6.68 (2 s, 8 H, Ar), 3.10, 3.09 (2 s, 8 H, C≡C-H), and 2.26, 2.25 (2 s, 24 H, CH₃) ppm.

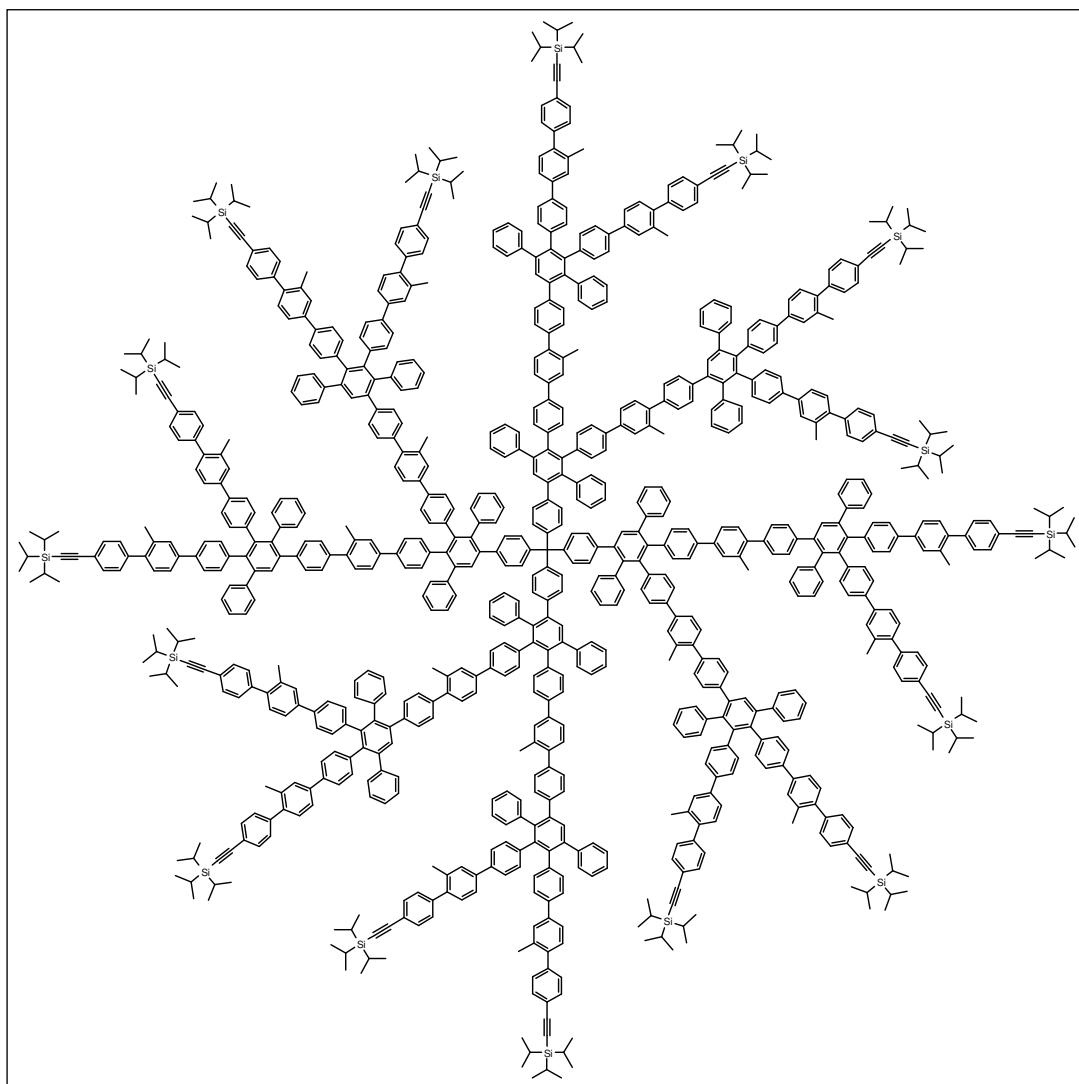
¹³C NMR (125 MHz, C₂D₂Cl₄, 350 K): δ=144.97, 142.58, 142.20, 141.50, 141.14, 141.05, 140.44, 140.22, 140.17, 140.14, 140.00, 139.77, 139.64, 139.19, 137.61, 137.34, 135.72, 135.70, 132.38, 132.36, 132.20, 131.96, 131.10, 130.62, 130.29, 130.14, 130.12, 129.37, 129.02, 128.92, 127.82, 127.03, 126.48, 125.75, 125.52, 125.26, 125.45, 120.96, 84.15, 77.78, and 20.55 ppm.

MALDI-TOF (dithranol): exact mass calcd for [M+H]⁺: C₂₆₅H₁₈₀: 3364.39, found 3362.

Second-generation dendrimer with sixteen TiPS protective groups (4.5)

A mixture of dendrimer **4.4** (50 mg, 0.015 mmol) and the branching unit (**4.1**) (190 mg, 0.18 mmol) in *o*-xylene (3 mL) was heated to reflux for 24 h under argon. After cooling to room temperature, the solvent was removed *in vacuo*. 1-2 mL of THF was added and the reaction

mixture was slowly dropped into acetone. After the filtration, the beige solid was washed with much acetone, followed by methanol, yielding colorless solid (153 mg, 88%).



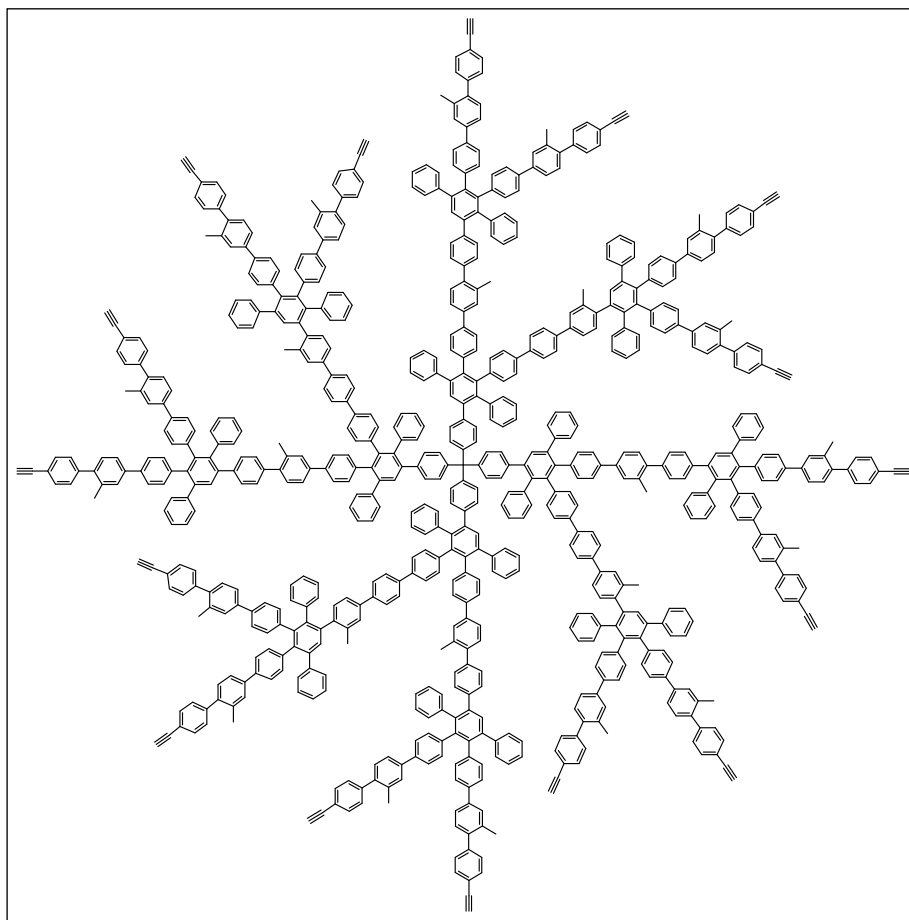
^1H NMR (700 MHz, $\text{C}_2\text{D}_2\text{Cl}_4$, 273 K): δ =7.59-6.70 (m, 412 H, Ar), 2.21, 2.20, 2.19, 2.19, 2.16, 2.16 (6 s, 72 H, CH_3), and 1.07, 1.06, 1.05 (3 s, 336 H, $i\text{Pr}_3\text{Si}$) ppm.

^{13}C NMR (175 MHz, $\text{C}_2\text{D}_2\text{Cl}_4$, 273 K): δ =142.02, 141.83, 141.48, 140.94, 140.80, 140.76, 140.47, 140.13, 140.05, 139.89, 139.70, 139.34, 139.04, 137.09, 136.08, 136.77, 136.08, 135.90, 135.86, 132.40, 132.20, 130.33, 129.96, 129.38, 128.93, 128.64, 127.98, 127.25, 126.54, 125.57, 125.27, 124.49, 124.31, 122.23, 107.10, 91.47, 20.91, 19.04, and 11.61 ppm.

MALDI-TOF (dithranol): exact mass calcd for $[\text{M}]^+$: $\text{C}_{873}\text{H}_{820}\text{Si}_{16}$: 11744, found 11709.

Second-generation dendrimer with sixteen ethynyl groups (4.6)

To the dendrimer **4.5** (132 mg, 0.011 mmol) in THF (5 mL) was added a solution of tetrabutylammonium fluoride trihydrate (62 mg, 0.197 mmol) in THF (2 mL). The reaction mixture was stirred under argon at room temperature for 40 min. After quenching with H₂O (1 mL), the mixture was concentrated *in vacuo*, a minimum amount of THF was added, and dropped into a methanol/water mixture (4/1) and stirred for 30 min. The precipitate was collected by filtration and was dried *in vacuo* to yield a colorless solid (84 mg, 81%).



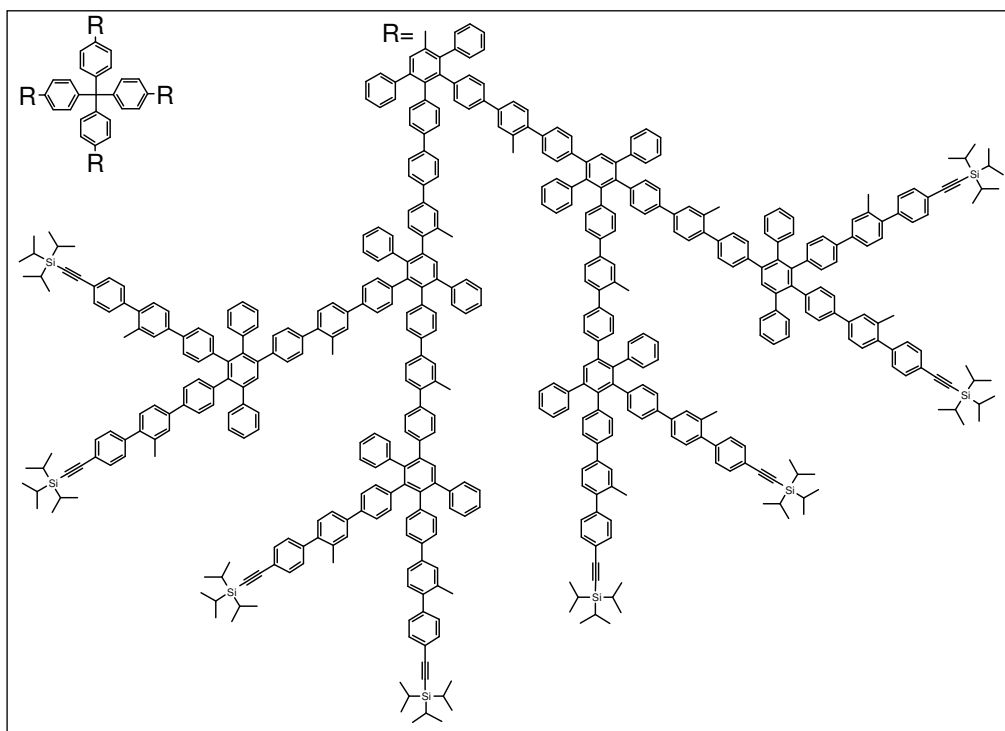
¹H NMR (500 MHz, C₂D₂Cl₄, 393 K): δ=7.61-6.77 (m, 412 H, Ar), 3.06 (s, br, 16 H, C≡C-H), and 2.21, 2.17 (2 s, br, 72 H, CH₃) ppm.

¹³C NMR (125 MHz, C₂D₂Cl₄, 350 K): δ=142.59, 142.25, 142.18, 141.65, 141.55, 141.12, 141.04, 140.97, 140.86, 140.60, 140.46, 140.37, 140.23, 140.16, 140.00, 139.99, 139.91, 139.74, 139.26, 137.81, 137.79, 137.76, 137.62, 137.54, 137.52, 137.33, 137.30, 135.91, 135.88, 135.71, 135.67, 132.36, 132.33, 132.18, 131.93, 131.36, 130.28, 130.18, 130.14, 130.10, 129.93, 129.36, 128.93, 128.78, 128.51, 127.82, 127.10, 126.47, 125.83, 125.51, 125.25, 124.45, 124.27, 120.95, 84.15, 77.78, and 20.53 ppm

MALDI-TOF (dithranol): exact mass calcd for [M+H]⁺: C₇₂₉H₅₀₀: 9260.11, found 9259.

Third-generation dendrimer with thirty two TiPS protective groups (4.7)

A mixture of the dendrimer **4.6** (70 mg, 0.0075 mmol) and the branching unit **4.1** (230 mg, 0.220 mmol) in *o*-xylene (5 mL) was heated to reflux for 36 h under argon. After cooling to room temperature, the solvent was removed *in vacuo* and the residue was worked up as described for **4.5** to give colorless solid (165 mg, 84%).



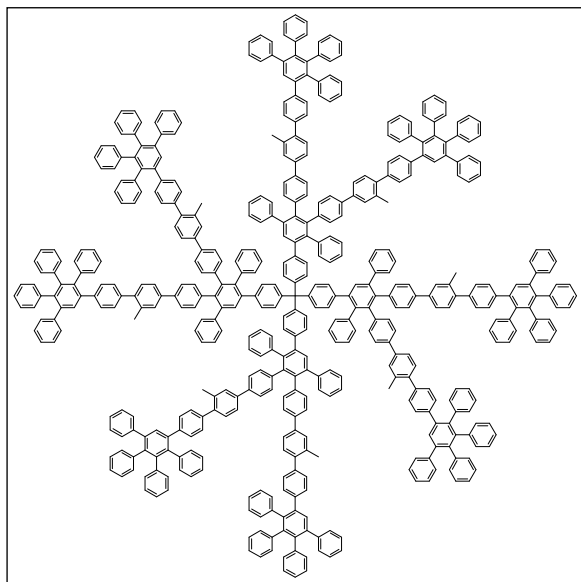
^1H NMR (500 MHz, $\text{C}_2\text{D}_2\text{Cl}_4$, 353 K): $\delta=7.60\text{--}6.74$ (m, 940 H, Ar), 2.21, 2.16 (2 s, br, 168 H, CH_3), and 1.12 (s, br, 672 H, $i\text{Pr}_3\text{Si}$) ppm.

^{13}C NMR (125 MHz, $\text{C}_2\text{D}_2\text{Cl}_4$, 350 K): $\delta=142.25$, 142.17, 142.06, 141.70, 141.66, 141.12, 140.95, 140.60, 140.37, 140.31, 140.09, 139.90, 139.72, 139.28, 137.62, 137.36, 135.90, 135.87, 135.72, 135.68, 132.35, 132.04, 131.93, 131.35, 130.28, 130.16, 130.12, 129.93, 129.25, 128.91, 128.78, 128.51, 127.81, 127.10, 126.47, 125.82, 125.50, 125.24, 124.45, 124.26, 122.47, 107.53, 20.56, 18.91, and 11.80 ppm.

MALDI-TOF (dithranol): exact mass calcd for $[\text{M}]^+$: $\text{C}_{1945}\text{H}_{1780}\text{Si}_{32}$: 26055, found 26064.

Compound 3.19

A mixture of dendrimer **4.4** (43 mg, 0.013 mmol) and tetraphenylcyclopentadienone (55 mg, 0.014 mmol) in *o*-xylene (2 mL) was heated to reflux for 24 h under argon. After cooling to



room temperature, the solvent was removed *in vacuo*. The reaction mixture was purified by means of the short silica column chromatography (PE/CH₂Cl₂:2/1) to collect branching unit, then dichloromethane to collect product yielding colorless solid (65 mg, 82%).

¹H NMR (700 MHz, C₂D₂Cl₄, 300 K): δ=7.31-6.67 (m, 316 H, Ar), and 2.14, 2.12 (2 s, 24 H, CH₃) ppm.

¹³C NMR (125 MHz, C₂D₂Cl₄, 350 K): δ=142.23, 142.00, 140.93, 140.86, 140.74,

140.63, 140.42, 140.37, 139.99, 139.94, 139.74, 139.64, 139.21, 137.77, 137.52, 135.90, 135.86, 132.33, 132.30, 131.90, 131.86, 131.82, 131.12, 130.60, 130.30, 130.24, 130.20, 130.17, 129.90, 129.01, 128.75, 128.46, 127.80, 127.67, 126.95, 126.69, 126.31, 125.65, 125.47, 125.37, 125.21, 124.24, and 20.52 ppm.

MALDI-TOF (dithranol): exact mass calcd for [M]⁺: C₄₈₉H₃₄₀: 6216.16, found 6218.

6.6 Syntheses of the dendrimers possessing eight internal -C≡C- triple bonds and their hydrogenation (for Chapter 3)

n-BuMgBr

The Grignard reagent. In the dried flask a powder of Mg (4.57 g, 0.17 mol) was covered with dried Et₂O (70 mL) and flushed with argon. 1-2 crystals of I₂ were added. Under cooling with an ice bath C₄H₉Br (19 mL, 17 mmol) was added dropwise. At the end of the reaction the mixture was heated until Mg had completely reacted. A turbid solution was obtained.

1,4-Di-*n*-butylbenzene

Kumada reaction. To a mixture of NiCl₂(dpe) (0.28 g, 0.39 mmol), *p*-dichlorobenzene (10 g, 68 mmol) and Et₂O (120 mL) at 0 °C was added via cannula *n*-BuMgBr (24.41 g, 0.15 mol). The resulting black mixture was heated at reflux for 20 hours to form much insoluble

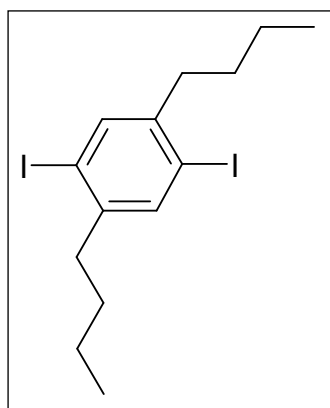
salt. During the reaction additional Et₂O (2x25 mL) was added. After hydrolysis with dilute HCl, the organic layer and ether extracts from the aqueous layer were combined, washed with water, dried over MgSO₄, and concentrated in *vacuo*. The crude material was purified by column chromatography using hexane as an eluent (R_F=0.73) to give a colorless oil (10.93 g, 84.5%).

¹H NMR (250 MHz, CD₂Cl₂, 300°K): δ=7.11 (s, 4H, Ar), 2.62-2.56 (t, 4H, 2 x CH₂), 1.66-1.52 (m, 4H, 2 x CH₂), 1.45-1.31 (m, 4H, 2 x CH₂), and 0.98-0.93 (t, 6H, 2 x CH₃) ppm.

¹³C NMR (62.5 MHz, CD₂Cl₂, 250 MHz, 300°K): δ=140.56, 128.67, 35.68, 34.35, 22.91, and 14.22 ppm.

EI (C₁₄H₂₂): m/z [ue⁻¹] 191.1 (100%), [M⁺]; calcd: 190.33

2,5-Di-*n*-butyl-1,4-diiodobenzene



Under argon in a 1 L flask were combined water (30 mL), acetic acid (300 mL), conc. sulphuric acid 9 mL, CCl₄ (60 mL), iodine (13.2 g, 52.0 mmol), periodic acid (5.93 g, 26 mmol), and 1,4-di-*n*-butylbenzene (10 g, 52 mmol). The mixture was heated to reflux overnight, then poured into water and extracted with hexane. The combined organic layers were washed with 1N Na₂CO₃ and 1N Na₂S₂O₃, and dried over MgSO₄. The solvent was removed in *vacuo*. The crude material was purified by column

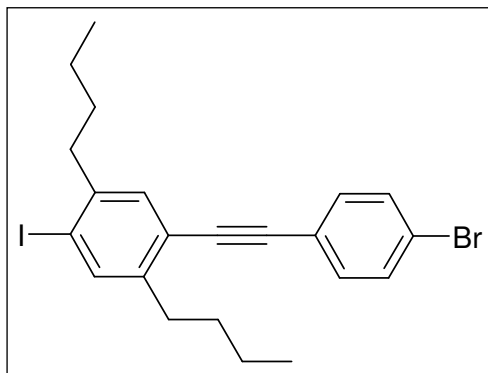
chromatography using hexane as eluent (R_F=0.73). After the evaporation of the solvent, the material was re-crystallized from EtOH to give a colorless solid (18.94 g, 81%), mp: 47.2-47.4 °C.

¹H NMR (250 MHz, CD₂Cl₂, 300 K): δ=7.63 (s, 2H, Ar), 2.64, 2.62, 2.58 (t, 4 H, 2 x CH₂), 1.59-1.32 (m, 8 H, overlap of 2 x CH₂), 0.98, 0.95, 0.92 (t, 6 H, 2 x CH₃) ppm.

¹³C NMR (62.5 MHz, CD₂Cl₂, 300°K): δ=145.27, 139.71, 100.60, 39.84, 32.73, 22.76, and 14.07 ppm

FDMS: m/z [ue⁻¹] 442.2 (100 %), [M⁺], (calcd. 442.12)

Anal.: Calcd for C₁₄H₂₀I₂: C, 38.03; H, 4.56. Found: C, 38.01; H, 4.45.

1-(4-Bromo-phenylethynyl)-2,5-dibutyl-4-iodo-benzene (5.3)

To a degassed solution of 2,5-dibutyl-1,4-diiodobenzene (6.34 g, 14.30 mmol), dry THF (50 mL), piperidine (10 mL), 1-bromo-4-ethynyl-benzene (1.73 g, 9.56 mmol) at 0 °C were added consecutively CuI (54 mg, 0.29 mmol) and Pd(PPh₃)₂Cl₂ (100 mg, 0.14 mmol). The reaction mixture was stirred overnight at r.t., thereafter dichloromethane and water were added. The two phases were separated, the

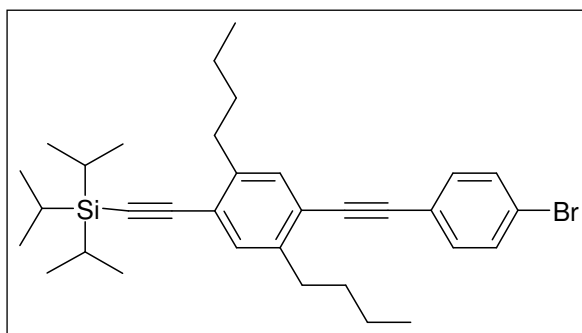
organic layer was washed with NH₄Cl (aq), cold 1N HCl, 10% NaHCO₃ (aq), dried over MgSO₄, the solvent was evaporated in *vacuo* and the crude material was purified by means of column chromatography using hexane as eluent (R_F=0.44). Upon evaporation of the solvent, a colorless oil, which slowly solidified, was obtained (2.07 g, 44%), mp: 46.5-47.5 °C.

¹H NMR (250 MHz, CD₂Cl₂, 300 K): δ=7.71 (s, 1 H, Ar), 7.51 (d, 2 H, Ar, ³J=8.53 Hz), 7.40 (d, 2 H, Ar, ³J=8.21 Hz), 7.32 (s, 1 H, Ar), 2.78-2.64 (m, 4 H, 2 x CH₂), 1.69-1.36 (m, 8 H, 2 x CH₂), and 1.00-0.93 (m, 6 H, 2 x CH₃) ppm.

¹³C NMR (62.5 MHz, CD₂Cl₂, 300 K): δ=144.49, 143.26, 139.96, 133.20, 132.56, 132.06, 122.83, 122.74, 122.70, 101.52, 92.66, 89.22, 40.21, 33.81, 33.19, 32.73, 22.95, 22.80, and 14.14 ppm.

FDMS: m/z [ue⁻¹] 494.8 (100%), 496.8 (100%) [M⁺], (calcd: 495.26, 497.26).

Anal.: Calcd for C₂₂H₂₄BrI: C, 53.36; H, 4.88. Found: C, 53.29; H, 4.82.

[4-(4-Bromo-phenylethynyl)-2,5-dibutyl-phenylethynyl]-triisopropyl-silane (5.2)

Under cooling with an ice bath to the degassed solution of **5.3** (2 g, 4 mmol), triisopropylsilylacetylene (1 mL, 4.4 mmol) in dried THF (30 mL) and Et₃N (10 mL) under argon were added consecutively CuI (0.03 g, 0.18 mmol), PdCl₂(PPh₃)₂ (0.06 g, 0.09 mmol). The reaction was stirred at r.t. for 15 hours,

then dichloromethane and water were added. The two phases were separated, the organic layer was washed with NH₄Cl (aq), cold 1N HCl, 10% NaHCO₃ (aq), and dried over MgSO₄.

The solvent was evaporated in *vacuo* and the crude material was purified by means of column chromatography using hexane as eluent ($R_F=0.49$) to give yellowish oil (2.13 g, 95.5%).

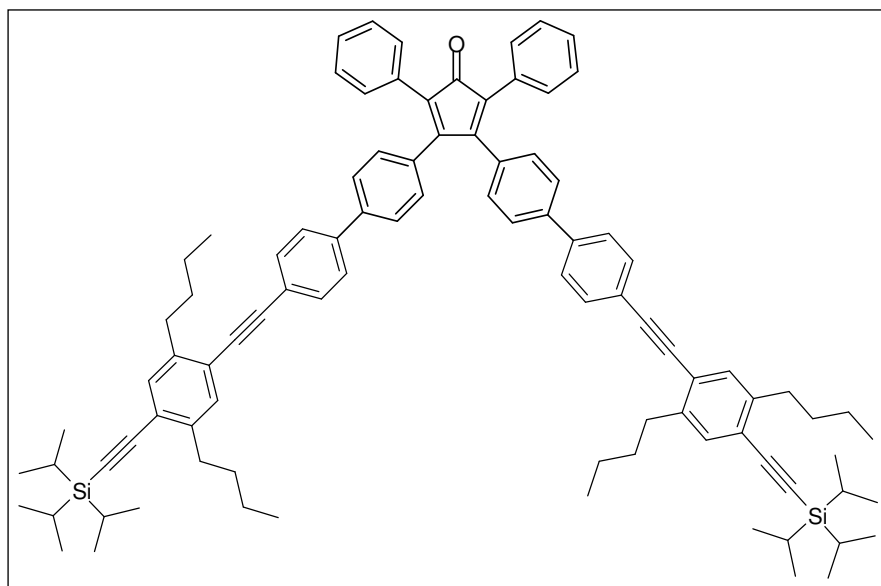
^1H NMR (250 MHz, CD_2Cl_2 , 300 K): $\delta=7.53$ (d, 2 H, Ar, $^3J=8.53$ Hz), 7.39 (d, 2H, Ar, $^3J=8.53$ Hz), 7.33, 7.32 (2 s, 2 H, Ar), 2.80-2.74 (t, 4H, CH_2), 1.70-1.56 (m, 4 H, CH_2), 1.46-1.34 (m, 4 H, CH_2), 1.15 (s, 21 H, iPr_3Si), and 0.98-0.91 (m, 6 H, CH_3) ppm.

^{13}C NMR (62.5 MHz, CD_2Cl_2 , 300 K): $\delta=143.07$, 142.65, 133.28 133.23, 132.61, 132.17, 123.48, 122.81, 122.77, 122.54, 105.89, 95.95, 93.00, 89.81, 34.41, 34.14, 33.35, 23.08, 23.04, 18.85, 14.16, and 11.76 ppm.

FDMS: m/z [ue^{-1}] 551.1 (100%), 553.0 (100%), [M^+], (calcd. for $\text{C}_{33}\text{H}_{45}\text{BrSi}$: 549.72, 551.72).

2,5-Diphenyl-3,4-di([4'-({2'',5''-dibutyl-4''-triisopropylsilyl}ethynyl)-phenylethynyl)-yl]-biphenyl-4-yl)-cyclopentadienone (5.1)

A mixture of 3,4-bis(4-(4,4,5,5-tetramethyl-1,3,2-dioxaborolan-2-yl)phenyl)-2,5-diphenylcyclopentadienone (540 mg, 0.85 mmol) and **5.2** (1.23 g, 2.20 mmol) were dissolved



in toluene (15 mL), the reaction mixture was degassed. K_2CO_3 (0.47 g, 3.40 mmol) in water (10 mL) was added, the system was again degassed and under argon $\text{Pd}(\text{PPh}_3)_4$ (0.12 g, 0.11 mmol) was added. The reaction mixture was refluxed overnight. After the reaction had

cooled to room temperature, two phases separated. The aqueous phase was extracted twice with dichloromethane, the organic phases were dried over MgSO_4 , and the solvents were evaporated. The product was purified by means of silica column chromatography using $\text{PE}/\text{CH}_2\text{Cl}_2$ as eluent (first 3:1 to remove starting material and then 2.5:1 to collect product, (TLC (1:1.5 $\text{PE}:\text{CH}_2\text{Cl}_2$), $R_F=0.36$) to give a reddish yellow powder (0.37 g, 33 %), $T_{\text{dec}}>250^\circ\text{C}$.

^1H NMR (700 MHz, $\text{C}_2\text{D}_2\text{Cl}_4$, 273 K): δ =7.56-7.51 (m, 8 H, Ar), 7.43 (d, 4H, Ar, ^3J =8.12 Hz), 7.28-7.23 (m, 14 H, Ar), 6.99 (d, 4 H, Ar, ^3J =8.13 Hz), 2.73-2.68 (m, 8H, CH_2), 1.62-1.54 (m, 8 H, CH_2), 1.39-1.31 (m, 8 H, CH_2), 1.08 (s, 42 H, iPr_3Si), and 0.91-0.86 (m, 12 H, CH_3) ppm.

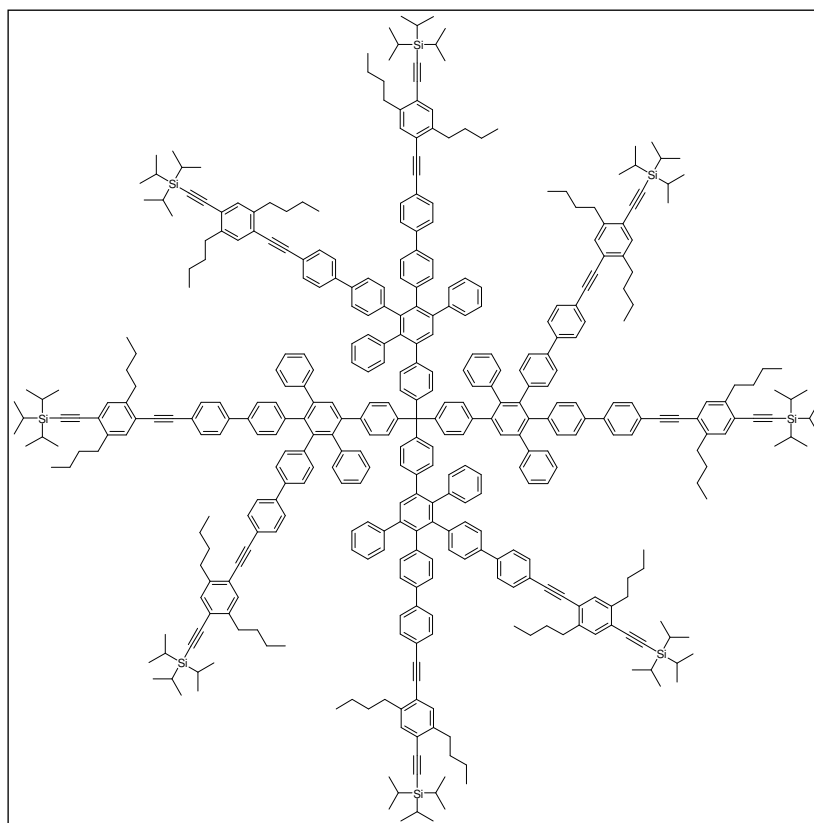
^{13}C NMR (175 MHz, $\text{C}_2\text{D}_2\text{Cl}_4$, 273 K): δ = 200.72, 154.22, 142.96, 142.44, 140.21, 139.97, 133.21, 132.50, 132.44, 132.28, 131.00, 130.49, 130.44, 128.52, 127.94, 127.13, 126.63, 125.89, 123.27, 123.07, 122.67, 105.79, 95.96, 94.04, 89.94, 34.43, 34.20, 33.24, 23.10, 19.05, 14.42, 14.38, and 11.66 ppm.

FDMS: m/z [ue^{-1}] 1324 (100 %), [M^+], (calcd. 1322.09)

Anal.: Calcd for $\text{C}_{95}\text{H}_{108}\text{OSi}_2$: C, 86.31; H, 8.23. Found: C, 86.28; H, 8.44.

First-generation dendrimer with protective TiPS groups (5.4)

A mixture of core tetra(4-ethynylphenyl)methane (20 mg, 0.048 mmol) and the branching unit **5.1** (305 mg, 0.230 mmol) in *o*-xylene (5 mL) was refluxed for 24 hours under argon. After cooling to room temperature, the solvent was removed *in vacuo*. The residue was purified by means of column chromatography using PE/ CH_2Cl_2 : (2.5/1) to give a colorless solid (178 mg, 66 %), $T_{\text{dec}} > 250\text{ }^\circ\text{C}$.



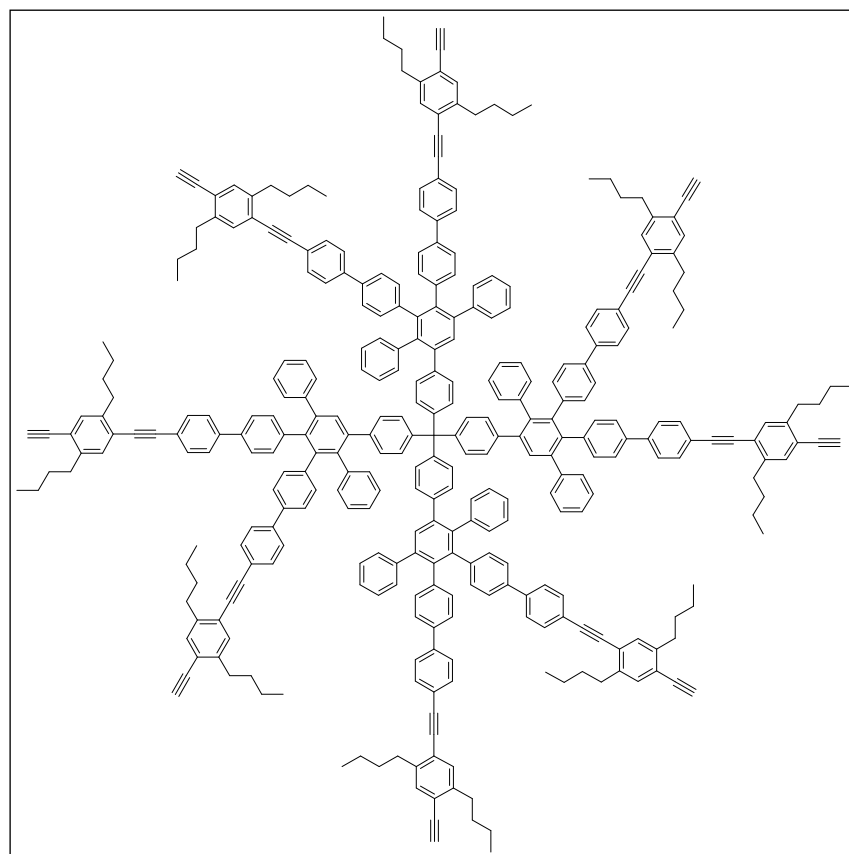
^1H NMR (700 MHz, $\text{C}_2\text{D}_4\text{Cl}_4$, 393 K): δ =7.58 (s, 4H, Ar), 7.44-7.39 (m, 30 H, Ar), 7.27-7.11 (m, 52 H, Ar), 6.97-6.74 (m, 54 H, Ar), 2.76 (m, 32 H, CH_2), 1.65 (m, 32 H, CH_2), 1.39 (m, 32 H, CH_2), 1.15 (s, 168 H, TIPS), and 0.92 (m, 48 H, CH_3) ppm.

^{13}C NMR (175 MHz, $\text{C}_2\text{D}_4\text{Cl}_4$, 273 K): δ =144.68, 142.92, 142.39, 141.95, 141.20, 141.11, 140.86, 140.75, 140.69, 140.35, 140.18, 139.98, 139.84, 139.52, 138.81, 136.99, 136.71, 133.18, 132.44, 132.06, 132.04, 131.38, 130.68, 130.34, 129.01, 128.02, 127.19, 126.97, 126.61, 125.68, 125.40, 123.13, 122.80, 123.13, 122.24, 105.84, 95.84, 94.21, 89.45, 34.42, 34.19, 33.22, 23.09, 19.05, 14.40, 14.37, and 11.66 ppm.

MALDI-TOF (dithranol): exact mass calcd for $[\text{M}+\text{Ag}]^+ \text{C}_{409}\text{H}_{452}\text{Si}_8\text{Ag}$: 5700.85, found 5700.

First-generation dendrimer with eight external ethynyl groups (5.5)

To a mixture of **5.4** (177 mg, 0.032 mmol) in THF (8 mL) under argon was added tetrabutylammonium fluoride trihydrate (88 mg, 0.27 mmol) in THF (2 mL). The reaction mixture was stirred at room temperature for 30 min. After quenching with H_2O , the mixture was concentrated *in vacuo*, a minimum amount of THF was added, and the solution was poured into a methanol/water mixture (4/1). The precipitated product was collected by filtration and was dried *in vacuo* to yield a colorless solid (116 mg, 85%).



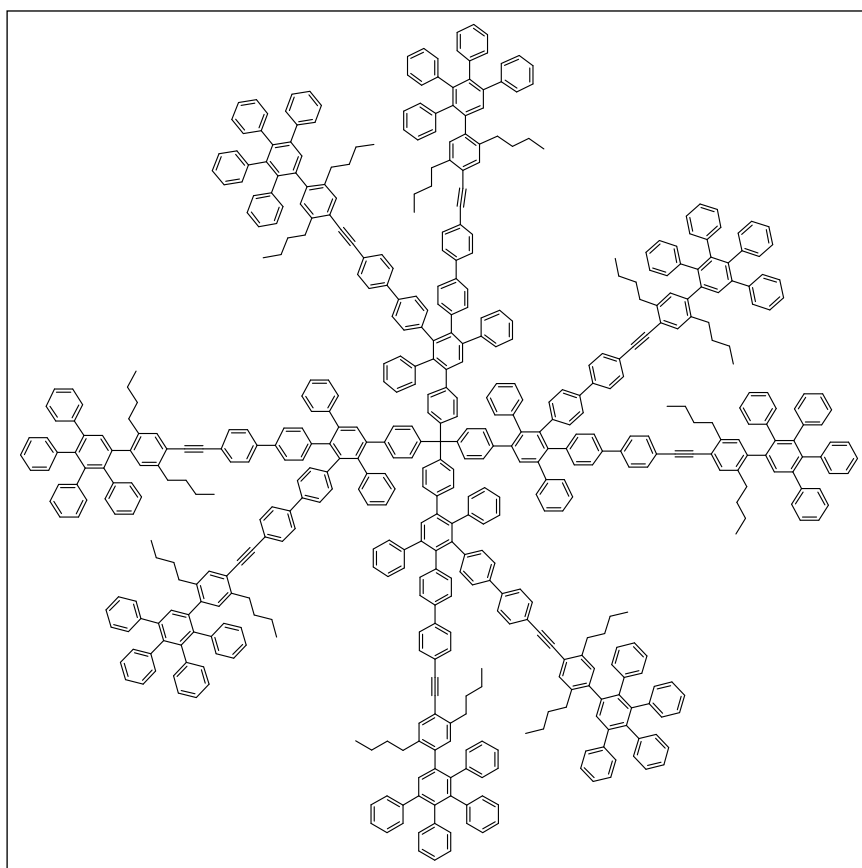
^1H NMR (500 MHz, CD_2Cl_2 , 273 K): δ =7.62 (s, 4H, Ar), 7.50-7.46 (30 H, Ar), 7.34-7.16 (m, 52 H, Ar), 7.03-6.72 (m, 54 H, Ar), 3.27, 3.35 (2 s, 8H, acetylene H), 2.80-2.73 (m, 32 H, CH_2), 1.68-1.58 (m, 32 H, CH_2), 1.42-1.36 (m, 32 H, CH_2), and 0.96-0.92 (m, 48 H, CH_3) ppm.

^{13}C NMR (125 MHz, CD_2Cl_2 , 273 K): δ =145.22, 145.14, 143.37, 142.74, 142.36, 141.73, 141.70, 141.59, 141.54, 140.98, 140.74, 140.68, 140.38, 140.34, 140.10, 139.44, 137.80, 137.73, 137.55, 133.56, 132.74, 132.25, 131.60, 130.90, 130.53, 129.33, 128.23, 127.43, 127.12, 126.94, 126.21, 125.88, 125.61, 123.72, 122.66, 122.62, 122.07, 94.49, 89.35, 82.87, 81.91, 34.20, 33.97, 33.28, 33.19, 23.05, 22.97, 14.20, and 14.13 ppm.

MALDI-TOF (dithranol): exact mass calcd for $[\text{M}+\text{H}]^+$ $\text{C}_{337}\text{H}_{292}$: 4342.08, found 4344.

Second-generation dendrimer bearing eight internal ethynyl groups (5.6)

The mixture of **5.5** (50 mg, 0.012 mmol) and tetraphenylcyclopentadienone (45 mg, 0.12 mmol) in *o*-xylene was heated at 130 °C for 3 days. After cooling to room temperature, the solvent was removed *in vacuo*. The residue was purified by means of column chromatography using PE/ CH_2Cl_2 : (1/1) to give a colorless solid (50 mg, 63 %), $T_{\text{dec}} > 216$ °C.



^1H NMR (700 MHz, $\text{C}_2\text{D}_4\text{Cl}_4$, 370 K): δ =7.58 (s, 4H, Ar), 7.43-7.34 (m, 38 H, Ar), 7.21-6.72 (m, 266 H, Ar), 2.76, 2.58, 2.44, 2.35 (4 s, br, 32 H), 1.50 (m, 32 H, CH_2), 1.28-1.23 (m, 32 H, CH_2), and 0.88-0.83 (m, 48 H, CH_3) ppm.

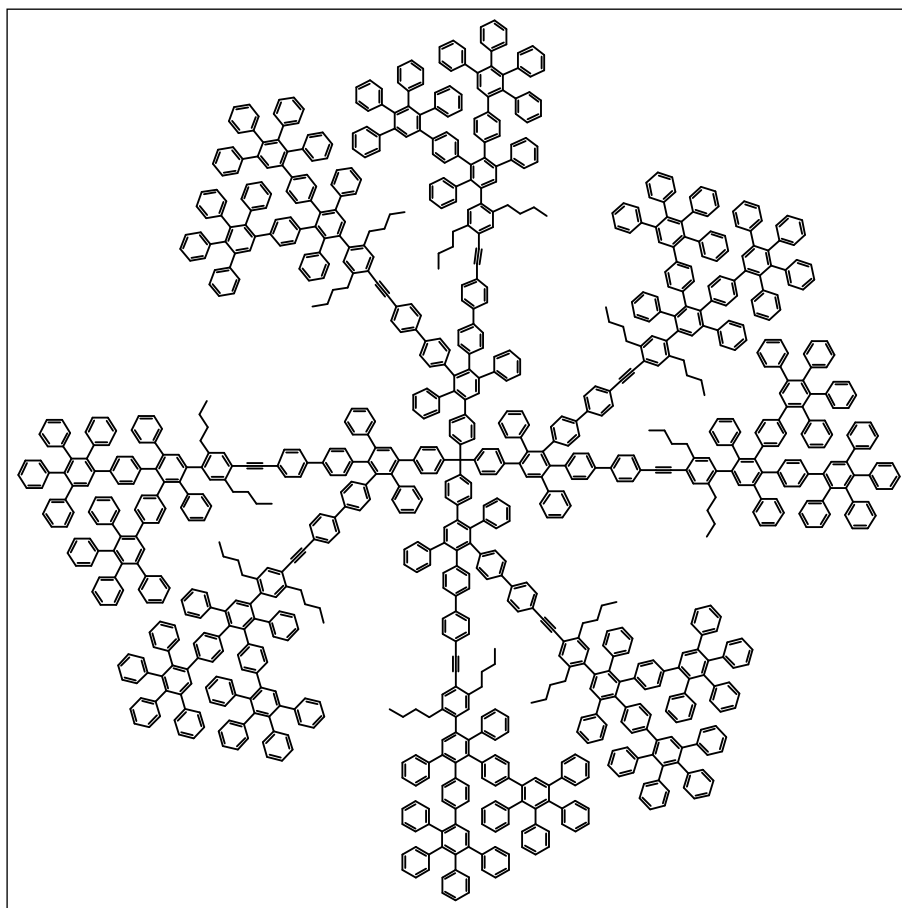
^{13}C NMR (175 MHz, $\text{C}_2\text{D}_4\text{Cl}_4$, 370 K): δ =144.97, 142.21, 142.12, 141.92, 141.74, 141.36, 141.20, 141.05, 140.72, 140.64, 140.58, 140.43, 140.36, 140.12, 140.08, 139.99, 139.61, 139.04, 138.13, 137.48, 137.24, 132.40, 131.94, 131.89, 131.84, 131.36, 131.16, 130.61, 130.18, 129.01, 127.66, 126.96, 126.76, 126.67, 126.28, 125.67, 125.36, 122.86, 122.80, 121.18, 92.55, 90.12, 33.91, 33.01, 32.93, 32.63, 22.86, 22.50, 14.12, and 13.95.

MALDI-TOF (dithranol): exact mass calcd for $[\text{M}+\text{Ag}]^+$ $\text{C}_{561}\text{H}_{452}\text{Ag}$: 7302.86, found 7307.

UV-vis (dichloromethane): $\lambda_{\text{max}}(\epsilon)$ = 321 nm (453916).

Third-generation dendrimer bearing eight internal ethynyl groups (5.7)

The mixture of **5.5** (40 mg, 0.0092 mmol) and second generation of cyclopentadienone dendron^[4] (0.13 g, 0.11 mmol) in Ph_2O (3 mL) was heated at 185 °C for 3 days. After cooling to room temperature, the solution was poured into acetone, the precipitated product was collected by filtration, washed with much acetone, methanol and was dried *in vacuo* to yield a colorless solid (94 mg, 75%), $T_{\text{dec}} > 280^\circ\text{C}$.



^1H NMR (700 MHz, $\text{C}_2\text{D}_4\text{Cl}_4$, 370 K): $\delta=7.57$ (s, 4 H, Ar), 7.40-6.50 (m, 624, Ar), 2.75, 2.57, 2.39, 2.29 (4 s, br, 32 H, CH_2), 1.48 (s, br, 32 H, CH_2), 1.24 (s, br, 32 H, CH_2), and 0.87-0.80 (m, 48 H, CH_3) ppm.

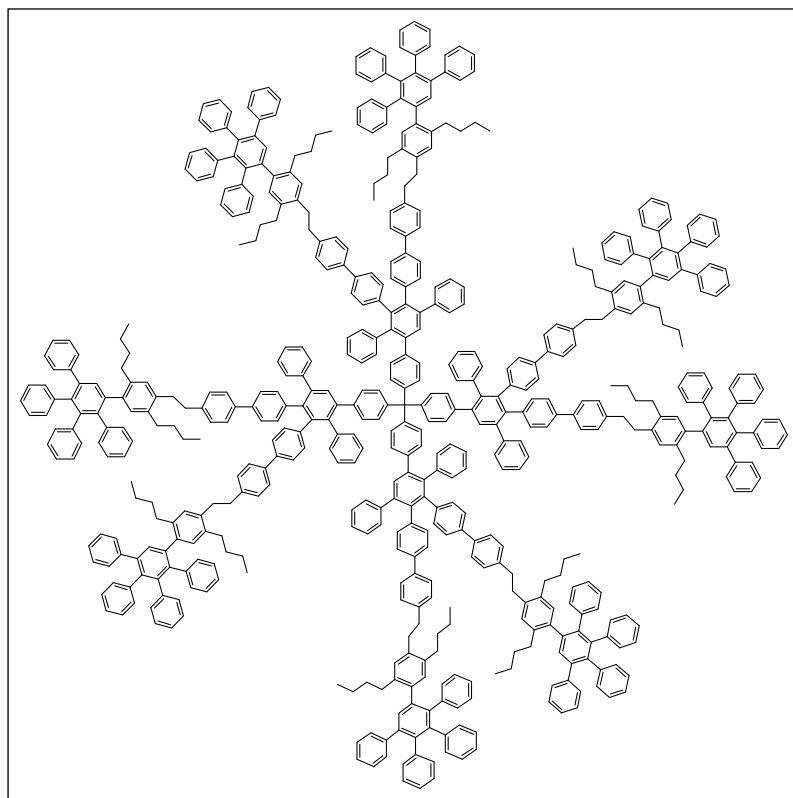
^{13}C NMR (175 MHz, $\text{C}_2\text{D}_4\text{Cl}_4$, 370 K): $\delta=144.94$, 142.28, 142.23, 142.07, 142.05, 141.80, 141.46, 141.31, 140.85, 140.78, 140.62, 140.43, 140.39, 140.31, 140.12, 140.07, 139.99, 39.53, 139.48, 139.43, 139.37, 139.19, 139.06, 138.74, 138.59, 138.32, 138.26, 138.09, 131.82, 131.27, 131.22, 130.23, 130.20, 128.85, 128.57, 127.67, 126.93, 126.78, 126.62, 126.29, 125.58, 125.30, 122.84, 121.11, 92.53, 90.14, 33.88, 32.93, 32.54, 22.82, 22.48, 14.13, and 13.98 ppm.

MALDI-TOF (dithranol): exact mass calcd for $[\text{M}+\text{K}]^+$ $\text{C}_{1041}\text{H}_{772}\text{K}$: 13320.76, found 13319; exact mass calcd for $2 \times [\text{M}+\text{K}]^+$, dimer of $\text{C}_{1041}\text{H}_{772}$: 26550, found 26587.

UV-vis (dichloromethane): $\lambda_{\text{max}}(\epsilon)=251$ (800681), and 315 nm (520769).

Hydrogenation of the second-generation dendrimer (5.8)

To a mixture of **5.8** (38 mg, 0.0052 mmol) chloroform (4 mL) a catalyst palladium on carbon (10% Pd/C) (4 mg) was



(10% Pd/C) (4 mg) was added. The reaction mixture was saturated with H_2 for 15 min. and was stirred at 50 °C in the presence of excess of hydrogen in atmosphere pressure for 1 week. The reaction mixture was then passed through the pipette filled with silica to separate the product from the catalyst. Upon evaporation of the solvent, a colorless solid was obtained (35 mg, 92%).

^1H NMR (700 MHz, $\text{C}_2\text{D}_4\text{Cl}_4$, 370 K): $\delta=7.58$ (s, 4 H, Ar), 7.40 -6.71 (m, 304 H, Ar), 2.77 (s, 32 H, CH_2 of $\text{CH}_2\text{-CH}_2$), 2.44, 2.40, 2.31 (3 s, br, 32 H, CH_2), 1.36-1.22 (m, 64 H), and 0.88-0.76 (m, 48 H, CH_3).

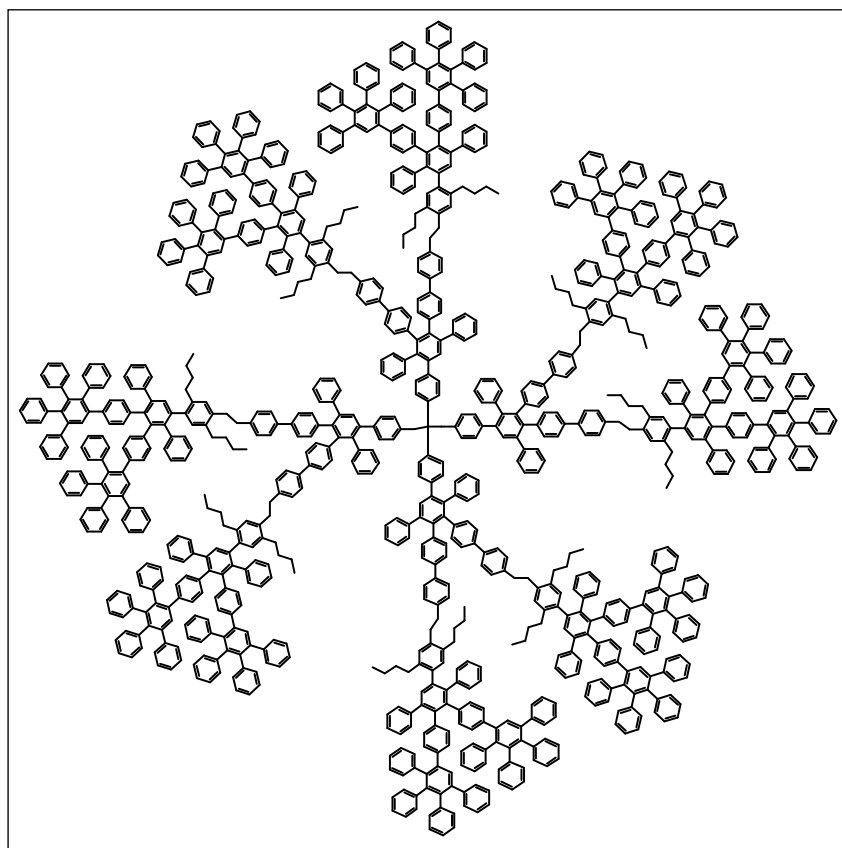
^{13}C NMR (175 MHz, $\text{C}_2\text{D}_4\text{Cl}_4$, 370 K): $\delta=144.93$, 142.40, 142.27, 141.72, 141.55, 141.23, 141.16, 141.05, 140.97, 140.73, 140.61, 140.45, 140.28, 140.14, 140.02, 139.67, 139.33, 139.23, 139.17, 138.83, 138.56, 138.50, 138.10, 137.84, 137.69, 137.66, 136.78, 132.27, 132.21, 131.95, 131.90, 131.50, 130.60, 130.22, 129.69, 129.48, 129.18, 128.99, 128.94, 128.76, 128.37, 127.77, 127.60, 127.41, 126.93, 126.81, 126.74, 126.63, 126.55, 126.41, 126.18, 125.93, 125.70, 125.55, 125.40, 125.27, 125.13, 37.32 (CH_2CH_2), 34.78 (CH_2CH_2), 33.46, 33.10, 32.77, 31.92, 22.86, 22.75, 14.14, and 14.00 ppm.

MALDI-TOF (dithranol): exact mass calcd for $[\text{M}+\text{K}]^+ \text{C}_{561}\text{H}_{484}\text{K}$: 7265.11, found 7263.

UV-vis (dichloromethane): $\lambda_{\text{max}}(\epsilon)=260$ nm (551596).

Hydrogenation of the third-generation dendrimer (5.9)

To the degassed mixture of **5.9** (70 mg, 0.0052 mmol), in 5 ml *o*-xylene palladium on carbon (10% Pd/C) (33 mg), was added as a catalyst. The reaction mixture was saturated with H_2 for 15 min. and was then stirred at 136 °C in the presence of hydrogen excess in atmosphere pressure for 1 week. After cooling the reaction mixture was passed through the pipette filled with silica to separate product from catalyst yielding a colorless solid (60 mg, 86 %).



^1H NMR ($\text{C}_2\text{D}_4\text{Cl}_4$, 700 MHz, 370 K): $\delta=7.56$ (s, 4 H, Ar), 7.40 -6.50 (m, 624 H, Ar), 2.74 (s, 32 H, CH_2 of $\text{CH}_2\text{-CH}_2$), 2.44, 2.40, 2.30 (m, 32 H, CH_2), 1.41-1.19 (m, 64 H, $2\times\text{CH}_2$), and 0.86-0.75 (m, 48 H, CH_3) ppm.

^{13}C NMR (700 MHz, $\text{C}_2\text{D}_4\text{Cl}_4$, 370 K): $\delta=144.94$, 142.41, 142.29, 142.07, 142.04, 141.55, 141.27, 141.05, 140.85, 140.81, 140.76, 140.69, 140.67, 140.46, 140.40,

140.34, 140.27, 140.18, 139.90, 139.69, 139.52, 139.45, 139.38, 139.26, 138.98, 138.88,

138.85, 138.76, 138.64, 138.58, 138.50, 138.45, 138.09, 137.81, 137.72, 137.68, 136.71, 136.59, 132.25, 131.82, 131.58, 131.32, 130.60, 130.24, 130.19, 129.88, 129.35, 129.26, 128.92, 128.82, 128.53, 127.76, 127.64, 126.91, 126.62, 126.55, 126.26, 126.19, 126.04, 125.63, 125.57, 125.43, 125.30, 125.12, 37.40, 37.36, 34.55, 34.51, 33.43, 33.05, 33.03, 32.70, 31.90, 22.81, 22.72, 14.12, and 13.99 ppm.

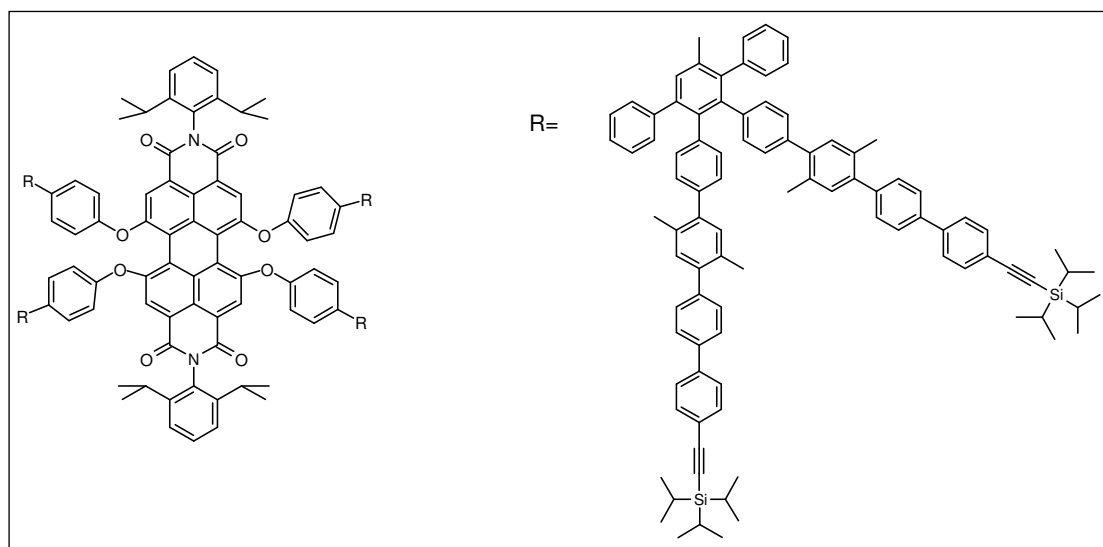
MALDI-TOF (dithranol): exact mass calcd for $[M+K]^+ C_{1041}H_{804}K$: 13352.76, found 13349.

UV-vis (dichloromethane): $\lambda_{\max}(\epsilon)=258$ nm (910565).

6.7 Syntheses of the extended arm polyphenylene dendrimers with perylenedimide core (for Chapter 4)

First-generation dendrimer with perylenedimide core bearing eight TiPS protective groups (6.1)

A mixture of 1,6,7,12-tetra-(*p*-ethynylphenoxy)-*N,N'*-(2,6-diisopropylphenyl)-perylene-3,4,9,10-tetracarboxdiimides **6.0** (40 mg, 0.034 mmol) and the extended cyclopentadienone **3.1** (0.22 g, 0.18 mmol) in 5 ml *o*-xylene was refluxed for 24 hours under argon. After cooling to room temperature, the solvent was removed *in vacuo*. The residue was purified by means of silica column chromatography (petroleum ether/ CH_2Cl_2 , 2/1) to yield a red solid (130 mg, 62%), $T_{\text{dec}} > 300^\circ\text{C}$



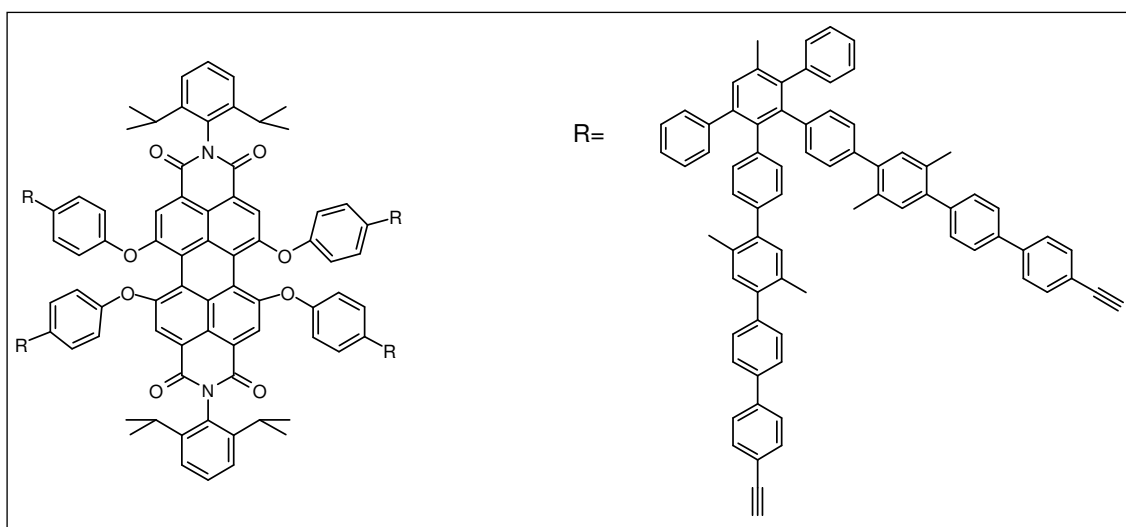
^1H NMR (700 MHz, CD_2Cl_2): δ =8.24 (s, 4H, Ar), 7.71-6.94 (m, 170 H, Ar), 6.79, 6.78 (d, 8H, J =7.69 MHz, Ar), 2.77 (t, 4H), 2.26, 2.25, 2.09, 2.07 (m, 48 H, CH_3), and 1.16 (s, 192 H of $i\text{Pr}_3\text{Si}$ and $i\text{Pr}$) ppm.

^{13}C NMR (175 MHz, CD_2Cl_2): δ =163.70, 156.18, 154.47, 146.46, 142.35, 142.12, 141.62, 141.38, 141.26, 141.23, 141.04, 140.49, 140.39, 140.34, 139.91, 139.85, 139.52, 139.22, 139.19, 138.92, 138.90, 138.66, 133.13, 133.12, 132.80, 131.96, 131.89, 131.84, 131.77, 130.54, 130.44, 130.17, 130.08, 128.20, 127.90, 127.51, 127.12, 126.96, 123.46, 122.81, 121.35, 120.88, 119.52, 107.35 and 91.79, 29.54, 24.16, 20.05, 19.94, 18.85, and 11.78 ppm

MALDI (dithranol): exact mass calcd for $[\text{M}+\text{H}]^+$ $\text{C}_{440}\text{H}_{426}\text{N}_2\text{O}_8\text{Si}_8$: 6095, found 6100.

First-generation dendrimer with perylenedimide core bearing eight ethynyl groups (6.2)

To **6.1** (88 mg, 0.014 mmol) in 8 ml THF under argon was added TBAF (40 mg, 0.13 mmol) in 3 ml THF and stirred at r.t. 40 min. After quenching with H_2O , the maximum amount of solvent was evaporated. The residue was dropped into the mixture of MeOH and water. The precipitation was collected and dried to yield a red solid (56 mg, 80%), $T_{\text{dec}} > 300^\circ\text{C}$



^1H NMR (700 MHz, CD_2Cl_2): δ =8,24 (s, 4H, Ar), 7.71-6.94 (m, 170 H, Ar), 6.81, 6.79 (d, 8H, J = 7.69 MHz), 3,19 (s, 8H), 2.78 (m, 4H), 2.26, 2.25, 2.10, 2.07 (m, 48 H), and 1.18 (s, 24 H) ppm.

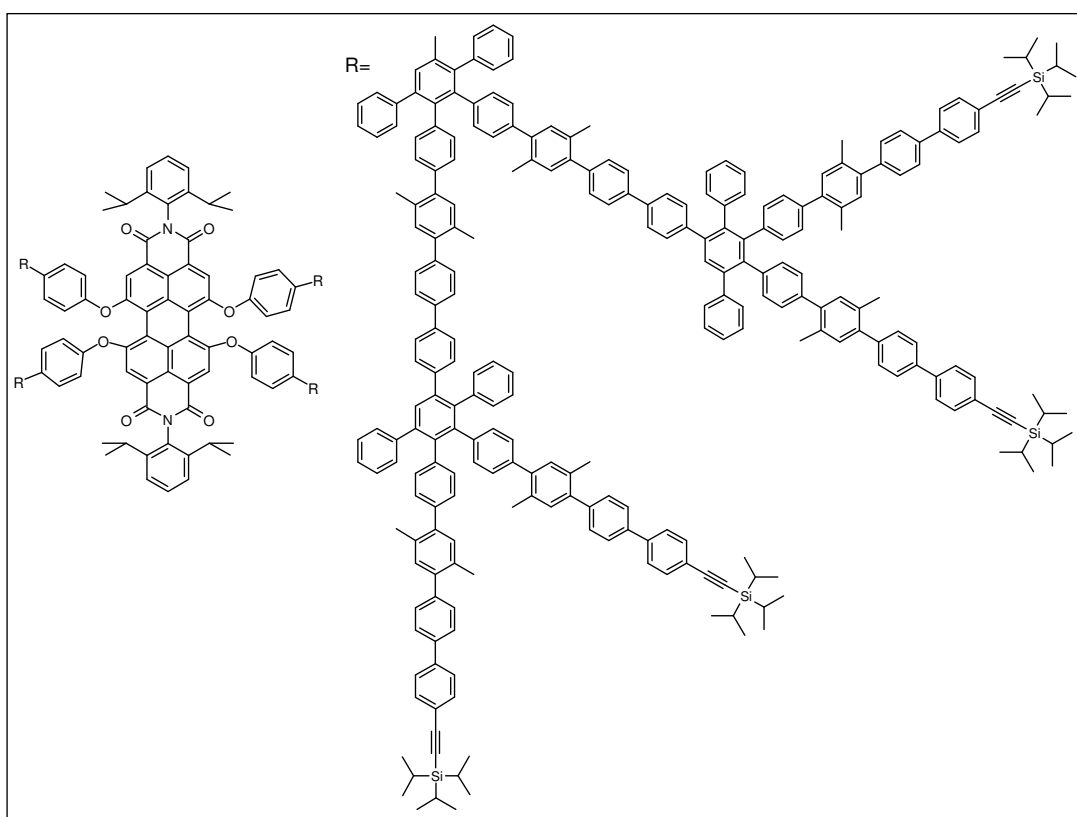
^{13}C NMR (175 MHz, CD_2Cl_2): δ =163.70, 156.19, 154.45, 146.46, 142.34, 142.12, 141.73, 141.55, 141.38, 141.28, 141.24, 140.49, 140.35, 139.91, 139.84, 139.52, 139.21, 138.78, 138.66, 133.14, 132.95, 132.77, 132.03, 131.95, 131.91, 131.84, 131.77, 130.54, 130.44,

130.18, 130.10, 128.20, 127.91, 127.52, 127.24, 127.00, 126.79, 123.45, 121.34, 120.88, 119.55, 83.76, 78.11, 29.55, 24.16, 20.05, and 19.94 ppm.

MALDI (dithranol): exact mass calcd for $[M]^+$ $C_{368}H_{266}N_2O_8$: 4844.23, found 4848.

Second-generation dendrimer with perylene-3,9-dimide core bearing sixteen protective TiPS groups (6.3)

A mixture of **6.2** (36 mg, 0.0074 mmol) and cyclopentadienone **3.1** (110 mg, 0.09 mmol) in 5 ml o-xylene was refluxed for 24 hours under argon. The reaction was worked up as described for **3.10** to yield a red solid, 79 mg (72 %).



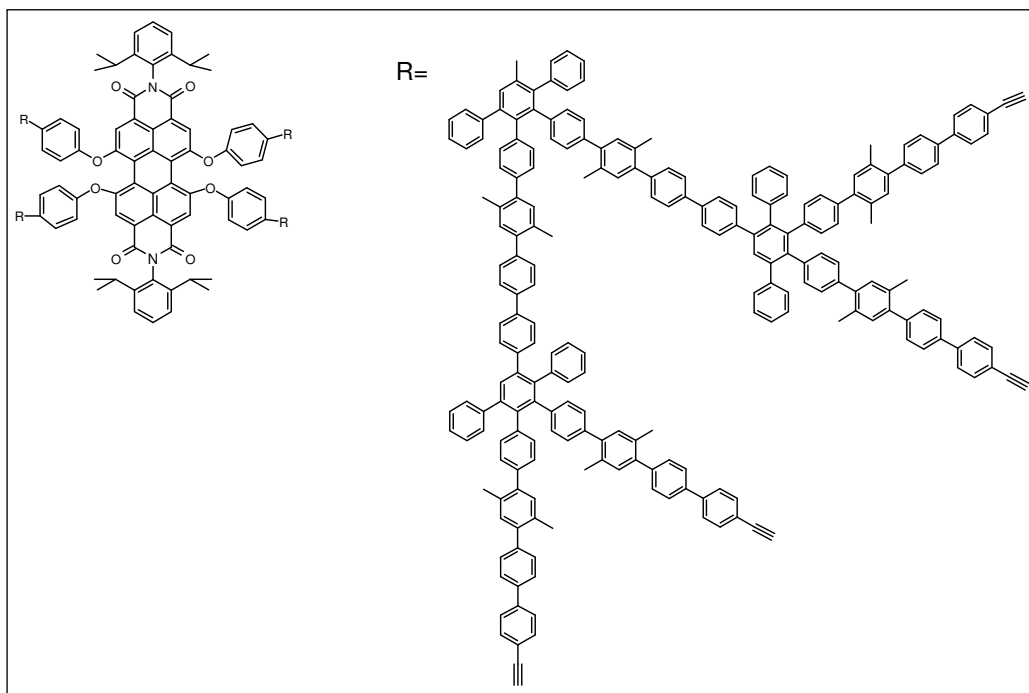
1H NMR (700 MHz, CD_2Cl_2 , 306 K): δ =8.24 (s, 4H, Ar), 7.73-6.79 (m, 490 H, Ar), 2.78 (s, br, 4H), 2.25, 2.10, 2.09, 2.09, 2.06 (m, 144 H), and 1.17, 1.16 (2 s, 360 H) ppm.

^{13}C NMR (175 MHz, CD_2Cl_2 , 306 K): δ =142.47, 142.19, 141.69, 141.33, 141.08, 140.80, 140.62, 140.40, 139.86, 139.58, 139.21, 138.94, 133.16, 132.85, 132.74, 131.93, 131.77, 130.99, 130.90, 130.56, 130.46, 130.19, 130.10, 128.16, 127.88, 127.15, 126.99, 126.54, 122.84, 107.38, 91.81, 30.00, 24.17, 20.06, 19.94, 18.86, and 11.81 ppm.

MALDI (dithranol): exact mass calcd for $[M+Ag]^+$ $C_{1088}H_{1002}N_2O_8Si_{16}Ag$: 14770, found 14787.

Second-generation dendrimer with perylene-3,4,9,10-tetracarboxylic diimide core bearing sixteen ethynyl groups (6.4)

To the mixture of **6.3** (47 mg, 0.0032 mmol) in 8 ml THF under argon was added TBAF (21 mg, 0.06 mmol) in 3 ml THF and stirred at r.t. 60 min. The reaction was worked up as described for **3.11** yielding a red solid, 35 mg (89 %).



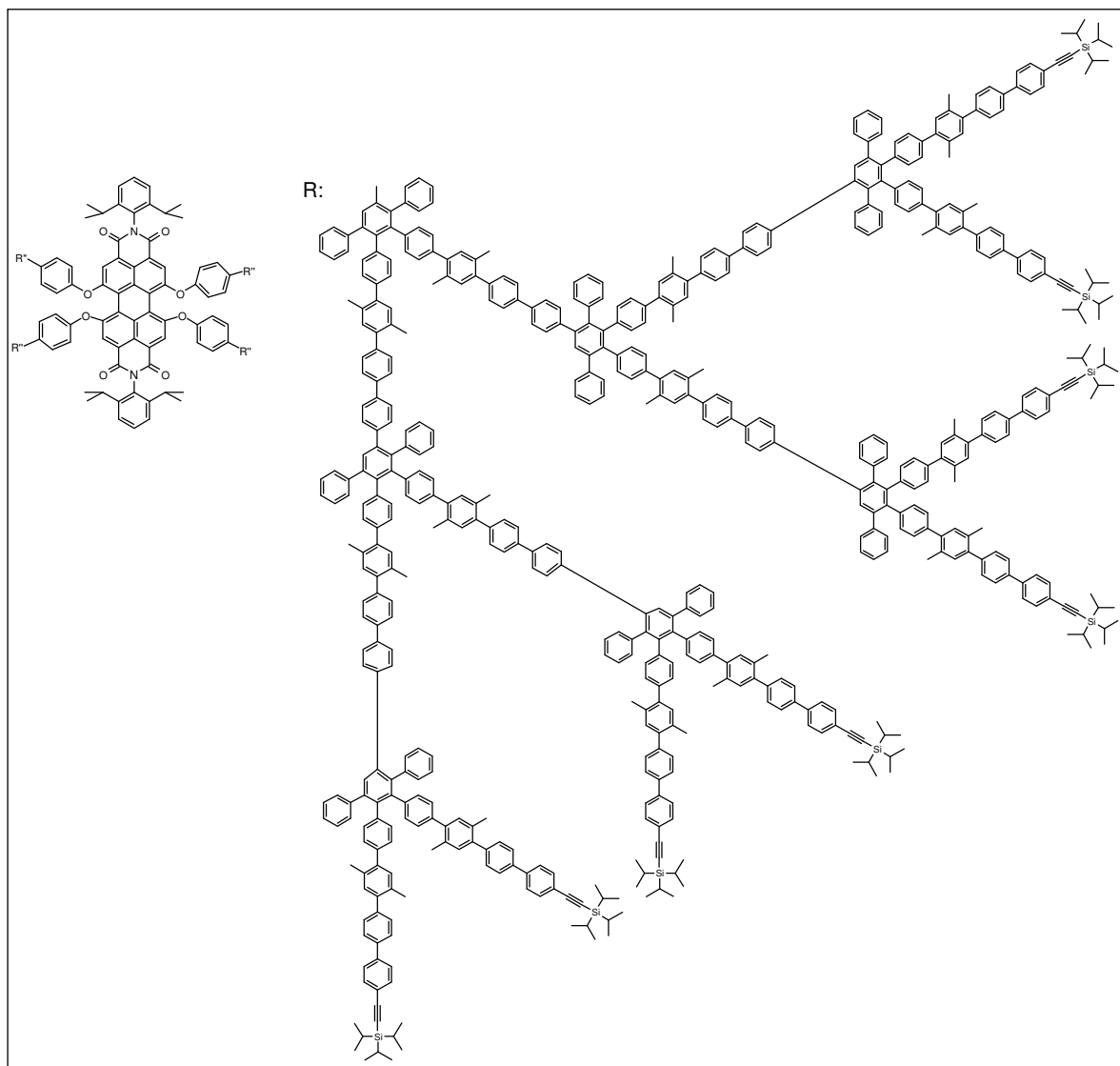
^1H NMR (700 MHz, $\text{C}_2\text{D}_2\text{Cl}_4$, 393 K): δ =8.19 (s, 4H, Ar), 7.63-6.80 (m, 490 H, Ar), 3.10 (br, 16H), 2.77 (s, br, 4H), 2.22, 2.07, 2.03 (m, 144 H), and 1.17, 1.05 (s, br, 17 H), and 1.05 (s, br, 17 H) ppm.

^{13}C NMR (175 MHz, $\text{C}_2\text{D}_2\text{Cl}_4$, 393 K): δ =142.25, 142.17, 141.78, 141.54, 141.30, 141.26, 141.18, 141.10, 140.64, 140.52, 140.47, 140.38, 140.26, 140.22, 139.80, 139.73, 139.48, 139.24, 139.13, 138.92, 138.64, 133.06, 132.91, 132.87, 132.74, 132.64, 132.52, 132.46, 132.00, 131.79, 131.63, 130.74, 130.38, 130.03, 129.89, 127.96, 127.75, 127.67, 127.30, 127.17, 127.05, 126.73, 126.48, 126.31, 126.10, 125.87, 121.41, 84.16, 78.11, 29.82, 24.26, 19.97, and 19.82 ppm.

MALDI (dithranol): exact mass calcd for $[\text{M}+\text{K}]^+$ $\text{C}_{944}\text{H}_{682}\text{N}_2\text{O}_8\text{Si}_{16}\text{K}$: 12221, found 12228.

Third-generation dendrimer with perylenedimide core bearing 32 protective TiPS groups (6.5)

A mixture of **6.4** (22 mg, 0.0018 mmol) and cyclopentadienone **3.10** (91 mg, 0.072 mmol) in 5 ml *o*-xylene was refluxed for 24 hours under argon 2 days. The reaction was worked up as described for **3.10** to yield a red solid, 43 mg (74 %).



^1H NMR (700 MHz, $\text{C}_2\text{D}_2\text{Cl}_4$, 370 K): δ =7.63–6.88 (m, 1114 H, Ar), 2.22, 2.21 (2 s, 168 H), 2.07, 2.03 (2 s, 168 H), 1.18, and 1.07 (br, 696 H) ppm.

^{13}C NMR (125 MHz, CD_2Cl_2): δ =142.12, 142.06, 141.91, 141.33, 141.04, 140.85, 140.00, 139.58, 139.54, 139.52, 139.35, 138.58, 135.98, 133.03, 132.87, 132.70, 132.65, 132.04, 131.98, 131.60, 130.88, 130.43, 130.06, 128.15, 127.92, 127.01, 126.90, 125.82, 122.71, 107.08, 91.93, 30.01, 24.28, 20.35, 20.22, 19.04, and 11.63 ppm.

MALDI (dithranol): exact mass calcd for $[\text{M}+\text{K}]^+$ $\text{C}_{2384}\text{H}_{2154}\text{N}_2\text{O}_8\text{Si}_{32}\text{K}$: 31853, found 32063.

6.8. Literature for Chapter 6.

1. U. Ziener; A. Godt, *J. Org. Chem.* **1997**, *62*, 6137-6143.
2. Varma; Raman. *J. Ind. Chem. Soc.* **1935**, *12*, 245-247.
3. Organikum. **1986**, VEB Deutscher Verlag der Wissenschaften, Berlin.
4. a) Y. Kiso; K. Yamamoto; K. Tamao; M. Kumada. *J. Am. Chem. Soc.* **1972**, *94*, 4374-4376; b) P.H. Lee; S.W. Lee; D. Seomoon. *Org. Lett.* **2003**, *5* (26), 4963-4966.
5. T. Weil; U.-M. Wiesler; A. Herrmann; R. Bauer; J. Hofkens; F. C. De Schryver; K. Müllen. *J. Am. Chem. Soc.* **2001**, *123*, 8101-8108.
6. U.M. Wiesler; K.Müllen, *Chem. Commun.* **1999**, 2293-2294.
7. a) O. Mongin; A. Gossauer. *Tetrahedron Letters*, **1996**, *37* (22), 3825-3828; b) D. Su; F.M. Menger. *Tetrahedron Letters*, **1997**, *38* (9), 1485-1488; c) U.-M. Wiesler; A. J. Berresheim; F. Morgenroth; G. Lieser; K. Müllen. *Macromolecule*. **2001**, *34*, 187-199.
8. A. Godt; Ö. Ünsal; M. Roos. *J. Org. Chem.* **2000**, *65*, 2837-2842.
9. a) D.Grebel-Koehler. Ph-D dissertation, University of Mainz, **2003**; b) J. Qu. Ph-D dissertation, University of Mainz, **2004**.
10. S. Huang; J.M. Tour. *J. Org. Chem.* **1999**, *64*, 8898.
11. U.-M. Wiesler; A. J. Berresheim; F. Morgenroth; G. Lieser; K. Müllen. *Macromolecules*. **2001**, *34*, 187-199.